

# Framing Strategies for Robustness in Steel Buildings

Submitted to the American Institute of Steel Construction  
Final Report August 2015

by

**Gustavo Cortés - LeTourneau University**

LeTourneau University  
2100 S. Mobberly Ave.  
Longview, TX 75602  
(903) 233-3937 / [gustavocortes@letu.edu](mailto:gustavocortes@letu.edu)

**Judy Liu - Purdue University**

School of Civil Engineering  
550 Stadium Mall Drive  
West Lafayette, IN 47907-2051  
(765) 494-2254 / [jliu@purdue.edu](mailto:jliu@purdue.edu)

## 1 Introduction

The main two components of this research are: (1) studying the concept of using stiff stories to limit deformations in the case of column loss and (2) performing an experimental study of half-scale beam-column gravity connections under column loss cases.

Stiff stories within a building are designed to support loads from failed columns underneath; a stiff-story is intended to be a more efficient framing strategy for mitigating effects of column loss than stiffening a conventional gravity frame. Figure 1 shows a 3-story 3-bay frame on the left, and a similar frame, but designed with a stiff-story at the roof, on the right. If one were to remove a column in the traditional building (Figure 1, left), the additional loads would have to be transferred to adjacent columns, introducing large catenary forces and inducing extreme deformations to the beam-column connections. Structural components of the floor are likely to collapse under the additional demand, potentially stressing other areas in the building to the point where they collapse as well. On the other hand, removing a column from a building with a stiff-story (Figure 1, right) would be less likely to result in collapse. The stiff-story would limit beam-column connection deformations, and transform the compressive force in the columns above the missing column to a tension, or hanger, force. Thus, the gravity load is redistributed through the stiff-story to the adjacent columns, as shown by the arrows (Figure 1, right).

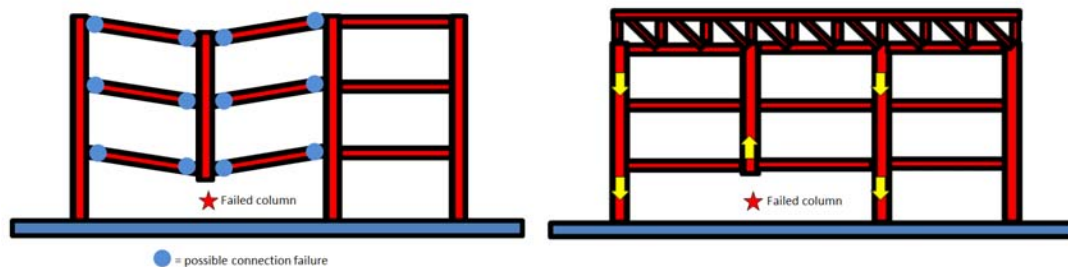


Figure 1. Traditional building (left); building with stiff-story (right).

The second main task of this project is an experimental study of the capacity of gravity connections subject to extreme deformations due to column removal. Although it is intended that the stiff stories would limit the deformation of the connections above the failed column, a balance between safety and cost may result in some deformations which need to be predicted and accommodated. While there have been a number of tests targeted at studying the behavior of beam-column connections under extreme deformations, only a very limited number of tests deal with simple gravity connections (e.g., Weigand, 2014; Hull, 2013; Johnson, 2014).

For the first task, existing buildings with large cantilevers or spans at the ground level were surveyed. Two of these buildings were selected as inspiration for the two case study buildings with stiff stories at the roof that were studied for this project. This building selection process and design are explained in Chapter 2 of the report. Chapters 3 and 4 describe the column removal linear analysis procedure and results for each of the two case study buildings, American Zinc and Lamar Construction, respectively. Chapter 5 presents the development of factors that rate the effectiveness of the different configurations studied. Chapter 6 compares the linear analysis procedure with a nonlinear approach. The second main task is covered in Chapter 7, which explains the experimental testing and results of simple gravity connections. Finally, conclusions and future work are presented in Chapter 8.

## 2 Building Analysis and Design Process

### 2.1 Building Selection

The initial tasks for the research were to survey existing buildings that serve as examples of stiff-story systems (i.e., with ‘missing’ columns at the ground level) and to catalog those systems and their properties. These tasks allowed buildings to be identified as potential case studies for the research. Additionally, trends in the case study building properties were used to provide guidance for design of stiff-story systems. For example, what types of framing strategies are preferred as the number of ‘missing’ columns increases or the number of stories supported increases? It could also help establish if certain types of framing systems are more effective for a cantilever configuration, for example.

Architectural and structural design publications were searched for buildings and their details. When possible, structural drawings were obtained from the owners or engineers of record with owner permission. In one case (Milstein Hall, No. 7), physical measurements were taken on site to supplement web-based materials. Otherwise, available architectural drawings and photographs were used, and best estimates were made. Twelve buildings were catalogued into three general categories of stiff-story systems. These general categories were the (A) cantilever / hanging perimeter, (B) large central span, and (C) cantilever truss, as shown schematically in Figure 2 and noted in Table 1.

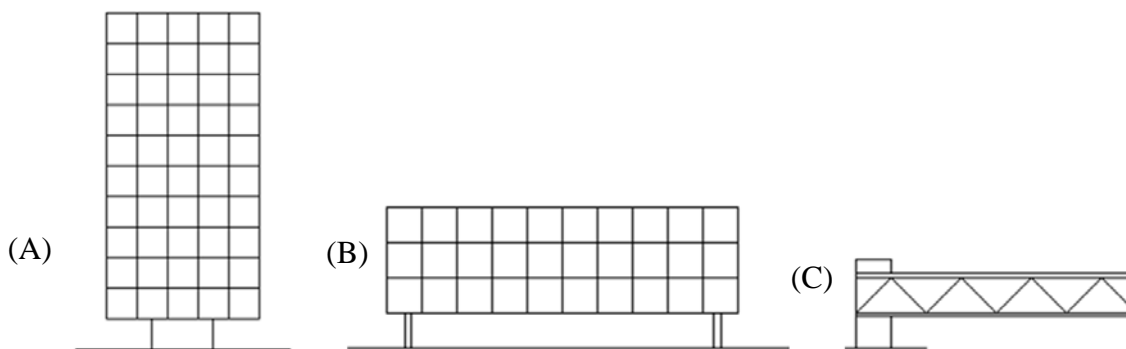


Figure 2. Structural system: (A) cantilever/hanging perimeter; (B) large center span; (C) cantilever.

Table 1. Stiff-story building examples.

No.	Building Name	Location	No. Stories#	Structural System*
1	Chauderon Administration Building	Lausanne, Switzerland	6	A
2	Kaden Tower	Louisville, KY	15	A
3	Tour Edipresse	Lausanne, Switzerland	13	A
4	Citicorp Center	New York, NY	59	A
5	American Zinc Building	St. Louis, MO	4	B
6	Fountain Place	Dallas, TX	63	B
7	Milstein Hall at Cornell University	Ithaca, NY	3	C
8	Tata Hall at Harvard University	Boston, MA	6	C
9	Samuel D. Proctor School of Education Building	Greensboro, NC	3	C
10	Cinepolis Headquarters	Morelia, Mexico	6	C
11	Clinton Library	Little Rock, AR	3	C
12	Lamar Construction Headquarters	Hudsonville, MI	2	C
#Total number of stories, including ground level, stiff and supported stories				
* Structural System (See Figure 2)				

The cantilever/hanging perimeter system (A) typically had no perimeter columns at ground level. In stories above, columns at the perimeter were generally supported by some cantilevered element from the top. For example, in the Chauderon Administration Building (No. 1) and Kaden Tower (No. 2), columns were hung from a stiff truss system at roof level. The cantilevered spans were approximately 40 feet to 50 feet, respectively. While the framing system for the cantilevered perimeter of the Tour Edipresse (No. 3) was not easily determined from public documents, the Citicorp Center (No. 4) is well known for its chevron framing allowing transfer of all loads to the “stilts” at each side of the building and enabling the corner of the multi-story structure to cantilever over the church on the same property.

The large central span (B) system allowed for mostly column-free spaces at ground level. These buildings typically utilized large trusses between vertical supports. The American Zinc building (No. 5) employed Vierendeel trusses over 80 foot spans. The system for Fountain Place (No.6) could not be determined from public documents.

Buildings No. 7 – 12 all featured long-span cantilevers, supported by large trusses. Spans ranged from 40 feet for the Tata Hall (No. 8) to 180 feet for the Clinton Library (No. 11). Most of these buildings utilized the cantilever truss (C) primarily for dramatic effect. The Milstein Hall (No. 7) system was used to span over a street and to maximize floor area within land space limitations. These buildings utilized trusses with diagonal web members regardless of span and typically supported a limited number of stories. For example, for the Lamar Construction Headquarters (No. 12) the stiff-story, a one-story 112-foot cantilever, was the main portion of the building. The two-story 52-foot cantilever in the Samuel D. Proctor building (No. 9) has story-deep trusses at both stories.

With the exception of the American Zinc building (No.5) with its Vierendeel truss for a large center span (B), buildings (for which the stiff-story system could be identified) employed story-deep trusses with diagonal web members. In the cantilever truss (C) systems, the trusses typically encompassed the depths of the buildings. In the cantilever/hanging perimeter (A) systems, the hanging columns were typically supported by trusses occupying the top story or located above the top story.

From this catalog two buildings were selected to study how effective stiff stories are in carrying loads when a column is missing. The selection was made based on type of stiff-story framing, as well as availability of information about that building. For example, most buildings utilized conventional trusses, with the exception of the American Zinc building's Vierendeel truss. Comparison of conventional and Vierendeel trusses would give additional depth to the study. Meanwhile, the original structural drawings were provided for the Lamar Construction Headquarters building (Wong, 2013), facilitating analysis and adaptation of the original structure for this study. Therefore, the Lamar Construction Headquarters building and the American Zinc building were selected and converted into "sister buildings".

## *2.2 Sister Buildings Design Process*

The concept of a sister building is to transform the existing case study building into a more typical structural system, while incorporating the existing stiff-story concepts. For instance, traditional bay sizes were established. Large spans and cantilevers were replaced with re-framed

orthogonal bays and columns that extended the full height of the building. The geometry of the truss stiff-story was maintained, however. Specific design assumptions for the American Zinc and Lamar sister buildings will be described in subsequent sections. Both sister buildings were designed to satisfy all typical loading conditions, except for seismic loading, and the designs were given the name Configuration 0.

### 2.3 American Zinc Building Design

The American Zinc building is a four story office building, with a total of 30,000 square feet, located in St. Louis, Missouri. The three upper floors measure 122' x 53'-4" in plan and are supported by two concrete piers on one end and on concrete walls on the other end. Figure 3 shows a picture of the building. The system has beams spanning the 53'-4" direction, framing into a 3-story high Vierendeel truss that runs the full 122' length of the building. This truss system transfers the building load from the long span into the supports.



Figure 3. Photograph of the American Zinc building in foreground (Sintelar, 1997).

Structural drawings were not found for the American Zinc building; only architectural drawings and photos were available. Thus, structural framing members had to be designed before column removal analyses could be performed. The design process is summarized below.

1. Model geometry of the structure based on dimensions found on architectural plans.
2. Model connections as pinned or fixed, based on the structural system and using engineering judgment.
3. Calculate gravity loads based on ASCE 7-10 (ASCE, 2010).

4. Design members based on strength and serviceability demands. A camber equivalent to the maximum deflection of the beams under service dead load was assumed when checking deflections.
5. Update model with designed members and run analysis.
6. Optimize members (optimization made in SAP2000). Even though members were optimized, uniform beam and column sizes were used throughout each story for economy in fabrication and erection.

### 2.3.1 Analysis of the Original Building

Figure 4 shows the plan view of the second story. The finite element model (FEM) used for analysis, created in SAP2000, is shown in Figure 5. Note that all beam-column connections in the Vierendeel truss are idealized as rigid. All beams spanning between gridlines 1 and 2 (see Figure 5) are pin connected. Lateral loads in the building are resisted by the concrete core (see Figure 4). This core was not designed. Instead, it was assumed to be rigid and restraints against translation in all three directions were modeled.

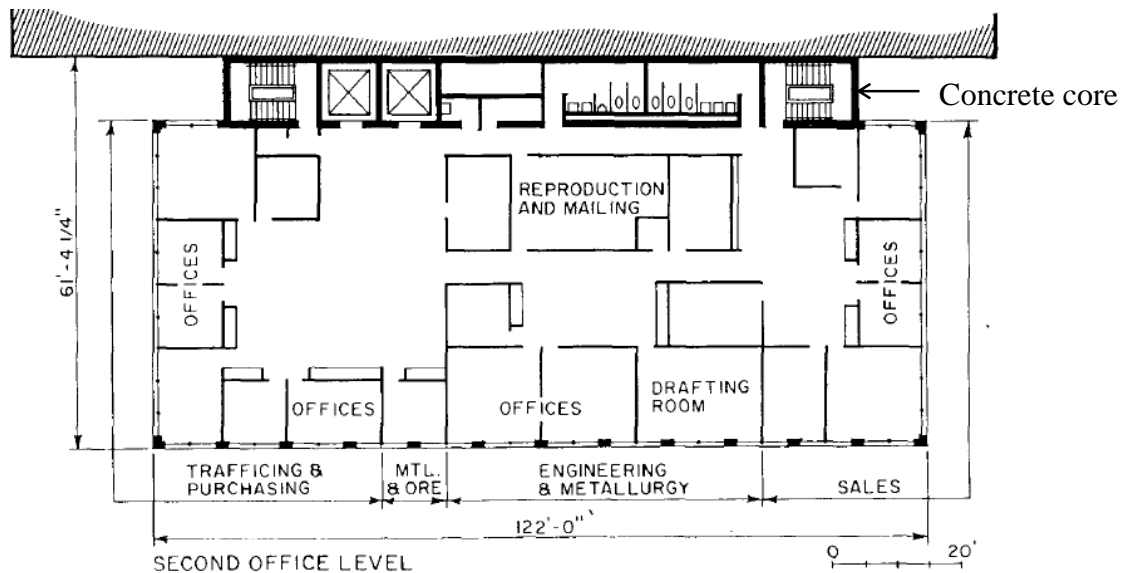


Figure 4. Plan view of the second story of the American Zinc building (National Register of Historic Places, 1998).

The design process included the generation of load assignments for the building. This was calculated using the ASCE 7-10 standard (ASCE, 2010). The loads were assigned in a one-way distribution to the main floor beams spanning 53'-4" between the two Vierendeel trusses. Table 2

summarizes the gravity loads applied at each story. Because this building has an open floor plan distribution and partition walls could be re-arranged, the 80 psf live load given in the ASCE 7-10 (ASCE, 2010) for corridors above the first floor in office buildings was used throughout. In addition, a partition live load of 20 psf was added, resulting in a total live load of 100 psf. The dead load used accounts for a concrete slab on steel deck (40 psf), for mechanical equipment (5 psf), and for the addition of tiles (16 psf), resulting in a total load of 61 psf. Finally, snow loads were calculated for the location of the building (St. Louis, MO), resulting in a 20 psf roof load. More detail for the load calculation is provided in Appendix A.

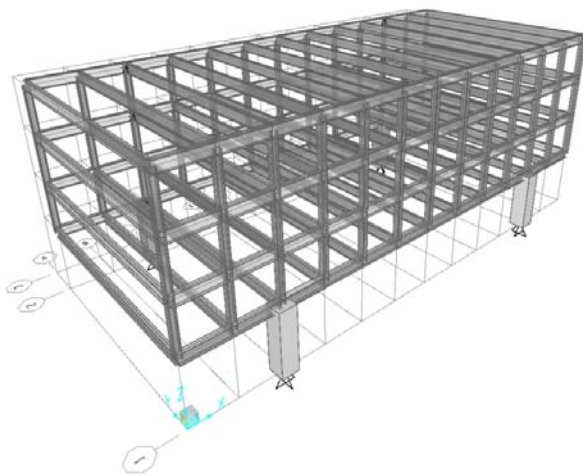


Figure 5. 3D view of the finite element model.

Table 2. Gravity loads used for design of the American Zinc building.

Story	Live Load	Dead Load	Snow Load
First Story	100 psf	61 psf	-
Second Story	100 psf	61 psf	-
Third Story	100 psf	61 psf	-
Roof	20 psf	61 psf	20 psf

Once the loads were assigned, members were designed to satisfy AISC Specifications (AISC, 2010). Members were designed to satisfy the combined flexural and axial force demands, as appropriate. SAP2000 was used to optimize the structure by analyzing the demand-capacity ratio of members but using the same section for all horizontal members of the Vierendeel truss, and one section for all vertical members of the truss. A plan view of the building indicating the structural shapes used is shown in Figure 6. Figure 7 shows the FEM of the building with the color-coded demand/capacity ratios. Note that members had demand capacity ratios varying from 0.4 to 0.9.

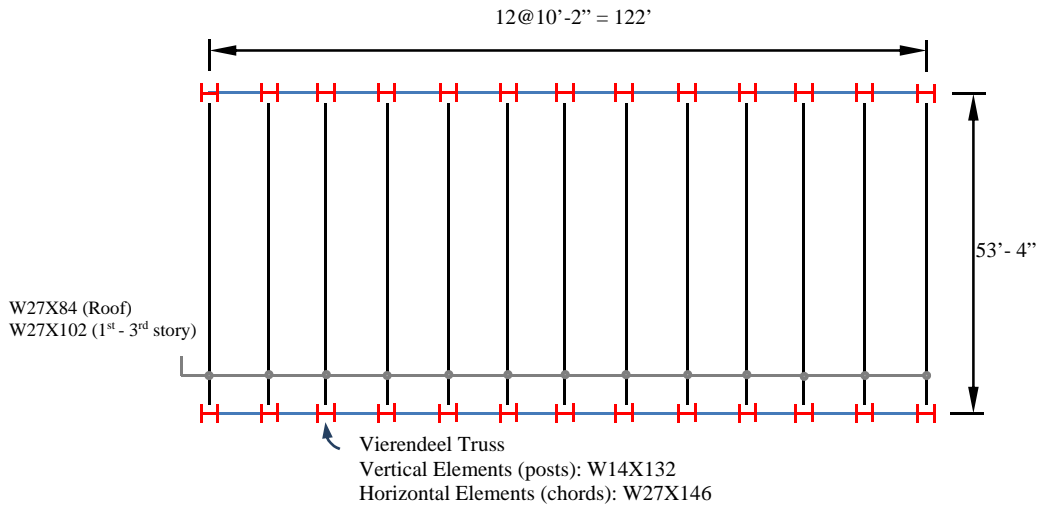


Figure 6. Plan view of the building.

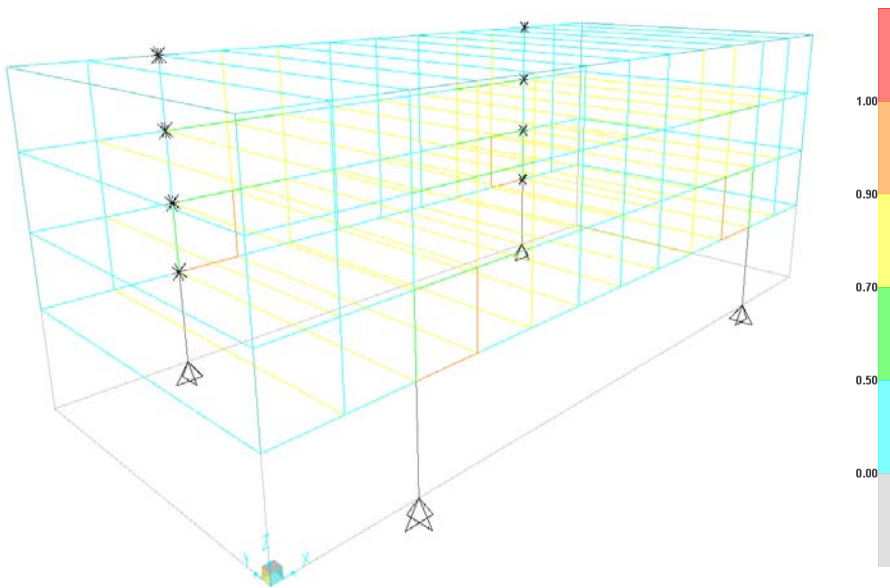


Figure 7. Demand capacity ratios of the structural system.

The American Zinc building was then transformed into a sister building, which is discussed in the next section.

### 2.3.2 Analysis and Design of Sister Building

Transforming the American Zinc into a typical structural system involved modifying the Vierendeel truss system, adding a central line of beams and columns and adding moment frames to resist lateral forces.

Perimeter columns and a gravity frame at the center, dividing the 53'-4" span into two 26'-8" spans, were added. 17 columns were added at the first story, and 7 columns added at stories 2, 3 and 4. The changes made can be seen in Figure 8, which shows the "original" configuration (left) and its sister building (right).

Figure 9 shows the plan view of the sister building at the upper levels. An interior frame and the two exterior frames along the short side of the building were converted to moment frames to resist the lateral load in that direction. In the direction parallel to the long side of the building, the Vierendeel trusses (including the new, first-story columns) serve as the lateral force resisting system. The interior columns are part of the gravity frames and do not contribute to the lateral stiffness of the building.

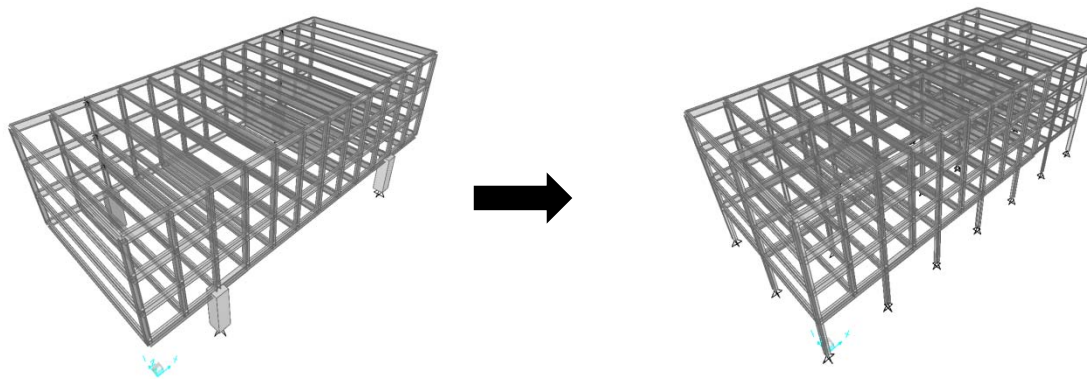


Figure 8. American Zinc building original (left) and sister building (right).

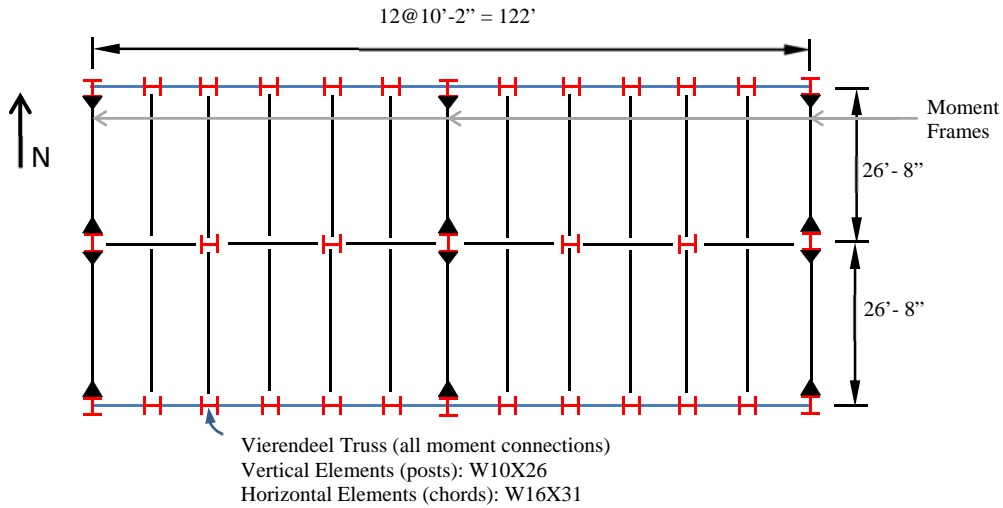


Figure 9. Plan view of American Zinc sister building.

	W16x31	W16x31	W16x31	W16x31	W16x31	W16x31	W16x31	W16x31	W16x31	W16x31	W16x31	W16x31	
W24x146	W16x31	W10x26	W10x26	W16x31	W10x26	W10x26	W16x31	W10x26	W10x26	W16x31	W10x26	W10x26	
W24x146	W16x31	W16x31	W16x31	W16x31	W16x31	W16x31	W24x146	W16x31	W16x31	W16x31	W16x31	W16x31	
W24x146	W16x31	W10x26	W10x26	W16x31	W10x26	W10x26	W16x31	W10x26	W10x26	W16x31	W10x26	W10x26	
W24x146	W16x31	W16x31	W16x31	W16x31	W16x31	W16x31	W24x146	W16x31	W16x31	W16x31	W16x31	W16x31	
W24x146		W14x74		W14x74		W24x146		W14x74		W14x74		W24x146	
	1	2	3	4	5	6	7	8	9	10	11	12	13

Figure 10. Configuration 0 beam and column sizes.

Loads for the sister building were determined according to ASCE 7-10 (ASCE, 2010). Dead, Live, Roof Live and Snow loads were the same as the original building loads, as outlined in Table 1. Wind loads were calculated for the location of the original building in Saint Louis, MO. A wind speed of 115 mph was obtained from the ASCE 7-10, resulting in the pressures shown in Table 3. Note that negative values indicate suction. The full wind calculation can be found in Appendix A.

Table 3. Wind pressure acting on the sister building (psf).

Wind Case	Windward (Floor 1)	Windward (Floor 2)	Windward (Floor 3)	Windward (Floor 4)	Leeward	Side	Roof
NS	13.8	16.1	17.9	19.3	-14.0	-17.8	-29.6 to 0.6*
EW	13.8	16.1	17.9	19.3	-10.0	-17.8	-21.8 to 0.6*

\* See Appendix A for full values.

The direct analysis method was used. Notional loads were applied to the SAP2000 model. Stiffness reduction factors were also applied and a second order analysis was used to account for P-Δ and P-δ effects. The steel members were optimized following the same process used in the original building design. Demand capacity ratios were initially targeted at near the 1.0 value while maintaining deflection limits. The demand capacity ratio of members in the lateral force resisting system remained over-designed for strength in order to satisfy deflection limits. Member sizes were kept uniform in groupings such as truss beams, truss columns, mid-span beams, mid-span columns and filler beams. The process followed for design is outlined below. A model showing the demand-capacity ratio of members can be seen in Figure 13.

1. Optimize member to have a demand-capacity ratio as close to 1.0 possible.
2. Check live load deflection on gravity beams to be within limits of IBC (ICC, 2009).
3. Check interstory drift (under service loading) to be within limits of ASCE Commentary C (ASCE, 2010).
4. Increase members if necessary to satisfy deflection limits.

Once the building was designed for strength, beam deflections and lateral drift were checked. Deflection limits due to gravity loads (dead and live) were satisfied according to the IBC (ICC, 2009). These deflection limits are outlined below.

$$\Delta_{D+L} \leq \frac{L}{240} = \frac{320''}{240} = 1.33''$$

$$\Delta_L \leq \frac{L}{360} = \frac{320''}{360} = 0.89''$$

A construction camber equal to the dead load deflection was assumed. The greatest live load deflection of a 26'-8" beam member was 0.61". Thus, the sister building satisfies the deflection limits suggested in the IBC (ICC, 2009).

Lateral drift limits were verified for wind loading per ASCE Commentary Appendix C (ASCE, 2010). This standard suggests a 10 year wind mean reoccurrence interval with service factored load combination: 1.0D+0.5L+0.7W. The commonly used wind interstory drift limit of  $h/400$  was used. Deflection limits were satisfied in both the North-South and the East-West direction as shown in Table 4 below. Members in the moment frame were increased in order to satisfy drift limits. Figure 11 and Figure 12 show the amplified deflected shapes for lateral loading in the NS and EW directions.

Table 4. Story drift summary.

Story	h (ft)	$\Delta_{\text{story}}$ Limit (in)	Interstory drift, NS (in)	Interstory drift, EW (in)
4	11	0.33	0.03	0.01
3	11	0.33	0.06	0.04
2	11	0.33	0.12	0.09
1	15	0.45	0.41	0.43

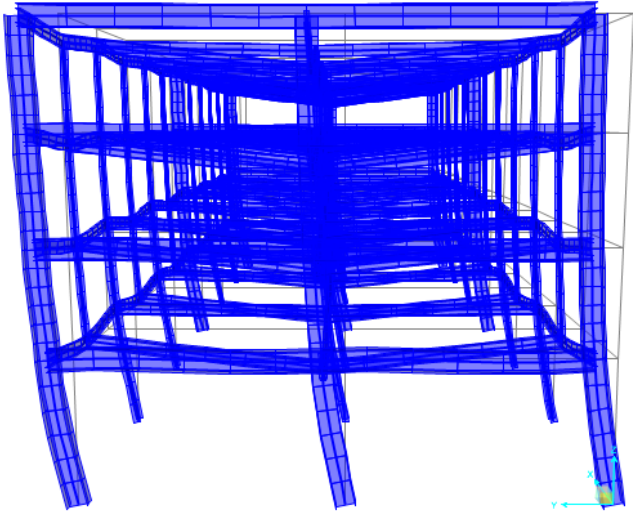


Figure 11. NS wind and gravity deflections (amplified).

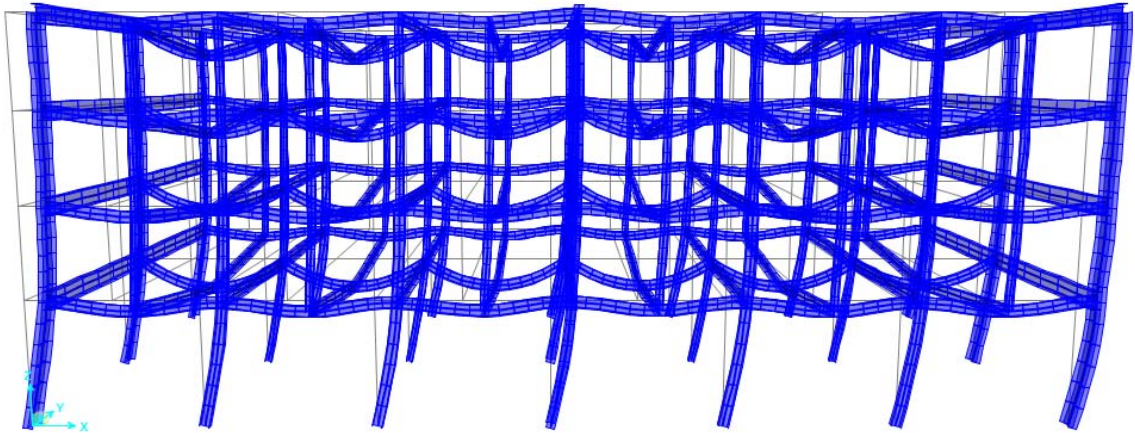


Figure 12. EW wind and gravity deflections (amplified).

The final design of the sister building that satisfies both demand-capacity ratios and deflection limits can be seen in Figures 14-17.

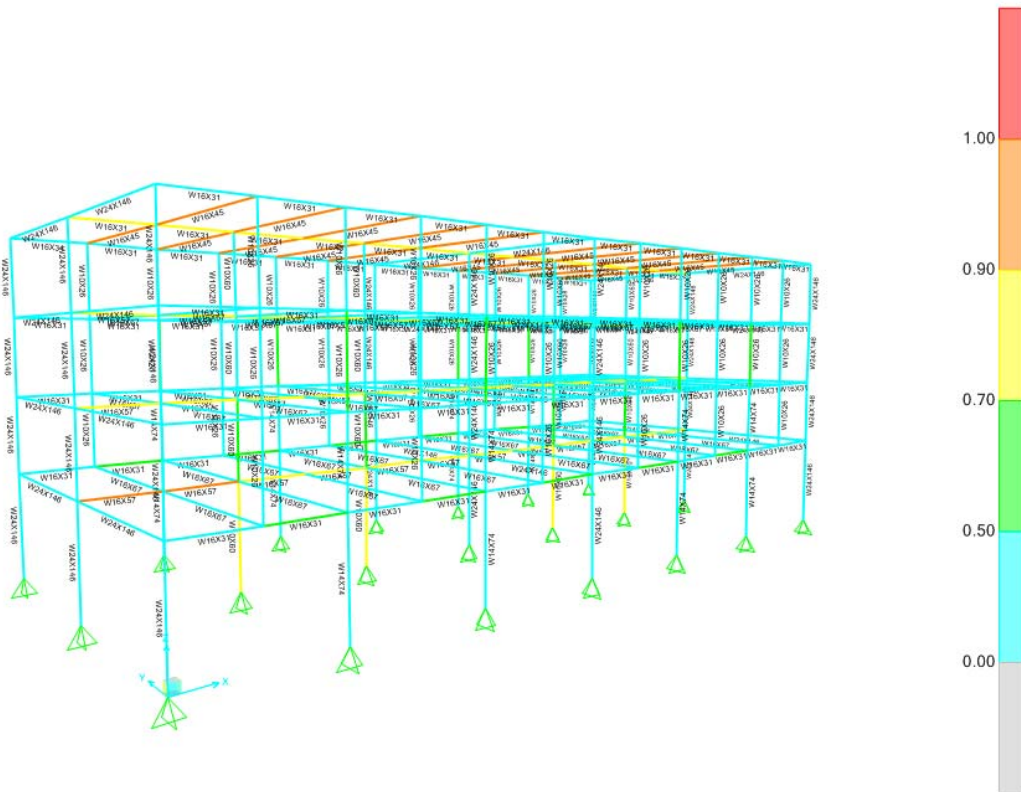


Figure 13. Sister building demand-capacity ratios (DCRs).



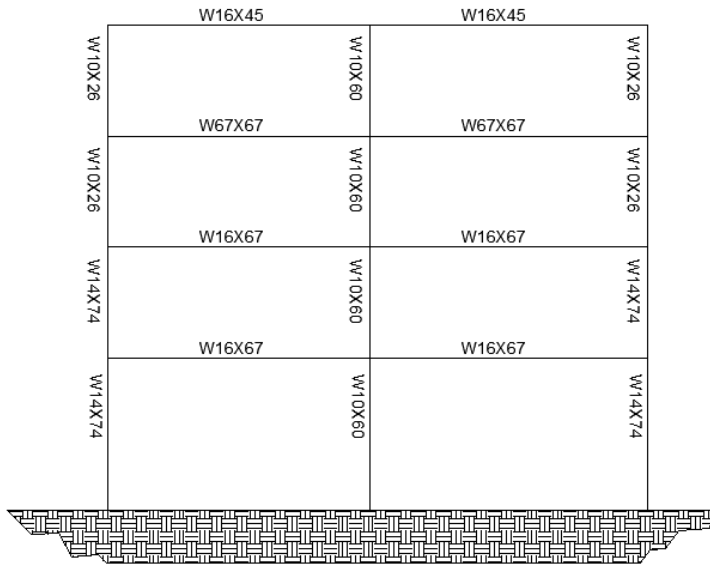


Figure 16. Typical interior gravity frame elevation.

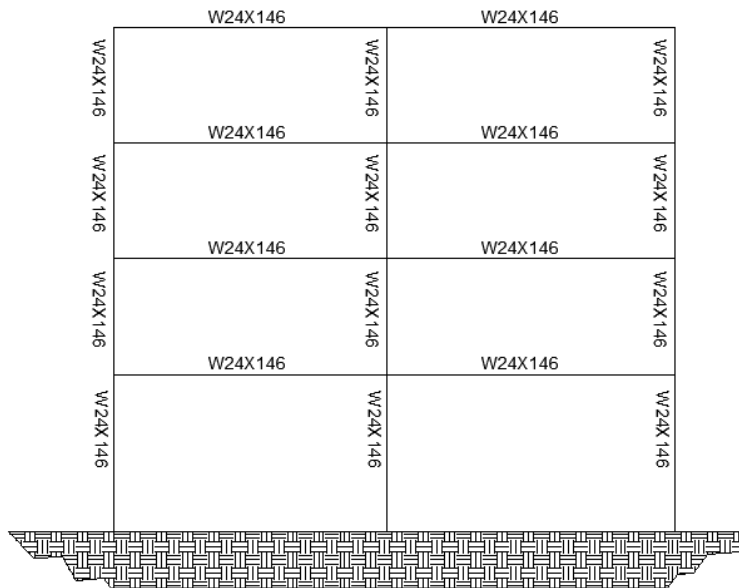


Figure 17. Typical moment frame elevation.

#### 2.4 Lamar Construction Building

The Lamar Construction Corporate Headquarters, located in Hudsonville, Michigan, is a 46,000 sq. ft. building constructed in 2007. The building has a 30,000 sq. ft. shop and 16,000 sq. ft. of office space. This steel building features a 52 ft. wide by 112 ft. long cantilever supported by a reinforced concrete core. Structural drawings were provided by the engineer of record for this





Figure 20. Photo of the Lamar Construction Corp. Headquarters (Lamar, n.d.)

#### 2.4.1 Analysis of “original” building

The 112 feet long cantilever has a story high truss system that is supported by a large steel-concrete composite core. Loading for the structure was provided in the structural plans. The floor has a 5 ½” slab with gage 20 composite metal deck with 2 ½” light weight concrete above the deck and is reinforced with 6x6 W2.1xW2.1 WWF. This slab contributes 40 psf to the dead loads. Other dead loads include 20 psf for the raised floor assembly consisting of a 1 ¼” light weight concrete topping on ¾” thick plywood and 15 psf for mechanical equipment. A 60 psf office live load and a 20 psf partition live load were also used.

The roof is composed of a 1 ½” 18 gage wide rib metal deck, which contributes to a total roof dead load of 20 psf. An additional 5 psf mechanical equipment load was also added to the roof’s dead load. A 35 psf flat roof snow load was applied at the roof based on the specified 50 psf ground snow load. The roof live load was 20 psf. Table 5 shows a summary of the loads used for the analysis.

The building was analyzed in SAP2000 to verify DCRs of the sections and deflections. Two 3D renderings of the FEM are shown in Figure 21.

Table 5. Gravity loads for design of the Lamar Construction building.

Load	First Floor	Roof
Dead Load	75 psf	25 psf
Live Load	80 psf	20 psf
Snow	-	35 psf

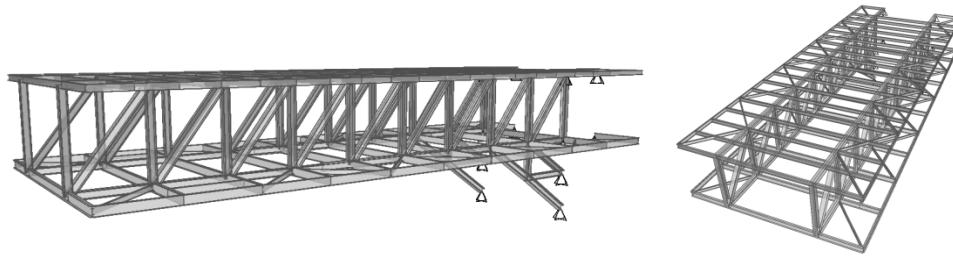


Figure 21. FEM rendering.

The model had a maximum deflection of 5.4", equivalent to a limit of  $L/250$ , under service loads (dead and live loads) at the free end of the cantilever (see Figure 22). Analysis results for gravity load combinations showed that members had demand capacity ratios varying from 0.1 to 0.7. This ratio, based on equations H1-1a and H1-1b of the AISC Specifications (AISC, 2010), considered the axial load and bending.

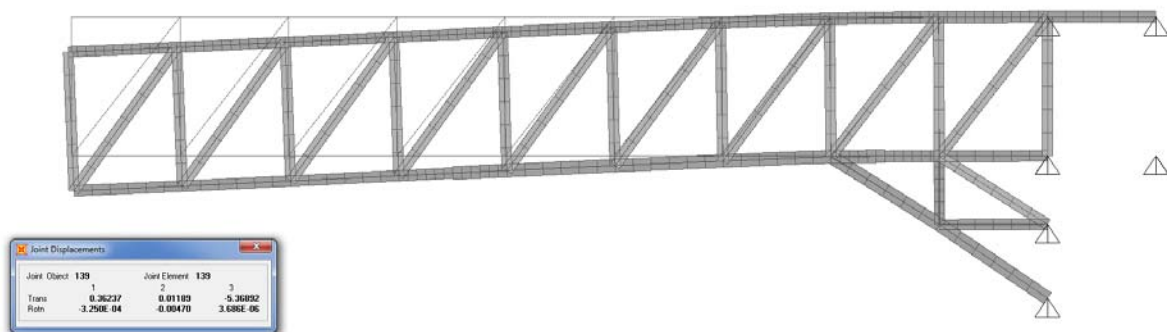


Figure 22. Deflected shape (results shown in inches).

#### 2.4.2 Sister Building Design

Following a similar approach as for the American Zinc building, the Lamar Construction building was converted into a sister building for further progressive collapse analysis and evaluation. Transforming the Lamar Construction building into a typical structural system involved mirroring the building over its elevation in order to make it a symmetrical building and adding columns at ground level. The building was converted into a 4 story building and, in its short direction, the 3 bays were modified to measure 26 feet each. Along the long direction, the building has 7 bays with spans of 25 feet. In addition, because the concrete core used in the original building was removed, lateral braces were added to the building in both orthogonal directions to provide lateral force resistance. The transformed model can be seen in Figures 25 through 29.

Gravity loads applied to the sister building were the same as those applied to the original building, noted in the previous section. Wind loads were calculated for the project site of Hudsonville, Michigan which has a basic wind speed of 115 mph. Table 6 summarizes the wind pressure.

Table 6. Wind pressure acting on the sister building (psf).

Wind Case	Windward (Floor 1)	Windward (Floor 2)	Windward (Floor 3)	Windward (Floor 4)	Leeward	Side	Roof
NS	22.3	24.2	25.9	27.2	-19.1	-24.5	-40.6 to 0.9*
EW	22.3	24.2	25.9	27.2	-13.8	-24.5	-29.9 to 0.9*

As for the American Zinc building, the direct analysis method was used. Notional loads were created and included in the analysis. SAP2000 directly applies the stiffness reduction factors. A second order analysis was used to account for P- $\Delta$  and P- $\delta$  effects. The analysis was performed and the members were sized according to the AISC Specifications (AISC, 2010). Beams were designed as simply supported and partially composite for gravity loads. A typical 3" metal deck with a 3.25" lightweight concrete topping reinforced with 6x6 W1.4xW1.4 welded wire reinforcement was used based on work by Francisco (2014). The shear studs are 3/4" x 4-7/8" spaced at 12" o.c. The design yielded a composite action of 38% for the beams and 36% for the girders. After sizing the elements for strength, deflections and lateral drifts were checked per IBC (ICC, 2009) and ASCE 7 (ASCE, 2010).

Lateral drift limits were verified for wind loading per ASCE Commentary Appendix C (ASCE, 2010). For details regarding the service load combination and the story drift limits please see Section 2.3.2. Table 7 summarizes the interstory drift results for the NS and EW directions. Note that drift limits are satisfied. Figure 23 and Figure 24 show the deflected shapes in the NS and EW directions, respectively. Final designs for the Lamar sister building are shown in Figure 25- Figure 29.

Table 7. Story drift summary.

Story	h (ft)	$\Delta_{\text{story}}$ Limit (in)	Interstory drift, NS (in)	Interstory drift, EW (in)
4	13	0.39	0.13	0.004
3	13	0.39	0.18	0.059
2	13	0.39	0.19	0.081
1	13	0.39	0.17	0.075

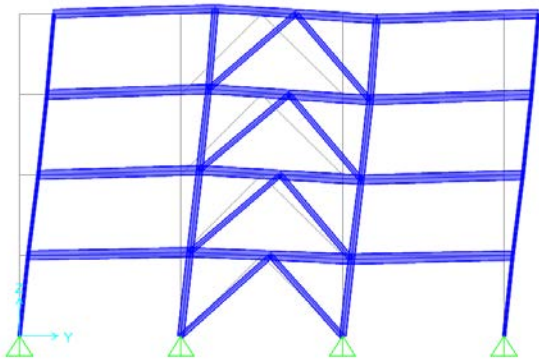


Figure 23. NS wind drift

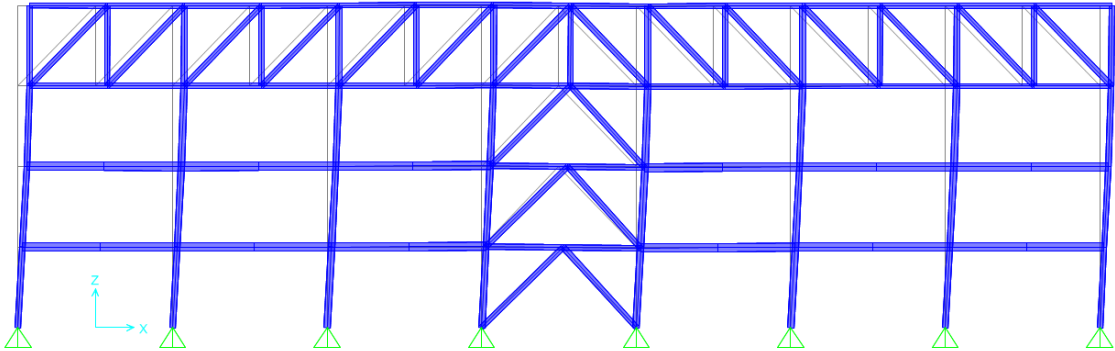


Figure 24. EW wind drift (scale factor = 100).

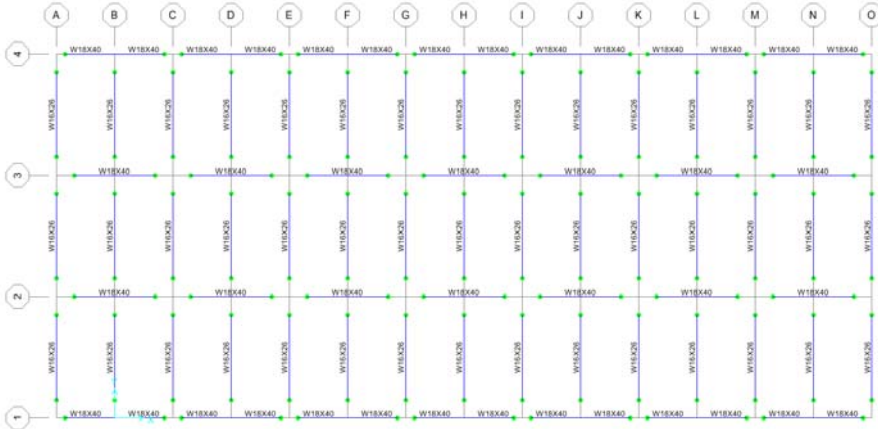


Figure 25. Roof plan view of Lamar Construction sister building.

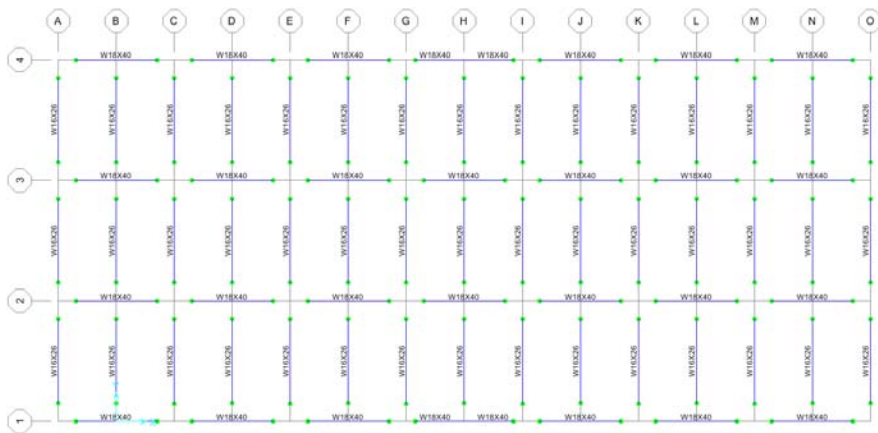


Figure 26. Floors 1-3 plan view of Lamar Construction sister building.

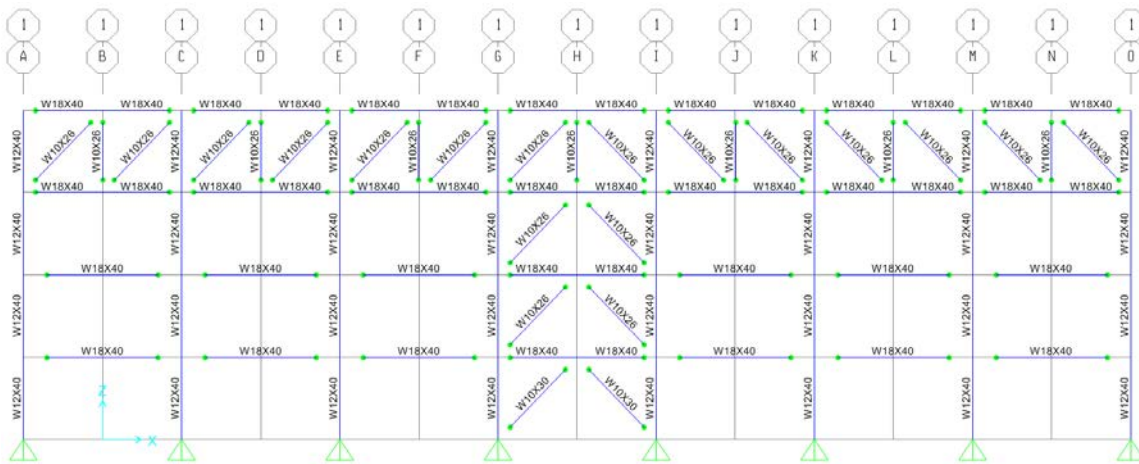


Figure 27. Elevation view of the external frame.

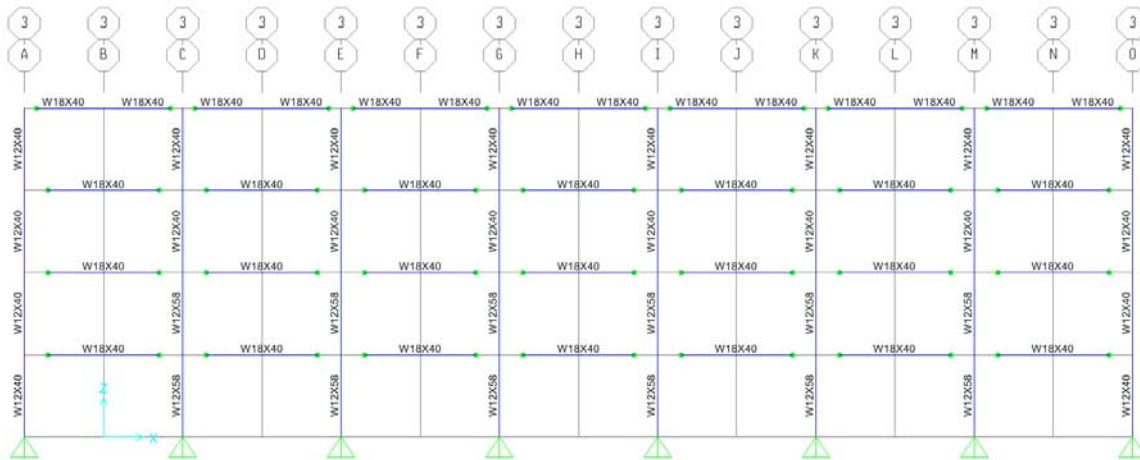


Figure 28. Elevation view of the internal frames.

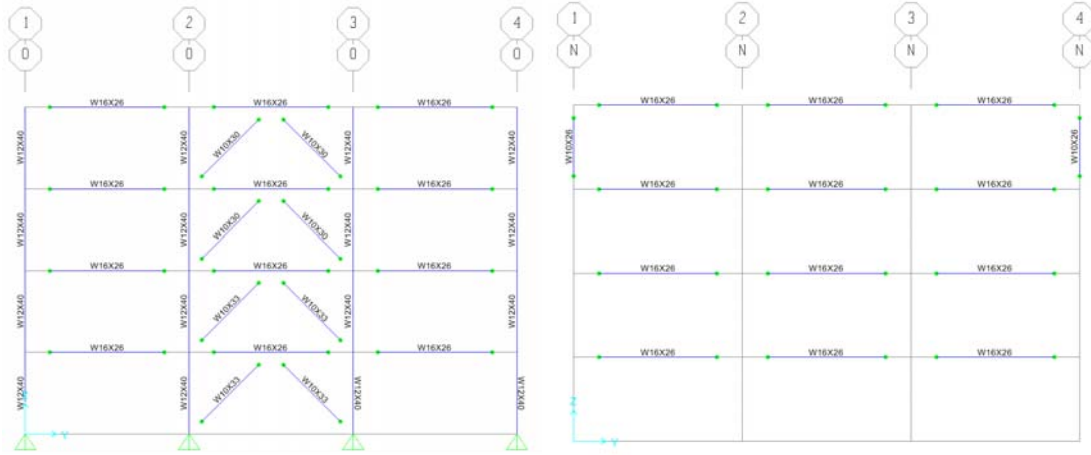


Figure 29. Elevation view of the NS external frames (left) and internal frames (right).

2.5 Progressive Collapse Resistance

After the sister buildings were fully designed, a column removal analysis was performed. The Alternate Path (AP) Linear Static Procedure (LSP) provided in the UFC 4-023-03 *Design of Buildings to Resist Progressive Collapse* was followed. The ASCE 41-06 *Seismic Rehabilitation of Existing Buildings* was also extensively used because the UFC guideline refers to it often.

2.5.1 General Procedure

The general procedure of column removal analysis involved selecting columns for removal, then performing a series of analytical steps to determine the structure’s response to progressive collapse. The beam-column connections of beams immediately adjacent to the removed column were first designed so that connection m-factors could be calculated. The m-factors of connections and beams adjoining the removed column were used to calculate amplified loads

that were then applied to the building models. Two models were created, one for deformation controlled (DC) actions and the other for force controlled (FC) actions. Results from the column removals of each model were then analyzed to determine which specific frame members would fail according to UFC and ASCE 41 criteria.

SAP2000 software was used for calculating member demands and capacities. A brief overview of the application of loads within the software follows. Load patterns, including dead loads, live loads, notional loads, etc., are used to apply loads directly to the structure. The load cases function has a nonlinear staged construction functionality which was used to create the column loss scenarios. These involved adding all the applicable loads, including the amplified load to account for dynamic effects, and removing the desired member(s).

### 2.5.2 Selection of Columns to be Removed

Column removal locations were selected to provide a representative group of unique exterior columns for each structure. Columns not supported by moment connections or braces were assumed to fail in column loss scenarios since these are modeled as pinned connections and do not have rotational resistance. Thus, these columns were not checked. Because the buildings are symmetrical, only one of each type of unique supported column was selected for removal. The supported columns that were not removed were assumed to act similarly to those their symmetric counterparts that were removed. Only the first story segments of the columns were removed, along with the adjoining brace if applicable. The column removal locations for the American Zinc and Lamar buildings can be found in Figure 33 and Figure 47, respectively.

### 2.5.3 M-Factors

M-factors are numerical values that are part of the acceptance criteria for structural members and elements. These were derived for seismic loads and are included in the ASCE 41 for linear procedures. ASCE 41 and the UFC both make use of m-factors in determining load increases and for the final evaluation of member suitability. See Appendix B for m-factor calculations.

Using the UFC procedure, m-factors were determined for all structural elements and critical connections. Most m-factors were determined using ASCE 41 Table 5-5, with the exception of m-factors for connections, which were found using UFC Table 5-1. Once the column removal locations were known, the m-factors for the beams, girders, and connections in the area affected by the removed element were found. Based on these m-factors, the increased loads around the column removal were determined (see Section 2.5.4). Once the model analysis had been run, m-

factors for all elements were used to determine the final acceptability of the members. Note that m-factors were used only for DC actions as required by the UFC.

Beam m-factors were determined using flange slenderness and web slenderness based on ASCE 41 Table 5-5. M-factors for beam-columns were divided into two categories based on the axial demand to capacity ratio ( $P_{UF}/P_{CL}$ ). Like beams, m-factors for beam-columns with a  $P_{UF}/P_{CL} < 0.2$  were based on flange and web slenderness values alone. M-factors for beam-columns with  $0.2 \leq P_{UF}/P_{CL} \leq 0.5$  were also affected by the  $P_{UF}/P_{CL}$  ratio. Beam-columns with  $P_{UF}/P_{CL} > 0.5$  were considered FC and m-factors were not defined for them. For certain slenderness values, linear interpolation was necessary to find the m-factor. M-factors for braces in compression were found based on the slenderness of the member. Tension in braces and columns used set m-factors.

#### 2.5.4 Column Removal Loads

Once the applicable m-factors had been found, the Load Increase Factors (LIFs) were found. For the DC model, the LIF ( $\Omega_{LD}$ ) for each column removal was based on the lowest m-factor ( $m_{LIF}$ ) for primary beams, girders, and wall elements (UFC 4-023-03, p. 44). Connections were also included in selection of  $m_{LIF}$  (UFC 4-023-03, p. 135).  $\Omega_{LD}$  was calculated according to Equation 1. For the FC model, the LIF ( $\Omega_{LF}$ ) was always 2.0. The LIFs were used to amplify loads in the affected bays around the column removal.

$$\Omega_{LD} = 0.9 \cdot m_{LIF} + 1.1 \quad \text{Equation 1}$$

In the SAP2000 models, the column removal load pattern was modeled with the same value as the load combination used for the rest of the structure (1.2D + 0.5L or 0.2S). The load case for each column removal increased the column removal load pattern by  $\Omega_{LD}-1$  (or  $\Omega_{LF}-1$ ), since the basic load combination was already applied throughout the structure. A summary of the load cases applied to the structure is shown below.

- a. For areas immediately adjacent to the removed column, in the DC model:

$$G_{LD} = \Omega_{LD}[1.2D + (0.5L \text{ or } 0.2S)]$$

- b. For areas immediately adjacent to the removed column, in the FC model:

$$G_{LF} = \Omega_{LF}[1.2D + (0.5L \text{ or } 0.2S)] = 2.4D + (1.0L \text{ or } 0.4S)$$

- c. For all areas away from the removed column, in both models (DC and FC):

$$G = 1.2D + (0.5L \text{ or } 0.2S)$$

### 2.5.5 Modeling

SAP2000 software was used for the analysis of each column removal's demand and capacity. Once the column removal loads described in Section 2.5.4 had been applied to the models, the load case feature of SAP2000 was used to create the column removal scenarios. Nonlinear Static Staged Construction (NSSC) with P-Delta effects was used to remove the first story column (and adjoining brace if applicable) and apply all applicable loads. Each load case included an add structure command (necessary to apply all structural elements to the load case); the dead, live, and snow load patterns using the combination  $1.2D + (0.5L \text{ or } 0.2S)$ ; the column removal load pattern (to amplify load in affected area); removed elements (which had to be below the add structure command in the stage data list); and notional load patterns using the combination  $1.2N_{DL} + (0.5N_{LL} \text{ or } 0.2N_{SL})$ . Four load cases were created for each column removal; each was identical except for the direction of the notional loads. The four load cases were grouped into a load combination for each column removal.

Since two models were used, one for FC actions and the other for DC actions, all load cases had to be applied to both models. This was easily done by setting up the load cases in one model and then copying the model and modifying to create the other model. The only difference between the two models was the LIF used ( $\Omega_{LD}$  or  $\Omega_{LF}$ ), which affected the scale factor applied to the column removal load patterns. Also, material strength in the DC model was based on expected yield strength, while the FC model was based on lower bound yield strength. All applicable load cases were then run in the analysis. Analysis results for each column removal were collected using SAP2000 Design Data tables (PMM Details and Shear Details) and then exported to Excel. The remaining portion of the structural evaluation was primarily completed using Excel spreadsheets. A single spreadsheet template was developed to simplify the analytical process (see Appendix C and Section 2.5.7).

### 2.5.6 Acceptance Procedure

The acceptance procedure followed UFC 3-2.11.7 and ASCE 41 chapter 5. The final acceptance of a member was determined by one of several interaction equations. The terms in the interaction equations are described in Table 8. Note that certain actions are classified as FC and others are

DC (see Table 9). DC actions typically consider the applicable m-factor (UFC 3-2.11.7.1) while FC actions do not (UFC 3-2.11.7.2). The basic procedure for analysis is as follows:

1. Based on the FC model results, classify all beam-columns with a  $P_{UF}/P_{CL}$  ratio greater than 0.5 as FC. Beam-columns with a  $P_{UF}/P_{CL}$  ratio less than 0.5 are classified as DC.
2. Check FC beam-columns in compression using Equation 2 *Interaction Equation for Force Controlled Members* (ASCE 41 Eq. 5-12).

$$\frac{P_{UF}}{\Phi P_{CL}} + \frac{M_{UFx}}{\Phi M_{CLx}} + \frac{M_{UFy}}{\Phi M_{CLy}} \leq 1.0 \quad \text{Equation 2}$$

3. Check DC beam-columns in compression using Equation 3 *Interaction Equation for*  $P_{UF}/P_{CL} < 0.2$  (based on ASCE 41 Eq. 5-11) and Equation 4 *Interaction Equation for*  $0.2 \leq P_{UF}/P_{CL} \leq 0.5$  (based on ASCE 41 Eq. 5-10).

$$\frac{P_{UF}}{2\Phi P_{CL}} + \frac{M_{UDx}}{\Phi m_c M_{CEx}} + \frac{M_{UDy}}{\Phi m_c M_{CEy}} \leq 1.0 \quad \text{Equation 3}$$

$$\frac{P_{UF}}{\Phi P_{CL}} + \frac{8}{9} \left[ \frac{M_{UDx}}{\Phi m_c M_{CEx}} + \frac{M_{UDy}}{\Phi m_c M_{CEy}} \right] \quad \text{Equation 4}$$

4. Check members with tension using Equation 5 *Interaction Equation for Tension Members* (Based on ASCE 41 Eq. 5-13).

$$\frac{P_{UD}}{\Phi m_b P_{TE}} + \frac{M_{UDx}}{\Phi m_c M_{CEx}} + \frac{M_{UDy}}{\Phi m_c M_{CEy}} \quad \text{Equation 5}$$

5. Check gravity beams with low axial demand (<10% of axial strength per ASCE 41 5.4.2.4.2) using Equation 3 or Equation 5. Failing members can be checked without axial demand if necessary.
6. Check all braces using Equation 6 *Interaction Equation for Braces in Compression* or Equation 7 *Interaction Equation for Braces in Tension* (based on ASCE 41 5.5.2.4.1), whichever is applicable.

$$\frac{P_{UD}}{\phi m_{br} P_{CE}} \leq 1.0$$

Equation 6

$$\frac{P_{UD}}{\phi m_{br} P_{TE}} \leq 1.0$$

Equation 7

7. Check shear in beams and columns using the FC model results. Ensure shear capacity is greater than demand and that shear capacity is based on actual  $F_y$  (not adjusted  $F_y$  for composite action).
8. Check connections to ensure capacity is greater than demand.
9. Summarize results and note which, if any, elements failed and would require redesign.

Table 8. Interaction equation variables.

Symbol	Description
$P_{UF}$	Axial demand from FC model
$P_{UD}$	Axial demand from DC model
$P_{CL}$	Lower-bound compression capacity
$P_{CE}$	Expected compression capacity
$P_{TE}$	Expected tension capacity
$M_{UFx}$	Major moment demand from FC model (x-x axis)
$M_{UFy}$	Minor moment demand from FC model (y-y axis)
$M_{UDx}$	Major moment demand from DC model
$M_{UDy}$	Minor moment demand from DC model
$m_c$	Applicable beam-column m-factor
$m_b$	Applicable beam m-factor
$m_{br}$	Applicable brace m-factor
$M_{CLx}$	Lower-bound major moment capacity
$M_{CLy}$	Lower-bound minor moment capacity
$M_{CEx}$	Expected major moment capacity
$M_{CEy}$	Expected minor moment capacity

Table 9. Action classification.

Member	Axial	Moment	ASCE 41 Reference
Columns - $P_{UF}/P_{CL} < 0.2$	FC	DC	5.4.2.4.2
Columns - $0.2 \leq P_{UF}/P_{CL} \leq 0.5$	FC	DC	5.4.2.4.2
Columns - $P_{UF}/P_{CL} > 0.5$	FC	FC	5.4.2.4.2
Columns in Tension	DC	DC	5.4.2.4.2
Beams (axial <10% capacity)	NA	DC	5.4.2.4.2
Beams in Chevron Frames	FC*	FC*	5.5.2.4.2
Braces in Compression	DC	NA	5.5.2.4.1
Braces in Tension	DC	NA	5.5.2.4.1
Brace Connections	FC		5.5.2.4.1

\*Treated as pin-connected beams throughout this study

NA stands for not applicable

### 2.5.7 Acceptance Analysis

Analytical model results (see Section 2.5.5) were evaluated according to the procedure outlined in Section 2.5.6. This evaluation was completed primarily using a master Excel spreadsheet template designed to simplify the process of classifying members and applying acceptance criteria equations. This spreadsheet is shown in Appendix C for individual building configuration results. Acceptance criteria equations were included in the spreadsheet and sometimes manually applied based on section size if required. Equations were set up to be used for both primary and secondary members. Members were manually classified as primary or secondary based on whether or not they directly contributed to collapse resistance. Examples of primary members include braces, beams and columns part of braced frames, columns supporting primary elements, and moment frames.

Equations checked whether members were braces, FC beam-columns, DC beam-columns, or tension members. Applicable acceptance criteria equations were applied. The last two columns displayed whether a member met the acceptance criteria or not.

## 3 Analysis of the American Zinc Building

### 3.1 *Introduction*

This chapter presents the study of the American Zinc sister building, called Configuration 0, and new configurations made which were inspired by that first configuration. Section 3.2 starts by presenting results from an alternate path linear static analysis performed on Configuration 0. Next, the procedure followed to integrate stiff stories with lateral force resisting system is presented in Section 3.3. Alternate configurations were then created and studied in Section 3.4.

### 3.2 *Initial Configuration (Configuration 0)*

#### 3.2.1 Introduction

The sister building, created from the original design of the American Zinc building, was analyzed using the Linear Static Procedure (LSP) within the Alternate Path (AP) method outlined in the UFC 4-023-03 guidelines (DoD, 2009). This analysis was performed using the Finite Element Analysis (FEA) software SAP2000, and is presented in this section.

#### 3.2.2 Design Information

The four-story steel building has moment frames in the short direction (column lines A, G and M) and Vierendeel trusses in the long direction along column lines 1 and 3. Figures 30 - 32 show the layout of the building and the member sections.

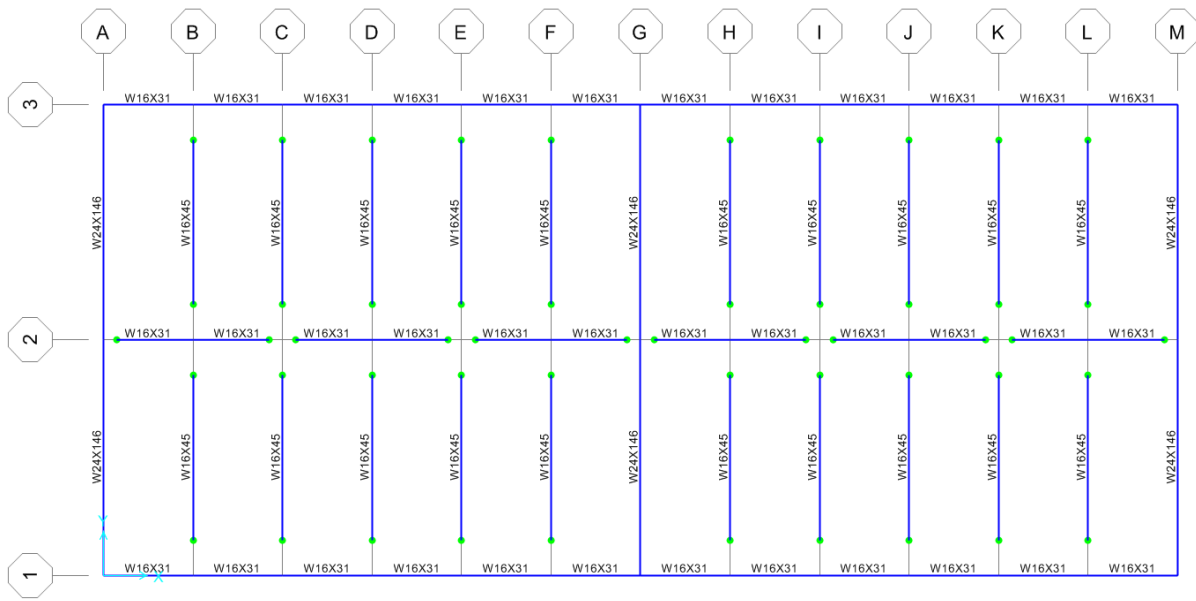


Figure 30. Sister building roof plan.

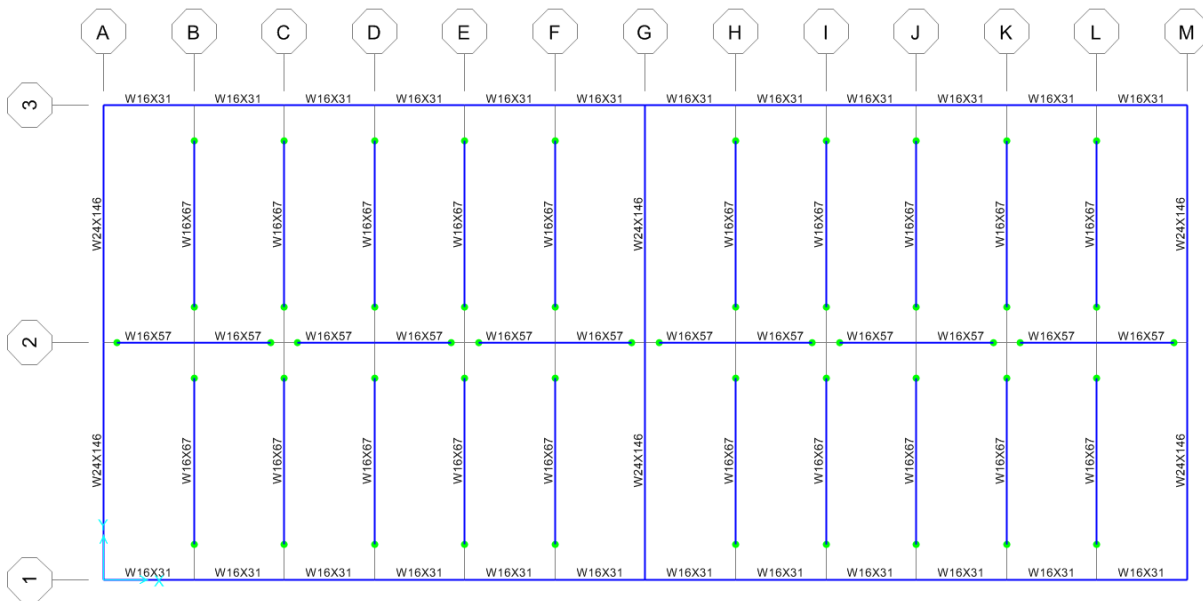


Figure 31. Sister building plan for floors 1 – 3.

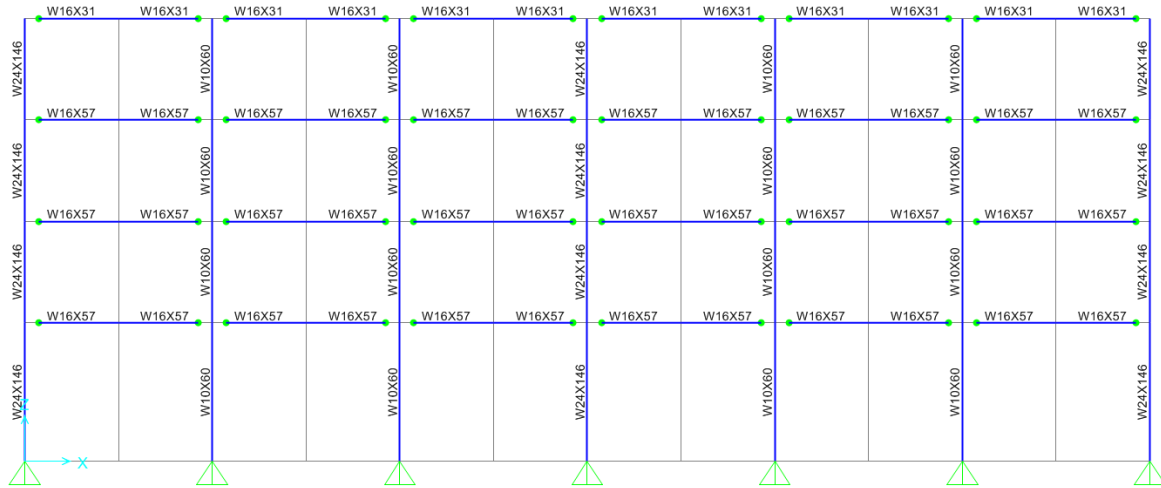


Figure 32. Sister building interior frame.

### 3.2.2.1 Analysis Model

The model contains sufficient amount of structural detail to allow proper transfer of vertical loads from the floor and roof to the primary elements and components, in accordance with ASCE 41, chapters 5 – 8 (ASCE, 2007). Section 3-2.11.2.2 of the UFC 4-023-03 states that secondary elements need not be included as their actions and deformations can be estimated based on a model that only includes primary elements. The model may be reanalyzed with the secondary components included, but their stiffness and resistance must be set to zero. This would allow the analyst to more easily check the secondary elements' deformation instead of performing hand calculations of the original model. Secondary elements were directly modeled in the American Zinc building analysis.

A number of assumptions were made when creating the model; these are numbered below:

1. Members are represented by centerline elements (i.e. zero end offset to account for joint flexibility)
2. All moment connections are improved welded unreinforced flange (WUF) with bolted web
3. Gravity framing connections are simple shear tabs modeled as pinned connections
4. Column to foundation connections are considered pinned
5. Each floor was assumed to behave as a rigid diaphragm
6. Gravity beams were designed as non-composite sections
7. All steel shapes are ASTM A992
8. Floor and roof system consists of a 3" composite steel deck with a 4 ½" concrete topping (total slab thickness = 7 ½")



The American Zinc Building does not have any of the irregularities listed, and therefore, does not need to satisfy the requirements of this section.

### 3.2.3.2 Load Cases for Deformation-Controlled and Force-Controlled Actions

As explained in Section 2.5.4, the load combinations applied during the column removal analysis depend on the  $\Omega_{LD}$  and the  $\Omega_{LF}$  factors. The  $\Omega_{LF}$  factor is used for the force controlled model and has a constant value of 2.0. The  $\Omega_{LD}$  factor depends on the m-factors of the members in the zone adjacent to the removed column. These m-factors were calculated for each of the beams and girders in the building and are summarized in Table 11. m-factors were also calculated for the two connections used in the building: WUF with bolted web and simple shear tabs.

Table 12 shows the equations used for calculating these m-factors, for primary and secondary members, where d is the depth of the beam in inches and  $d_{bg}$  is the depth of bolt group in inches.

Table 11. Beam and girder m-factors (from ASCE 41 Table 5-3 for life safety (LS)).

Beam	Primary or Secondary	Beam Girder m Factor (ASCE 41)
W16X67 (filler beam)	Secondary	10
W16X45 (filler beams)	Secondary	10
W16X31 (Vierendeel truss)	Primary	6
W16X57 (girder)	Secondary	10
W16X31 (girder)	Secondary	10
W24X146 (moment frame)	Primary	6

Table 12. m-factor equations per connection type (UFC 4-023-03 Table 5-1).

Fully Restrained Moment Connections	Primary
Improved WUF with Bolted Web	$2.3 - 0.021d$
Partially Restrained Simple Connections	Secondary
Simple Shear Tab	$8.7 - 0.161d_{bg}$

Table 13 shows the m-factors for all members and connections, for each of the stories affected during each of the four column removal cases. Table 14 summarizes the controlling m-factors for each column removal case, for deformation-controlled and force-controlled actions and the corresponding  $\Omega_{LD}$  and  $\Omega_{LF}$ .

Table 13. Component m-factors for deformation-controlled actions.

Removed Column	Level	Beam/Girder	Primary or secondary	d or d <sub>bg</sub> (in)	Beam/Girder m-factor	Simple Connection m-factor	Fixed Connection m-factor
1 (G-3)	2, 3, 4, roof	W24X146	Primary	d = 24.7"	6	--	1.78
	2, 3, 4, roof	W16X67	Secondary	d <sub>bg</sub> = 6"	10	7.73	--
		W16X45	Secondary	d <sub>bg</sub> = 6"	10	7.73	--
	2, 3, 4, roof	W16X31	Primary	d = 15.9"	6	--	1.97
	2, 3, 4, roof	W16X57	Secondary	d <sub>bg</sub> = 6"	10	7.73	--
		W16X31	Secondary	d <sub>bg</sub> = 6"	10	7.73	--
2 (A-3)	2,3,4, roof	W24X146	Primary	d = 24.7"	6	--	1.78
	2,3,4, roof	W16X67	Secondary	d <sub>bg</sub> = 6"	10	7.73	--
		W16X45	Secondary	d <sub>bg</sub> = 6"	10	7.73	--
	2,3,4, roof	W16X31	Primary	d = 15.9"	6	--	1.97
	2,3,4, roof	W16X57	Secondary	d <sub>bg</sub> = 6"	10	7.73	--
		W16X31	Secondary	d <sub>bg</sub> = 6"	10	7.73	--
3 (M-2)	2,3,4, roof	W24X146	Primary	d = 24.7"	6	--	1.78
	2,3,4, roof	W16X67	Secondary	d <sub>bg</sub> = 6"	10	7.73	--
		W16X45	Secondary	d <sub>bg</sub> = 6"	10	7.73	--
	2,3,4, roof	W16X31	Primary	d = 15.9"	6	--	1.97
	2,3,4, roof	W16X57	Secondary	d <sub>bg</sub> = 6"	10	7.73	--
		W16X31	Secondary	d <sub>bg</sub> = 6"	10	7.73	--
4 (C-1)	2,3,4, roof	W24X146	Primary	d = 24.7"	6	--	1.78
	2,3,4, roof	W16X31	Primary	d = 15.9"	6	--	1.97
	2,3,4, roof	W16X67	Secondary	d <sub>bg</sub> = 6"	10	7.73	--
		W16X45	Secondary	d <sub>bg</sub> = 6"	10	7.73	--
	2,3,4, roof	W16X57	Secondary	d <sub>bg</sub> = 6"	10	7.73	--

Table 14. Load increase factors.

Removed Column	Lowest m-factor	$\Omega_{LD} = 0.9m_{LIF} + 1.1$	$\Omega_{LF}$ , LIF for Force Controlled Actions
1	1.78	2.70	2
2	1.78	2.70	2
3	1.78	2.70	2
4	1.78	2.70	2

### 3.2.3.3 Column Removal Loads

Once the load increase factors were found for each column removal analysis, the load combinations were applied to the building. For all column removal cases, the load combinations became:

1. For area immediately adjacent to column removed, in deformation-controlled load case:

$$G_{LD} = \Omega_{LD} [1.2 D + (0.5 L \text{ or } 0.2 S)] = 2.70 [1.2 D + (0.5 L \text{ or } 0.2 S)]$$

$$= 3.24 D + (1.35 L \text{ or } 0.54 S)$$

$$G_{LD, 1-3} = 3.24(61) + 1.35(100) = 332.6 \text{ psf}$$

$$G_{LD, \text{roof}} = 3.24(61) + 0.54(20) = 208.4 \text{ psf}$$

2. For area immediately adjacent to column removed, in force-controlled load case:

$$G_{LF} = \Omega_{LF} [1.2 D + (0.5 L \text{ or } 0.2 S)] = 2.0 [1.2 D + (0.5 L \text{ or } 0.2 S)]$$

$$= 2.4 D + (1.0 L \text{ or } 0.4 S)$$

$$G_{LF, 1-3} = 2.4 (61) + 1.0(100) = 246.4 \text{ psf}$$

$$G_{LF, \text{roof}} = 2.4 (61) + 0.4 (20) = 154.4 \text{ psf}$$

3. For the area away from the column removed, for deformation and force-controlled load cases:

$$G = 1.2 D + (0.5 L \text{ or } 0.2 S)$$

$$G_{1-3} = 1.2(61) + 0.5(100) = 123.2 \text{ psf}$$

$$G_{\text{roof}} = 1.2(61) + 0.2(20) = 77.2 \text{ psf}$$

A summary of the resulting loads on the building, for each column removal case, is presented in Table 15. Appendix D shows the load assigned to each member, for each column removal case.

Table 15. Gravity loads.

Column Removed	$G_{LD}$ (psf)		$G_{LF}$ (psf)		G (psf)	
	Levels 2-4	roof	Levels 2-4	roof	Levels 2-4	roof
Col 1	332.6	208.4	246.4	154.4	123.2	77.2
Col 2	332.6	208.4	246.4	154.4	123.2	77.2
Col 3	332.6	208.4	246.4	154.4	123.2	77.2
Col 4	332.6	208.4	246.4	154.4	123.2	77.2

### 3.2.4 Results

After running the analysis, deformation controlled and force controlled actions are checked for all members as outlined in Section 2.5. Figure 34 shows the building deformation under the first

column removal case. Figure 35 shows DCR (per AISC Specifications Eq. H1-1) for column removal case 1. As it is expected, members experiencing the greatest stresses are the ones immediately adjacent to the removed column. The procedure explained in Section 2.5 was followed and is applied to the American Zinc sister building in the following sections.

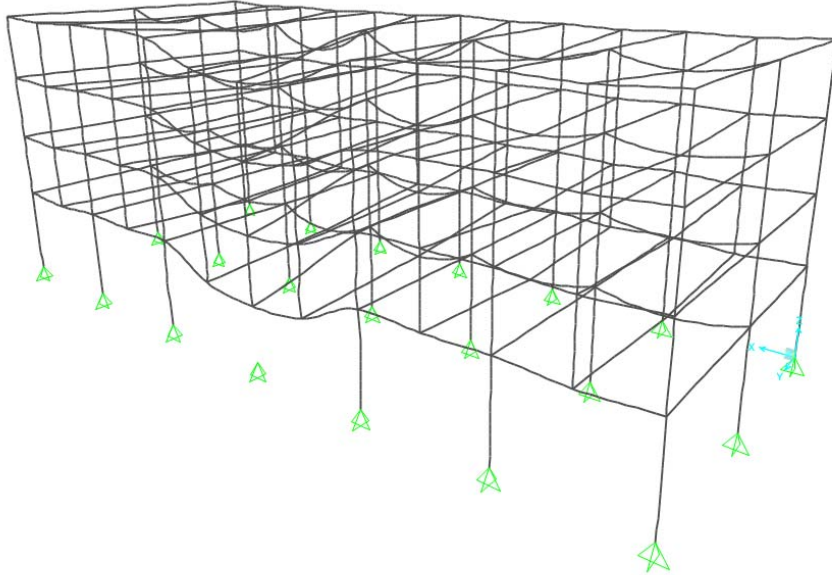


Figure 34. Frame deflection due to column 1 removal.

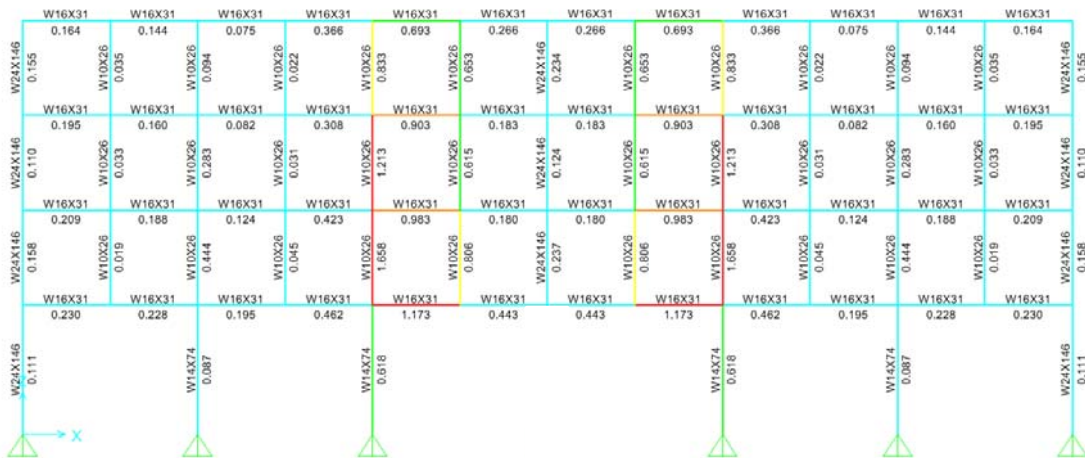


Figure 35. DCRs due to column 1 removal.

### 3.2.4.1 Columns Axial and Flexure

Beam-column members are checked for compliance using equations shown in Section 2.5, replicated in Table 16 below. m-factors for beams, girders and connections are shown in Table

13. In the case of columns, the m-factor depends on the slenderness of the cross section and on the ratio of axial load from the force-controlled model,  $P_{UF}$ , to the lower-bound compressive strength,  $P_{CL}$ . Table 16 shows the three ranges of axial load ratio ( $P_{UF}/P_{CL}$ ) on which the m-factors depend. This table also shows the acceptance criteria equations defined in the ASCE 41 (ASCE, 2006).

Table 16. Interaction equations for beam-columns.

Axial Load Ratio	Model	Equation
$\frac{P_{UF}}{P_{CL}} < 0.2$	Deformation-Controlled	$\frac{P_{UF}}{2P_{CL}} + \frac{M_{UDx}}{\phi m_c M_{CEx}} + \frac{M_{UDy}}{\phi m_c M_{CEy}} \leq 1.0$
$0.2 \leq \frac{P_{UF}}{P_{CL}} \leq 0.5$	Deformation-Controlled	$\frac{P_{UF}}{P_{CL}} + \frac{8}{9} \left[ \frac{M_{UDx}}{\phi m_c M_{CEx}} + \frac{M_{UDy}}{\phi m_c M_{CEy}} \right] \leq 1.0$
$\frac{P_{UF}}{P_{CL}} > 0.5$	Force-Controlled	$\frac{P_{UF}}{P_{CL}} + \frac{M_{UFx}}{\phi M_{CLx}} + \frac{M_{UFy}}{\phi M_{CLy}} \leq 1.0$

In case of  $P_{UF}/P_{CL} \leq 0.5$  (cases 1 or 2 in Table 16), the Life Safety values given in Table 5-5 of the ASCE 41 (ASCE, 2007) document are used to find the beam/girder m-factor. For case 1,  $P_{UF}/P_{CL} < 0.2$ , the m-factor is between 1.25 and 6, depending on the slenderness of the cross section. The m-factor for case 2 ( $0.2 \leq P_{UF}/P_{CL} \leq 0.5$ ) also depends on the slenderness of the cross section and varies between 1.25 and the value given by Equation 8.

$$m = 9 \left( 1 - \frac{5}{3} \frac{P}{P_{CL}} \right) \quad \text{Equation 8}$$

For higher  $P_{UF}/P_{CL}$  ratios (i.e.,  $P_{UF}/P_{CL} > 0.5$ ), the column becomes force-controlled and its DCR is checked against 1.0. Table 17 shows a summary of the m-factors that apply to the beam-columns used in the American Zinc building. Note that for beams (horizontal members), the connection m-factor controls. This m-factor is also shown in Table 17.

Table 17. m-factor in deformation-controlled columns.

Column Section	$\frac{b_f}{2t_f}$	$\frac{h}{t_w}$	m-factor		m-factor (connection)
			$P_{UF}/P_{CL} < 0.2$	$0.2 \leq P_{UF}/P_{CL} \leq 0.5$	
W14X74	6.41	25.4	6	$9 \left( 1 - \frac{5 P}{3 P_{CL}} \right)$	-
W24X146	5.92	33.2	6	$9 \left( 1 - \frac{5 P}{3 P_{CL}} \right)$	1.78
W10X26	6.52	34.0	6	$9 \left( 1 - \frac{5 P}{3 P_{CL}} \right)$	-
W16X31	6.28	51.6	3.5	~1.25 (or interpolate)	1.97
W10X60 (secondary)	7.41	18.7	4.92	Interpolate	See secondary connections

The  $P_{UF}/P_{CL}$  ratio of columns was first checked using the force-controlled model. Columns with a ratio greater than 0.5 were identified and checked using the force-controlled model. Other columns were checked using the deformation-controlled model.

#### *Force-Controlled Columns*

Columns with a  $P_{UF}/P_{CL}$  ratio greater than 0.5 are identified in Table 18, along with the axial and bending demands and capacities, and the demand capacity ratio (DCR). The highlighted members, 166, 179, 160, 114 and 115, do not pass and would need to be re-designed. A discussion of these failed elements is presented in Section 3.2.4.5.

Table 18. Force-controlled elements.

Frame	Section	P <sub>UF</sub> (kip)	M <sub>rx</sub> (kip- in)	M <sub>ry</sub> (kip- in)	P <sub>CL</sub> (kip)	M <sub>CLx</sub> (kip-in)	M <sub>CLy</sub> (kip- in)	DCR
Column Removal 1								
166	W10X26	-171.5	506.9	-0.6	172.2	1408.5	337.5	1.36
167	W10X26	-105.0	-540.4	-0.5	172.2	1408.5	337.5	1.00
179	W10X26	-171.5	-506.9	-0.6	172.2	1408.5	337.5	1.36
180	W10X26	-105.0	540.4	-0.5	172.2	1408.5	337.5	1.00
241	W10X60	-302.8	56.6	-5.7	552.9	3357.0	1575.0	0.57
243	W10X60	-302.8	-56.6	-5.7	552.9	3357.0	1575.0	0.57
Column Removal 2								
160	W10X26	-160.2	-406.1	-0.8	172.2	1408.5	337.5	1.22
161	W10X26	-98.0	429.9	-0.8	172.2	1408.5	337.5	0.88
239	W10X60	-302.8	64.7	7.8	552.9	3357	1575	0.57
Column Removal 3								
126	W10X26	-91.9	122.4	-0.3	172.2	1408.5	337.5	0.62
132	W10X26	-155.6	85.7	0.4	172.2	1408.5	337.5	0.97
133	W10X26	-94.9	-80.8	-0.4	172.2	1408.5	337.5	0.61
179	W10X26	-91.9	122.4	-0.3	172.2	1408.5	337.5	0.62
185	W10X26	-155.6	85.7	-0.4	172.2	1408.5	337.5	0.97
186	W10X26	-94.9	-80.8	-0.4	172.2	1408.5	337.5	0.61
240	W10X60	-454.4	-66.4	3.7	552.9	3357.0	1575.0	0.84
264	W10X60	-329.1	-66.5	3.7	652.8	3357.0	1575.0	0.53
Column Removal 4								
114	W10X26	-223.2	-953.6	0.3	172.2	1408.5	337.5	1.97
115	W10X26	-137.1	1047.6	0.3	172.2	1408.5	337.5	1.54
239	W10X60	-363.5	98.9	-3.7	552.9	3357.0	1575.0	0.69
241	W10X60	-302.8	100.1	3.3	552.9	3357.0	1575.0	0.58

### *Deformation-Controlled Columns*

All beam-columns, including the beams in the moment frames and the Vierendeel trusses, were checked using the interaction equations shown in Table 16. The m-factors for the deformation-controlled columns (beam-columns) are shown in Table 17. These m-factors depend on the slenderness ratio of the cross section and on the ratio of axial load to axial load capacity. Table 19 shows one example of a member check as performed in a spreadsheet. All deformation-controlled elements satisfied their acceptance criteria.

Table 19. Demand on a deformation-controlled beam-column due to column removal 1.

Frame	Section	P <sub>UF</sub> (kip)	P <sub>CL</sub> (kip)	m	M <sub>rx</sub> (kip-in)	M <sub>ry</sub> (kip-in)	M <sub>CLx</sub> (kip-in)	M <sub>CLy</sub> (kip-in)	DCR
132	W10X26	-82.7	176.8	1.8	-35.9	-0.6	1549	371	0.49

### 3.2.4.2 Beam Flexure

Beam in the moment frames and the Vierendeel trusses were treated as beam-columns and checked in the previous section. This section covers beam that were subject only to flexure (i.e., gravity beams). These were checked against the acceptance criteria for secondary members. The acceptance criteria, given in Table 5-5 of the ASCE 41 (ASCE, 2006) and shown in Table 20, depends on the slenderness ratio of the cross section.

Table 20. m-factor for flexure in secondary beams.

Slenderness Limits	m-factor
$\frac{b_f}{2t_f} \leq \frac{52}{\sqrt{F_{ye}}} = 7.01$ and $\frac{h}{t_w} \leq \frac{418}{\sqrt{F_{ye}}} = 56.4$	10
$\frac{b_f}{2t_f} \geq \frac{65}{\sqrt{F_{ye}}} = 8.76$ and $\frac{h}{t_w} \geq \frac{640}{\sqrt{F_{ye}}} = 86.3$	3

The m-factor for the four sections used for gravity framing is shown in Table 21. This table also shows the beam capacity, the maximum moment demand, the controlling case(s) and the DCR. The assigned m-factor is greater than the DCR for all gravity beams.

Table 21. Secondary beam flexure DCR check.

Section	$\frac{b_f}{2t_f}$	$\frac{h}{t_w}$	m-factor	$\Phi M_n$ (kip-in)	Max Mu (kip-in)	Controlling Case	Max $\frac{M_u}{\Phi M_n}$
W16x31	6.28	51.6	10	2680	3449	Col Rem 3	1.29
W16X45	6.45	41.1	10	4079	2262	Col Rem 1-4	0.55
W16x57	4.98	33.0	10	5201	5499	Col Rem 3	1.06
W16X67	7.70	35.9	7.2	6442	3607	Col Rem 1-4	0.56

Gravity beams were also checked including the secondary moments generated at the beam-column connections due to the partial restraint caused by the shear tab connections. These moments at the ends of gravity beams were calculated by multiplying the approximate stiffness

of the shear tabs,  $k_o$ , times the rotation undergone during the column removal cases. This is expressed in Equation 9.

$$M_{shear\ tab} = k_o \theta \quad \text{Equation 9}$$

The rotation,  $\theta$ , is found by dividing the relative displacement at the end of the filler beam by its length. This is normally called the chord rotation,  $k_o$ , and is estimated using Eq. 5-15 of ASCE 41 (ASCE, 2006), shown in Equation 10.

$$k_o = \frac{M_{CE}}{0.005} \quad \text{Equation 10}$$

$M_{CE}$  is the probable flexural demand caused by the shear tab and is found by multiplying the shear strength of the shear tab connection times the eccentricity,  $e$ , given in Table 10-9 of the AISC Manual (AISC, 2011).

The maximum moment at each of the beams,  $M_{UD}$ , can be calculated once the end moments are estimated. AISC Manual (AISC, 2011) Table 3-23 was used to analyze the beams with a span loading and end moments. Table 22 shows a summary of the calculations made for column removal case 3, including the beam section, load demand, relative end deflection ( $\Delta$ ), connection eccentricity ( $e$ ), shear tab moment ( $M_{CE}$ ), shear tab rotational stiffness ( $k_o$ ), end moments ( $M_1$  and  $M_2$ ), maximum moment demand ( $M_{UD}$ ), moment capacity of the section ( $M_{CE}$ ), demand capacity ratio (DCR) and the member m-factor. All DCRs are below the m-factors for all four column removal analyses; thus, all sections pass. It is interesting to compare Table 21, which does not consider the secondary moments from the shear tab restraint, with Table 22, which considers the secondary moments. Note that the difference is negligible since the restraint provided by the shear tabs is very small.

Table 22. Gravity beams flexure check (column removal 3).

Story	Beam Section	$w_u$ (kip/ft) or $P_u$ (kip)	$\Delta$ (in)	$e$ (in)	MCE conn (kip- in)	$k_o$ (kip- in/rad)	$M_1$ (kip-in)	$M_2$ (kip-in)	$M_{UD}$ (kip-in)	$M_{CE}$ (kip- in)	DCR	m- factor
1, 2, 3	W16x67	3.38	1.32	1.5	57.5	11490	47.4	-47.4	3607.4	6442	0.56	7.2
Roof	W16x45	2.12	1.32	1.5	57.5	11490	47.4	-47.4	2260.7	4079	0.55	10
1, 2, 3	W16X57	90.2 ( $P_u$ )	2.47	1.5	57.5	11490	116.3	-116.3	5501.1	5201	1.06	10
Roof	W16X31	56.5 ( $P_u$ )	2.47	1.5	57.5	11490	116.3	-116.3	3447.1	2680	1.29	10

### 3.2.4.3 Shear in Beams and Columns

Shear is considered a force-controlled action and, therefore, was checked using the force-controlled model. According to the AISC Specifications (AISC, 2010), the capacity of a W shape is given by Equation 11.

$$V_n = 0.6F_y A_w C_v \quad \text{Equation 11}$$

Where  $F_y$  is the lower bound yield strength (50 ksi);  $A_w$  is the area of the web ( $dt_w$ ); and  $C_v$  is the web shear coefficient that accounts for web buckling. For sections with  $h/t_w \leq 2.24\sqrt{E/F_y} = 53.9$ ,  $C_v = 1.0$  and  $\phi = 1.0$ . All sections used had a slenderness ratio under the buckling limit, and thus, yielding controlled. Table 23 summarizes the shear strength for all sections used.

Table 23. Shear strength of sections in model.

Section	$h/t_w$	$\phi V_n$ (kips)
W10X26	34.0	80.3
W10X60 (secondary)	18.7	129
W14X74	25.4	192
W16x31 (primary and secondary)	51.6	131
W16X45 (secondary)	41.1	167
W16x57 (secondary)	33.0	212
W16X67 (secondary)	35.9	193
W24X146	33.2	482

Shear in the columns is checked by verifying that the capacity is greater than the demand for all column removal cases. This was the case for all columns. For beams, the additional shear demand arising from the partial restraint provided by the shear tabs was considered. The process

followed to calculate the additional shear is similar to the explanation in the previous section, where the approximate moment from the shear connections is first found, then the shear corresponding to that moment is calculated. Table 24 shows the results for column removal 3. All DCRs are well below the limit of 1.0 for all four column removal analyses.

Table 24. Gravity beams shear check (column removal 3).

Story	Beam Section	$w_u$ (kip/ft) or $P_u$ (kip)	$\Delta$ (in)	MCE conn. (kip-in)	$k_o$ (kip-in/rad)	$M_1$ (kip-in)	$M_2$ (kip-in)	$V_{uF}$ (kip)	$V_{CL}$ (kip)	DCR
1, 2, 3	W16x67	2.51	1.32	57.5	11490	47.4	-47.4	33.7	193	0.17
Roof	W16x45	1.57	1.32	57.5	11490	47.4	-47.4	21.2	167	0.13
1, 2, 3	W16X57	66.8 ( $P_u$ )	2.47	57.5	11490	116.3	-116.3	34.4	212	0.16
Roof	W16X31	41.9 ( $P_u$ )	2.47	57.5	11490	116.3	-116.3	21.9	131	0.17

#### 3.2.4.4 Connections

Welded unreinforced flange with bolted web (WUF-B) connections were used for all rigid connections. Complete joint penetration (CJP) welds between the beam's top and bottom flanges and the column flange transfer the beam's moment into the column. Flexure was already checked when checking beam elements in the section above. Shear in the connection is checked using the force-controlled model. A simple inspection of the shear demand reveals that shear was easily satisfied. The maximum shear demand on a beam is 34.4 kips (see Table 24). A shear tab with (3) 3/4" A325-N bolts (see Figure 36) would suffice for this demand.

Shear tabs were modeled as pure pins and therefore are considered secondary elements. Figure 36 shows a drawing of the shear tab connection used throughout the building. The design checks are shown in Table 25. According to the UFC 4-023-03 (DoD, 2009) document, both shear and flexure actions need to be verified against the capacity of these connections. As with the gravity beam checks, the shear and moment contributions from the partial restraint provided by the shear tab were calculated and included in the demand.

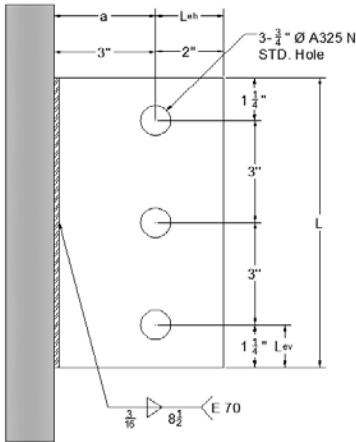


Figure 36. Shear tab connection.

Table 25. Shear connection design (3/4" A325-N bolts).

Story	Beam Section	T (in)	Vu,max (kips)[a]	No. Bolts	Bolt Spacing (in)[b]	tw (in)	tplate (in)	L (in)	Lev ≥ 1" (in)	a ≤ 3 1/2" (in)	Leh ≥ 2d" (in)	Shear Plate Capacity (kips)[c]
1 - 3	W16x67	13 1/4	33.3	3	3	0.395	1/4	8 1/2	1 1/4	3	1 1/2	38.3
Roof	W16x45	13 5/8	12.7	3	3	0.345	1/4	8 1/2	1 1/4	3	1 1/2	38.3
1 - 3	W16X57	13 5/8	34	3	3	0.43	1/4	8 1/2	1 1/4	3	1 1/2	38.3
Roof	W16X31	13 5/8	16	3	3	0.275	1/4	8 1/2	1 1/4	3	1 1/2	38.3

[a] : Vu max: under load case 1.2D+1.6L+0.5Lr+Notional load in SAP 2000

[b] : AISC J3.3

[c] : AISC Table 10-10a

The flexural demand was estimated from two components: (1) the shear reaction from the beam times the eccentricity of the shear tab, and (2) the moment generated by the relative displacement at the end of the gravity beam. These demands were calculated using the deformation-controlled model. The probable flexural demand caused by the shear tab is estimated by multiplying its shear strength times the eccentricity given in Table 10-9 of the AISC Manual (AISC, 2011). The DCR was then compared to the m-factors of these connections. Table 26 shows a summary of the results for the most critical column removal case (case 3). The m-factor is greater than the DCR for all cases.

Table 26. Shear tab flexure check (column removal 3).

Story	Beam Section	$w_u$ (kip/ft) or $P_u$ (kip)	$\Delta$ (in)	$M_{CE}$ conn. (kip-in)	$k_o$ (kip-in/rad)	$V_{uD}$ (kip)	$M_{DLoad}$ (kip-in)	$M_{DLoad}$ (kip-in)	$M_{DLoad}$ (kip-in)	DCR	m-factor
1, 2, 3	W16x67	3.38	1.32	57.5	11490	33.7	68.1	47.4	115.5	2.0	7.73
Roof	W16x45	2.12	1.32	57.5	11490	21.2	42.8	47.4	90.2	1.6	7.73
1, 2, 3	W16X57	90.2 ( $P_u$ )	2.47	57.5	11490	34.4	69.1	116.3	185.4	3.2	7.73
Roof	W16X31	56.5 ( $P_u$ )	2.47	57.5	11490	21.9	43.8	116.3	160.1	2.8	7.73

The shear capacity of the connection is checked against the demand, which is caused by the reaction of the load acting on the beam, plus the shear demand caused by the moment created by the relative displacements at the end of the gravity beam (Equation 12). Table 27 shows a summary of the check for column removal case 3. All connections satisfied the DCR limit of 1.0.

$$V_{disp} = \frac{2M_{Ddisp}}{L} \quad \text{Equation 12}$$

Table 27. Shear tab shear check (column removal 3).

Story	Beam Section	$w_u$ (kip/ft) or $P_u$ (kip)	$\Delta$ (in)	$k_o$ (kip-in/rad)	$V_{uDLoad}$ (kip)	$V_{uDisp}$ (kip)	$V_{uTot}$ (kip)	$\phi V_n$ (kip)	DCR
1, 2, 3	W16x67	3.38	1.32	11490	33.7	0.3	34	38.3	0.89
Roof	W16x45	2.12	1.32	11490	21.2	0.3	21.5	38.3	0.56
1, 2, 3	W16X57	90.2 ( $P_u$ )	2.47	11490	34.4	0.9	35.3	38.3	0.92
Roof	W16X31	56.5 ( $P_u$ )	2.47	11490	20.9	0.9	22.8	38.3	0.60

### 3.2.4.5 Redesign

Only the five members identified in Table 28 did not pass the check. The sections used for these members need to be increased, until the check is satisfied. All these unsatisfactory members were beam-columns checked with the force-controlled model ( $P_{UF}/P_{CL} > 0.5$ ). Figures 37 - 39 show the deflected shape of the controlling column removal cases (given in Table 28) and highlight the members not passing.

All the failed elements are Vierendeel truss columns adjacent to a missing column, which are carrying a portion of the load originally carried by the missing column. These results should be expected since the building was designed (and optimized) for typical gravity and lateral loads without consideration for possible missing columns. Table 29 shows the compressive capacity of the five failed members along with the compression load demand under the original design

(gravity and lateral loads) and under the AP analysis (column removal). Note that the demand under the AP analysis is as high as 52.5% higher for one of the cases. Another interesting point is that the first story columns did not fail. The reason is that the sections used for these columns had been significantly increased in order to satisfy inter-story drift limits.

Table 28. Members requiring redesign.

Frame No.	Section	Story	Location	Controlling Column Removal Case	DCR
166	W10X26	2	3E	COL 1	1.36
179	W10X26	2	3I	COL 1	1.36
160	W10X26	2	3C	COL 2	1.22
114	W10X26	2	1E	COL 4	1.97
115	W10X26	3	1E	COL 4	1.54

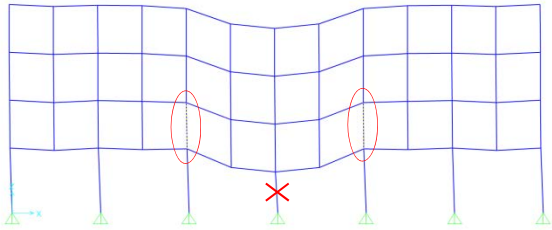


Figure 37. Column removal 1 deflected shape. Two unsatisfactory members identified.

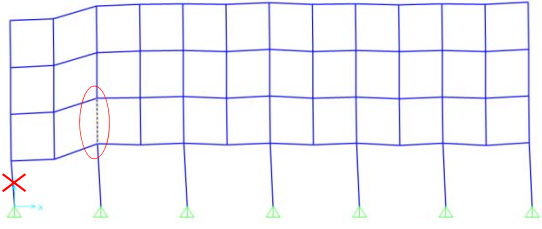


Figure 38. Column removal 2 deflected shape. Unsatisfactory member identified.

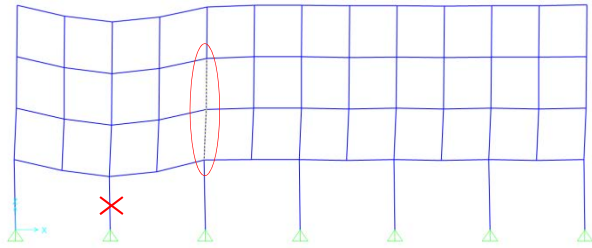


Figure 39. Column removal 4 deflected shape. Unsatisfactory member identified.

Table 29. Demand on members requiring redesign.

Frame No.	Controlling Column Removal Case	Section	$\phi P_n$	$P_u$ (design)	$P_u$ (AP analysis)	Compression Demand Increase
166	COL 1	W10X26	172.2 kip	152.1 kip	171.5 kip	12.7%
179	COL 1	W10X26	172.2 kip	152.1 kip	171.5 kip	12.7%
160	COL 2	W10X26	172.2 kip	155.2 kip	160.2 kip	3.2%
114	COL 4	W10X26	172.2 kip	152.1 kip	223.2 kip	46.7%
115	COL 4	W10X26	172.2 kip	89.9 kip	137.1 kip	52.5%

### 3.3 Integration of stiff-story with LFRSs

After the American Zinc sister building was analyzed for column removal, a subsequent study was made to integrate Lateral Force Resisting Systems (LFRS) with the stiff-story solutions designed to prevent disproportionate collapse in the event of a column-loss scenario. The process was as follows:

1. Convert the building to a more standard configuration by removing the Vierendeel truss system, but keeping some of the stiff-story concepts.
2. Calculate seismic loads using ASCE 7-10 based on the location of the original American Zinc building and apply them to the SAP2000 analytical model.
3. Modify the members as needed to satisfy seismic loading. This includes satisfying the ASCE 7-10 interstory drift limitations.
4. Consider different buildings with different LFRS locations and stiff-story configurations.
5. Remove individual columns for all the different configurations and compare them to determine the effectiveness of the LFRS and stiff-story combination.

### 3.3.1 Seismic Load Design

For each of the different LFRS and stiff story configurations the building was designed for earthquake loads. From the building's coordinates, 38°37'36.5" North and 90°11'51.7" East, and a Class C soil type, the values obtained for  $S_S$ ,  $S_1$ , and  $T_L$  from the USGS website were 0.432 %g, 0.166 %g, and 12 s, respectively (US Seismic Design Maps, 2014). Values for the adjusted site class effects,  $S_{MS}$  and  $S_{M1}$ , when combined are 0.5184 and 0.271. Two-thirds of those values were used to find the initial period,  $T_0$ , and the secondary period,  $T_S$ . Table 30 shows the values used in the design response spectrum shown in Figure 40.

Table 30. Period and design response spectrum values.

T (s)	$S_a$ (g)
0	0.14
0.11	0.35
0.52	0.35
1	0.18
2	0.09
3	0.06
4	0.05
12	0.04

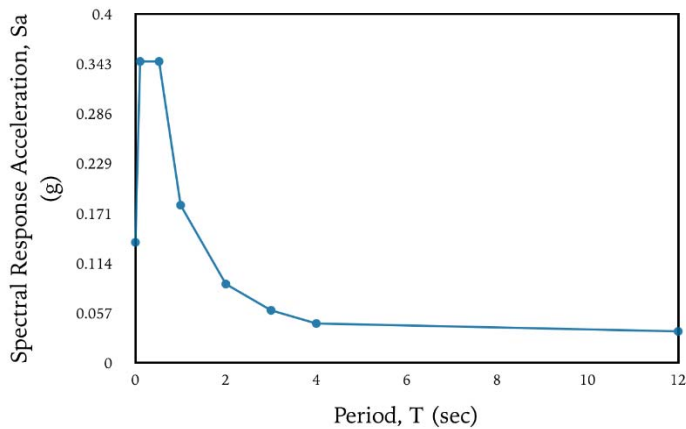


Figure 40. Design response spectrum.

American Zinc was classified as Seismic Design Category C and designed as an ordinary steel moment frame structure. Because no special seismic detailing was desired, an R factor equal to 3 was used.  $\Omega_0$  and  $C_d$  values were also equal to 3, while the importance factor,  $I_e$ , was 1.0. The

redundancy factor,  $\rho$ , for American Zinc is 1.0 due to its seismic design category. The fundamental period  $T_a$  was calculated to be 0.62 seconds. The length of the building is 122' by 53'4" wide, which was rounded up to 53.5' as a conservative value. The area of a floor is therefore about 6527 sq. ft. and multiplying that area by the dead load of 61 psf gives a weight per floor of approximately 398 kips. The total weight was assumed to be evenly distributed across the floors. The total building shear was calculated to be 154.9 kips. Table 31 shows a summary of the lateral seismic forces and shears for each floor.

Table 31. Lateral seismic forces and shears.

Story	Weight, $w_i$ (kip)	Height, $h_i$ (ft)	$w_i \times h_i^k$	$C_{vx}$	$F_x$ (kip)	$V_x$ (kip)
1	398	15	7020.0	0.11	17.6	154.9
2	398	26	12575.1	0.20	31.4	137.3
3	398	37	18277.1	0.30	45.7	105.9
4	398	48	24083.0	0.39	60.2	60.2
Total	1592	--	61955.2	1.00	154.9	--

### 3.3.2 Seismic Load Modeling

The calculated seismic story forces were then applied to the SAP2000 model. According to ASCE 7-10 section 12.8.4.2, accidental torsion provisions must be included. These loads were applied at a 5% offset from the center of mass of the structure (the geometric center due to symmetry) as specified by ASCE 7-10 12.8.4.2. Figure 41 shows the locations of loads  $EQX_n$ ,  $EQX_s$ ,  $EQY_e$ , and  $EQY_w$ .  $EQX_n$  and  $EQX_s$  are 2.67 ft. off centered from the center of mass and  $EQY_e$  and  $EQY_w$  are 6.1 ft. off centered from the center of mass. The steel design feature on SAP2000 was then used to redesign the structure for the added seismic loads.

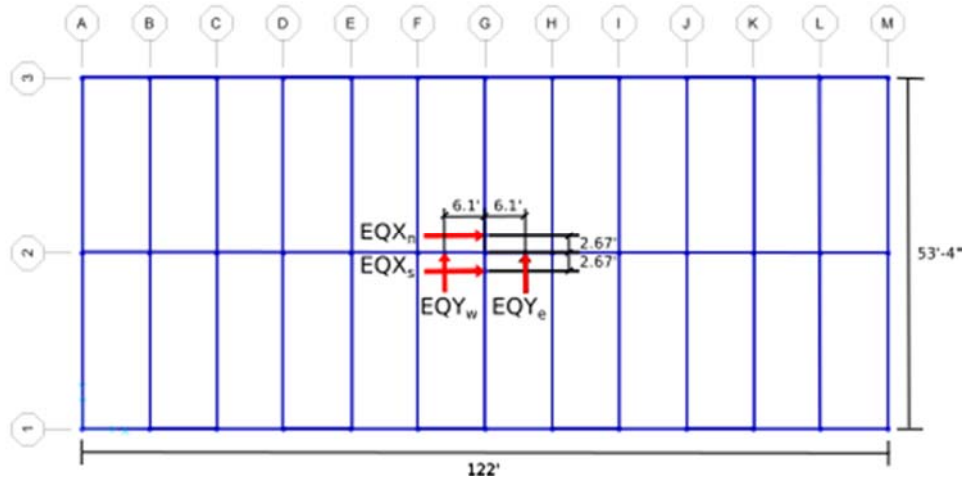


Figure 41: Plan view of seismic loads as applied in SAP2000.

### 3.3.3 Lateral Load Comparison

The building was designed for wind and earthquake loads, per ASCE 7-10 Chapter 2 load combinations. Table 32 shows a summary of the earthquake and wind story shears for the two main orthogonal directions (EW and NS). Note that earthquake story shears are higher for both directions.

Table 32. Earthquake and wind load comparison (story shears).

Story	Wind EW (kip)	Wind NS (kip)	Earthquake (kip)
1	65.6	153.2	154.9
2	46.3	109.1	137.3
3	28.6	68.7	105.9
4	9.8	25.9	60.2

### 3.3.4 Interstory drift

Once the American Zinc sister building was redesigned for seismic loads, interstory drift limitations, as specified in ASCE 7-10 Appendix B, were checked. The procedures outlined in ASCE 7-10 sections 12.8.6 and 12.12.1 were followed. A wind drift limit of  $h/400$  and an earthquake drift limit of  $0.025h$  were used, where  $h$  is the story height (ASCE 7-10 section 12.12.1). The earthquake story drift  $\delta_x$  was determined by using Equation 13.

$$\delta_x = \frac{C_d \delta_{xe}}{I_e}$$

Equation 13

Elastic deflections from the SAP2000 model were used to calculate drift, and members were resized until drift was satisfied. Wind interstory drift was also calculated for completeness, and a summary of the calculations can be found in Table 33 for configuration A0, which is the same American Zinc Configuration 0 but now designed with consideration for seismic effects.

Table 33. Summarized interstory drift values for A0.

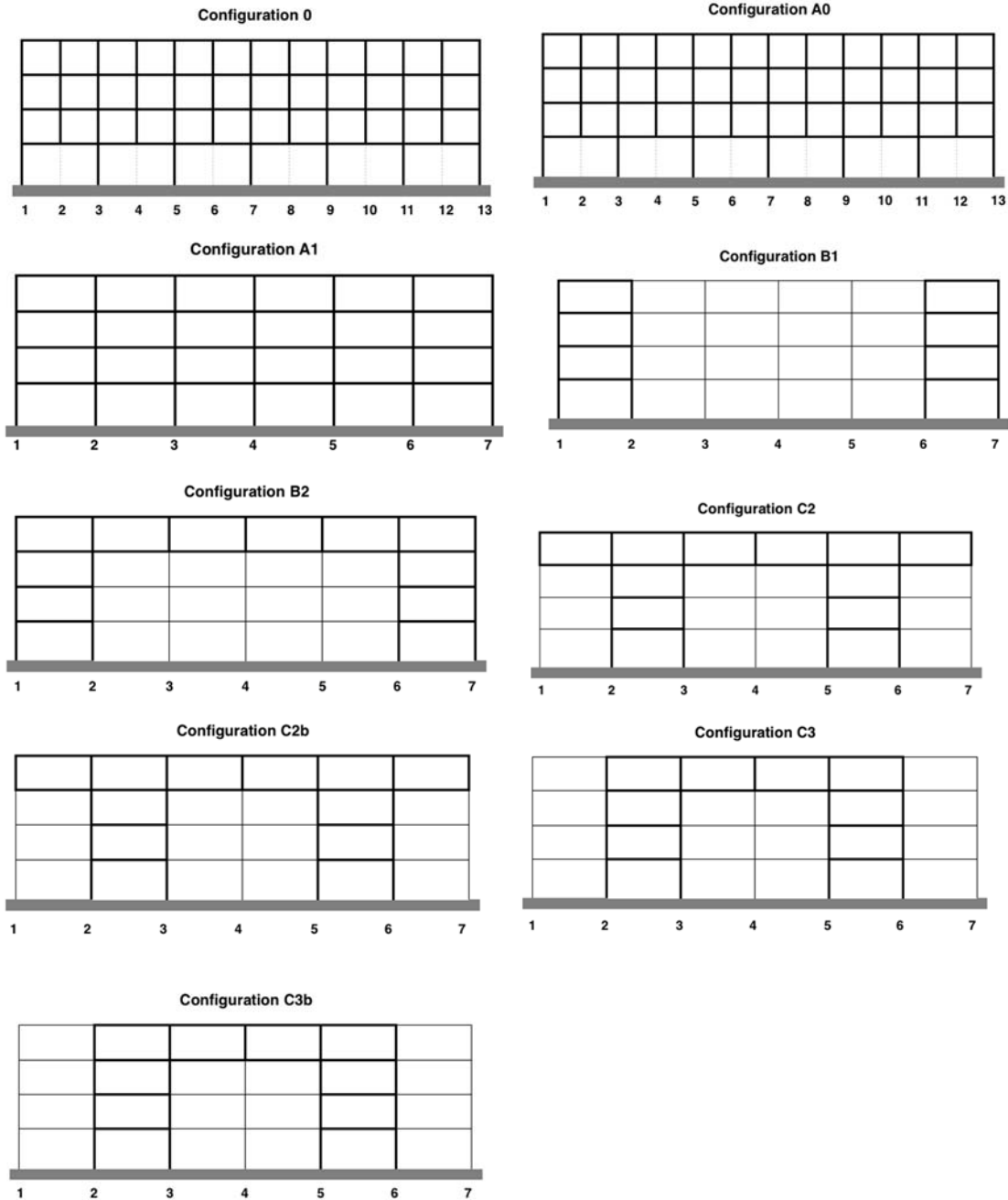
Story	Seismic $\bar{\delta}x$ NS (in)	Seismic $\bar{\delta}x$ EW (in)	Seismic $\bar{\delta}x$ Limit (in)	Wind $\bar{\delta}x$ NS (in)	Wind $\bar{\delta}x$ EW (in)	Wind $\bar{\delta}x$ Limit (in)
1	2.24	4.49	4.50	0.42	0.45	0.45
2	0.74	0.45	3.30	0.12	0.10	0.33
3	0.47	0.26	3.30	0.06	0.04	0.33
4	0.29	0.16	3.30	0.03	0.01	0.33

### 3.4 Alternative Structural Configurations

The next step of the design process was to integrate different stiff-story geometries with LFRSs in order to create several building configurations. The objective of this task was to learn from the behavior of these different building configurations, but also to compare them and determine if there are any clear trends as to what works best. Because different stiff-stories and LFRS configurations were used, each building configuration was checked for strength and serviceability.

Seven additional configurations were created. Each configuration is capable of resisting lateral forces, but some also provide additional redundancy for column loss scenarios. The EW side of the building for each configuration can be seen in Figure 42. Figure 43 shows the NS exterior frames. A thick, black line designates a moment frame. Most configurations have moment frames at 1, 4 and 7, with the exception of configuration C3b which only has moment frames at 1 and 7, and C2b which uses braced frames at 1 and 7 (see Figure 43). Configuration 0 represents the first version of the American Zinc model which does not include seismic loads (see Section 3.2). Configuration A0 has the same geometry as configuration 0, however its members were redesigned to consider seismic loads. Configuration A1 is the starting point for all of the configurations, it is similar to configuration A0 which has the Vierendeel truss on the exterior EW frames, but the vertical struts between main columns were removed to convert it to a more typical building. Note that the moment connections were kept for all beam-column connections in the exterior EW frames. Configurations B1, C1, and D1 all have moment frames at different locations in the exterior EW frames. For B1, the moment frames are located on the outside bays, for C1

on the next to outside bays (between column lines 2-3 and 5-6), and for D1 on the two central bays. Configurations B2, C2, and D2 all utilize a stiff-story element to limit the amount of vulnerable columns. Configuration C3 uses a partial stiff-story. Models C2 and C3 have secondary models (C2b and C3b) for column removal analysis. Figure 43 shows the NS elevation used for C2b. This model removed any moment frame in the NS direction that connected to an EW moment frame.



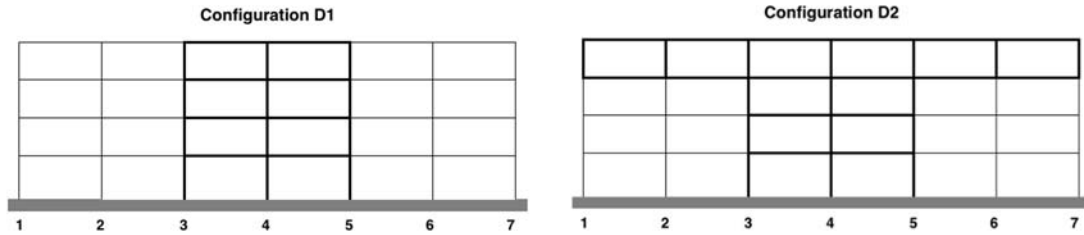


Figure 42. American Zinc configuration external EW Elevations

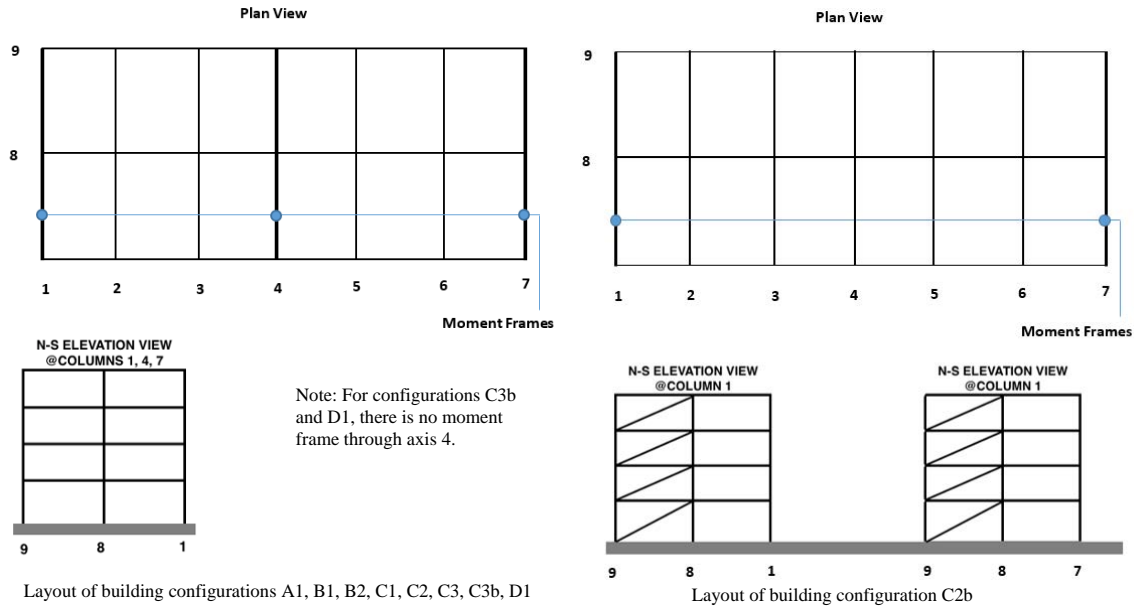


Figure 43. American Zinc building NS layouts.

### 3.4.1 American Zinc Column Removal Analysis

This section describes the column removal analysis procedure and results as they apply to the American Zinc building configurations. UFC guidelines require that at least one column near the middle of the structure on the long side, one column near the middle of the structure on the short side, and one corner column be removed. In the case of the American Zinc configurations, two additional columns between the corner and the middle column on the long side were also removed in order to better determine the effectiveness of the stiff-story solutions. Because of time limitations, only configurations C1, C2b, C3b and D1, shown in Figure 44, were analyzed.

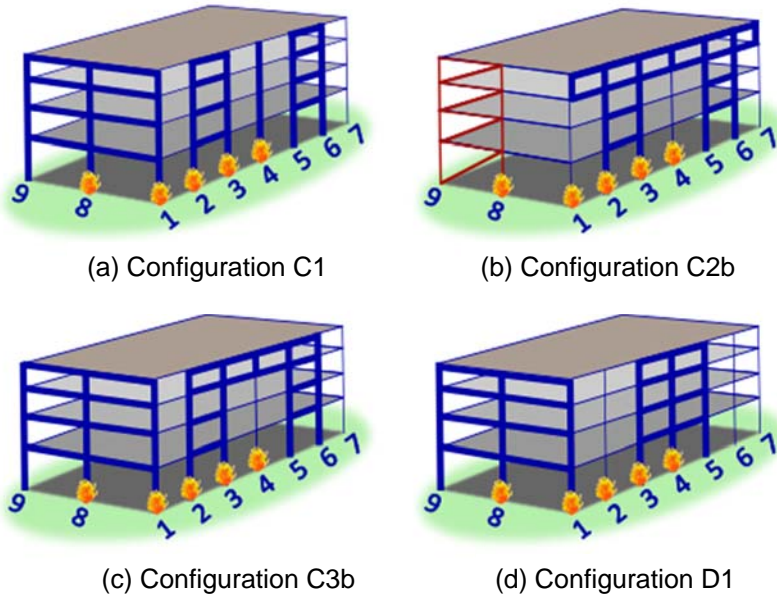


Figure 44. American Zinc column removal locations.

Flames at column bases indicate columns that were removed, individually, for the alternate path analysis (see Figure 44). Bold lines represent moment frames. Configuration C2b has a braced frame between columns 8 and 9. As seen in Figure 44, only exterior first-story columns were removed because the building was assumed to have controlled public access and is, therefore, excluded from the UFC interior column removal requirement. Figure 45 shows the immediate affected areas of removed columns applicable to all configurations. In order to show all removed columns and their respective affected zones in the same plan view, column removals 2, 4 and 5 were illustrated at a mirrored location (equivalent because the building is symmetrical). In the actual analysis, column removals 1-4 occurred along column line 1, and the removal of column 5 occurred at location A-2.

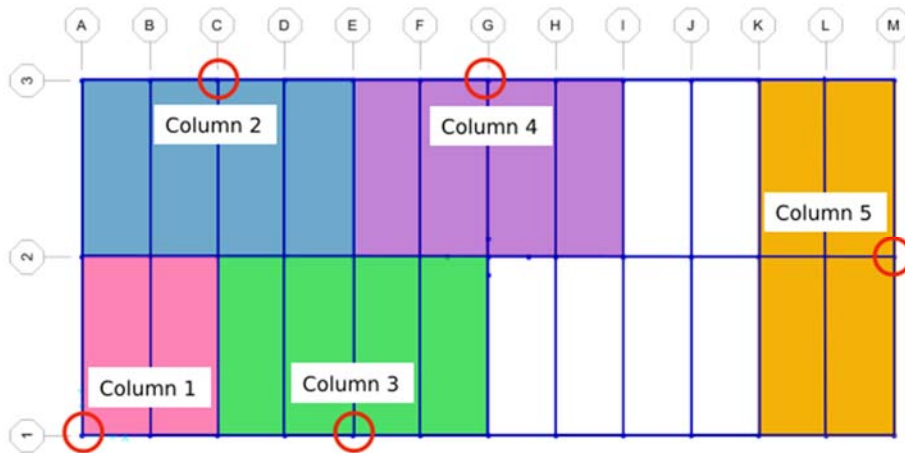


Figure 45. Removed column and affected areas.

### 3.4.2 Configuration C1

This section details the column removal procedure and its results as applicable to configuration C1. The geometry used for C1 was chosen because, although it does not have a stiff-story, every exterior column is part of a moment frame, theoretically reducing the likelihood of failure in the event of a column loss. Refer to Figure 44 and Figure 45 for moment frame configuration and column removal locations.

#### 3.4.2.1 M-factors

The m-factors for all beams, girders, and beam-to-column connections are shown in Table 34. All gravity connections in the structure were shear tab connections with  $d_{bg} = 6''$ . Rigid connections were treated as improved WUF with bolted web. Table 34 shows that the smallest m-factors for all column removal cases is 1.78.

Table 34. Configuration C1 m-factors for determining increased loads.

Removed Column	Level	Beam/Girder	Primary or secondary	d or d <sub>bg</sub> (in)	Beam/Girder m-factor	Simple Connection m-factor	Fixed Connection m-factor
1 (A-1)	2, 3, 4, roof	W24X146	Primary	d = 24.7"	6	--	1.78
	2, 3, 4, roof	W16X67	Secondary	d <sub>bg</sub> = 6"	10	7.73	--
		W16X45	Secondary	d <sub>bg</sub> = 6"	10	7.73	--
	2, 3, 4, roof	W16X31	Secondary	d <sub>bg</sub> = 6"	10	7.73	--
	2, 3, 4	W16X57	Secondary	d <sub>bg</sub> = 6"	10	7.73	--
2 (C-1)	2,3,4, roof	W24X146	Primary	d = 24.7"	6	--	1.78
	2,3,4, roof	W16X67	Secondary	d <sub>bg</sub> = 6"	10	7.73	--
		W16X45	Secondary	d <sub>bg</sub> = 6"	10	7.73	--
	2,3,4, roof	W16X31	Secondary	d <sub>bg</sub> = 6"	10	7.75	--
	2,3,4	W16X57	Secondary	d <sub>bg</sub> = 6"	10	7.73	--
3 (E-1)	2,3,4, roof	W24X146	Primary	d = 24.7"	6	--	1.78
	2,3,4, roof	W16X67	Secondary	d <sub>bg</sub> = 6"	10	7.73	--
		W16X45	Secondary	d <sub>bg</sub> = 6"	10	7.73	--
	2,3,4, roof	W16X31	Secondary	d <sub>bg</sub> = 6"	10	7.73	--
	2,3,4	W16X57	Secondary	d <sub>bg</sub> = 6"	10	7.73	--
4 (G-1)	2,3,4, roof	W24X146	Primary	d = 24.7"	6	--	1.78
	2,3,4, roof	W16X31	Secondary	d <sub>bg</sub> = 6"	10	7.73	--
	2,3,4, roof	W16X67	Secondary	d <sub>bg</sub> = 6"	10	7.73	--
		W16X45	Secondary	d <sub>bg</sub> = 6"	10	7.73	--
	2,3,4	W16X57	Secondary	d <sub>bg</sub> = 6"	10	7.73	--
5 (M-2)	2,3,4, roof	W24X146	Primary	d = 24.7"	6	--	1.78
	2,3,4, roof	W16X31	Secondary	d <sub>bg</sub> = 6"	10	7.73	--
	2,3,4, roof	W16X67	Secondary	d <sub>bg</sub> = 6"	10	7.73	--
		W16X45	Secondary	d <sub>bg</sub> = 6"	10	7.73	--
	2,3,4	W16X57	Secondary	d <sub>bg</sub> = 6"	10	7.73	--

\*Fixed connection

†Shear tab connection

### 3.4.2.2 Column Removal Loads

Load increase factors (LIF) for deformation controlled actions ( $\Omega_{LD}$ ) and force controlled actions ( $\Omega_{LF}$ ) are based on the lowest m-factor for each column removal. Table 35 summarizes the increase factors for each removal for this configuration.

Table 35. Configuration C1 load increase factors.

Removed Column	Lowest m-factor	$\Omega_{LD} = 0.9mLIF + 1.1$	$\Omega_{LF}$ , LIF for Force Controlled Actions
1	1.78	2.7	2
2	1.78	2.7	2
3	1.78	2.7	2
4	1.78	2.7	2
5	1.78	2.7	2

The determined load increase factors,  $\Omega_{LD}$  and  $\Omega_{LF}$  were then applied to the building for each column removal scenario. The load combinations applied are:

- a. For area immediately adjacent to removed column (deformation-controlled load case):

$$G_{LD,1-3} = 2.70[1.2(61 \text{ psf}) + 0.5(100 \text{ psf})] = 332.6 \text{ psf}$$

$$G_{LD,roof} = 2.70[1.2(61 \text{ psf}) + 0.2(20 \text{ psf})] = 208.4 \text{ psf}$$

- b. For area immediately adjacent to removed column (force-controlled load case):

$$G_{LF,1-3} = 2.00[1.2(61 \text{ psf}) + 0.5(100 \text{ psf})] = 246.4 \text{ psf}$$

$$G_{LF,roof} = 2.00[1.2(61 \text{ psf}) + 0.2(20 \text{ psf})] = 154.4 \text{ psf}$$

- c. For the area away from removed column (deformation and force-controlled load cases):

$$G_{1-3} = 1.2(61 \text{ psf}) + 0.5(100 \text{ psf}) = 123.2 \text{ psf}$$

$$G_{roof} = 1.2(61 \text{ psf}) + 0.2(20 \text{ psf}) = 77.2 \text{ psf}$$

### 3.4.2.3 Results

The procedures outlined in Section 2.5 were used for the rest of the evaluation of C1. See Appendix C for an example of the results spreadsheet used to determine whether the members conformed to the acceptance criteria. This spreadsheet was used for all column removal analyses. All members passed the acceptance criteria, suggesting that the loads were properly redistributed. It should be noted that each column removed was part of a moment frame. Therefore, the loads were carried through bending action to the columns part of the moment frame, and down to the foundations. Results from this configuration showed that although a stiff-story was not directly employed in this building, a strategic location of the moment frames was sufficient to eliminate disproportionate collapse due to column loss. In order to compare this configuration against the following models and to evaluate the stiff-story's effectiveness, members with a DCR value above 0.50 are identified and are shown in Table 36.

Table 36. Configuration C1 column removal results.

Column Removal 1				
Frame #	Section	Type	Controlling Load Type	DCR
239	W10x60	Column	FC axial compression	0.60
Column Removal 2				
Frame #	Section	Type	Controlling Load Type	DCR
239	W10x60	Column	FC axial compression	0.71
241	W10x60	Column	FC axial compression	0.60
Column Removal 3				
Frame #	Section	Type	Controlling Load Type	DCR
239	W10x60	Column	FC axial compression	0.60
241	W10x60	Column	FC axial compression	0.71
Column Removal 4				
Frame #	Section	Type	Controlling Load Type	DCR
241	W10x60	Column	FC axial compression	0.60
242	W24x146	Column	DC axial compression	0.61
243	W10x60	Column	FC axial compression	0.60
Column Removal 5				
Frame #	Section	Type	Controlling Load Type	DCR
239	W10x60	Column	FC axial compression	0.70

### 3.4.3 Configuration C2b

This section details the column removal procedure and the results for configuration C2b. C2b is a modification of configuration C1 and has a stiff-story extending across the EW direction of the building. Configuration C1 has three moment frames in the NS direction, but for C2b the moment frames were removed and instead two braced frames were used. Figure 44 and Figure 45 show column removal locations and the moment frame configuration.

#### 3.4.3.1 M-factors

The m-factors for all beams, girders, and beam-to-column connections are shown in Table 37. Gravity connections in the structure are shear tab connections with  $d_{bg} = 6''$  while rigid connections are improved WUF with bolted web. Table 37 shows that the smallest m-factor for all column removal cases is 1.78.

Table 37. Configuration C2b m-factors for determining increased loads.

Removed Column	Level	Beam/Girder	Primary or secondary	d or d <sub>bg</sub> (in)	Beam/Girder m-factor	Connection m-factor
1 (A-1)	4, roof	W24X146	Primary	d = 24.7"	6	1.78*
	2, 3, 4	W16X67	Secondary	d <sub>bg</sub> = 6"	10	7.73
	roof	W16X45	Secondary	d <sub>bg</sub> = 6"	10	7.73
	2, 3, roof	W16X31	Secondary	d <sub>bg</sub> = 6"	10	7.73
	2, 3, 4	W16X57	Secondary	d <sub>bg</sub> = 6"	10	7.73†
2 (C-1)	2,3,4, roof	W24X146	Primary	d = 24.7"	6	1.78*
	2,3,4	W16X67	Secondary	d <sub>bg</sub> = 6"	10	7.73†
	roof	W16X45	Secondary	d <sub>bg</sub> = 6"	10	7.73†
	2, 3, roof	W16X31	Secondary	d <sub>bg</sub> = 6"	10	7.73†
	2,3,4	W16X57	Secondary	d <sub>bg</sub> = 6"	10	7.73†
3 (E-1)	2,3,4, roof	W24X146	Primary	d = 24.7"	6	1.78*
	2,3,4	W16X67	Secondary	d <sub>bg</sub> = 6"	10	7.73†
	roof	W16X45	Secondary	d <sub>bg</sub> = 6"	10	7.73†
	2,3, roof	W16X31	Secondary	d = 15.9"	10	7.73†
	2,3,4	W16X57	Secondary	d <sub>bg</sub> = 6"	10	7.73†
4 (G-1)	4, roof	W24X146	Primary	d = 24.7"	6	1.78*
	2, 3, 4	W16X67	Secondary	d <sub>bg</sub> = 6"	10	7.73†
	roof	W16X45	Secondary	d <sub>bg</sub> = 6"	10	7.73†
	2, 3, roof	W16X31	Secondary	d <sub>bg</sub> = 6"	10	7.73†
	2, 3, 4	W16X57	Secondary	d <sub>bg</sub> = 6"	10	7.73†
5 (M-2)	4, roof	W24X146	Primary	d = 24.7"	6	1.78*
	2, 3, 4	W16X67	Secondary	d <sub>bg</sub> = 6"	10	7.73†
	roof	W16X45	Secondary	d <sub>bg</sub> = 6"	10	7.73†
	2, 3, roof	W16X31	Secondary	d <sub>bg</sub> = 6"	10	7.73†
	2, 3, 4	W16X57	Secondary	d <sub>bg</sub> = 6"	10	7.73†

\*Fixed connection

†Shear tab connection

### 3.4.3.2 Column Removal Loads

The loads remain the same as those applied in C1 for all column removal cases, as can be seen in Table 38.

Table 38. Configuration C2b load increase factors.

Removed Column	Lowest m-factor	$\Omega_{LD} = 0.9mLIF + 1.1$	$\Omega_{LF}$ , LIF for Force Controlled Actions
1	1.78	2.7	2
2	1.78	2.7	2
3	1.78	2.7	2
4	1.78	2.7	2
5	1.78	2.7	2

### 3.4.3.3 Results

The procedures outlined in Section 2.5 were used for the rest of the evaluation of C2b. See Appendix C for an example of the results spreadsheet used to determine whether the members conformed to the acceptance criteria. For illustration purposes, results for members with a DCR ratio above 0.5 are presented for each column removal in Table 39. Note that one member under column removal 5 did not pass the check.

Table 39. Configuration C2b column removal results.

Column Removal 1				
Frame #	Section	Type	Controlling Load Type	DCR
239	W10x60	Column	FC axial compression	0.65
241	W10x60	Column	FC axial compression	0.50
242	W10x60	Column	FC axial compression	0.50
Column Removal 2				
Frame #	Section	Type	Controlling Load Type	DCR
239	W10x60	Column	FC axial compression	0.71
241	W10x60	Column	FC axial compression	0.60
Column Removal 3				
Frame #	Section	Type	Controlling Load Type	DCR
140	W10x60	Column	FC axial compression	0.55
239	W10x60	Column	FC axial compression	0.60
241	W10x60	Column	FC axial compression	0.71
242	W10x60	Column	FC axial compression	0.59
Column Removal 4				
Frame #	Section	Type	Controlling Load Type	DCR
241	W10x60	Column	FC axial compression	0.59
242	W10x60	Column	FC axial compression	0.70
243	W10x60	Column	FC axial compression	0.59
Column Removal 5				
Frame #	Section	Type	Controlling Load Type	DCR
97	W10x60	Column	FC axial compression	0.71
98	W10x60	Column	DC	0.70
103	W24x146	Column	DC	0.57
239	W10x60	Column	FC axial compression	0.72
250	W10x60	Column	FC axial compression	1.10
251	W10x60	Column	FC axial compression	0.79
267	W10x60	Column	FC axial compression	0.55
293	W10x60	Column	FC axial compression	0.94
294	W10x60	Column	FC axial compression	0.80

While this configuration had one force-controlled secondary column fail and several members with DCRs higher than 0.50, these were mostly for column removal 5 which was part of the braced frame system and not part of the stiff-story. The removal of column 5 caused a rotation of the plan of the building as illustrated in Figure 46 (scale factor of 2). This column was removed for completeness but is not part of the moment frame stiff-story which is the main intention for studying this building.

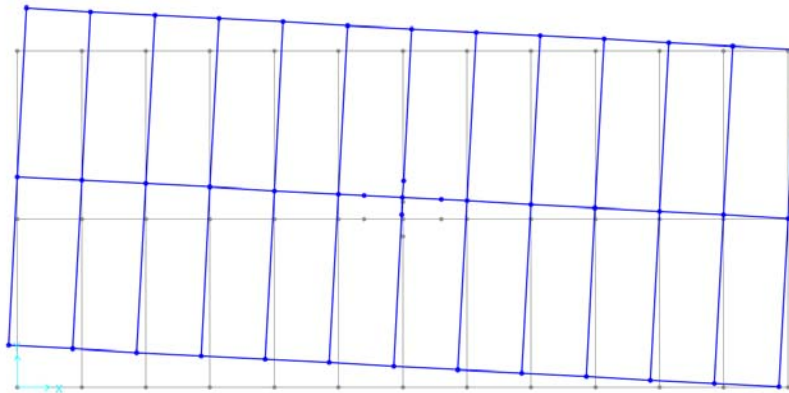


Figure 46. Configuration C2b removal 5 torsion (scale factor = 2).

### 3.4.4 Configuration C3b

This section details the column removal procedure and its results as it applicable to Configuration C3b. C3b is a modified version of configuration C2b. Its stiff-story does not extend across the entire length of the building, which allows the implementation of end moment frames in the NS direction. Because only two moment frames were used, the size of the beams and the columns were increased from W24X146 (used for C1) to W24X192 in order to satisfy drift in the NS direction. Moment frames and stiff-story elements were kept W24X146 in the EW direction of the building.

#### 3.4.4.1 M-factors

The m-factors for all beams, girders, and beam-to-column connections are shown in Table 40. As for previous configurations, gravity connections in the structure are shear tab connections with  $d_{bg} = 6''$ . Rigid connections are improved WUF with bolted web. Table 37 shows that the smallest m-factor for column removal cases 1, 2 and 5 is 1.76 and for column removal cases 3 and 4 is 1.78.

Table 40. Configuration C3b m-factors for determining increased loads.

Removed Column	Level	Beam/Girder	Primary or secondary	Beam/ Girder m-factor	Connection m-factor
1 (A-1)	2, 3, 4, roof	W24X192	Primary	6	1.76*
	2, 3, 4	W16X67	Secondary	10	7.73 <sup>†</sup>
	roof	W16X45	Secondary	10	7.73 <sup>†</sup>
	2, 3, roof	W16X31	Secondary	10	7.73 <sup>†</sup>
	2, 3, 4	W16X57	Secondary	10	7.73 <sup>†</sup>
2 (C-1)	2,3,4, roof	W24X146	Primary	6	1.78*
	2, 3, 4, roof	W24X192	Primary	6	1.76*
	2,3,4	W16X67	Secondary	10	7.73 <sup>†</sup>
	roof	W16X45	Secondary	10	7.73 <sup>†</sup>
	2, 3, roof	W16X31	Secondary	10	7.73 <sup>†</sup>
3 (E-1)	2,3,4, roof	W24X146	Primary	6	1.78*
	2,3,4	W16X67	Secondary	10	7.73 <sup>†</sup>
	roof	W16X45	Secondary	10	7.73 <sup>†</sup>
	2,3,4, roof	W16X31	Secondary	10	7.73 <sup>†</sup>
	2,3,4	W16X57	Secondary	10	7.73 <sup>†</sup>
4 (G-1)	4, roof	W24X146	Primary	6	1.78*
	2, 3, 4	W16X67	Secondary	10	7.73 <sup>†</sup>
	roof	W16X45	Secondary	10	7.73 <sup>†</sup>
	2, 3, roof	W16X31	Secondary	10	7.73 <sup>†</sup>
	2, 3, 4	W16X57	Secondary	10	7.73 <sup>†</sup>
5 (M-2)	2, 3, 4, roof	W24X192	Primary	6	1.76*
	2, 3, 4	W16X67	Secondary	10	7.73 <sup>†</sup>
	roof	W16X45	Secondary	10	7.73 <sup>†</sup>
	2, 3, 4, roof	W16X31	Secondary	10	7.73 <sup>†</sup>
	2, 3, 4	W16X57	Secondary	10	7.73 <sup>†</sup>

\*Fixed connection

<sup>†</sup>Shear tab connection

### 3.4.4.2 Column Removal Loads

As with previous configurations, connection m-factors controlled for all column removal cases. Because only two moment frames were used in this configuration, increased beam sizes (as compared to previous configurations) for the NS moment frames were required, resulting in different connection m-factors. For column removal cases 1, 2 and 5 the smallest m-factor was 1.76 while for column removal cases 3 and 4 the m-factor was 1.78. Because of the small difference, the  $\Omega_{LD}$  factor is only reduced from 2.7 to 2.68 for cases 1, 2 and 5. For the analysis this difference was neglected and an amplification factor of 2.7 was used for all cases, resulting in the same loads as those applied to Configuration C2b.

### 3.4.4.3 Results

As for previous configurations, the procedures outlined in Section 2.6 were used for the rest of the evaluation of C3b. Appendix C shows an example of the spreadsheet used to determine if

members conformed to the acceptance criteria. The DCR values above 0.50 for each column removal are summarized in Table 41. All members passed the acceptance criteria. Note that cases 1, 2 and 8 are essentially the same as for configuration C1. Thus, it was expected that these would not have failure. The stiff-story, employed especially in column removal 4, performed satisfactorily.

Table 41. Configuration C3b column removal results.

Column Removal 1				
Frame #	Section	Type	Controlling Load Type	DCR
239	W10x60	Column	FC axial compression	0.60
Column Removal 2				
Frame #	Section	Type	Controlling Load Type	DCR
239	W10x60	Column	FC axial compression	0.71
241	W10x60	Column	FC axial compression	0.60
Column Removal 3				
Frame #	Section	Type	Controlling Load Type	DCR
140	W10x60	Column	FC axial compression	0.56
239	W10x60	Column	FC axial compression	0.60
241	W10x60	Column	FC axial compression	0.70
242	W10x60	Column	FC axial compression	0.59
Column Removal 4				
Frame #	Section	Type	Controlling Load Type	DCR
241	W10x60	Column	FC axial compression	0.59
242	W10x60	Column	DC axial compression	0.70
243	W10x60	Column	FC axial compression	0.59
Column Removal 8				
Frame #	Section	Type	Controlling Load Type	DCR
239	W10x60	Column	FC axial compression	0.70

### 3.4.5 Configuration D1

This configuration has two moment frames side-by-side in the center of the EW direction of the building but does not employ a stiff-story. Its NS direction has end moment frames similar to those used in C3b.

### 3.4.5.1 M-factors

The m-factors for all beams, girders, and beam-to-column connections in Configuration D1 are shown in Table 42.

Table 42. Configuration D1 m-factors for determining increased loads.

Removed Column	Level	Beam/Girder	Primary or secondary	Beam/Girder m-factor	Connection m-factor
1 (A-1)	2, 3, 4, roof	W24X192	Primary	6	1.76*
	2, 3, 4	W16X67	Secondary	10	7.73†
	roof	W16X45	Secondary	10	7.73†
	2, 3, 4, roof	W16X31	Secondary	10	7.73†
	2, 3, 4	W16X57	Secondary	10	7.73†
2 (C-1)	2, 3, 4, roof	W24X192	Primary	6	1.76*
	2,3,4	W16X67	Secondary	10	7.73†
	roof	W16X45	Secondary	10	7.73†
	2, 3, 4, roof	W16X31	Secondary	10	7.73†
	2,3,4	W16X57	Secondary	10	7.73†
3 (E-1)	2,3,4, roof	W24X146	Primary	6	1.78*
	2,3,4	W16X67	Secondary	10	7.73†
	roof	W16X45	Secondary	10	7.73†
	2,3,4, roof	W16X31	Secondary	10	7.73†
	2,3,4	W16X57	Secondary	10	7.73†
4 (G-1)	2,3,4, roof	W24X146	Primary	6	1.78*
	2, 3, 4	W16X67	Secondary	10	7.73†
	roof	W16X45	Secondary	10	7.73†
	roof	W16X31	Secondary	10	7.73†
	2, 3, 4	W16X57	Secondary	10	7.73†
5 (M-2)	2, 3, 4, roof	W24X192	Primary	6	1.76*
	2, 3, 4	W16X67	Secondary	10	7.73†
	roof	W16X45	Secondary	10	7.73†
	2, 3, 4, roof	W16X31	Secondary	10	7.73†
	2, 3, 4	W16X57	Secondary	10	7.73†

\*Fixed connection

†Shear tab connection

### 3.4.5.2 Column Removal Loads

The loads remain the same as those applied in C3b for all column removal cases as shown in Table 43. As was the case with Configuration C3b, the  $\Omega_{LD}$  factor was rounded to 2.7 for all cases.

Table 43. Configuration D1 load increase factors.

Removed Column	Lowest m-factor	$\Omega_{LD} = 0.9m_{LIF} + 1.1$	$\Omega_{LF}$ , LIF for Force Controlled Actions
1	1.76	2.68	2
2	1.76	2.68	2
3	1.78	2.70	2
4	1.78	2.70	2
5	1.76	2.68	2

### 3.4.5.3 Results

The procedures outlined in Section 2.5 were used for the rest of the evaluation of D1. See Appendix C for an example of the results spreadsheet used to determine whether the members conformed to the acceptance criteria. Column removal 2 is not part of a moment frame, and, therefore, its removal would result in a collapse mechanism. One possible solution to eliminate the vulnerability arising from the collapse mechanism would be to add a stiff-story in the upper story between columns 2-3 and 5-6 (see Figure 44). Under the remaining column removals, all members passed the acceptance criteria. The DCR values above 0.50 for each column removal are summarized in Table 44.

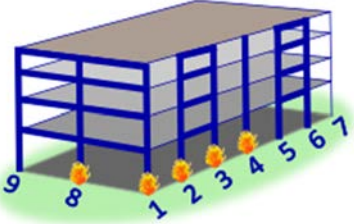
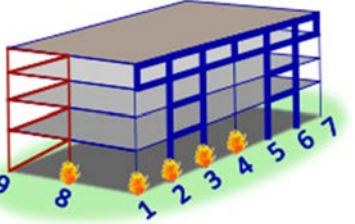
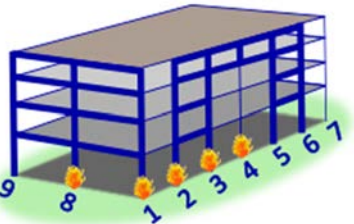
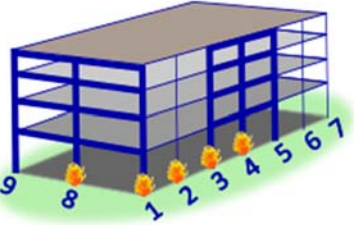
Table 44. Configuration D1b column removal results.

Column Removal 1				
Frame #	Section	Type	Controlling Load Type	DCR
239	W10x60	Column	FC axial compression	0.60
Column Removal 2				
<i>failure mechanism</i>				
Column Removal 3				
Frame #	Section	Type	Controlling Load Type	DCR
140	W10x60	Column	FC axial compression	0.60
239	W10x60	Column	FC axial compression	0.60
241	W10x60	Column	FC axial compression	0.71
242	W10x60	Column	FC axial compression	0.60
Column Removal 4				
Frame #	Section	Type	Controlling Load Type	DCR
241	W10x60	Column	FC axial compression	0.59
242	W10x60	Column	FC axial compression	0.70
243	W10x60	Column	FC axial compression	0.59
Column Removal 5				
Frame #	Section	Type	Controlling Load Type	DCR
239	W10x60	Column	FC axial compression	0.70

### 3.4.6 Summary and Concluding Remarks

Table 45 summarizes the results from all four buildings analyzed. Note that CM refers to the number of columns whose removal would result in a collapse mechanism. Only D1 has possible collapse mechanisms. All other configurations prevent collapse mechanisms by either using stiff-stories or by having all external columns form part of a moment frame (C1).

Table 45. American Zinc results summary.

 <p>C1    CM = 0    RE = 0</p>	 <p>C2b    CM = 0    RE = 1</p>	 <p>C3b    CM = 0    RE = 0</p>
 <p>D1    CM = 4    RE = 0</p>		
<p>CM = collapse mechanism RE = elements requiring redesign</p>		

A summary of both configurations (C and D) is presented next:

C series:

- The C series involved buildings with two moment frames for each external frame in the EW direction, between columns 2-3 and 5-6. C1 did not have a stiff-story element. C2b had a full stiff-story in the upper level and C3b had a partial stiff-story.
- The LFRS in the NS direction was different for all three systems:
  - o C1 had three MFs
  - o C2b had two braced frames; on the exterior frames
  - o C3b had two moment frames; on the exterior frames
- For C1, each column removed was part of a moment frame. Therefore, the loads were carried through bending action to the columns part of the moment frame, and down to the foundation.
- Although a stiff-story was not directly employed in C1, a strategic location of the moment frames was sufficient to eliminate column loss risk.
- C2b experienced no failure when removing a column part of the stiff-story.
- For C2b, column removal 5 caused a plan rotation which resulted in failure of one force controlled secondary column.
- For C3b, all members passed the acceptance criteria.

- Note that column removals 1, 2 and 5 for C3b are essentially the same as for configuration C1. Thus, it was expected that these would not have failure.

D series:

- D1 has 4 columns (2, 6 and the same columns on the opposite side of the building) which would result in a collapse mechanism if removed.
- For D1 all members for column removals 1, 3, 4 and 5 passed.
- While D1 has vulnerable columns, this could be mitigated by adding a stiff-story in the spans between columns 2-3 and 5-6.

In conclusion, the analysis of this building showed that stiff-stories have a beneficial effect in redistributing loads in column loss scenarios. This was evidenced in both configurations C2b and C3b. It is believed that because moment frames were oversized in order to limit interstory drifts, its capacity to carry additional loads from column loss was significant and no failure was observed for any of the stiff-story components. Future work should look at optimizing members in the stiff-story system. Plan torsion caused by the removal of column 5 for configuration C2b was not expected. This issue is further discussed in the next chapter.

## 4 Analysis of the Lamar Construction Building

### 4.1 Introduction

This chapter presents the study of the Lamar Construction sister building, called Configuration 0, and new configurations made which were inspired by that first configuration. Section 4.2 presents the results from an alternate path linear static analysis performed on Configuration 0. The procedure followed to integrate stiff stories with lateral force resisting system is then presented in Section 4.3. Alternate configurations were then created and studied in Section 4.4.

### 4.2 Initial Configuration (Configuration 0)

#### 4.2.1 Introduction

The Lamar Construction sister building was analyzed using the LSP within the AP method outlined in the UFC 4-023-03 guidelines (DoD, 2009). This analysis is presented in this chapter.

#### 4.2.2 Design Information

##### 4.2.2.1 Column Removal Locations

The four column removal locations selected are shown in Figure 47 along with the affected areas for each location. The columns were removed only from the first floor.



Figure 47. Columns removed.

#### 4.2.2.2 Load Cases for Deformation-Controlled and Force-Controlled Actions

The load combinations used in force-controlled and deformation-controlled models are explain in Section 2.5. These combinations depend on the m-factors of each of the beams, girders, spandrels and beam-column connections in the zone immediately adjacent to the removed column. Table 46 shows the m-factor for each beam section and its connection, for each column removal case.

Shear tabs and double angles are used throughout the building for all beam-column connections. These were modeled as pinned connections with no rotational restraint. One exception is at locations where diagonal braces join a beam-column connection. Those connections have a higher rotational stiffness and were modeled as partially restrained connections. Thus, these were treated as primary members and its stiffness was modeled using rotational springs.

The stiffness used for the rotational spring was obtained from Equation 10, resulting in a rotational stiffness of 11,490 kip-in/rad for the connections of W10X26 beams, and 12,960 kip-in/rad for the connections of W16X26 and W18X40 beams. This stiffness is conservative since it neglects the contribution from the gusset plates. A more realistic force-deformation relationship for gravity connections restrained by gusset plates (e.g. Stoakes and Fahnestock, 2011) could be used in future work if found suitable. The capacity of the shear connections is given in Table 47.

Table 46. Component m-factors for deformation-controlled actions.

Removed Column	Level	Beam/Girder	Primary or secondary	$d_{bg}$ (in)	Beam/ Girder m-factor	Connection (m-factor)
1 (G-4)	2, 3, 4, Roof	W18x40	Primary	$d_{bg} = 3''$	6	1.5
	4, Roof	W18x40	Primary	$d_{bg} = 6''$	6	5.16
	2, 3	W18x40	Secondary	$d_{bg} = 6''$	10	7.73
	2, 3, 4, roof	W16x26	Secondary	$d_{bg} = 6''$	6.17	7.73
2 (A-4)	4	W18x40	Primary	$d_{bg} = 3''$	6	1.5
	Roof	W18x40	Primary	$d_{bg} = 6''$	6	5.16
	2, 3	W18x40	Secondary	$d_{bg} = 6''$	10	7.73
	2, 3, 4, roof	W16x26	Secondary	$d_{bg} = 6''$	6.17	7.73
3 (O-2)	2, 3, 4	W16x26	Primary	$d_{bg} = 3''$	3.81	1.5
	Roof	W16x26	Primary	$d_{bg} = 6''$	3.81	5.16
	2, 3, 4, roof	W16x26	Secondary	$d_{bg} = 6''$	6.17	7.73
	2, 3, 4, roof	W18x40	Secondary	$d_{bg} = 6''$	10	7.73
	4, Roof4, roof	W10X26	Primary	$d_{bg} = 6''$	6	5.16
4 (C-1)	4, Roof2, 3, 4	W18x40	Primary	$d_{bg} = 3''$	6	1.5
	2, 3, 2, 3, roof	W18x40	Primary	$d_{bg} = 6''$	6	5.16
	2, 3, 4, roof	W18x40	Secondary	$d_{bg} = 6''$	10	7.73
		W16x26	Secondary	$d_{bg} = 6''$	6.71	7.73

Table 47. Shear tab connections (3/4" A325-N bolts).

Story	Beam Section	T (in)	$V_u, \max$ (kips)	No. Bolts	Bolt Spacing (in)	$t_w$ (in)	$t_{plate}$ (in)	L (in)	$Le_v \geq 1''$ (in)	$a \leq 3 \frac{1}{2}''$ (in)	$Le_h \geq 2d''$ (in)	Shear Plate Capacity (kips)[a]
All	W16X26	13 5/8	19.9	3	3	0.250	5/16	8 1/2	1 1/4	3	1 1/2	43.4
All	W18X40	15 1/2	39.2	3	3	0.315	5/16	8 1/2	1 1/4	3	1 1/2	43.4

[a] : AISC 360-10 Table 10-10a

Table 46 shows that the smallest m-factor for every column removal case is 1.5, corresponding to the double angle connections used to attach W18X40 and W16X26 sections acting as the top and bottom chords of the top-story truss members where gusset plates are present.

Force-controlled actions have a load increase factor of 2.0. Members not immediately adjacent to the removed column are loaded with the same gravity combination as for the deformation-controlled case.

A summary of controlling m-factors for each column removal case, for deformation-controlled and force-controlled actions, is shown in Table 48.

Table 48. Load increase factors.

Removed Column	Lowest m-factor	$\Omega_{LD} = 0.9m_{LIF} + 1.1$	$\Omega_{LF}$ , LIF for Force Controlled Actions
1	1.5	2.45	2
2	1.5	2.45	2
3	1.5	2.45	2
4	1.5	2.45	2

#### 4.2.2.3 Column Removal Loads

The load combinations used for all column removal cases are presented next.

1. For area immediately adjacent to column removed, in deformation-controlled load case:

$$G_{LD} = \Omega_{LD} [1.2 D + (0.5 L \text{ or } 0.2 S)] = 2.45 [1.2 D + (0.5 L \text{ or } 0.2 S)]$$

$$= 2.94 D + (1.23 L \text{ or } 0.49 S)$$

$$G_{LD, 1-3} = 2.94(75) + 1.23(80) = 318.9 \text{ psf}$$

$$G_{LD, \text{roof}} = 2.94(25) + 1.23(35) = 116.6 \text{ psf}$$

2. For area immediately adjacent to column removed, in force-controlled load case:

$$G_{LF} = \Omega_{LF} [1.2 D + (0.5 L \text{ or } 0.2 S)] = 2.0 [1.2 D + (0.5 L \text{ or } 0.2 S)]$$

$$= 2.4 D + (1.0 L \text{ or } 0.4 S)$$

$$G_{LF, 1-3} = 2.4 (75) + 1.0(80) = 260 \text{ psf}$$

$$G_{LF, \text{roof}} = 2.4 (25) + 0.4 (35) = 74 \text{ psf}$$

3. For the area away from the column removed, for deformation and force-controlled load cases:

$$G = 1.2 D + (0.5 L \text{ or } 0.2 S)$$

$$G_{1-3} = 1.2(75) + 0.5(80) = 130 \text{ psf}$$

$$G_{\text{roof}} = 1.2(75) + 0.2(35) = 37 \text{ psf}$$

A summary of the resulting loads on the building, for each column removal case, is presented in Table 49.

Table 49. Gravity loads.

Column Removed	$G_{LD}$ (psf)		$G_{LF}$ (psf)		G (psf)	
	Levels 1-3	roof	Levels 1-3	roof	Levels 1-3	roof
Col 1	318.9	116.6	260	74	130	37
Col 2	318.9	116.6	260	74	130	37
Col 3	318.9	116.6	260	74	130	37
Col 4	318.9	116.6	260	74	130	37

#### 4.2.3 Results

The procedure outlined in Section 2.5 was implemented for this analysis and is shown in the following sections. For column removals 1 and 3, the column and also the attached diagonal brace were removed, per the UFC guidelines (DoD, 2009). Figure 48 shows the deflected shape of the force-controlled building model under column removal case 1, and Figure 49 displays the DCRs for the same column removal case. Red means that the member was over stressed.

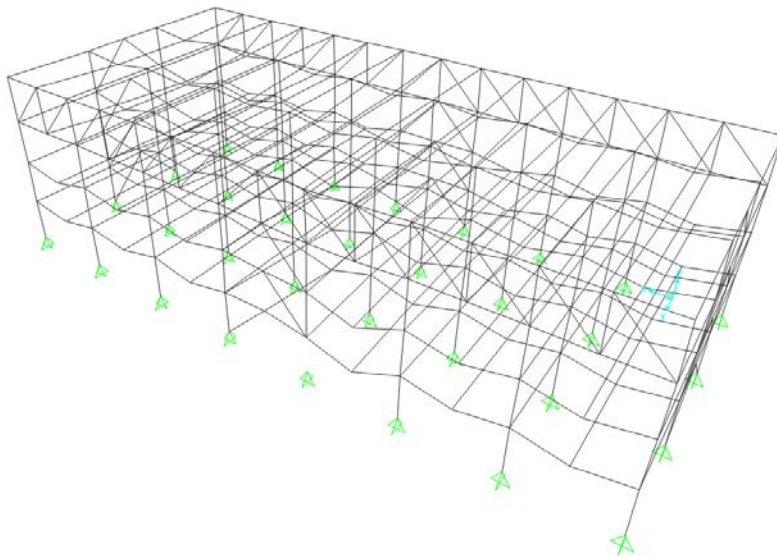


Figure 48. Frame deflection due to column 1 removal.

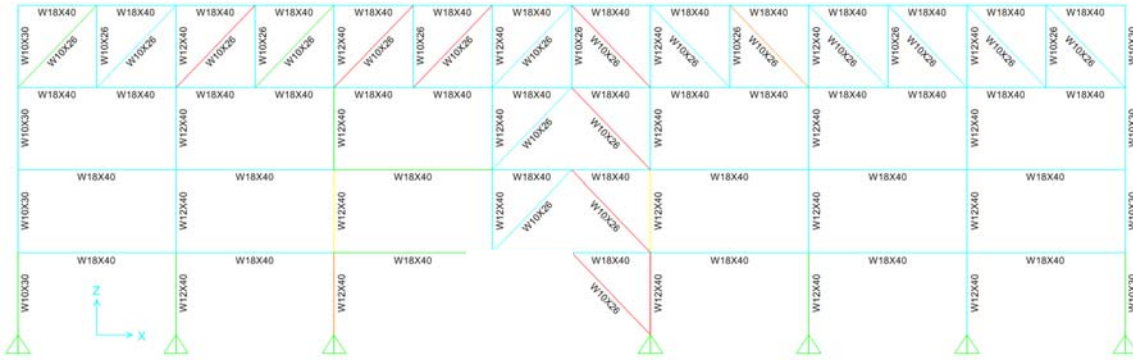


Figure 49. Moment ratios due to column 1 (and adjacent brace) removal.

### Force-Controlled Columns and Braces

Columns with a  $P_{UF}/P_{CL}$  ratio greater than 0.5 were checked in the force-controlled model. Table 50 shows the elements with  $P_{UF}/P_{CL}$  greater than 0.5, which are overstressed. These members would need to be re-designed.

Table 50. Force-controlled elements.

Column Removal 1								
Frame #	Section	$P_{UF}$ (kip)	$M_{rx}$ (kip-in)	$M_{ry}$ (kip-in)	$P_{CL}$ (kip)	$M_{CLx}$ (kip-in)	$M_{CLy}$ (kip-in)	DCR
1555	W12X40	-349.1	-3.74	0.0	329.9	2587.5	756.0	1.08
Column Removal 3								
1523	W12X40	-328.7	-4.5	3.47	329.9	2587.5	756.0	1.07
1555	W12X40	-328.6	4.5	4.4	329.9	2587.5	756.0	1.09
69	W12X40	-445.7	-6.9	0.1	329.9	2587.5	756.0	1.38
90	W12X40	-338.6	-7.2	0.1	329.9	2587.5	756.0	1.06
587	W12X40	-464.9	-38.3	-0.1	329.9	2587.5	756.0	1.59
591	W12X40	-361.0	-46.1	-0.1	329.9	2587.5	756.0	1.31
Column Removal 4								
1521	W12X40	-333.1	-0.1	0.1	329.9	2587.5	756.0	1.01
75	W10X30	-246.7	0.1	0.0	155.1	1647.0	397.8	1.59
76	W10X30	-202.3	1.0	0.0	155.1	1647.0	397.8	1.31
251	W10X30	-290.4	0.0	-0.1	155.1	1647.0	397.8	1.88

### Deformation-Controlled columns and braces

m-factors for the deformation-controlled columns (beam-columns) are shown in Table 51 and Table 52. These values depend on the slenderness ratio of the cross section and on the ratio of

axial load to axial load capacity. Table 53 shows one example of a member check as performed in a spreadsheet. All deformation-controlled elements satisfied their acceptance criteria.

It should be mentioned that the removal of columns caused some members to have tension loads. These members were identified and verified in the deformation-controlled model using the interaction equation (Equation 14). All members subjected to tension passed.

$$\frac{T}{\phi m_t T_{CE}} + \frac{M_x}{\phi m_x M_{CEx}} + \frac{M_y}{\phi m_y M_{CEy}} \leq 1.0 \quad \text{Equation 14}$$

Where T is the tension demand;  $m_t$  is the m-factor for tension (3 for beams and columns and 6 for braces);  $T_{CE}$  is the tension capacity. All other parameters were previously defined.

Table 51. m-factor in deformation-controlled columns with  $P_{UF}/P_{CL} < 0.2$

Column Section	$\frac{b_f}{2t_f}$	$\frac{h}{t_w}$	m-factor for $P_{UF}/P_{CL} < 0.2$	
			Primary	Secondary
W12X40	7.77	33.6	3.95	6.54
W10X30	5.7	29.5	6	10
W10X26	6.56	34	6	10
W12X58	7.82	27	3.81	6.31
W10X33	9.15	27.1	1.25	2

Table 52. m-factor in deformation-controlled columns with  $0.2 \leq P_{UF}/P_{CL} \leq 0.5$

Column Section	$\frac{b_f}{2t_f}$	$\frac{h}{t_w}$	m-factor for $0.2 \leq P_{UF}/P_{CL} \leq 0.5$	
			Primary	Secondary
W12X40	7.77	33.6	Between 1.25 and $9\left(1 - \frac{5P}{3P_{CL}}\right)$	Between 2 and $15\left(1 - \frac{5P}{3P_{CL}}\right)$
W10X30	5.7	29.5	$9\left(1 - \frac{5P}{3P_{CL}}\right)$	$15\left(1 - \frac{5P}{3P_{CL}}\right)$
W10X26	6.56	34	$9\left(1 - \frac{5P}{3P_{CL}}\right)$	$15\left(1 - \frac{5P}{3P_{CL}}\right)$
W12X58	7.82	27	Between 1.25 and $9\left(1 - \frac{5P}{3P_{CL}}\right)$	Between 2 and $15\left(1 - \frac{5P}{3P_{CL}}\right)$
W10X33	9.15	27.1	1.25	2

Table 53. Demand on a deformation-controlled beam-column due to column removal 1.

Frame	Section	P <sub>UF</sub> (kip)	P <sub>CL</sub> (kip)	m-factor	M <sub>rx</sub> (kip-in)	M <sub>ry</sub> (kip-in)	M <sub>CLx</sub> (kip-in)	M <sub>CLy</sub> (kip-in)	DCR
4	W12X40	-122.1	329.9	2.5	-5.65	237.19	-0.10	69.30	0.378

#### 4.2.3.1 Beam Flexure

The m-factor for the three sections used for gravity beams are shown in Table 54. This table shows the section capacity, the maximum moment demand, the controlling case(s) and the DCR. Note that the assigned m-factor is greater than the DCR for all gravity beams.

Table 54. Secondary beam flexure DCR check.

Section	$\frac{b_f}{2t_f}$	$\frac{h}{t_w}$	m-factor	$\Phi M_n$ (kip-in)	Max Mu (kip-in)	Controlling Case	Max $\frac{M_u}{\Phi M_n}$
W16X26 Edge	7.97	56.8	6.17	3420	4044	Col Rem 1-4	1.2
W16x26 Interior	7.97	56.8	6.17	3420	4044	Col Rem 1-4	1.2

The contribution from the secondary moment generated at the shear tab connections was not considered here. These are very small as was the case for the American Zinc building (see Section 3.2.4.2).

#### 4.2.3.2 Shear in Beams and Columns

The shear demand was checked using the force-controlled model. Shear capacity was obtained from Equation 11, per AISC Specifications (AISC, 2010). The shear strength for all sections. Note that the slenderness ratio of all sections was less than the shear buckling limit.

Table 55. Shear strength of sections in model.

Section	$h/t_w$	$\phi V_n$ (kips)
W18X40	50.9	169
W16X26	56.8	106
W12X40	33.6	106
W12X58	28.1	132
W10X30	29.5	94.2
W10X26	34.0	80.3
W10X33	27.1	84.7

Shear in all sections was checked by verifying that the shear capacity was greater than the demand for all column removal cases. This was the case for all sections. For beams, the additional shear demand arising from the partial restraint provided by the shear tabs was neglected.

#### 4.2.3.3 Connection Analysis

Connections in the Lamar Construction Sister Building included shear tabs for gravity beams, double angle connections for beam-column connections in joints with braces and gusset plate connections for the braces. These connections were designed for the original demands, and then checked against the increased demands present in the column removal scenario. All shear tab and double angle connections passed the check. However, several connection failures occurred in the gusset-plate to brace connection. These were excluded from the current project scope.

### 4.3 *Integration of stiff-story with LFRSs*

The next step was to integrate stiff-story solutions with LFRSs. First, seismic loads were determined according to ASCE 7-10. Once these lateral loads were found, interstory drift was checked to ensure compliance with applicable standards.

Section 4.4 describes the development, comparison, and design of multiple unique bracing configurations for the Lamar sister building. All configurations included LFRS bracing to evaluate whether a LFRS designed solely for lateral loads could also resist disproportionate collapse. Several configurations also featured stiff-story bracing. Since the Lamar sister building featured pin connections throughout the building, forces in the lost column were primarily transmitted through the LFRS braces. Therefore, a column not adjacent to the LFRS or supported by a stiff-story was assumed to be much more vulnerable to collapse.

Several configurations were selected for column removal analysis and then analyzed in Section 4.4.2. The configurations that were selected provide a parametric study of the effectiveness of the stiff-story concept and two different LFRS locations.

#### 4.3.1 Seismic Load Design

Seismic loads were calculated assuming that the sister building is located at the site of the original Lamar Construction Corporate Headquarters, which is in Hudsonville, Michigan at 42.8448°N and 85.8708°W. The site soil classification is assumed to be Class D and the risk category is level II.

Using the USGS seismic data website (US Seismic Design Maps, 2014), the seismic design values  $S_s$  and  $S_1$  were found to be 0.073 and 0.045, respectively.

The building parameters for the sister building were found by assuming the structure uses an ordinary concentrically braced frame. Based on ASCE 7-10 Table 12.2-1, the overstrength factor,  $\Omega_0$ , is 2.0, the deflection amplification factor,  $C_d$ , is 3.25, and the response modification coefficient,  $R$ , was taken as 3.0 to avoid special seismic detailing. The design load includes a dead load of 75 psf for the floors and 25 psf for the roof. Since the building includes partition walls, a 20 psf partition live load is also included for each floor as required by ASCE 7-10 Section 12.7.2. The roof snow load of 35 psf is large enough to be included in the seismic weight as well, though ASCE 7-10 Section 12.7.2 specifies using only 20% of the value. Table 56 summarizes the seismic loads for Lamar, including the force applied to each story and the story shear.

Table 56. Lamar seismic loads.

Story	Weight (kip)	Height (ft)	Seismic Force (kip)	Shear force (kip)
1	1296.8	13	15.3	112.3
2	1296.8	26	30.6	97.0
3	1296.8	39	45.9	66.5
4	436.8	52	20.6	20.6
Total	4327.2	---	112.3	---

#### 4.3.2 Seismic Load Modeling

The seismic loads found above were then applied to the sister building model in SAP2000. Because the sister building structure is symmetrically braced, the center of rigidity for each floor is located at the same point as the center of mass, and therefore the earthquake loads do not create any eccentricity. However, ASCE 7-10 Section 12.8.4.2 specifies provisions for accidental torsion in non-flexible diaphragms by stipulating that earthquake loads shall be offset a distance of 5% of the building dimension perpendicular to the load direction.

#### 4.3.3 Lateral Load Comparison

The wind pressures for each level were calculated and then used to find the wind load for each of the two building directions. Wind load calculations are presented in Appendix A and compared with seismic loads in Table 57. Wind shears are greater for the NS direction and for the first two

stories in the EW direction. The earthquake story shear is higher for story 3 and yield the same demand in the EW direction for story 4.

Table 57. Lateral load controlling case (story shears).

Story	Wind EW (kip)	Wind NS (kip)	Earthquake (kip)
1	136	348	112
2	100	254	97
3	61	155	67
4	21	53	21

#### 4.3.4 Interstory drift

Interstory drift was calculated for both wind and earthquake loads. Interstory drift due to wind was compared with the limits recommended in ASCE 7-10 Commentary CC.1.2. A limit of  $h/400$  was used for wind service loads, with  $h$  being the story height. Interstory drift due to earthquake loads was calculated according to ASCE 7-10 sections 12.8.6 and 12.12.1. Earthquake drift limits are less conservative, with a limit of  $0.025h$  applicable to the Lamar sister building (ASCE 7-10 Table 12.12-1). Equation 15 (ASCE 7-10 Equation 12.8-15) was used to calculate story drift for the Lamar sister building.  $\delta_{xe}$  represents the story drift found directly from elastic analysis of the building, which in this case was found using SAP2000.  $C_d$  and  $I_e$  were previously defined.

The story drift due to both the wind and earthquake loads was below the applicable limits. Story drift was checked for each configuration that was selected for design in Section 4.4.2. A summary of these results is presented in Table 58. Story drift was calculated in both the NS and EW building directions.

$$\delta_x = \frac{C_d \delta_{xe}}{I_e}$$

Equation 15

Table 58. Story drift summary (Configuration A1).

Story	Wind $\delta x$ Limit (in)	Wind $\delta x$ NS (in)	Wind $\delta x$ EW (in)	Seismic $\delta x$ NS (in)	Seismic $\delta x$ EW (in)
1	0.39	0.09	0.04	0.17	0.19
2	0.39	0.12	0.06	0.24	0.27
3	0.39	0.13	0.06	0.24	0.29
4	0.39	0.12	0.06	0.18	0.24

#### 4.4 *Alternative Structural Configurations*

In order to identify effective structural systems resistant to disproportionate collapse, the Lamar sister building concept was developed further. As part of the process, several additional building configurations were created, using various combinations of lateral bracing. These configurations are described in Section 4.4.1. All configurations use the basic four story structure of the original sister building. These configurations were intended to be used as part of a parametric study to explore optimal relationships between structural economy and robustness.

Several of these configurations were designed and evaluated under column removal scenarios. The goal was to discern structural configurations that maximize efficiency while minimizing the risk of disproportionate collapse from column removal.

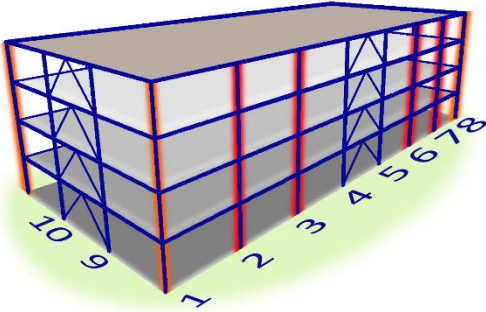
##### 4.4.1 Configuration Description

21 different configurations were created and are shown in Figure 50. Configuration A0 in represents the original Lamar sister building described in Section 2.4.2. Configurations A2, B2, C2, D2, and E2 share stiff stories on the EW sides of the fourth level, which are intended to provide column support for any column that is removed. Configurations A3, B3, C3, and D3 also feature stiff stories on the NS sides of the building to further enhance robustness. The stiff-story concept is derived from the cantilever of the original Lamar Construction headquarters. Configurations A1, A1B, B1 C1, D1, and E1 do not feature the stiff-story, allowing a comparison of the effects of the stiff-story on collapse resistance.

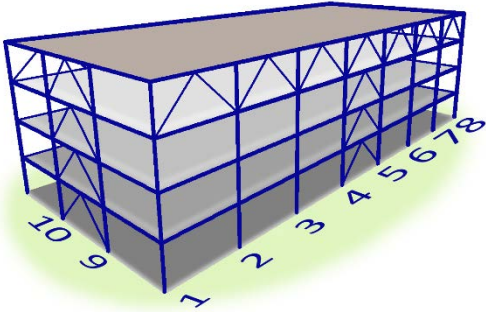
Configurations G, H, I, J, and K feature unconventional bracing configurations and are included to provide an index comparison with the more traditional configurations. These configurations would need to be considered separately due to their unconventional bracing, which could pose

unique design challenges. Accordingly, configurations A-F were favored during selection of configurations for design and column removal analysis.

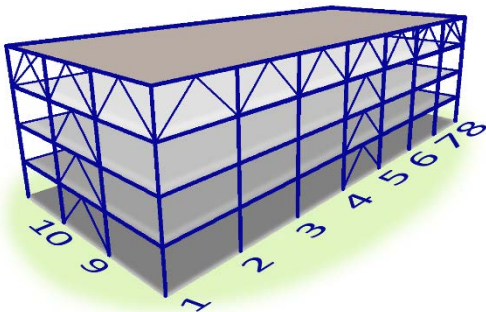
a. Configuration A1



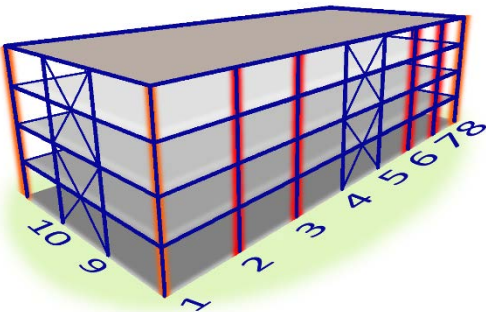
b. Configuration A2



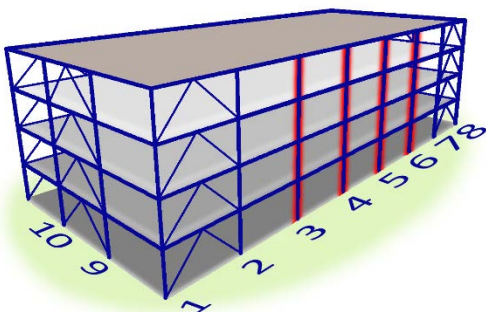
c. Configuration A3



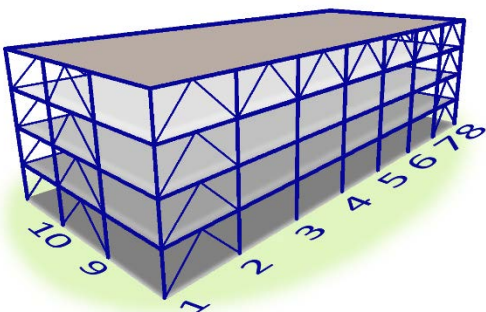
d. Configuration A1b



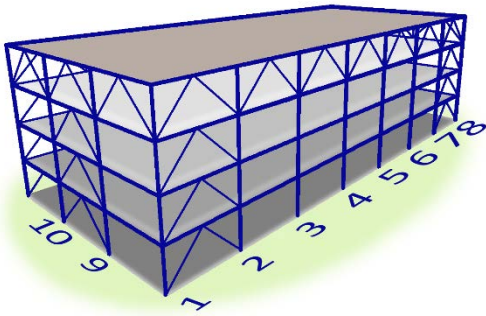
e. Configuration B1



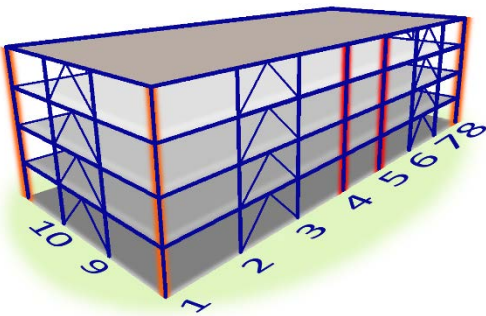
f. Configuration B2



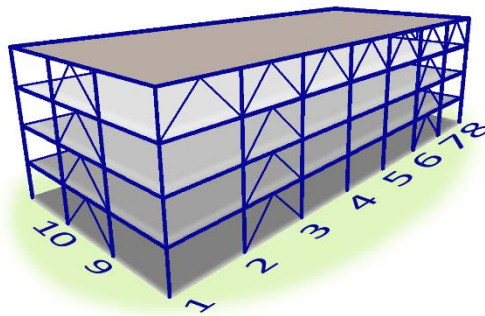
g. Configuration B3



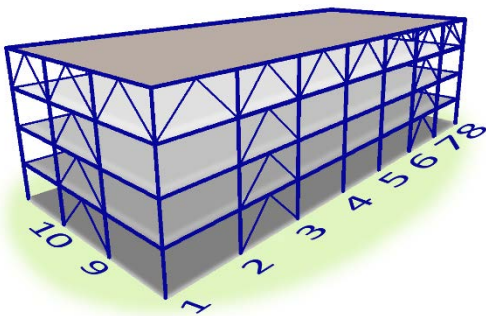
h. Configuration C1



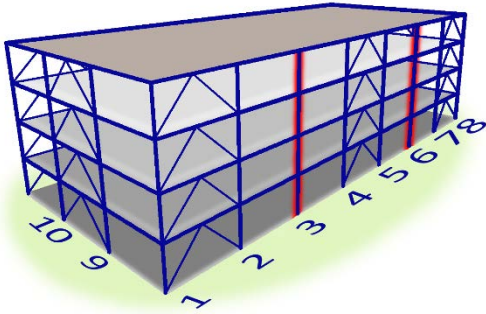
i. Configuration C2



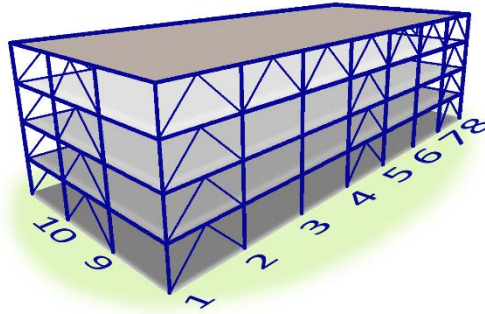
j. Configuration C3



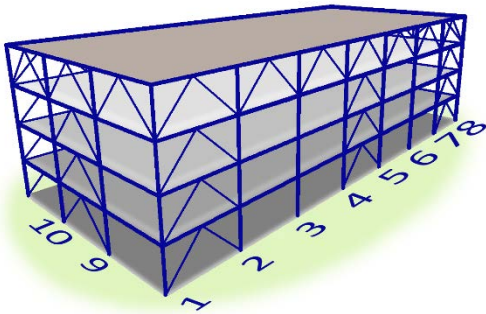
k. Configuration D1



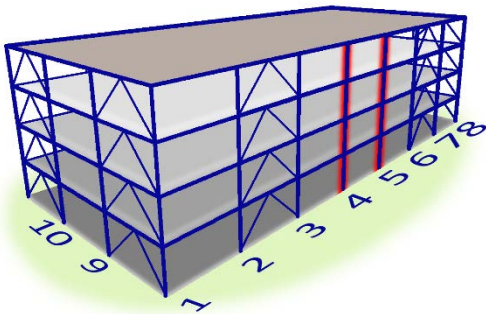
l. Configuration D2



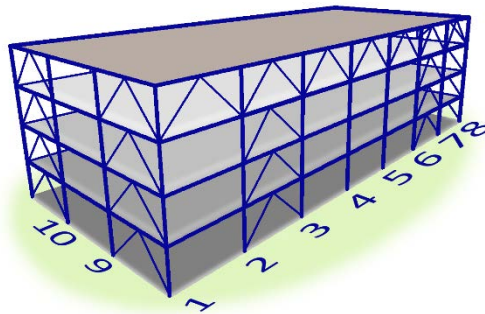
m. Configuration D3



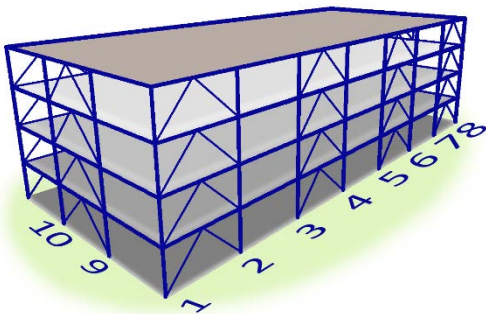
n. Configuration E1



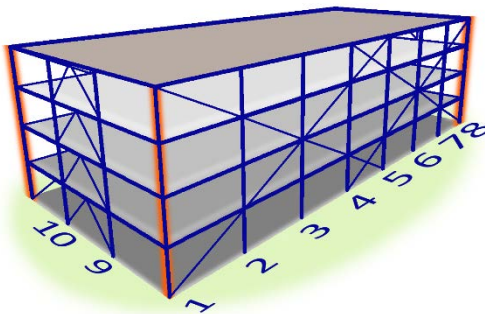
o. Configuration E2



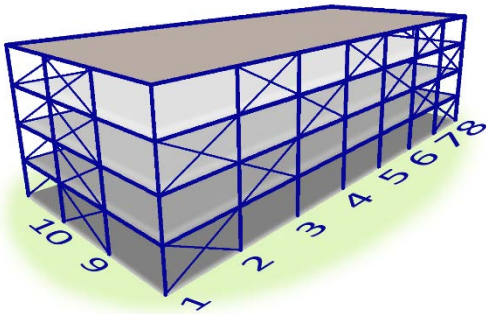
p. Configuration F



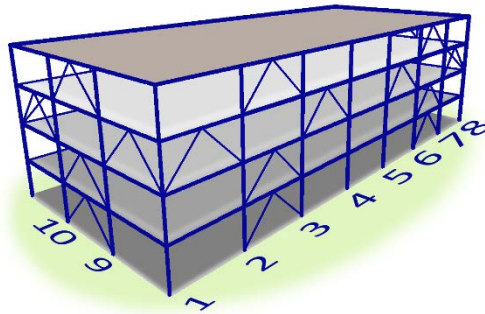
q. Configuration G



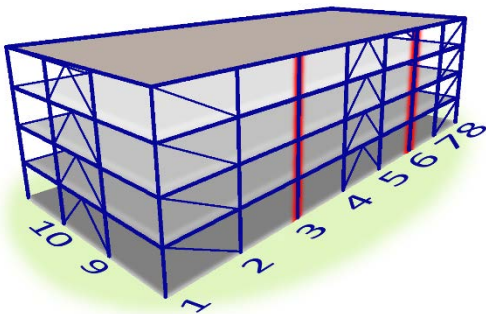
r. Configuration H



s. Configuration I



t. Configuration J



u. Configuration K

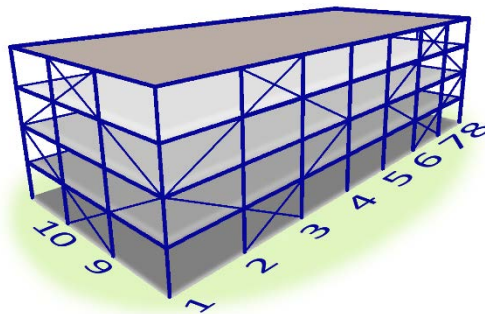
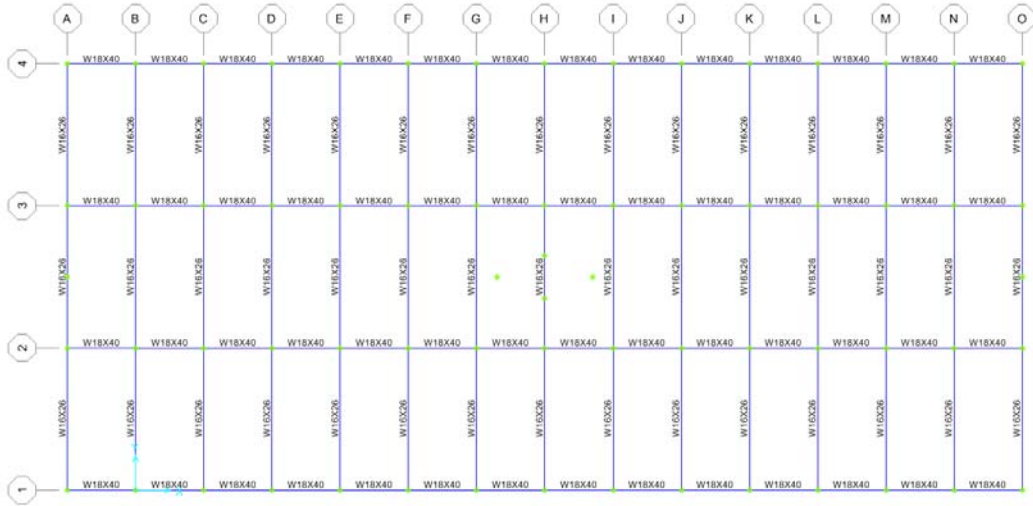


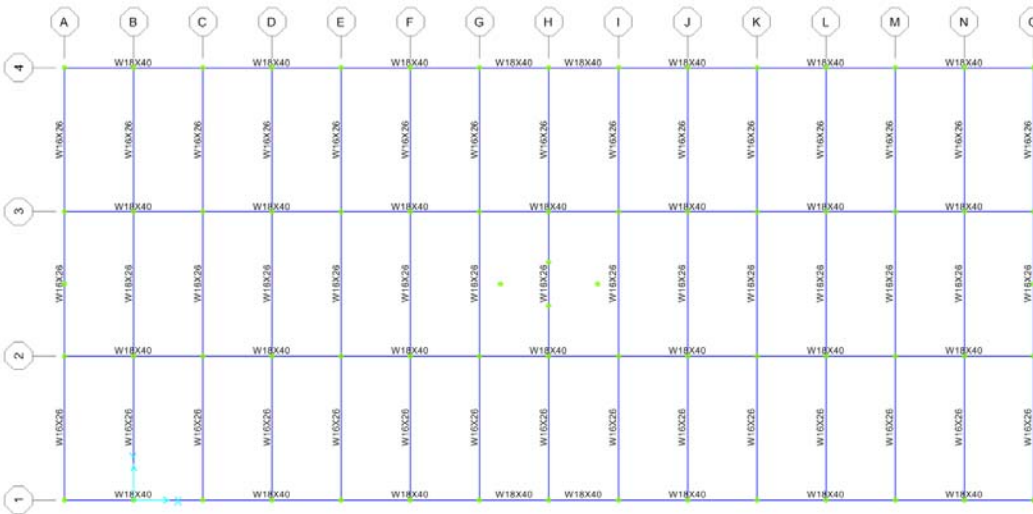
Figure 50. Lamar configuration diagrams.

Building design considered earthquake loads, interstory drift checks, and composite action design as explained in previous sections. Figure 51 shows the section views of configuration A1, which is typical of the other configurations. The EW brace sizes were different in B1-B3 than A1-A3; B1-B3 used W6X15 braces while A1-A3 used W10X26.

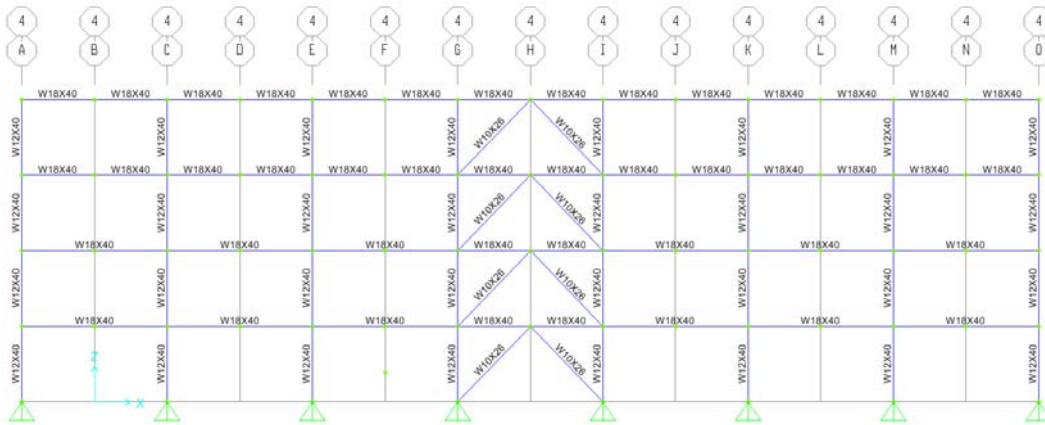
a. Roof plan view



b. Floors 1-3 plan view



c. Elevation view of EW external frame



d. Elevation view of EW internal frame



e. Elevation view of NS external frame (left) and internal frame (right)



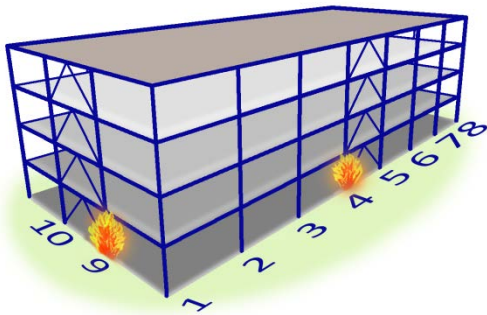
Figure 51. Lamar A1 section views.

#### 4.4.2 Column Removal Analysis

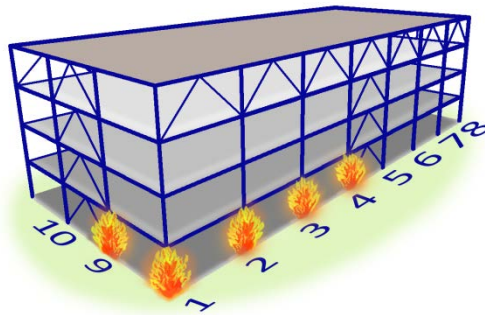
This section describes the column removal analysis procedure and results as they apply to Lamar configurations A1-B3. A1 and A2 were similar to the original Lamar sister building. B1 and B2 were also similar, except that the EW building faces feature two sets of braced frames instead of one.

Figure 52 shows the basic column removal locations for the Lamar configurations that were analyzed. The exact column removal locations are shown in greater detail in each configuration section.

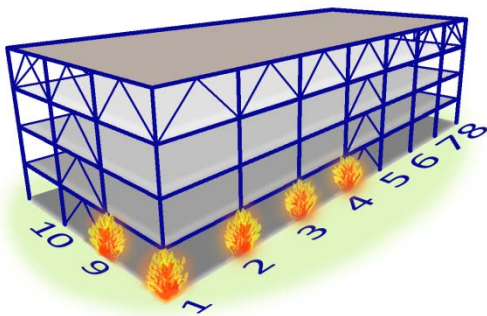
a. Configuration A1



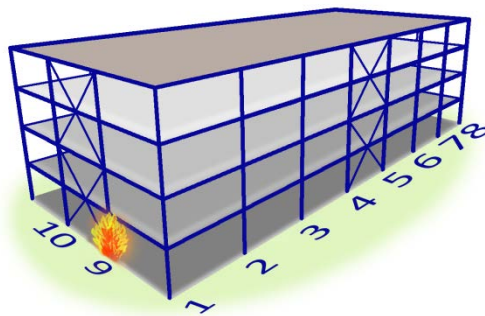
b. Configuration A2



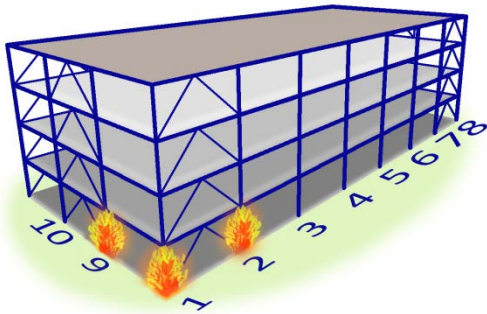
c. Configuration A3



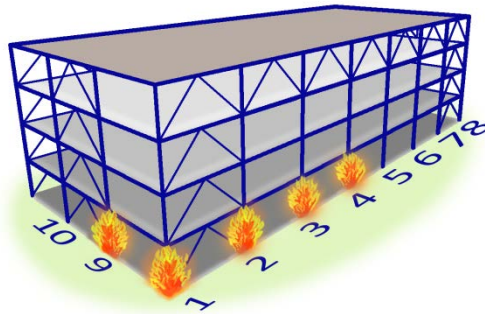
d. Configuration A1B



e. Configuration B1



f. Configuration B2



g. Configuration B3

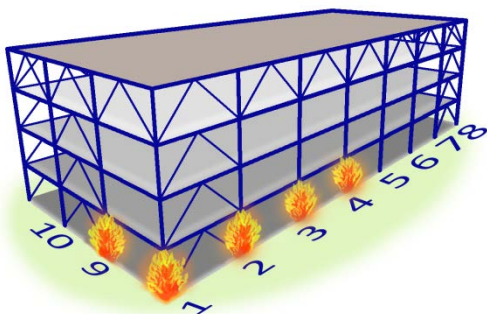


Figure 52. Lamar column removal.

#### 4.4.3 Configuration A1

This section details the column removal procedure and results as applicable to Configuration A1.

##### 4.4.3.1 Column Removal Locations

Column removals were selected according to the rationale described in Section 2.5.2. Two first-story columns were removed from A1 and are shown in Figure 53 along with their areas of increased load. Column removal 1 removed members 1523 (column) and 3 (brace) from the structure. Column removal 2 removed members 69 (column) and 168 (brace). Since A1 is a symmetrical structure, the two column removals were considered representative of their corresponding members on other sides of the structure. A1 does not have a stiff-story, so gravity columns were not removed as they form a collapse mechanism.

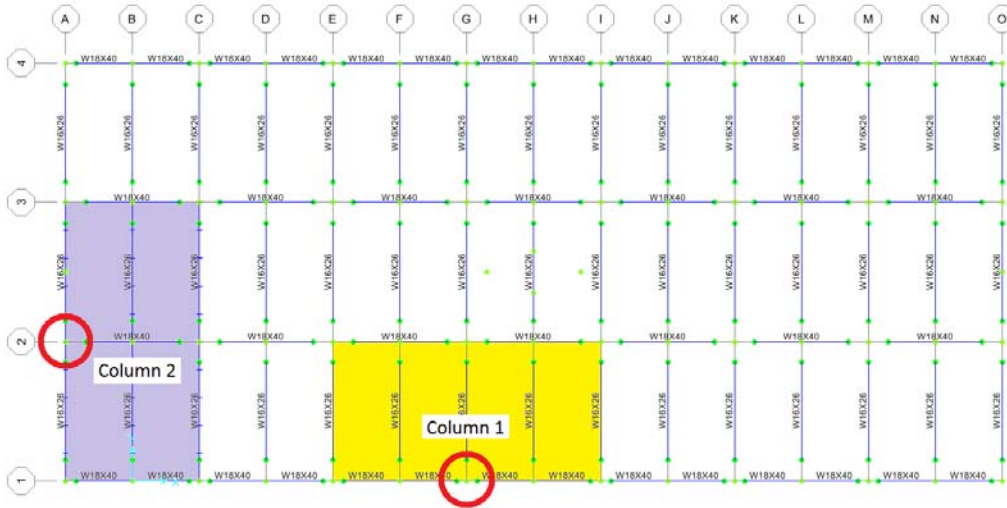


Figure 53. Configuration A1 column removals.

#### 4.4.3.2 M-factors

The m-factors for all beams, girders, and beam-to-column connections used to determine the increased loads for A1 are shown in Table 59. Most connections in the structure are simple shear tabs with  $d_{bg} = 6"$ . The connections to the braces include a gusset plate, with double angles connecting to the beams. For double angle connections,  $d_{bg} = 3"$ . Table 59 shows that the smallest m-factor for each column removal case is 1.50, based on primary double angle connections.

Table 59. Configuration A1 m-factors for determining increased loads.

Removed Column	Level	Beam / Girder	Primary or Secondary	Beam / Girder m-factor	Connection m-factor
1 (G-1)	2, 3, 4	W18X40	Primary	6.00	1.50*
	roof	W18X40	Primary	6.00	5.16†
	2, 3, 4, roof	W18X40	Secondary	10.00	7.73†
	2, 3, 4, roof	W16X26	Secondary	6.17	7.73†
2 (A-2)	2, 3, 4	W16X26	Primary	3.81	1.50*
	roof	W16X26	Primary	3.81	5.16†
	2, 3, 4, roof	W16X26	Secondary	6.17	7.73†
	2, 3, 4, roof	W18X40	Secondary	10.00	7.73†

\*Double angle connection

†Shear tab connection

In addition to the m-factors listed above, additional m-factors were used for all beam-columns, tension members, and braces to determine acceptability. Table 60 shows the m-factors for all DC beam-columns. For the sections with  $0.2 \leq P_{UF}/P_{CL} \leq 0.5$ , the m-factor had to be interpolated between a lower limit value and the upper limit value which is dependent on the  $P_{UF}/P_{CL}$  ratio (ASCE 41 Table 5-5). Table 61 shows the m-factors for all braces (based on ASCE 41 Table 5-5). All beam-columns in tension used an m-factor of 3.00 for primary members and 6.00 for secondary members.

Table 60. Configuration A1 beam-column m-factors.

Column Section	$\frac{b_f}{2t_f}$	$\frac{h}{t_w}$	$P_{UF}/P_{CL} < 0.2$		$0.2 \leq P_{UF}/P_{CL} \leq 0.5$	
			Primary m-factor	Secondary m-factor	Primary m-factor	Secondary m-factor
W12X40	7.77	33.6	3.95	6.54	Varies	Varies
W12X58	7.82	27.0	3.81	6.31	Varies	Varies

Table 61. Configuration A1 brace m-factors.

Brace Section	L (ft.)	$\frac{kl}{r}$	Compression		Tension	
			Primary m-factor	Secondary m-factor	Primary m-factor	Secondary m-factor
W10X26	18.0	158.8	6.00	7.00	6.00	8.00
W10X30	18.4	161.2	6.00	7.00	6.00	8.00
W10X33	18.4	113.8	6.00	7.00	6.00	8.00

#### 4.4.3.3 Column Removal Loads

The LIF for DC actions ( $\Omega_{LD}$ ) is based on the lowest m-factor ( $m_{LIF}$ ) for each column removal. Table 62 shows the LIFs for A1.

Table 62. Configuration A1 load increase factors.

Removed Column	Lowest m-factor	$\Omega_{LD}$	$\Omega_{LF}$
1 (G-1)	1.50	2.45	2.00
2 (A-2)	1.50	2.45	2.00

Based on these LIFs and the loads specific to Lamar, a summary of the load cases applied to the structure is shown below. Since the LIFs were the same for both column removals, the applied loads were also the same. Snow loads controlled for the roof.

- a. For areas immediately adjacent to the removed column, in the DC model:

$$G_{LD, 1-3} = 2.45[1.2(75 \text{ psf}) + 0.5(80 \text{ psf})] = 318.9 \text{ psf}$$

$$G_{LD, \text{ roof}} = 2.45[1.2(25 \text{ psf}) + 0.2(35 \text{ psf})] = 90.7 \text{ psf}$$

- b. For areas immediately adjacent to the removed column, in the FC model:

$$G_{LF, 1-3} = 2.00[1.2(75 \text{ psf}) + 0.5(80 \text{ psf})] = 260 \text{ psf}$$

$$G_{LF, \text{ roof}} = 2.00[1.2(25 \text{ psf}) + 0.2(35 \text{ psf})] = 74 \text{ psf}$$

- c. For all areas away from the removed column, in both models:

$$G_{1-3} = 1.2(75 \text{ psf}) + 0.5(80 \text{ psf}) = 130 \text{ psf}$$

$$G_{\text{ roof}} = 1.2(25 \text{ psf}) + 0.2(35 \text{ psf}) = 37 \text{ psf}$$

#### 4.4.3.4 Acceptance Results

The procedures outlined in Sections 2.5.5, 2.5.6, and 2.5.7 were used for the rest of the evaluation of A1. See Appendix C for the spreadsheet with results and acceptance criteria. The members not passing the acceptance criteria are shown in Figure 65 and are highlighted in Figure 54 and Figure 55. A total of two members, both columns, failed in column removal 1, while 15 members, including columns, braces, and beams, failed in column removal 2. Several members in removal 2 failed away from the area of increased loads due to column removal, possibly due to plan torsion stemming from the floors acting as diaphragms.

Table 63. A1 column removal results.

Column Removal 1 (G-1)				
Frame #	Section	Type	Controlling load type	DCR
1534	W12X40	Column	FC axial compression	1.42
1544	W12X40	Column	FC axial compression	1.27
Column Removal 2 (A-2)				
Frame #	Section	Type	Controlling load type	DCR
8	W12X40	Column	FC axial compression	1.95
16	W12X58	Column	FC axial compression	1.05
24	W12X40	Column	DC axial tension	1.28
44	W10X26	Brace	DC axial compression	1.37
56	W12X40	Column	DC axial tension	1.35
66	W12X40	Column	FC axial compression	1.86
122	W10X26	Brace	DC axial compression	1.36
1523	W12X40	Column	DC axial tension	2.16
1534	W12X40	Column	FC axial compression	2.95
1544	W12X40	Column	FC axial compression	3.04
1555	W12X40	Column	DC axial tension	2.09
91	W16X26	Beam	DC Flexure	2.76
176	W12X40	Column	FC axial compression	1.44
243	W12X40	Column	FC axial compression	1.93
569	W12X40	Column	FC axial compression	1.49

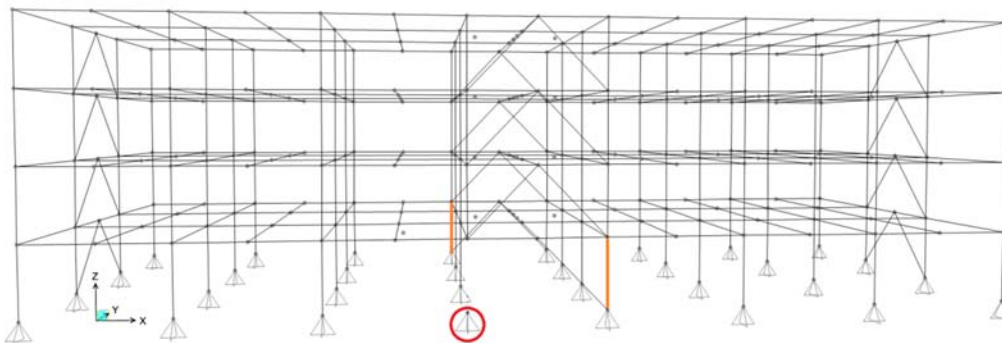


Figure 54. Configuration A1 column removal 1 failed members.

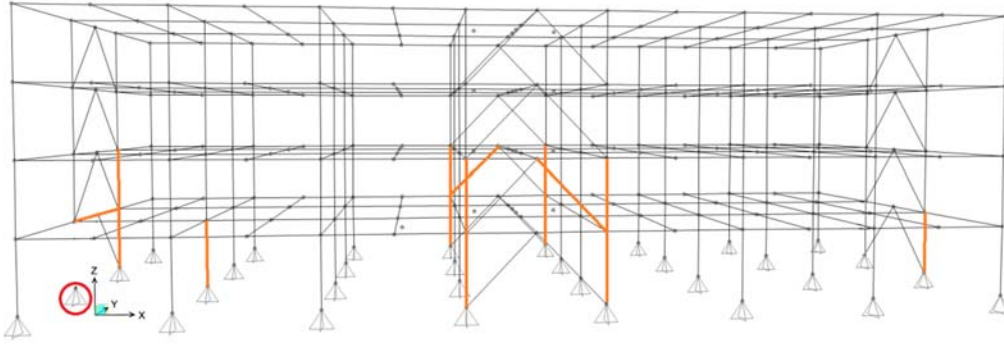


Figure 55. Configuration A1 column removal 2 failed members.

The plan torsion produced by both column removals, especially removal 2, was a significant result of the configuration study. Both Figure 54 and Figure 55 show that member failures occurred throughout the building, even away from the removed members. Torsion can also be seen in the deflected shape of the building in Figure 56. Note that the deflection is amplified in the figure.

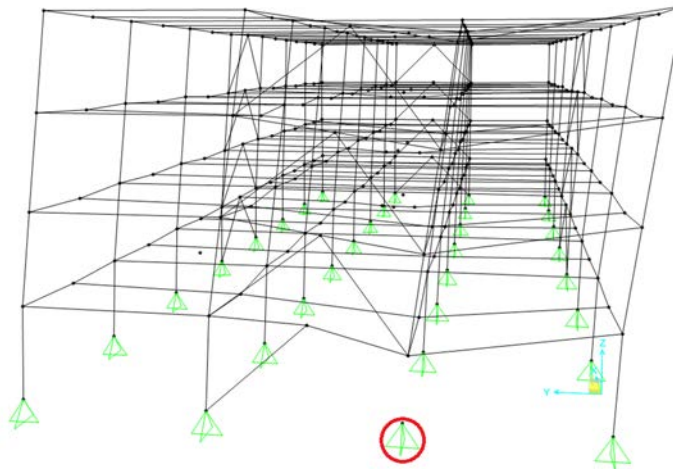


Figure 56. A1 column removal 2 deflected shape.

The torsion and the member failures it caused can be explained by the limited lateral bracing in the NS building direction (the direction with the column removal) and the floor diaphragm behavior. Because each floor included a concrete slab, the floors were modelled as rigid diaphragms in SAP2000. With the column removed, the now unbalanced bracing allowed the ends of the floors to twist. As the ends of the floors twisted, the whole diaphragm rotated, placing the braces under extra load which was transmitted to the columns. The NS bracing was not adequate to resist the torsion from column removal 2.

Although the effects of torsion are seen in both column removals, the effects were much worse with column removal 2. This is best explained by comparing the lateral resistance of the braces to moments acting about the center of the structure. In column removal 2, the unbalanced resistance of the affected frame created a large moment. The EW braced frames, where most failures occurred, had a shorter moment arm, which increased the loads on the frames. In column removal 1, the unbalanced resistance of the affected frame created a smaller moment, and the NS braces had a larger moment arm which more effectively resisted the torsion.

#### 4.4.4 Configuration A1B

This section details the column removal procedure and results as applicable to Configuration A1B. A1B was developed after observing the torsion effects in A1, with the goal of determining if a modified bracing configuration would enhance robustness. A1B did not undergo the same design process as the other configurations, and the bracing configuration was the only change. All member sizes remained the same.

##### 4.4.4.1 Column Removal Locations

Only one first-story column removal was performed on A1B and is shown in Figure 57 along with the area of increased load. Column removal 1 removed members 69 (column) and 168 (brace) from the structure, the same as A1 column removal 2. Since the torsional effect caused the most effects with this column removal, no other column removals were performed on A1B.

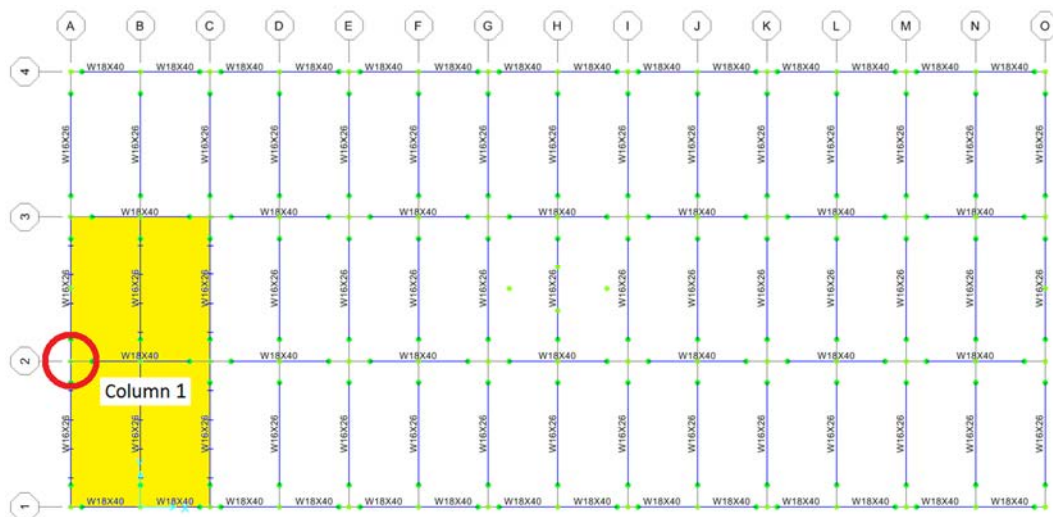


Figure 57. Configuration A1B column removal.

#### 4.4.4.2 M-factors

A1B used the same m-factors as A1. See Section 4.4.4.2 and column removal 2 of Table 59.

#### 4.4.4.3 Column Removal Loads

See Section 4.4.4.3.

#### 4.4.4.4 Acceptance Results

The procedures outlined in Sections 2.5.5, 2.5.6, and 2.5.7 were used for the rest of the evaluation of A1B. See Appendix C for the spreadsheet with results and acceptance criteria. The members not passing the acceptance criteria are shown in Table 64 and are highlighted in Figure 58. A total of 14 members, including 10 columns and braces, failed. All members that failed were away from the area of increased load at the column removal.

Table 64. A1B column removal results.

Column Removal 1 (A-2)				
Frame #	Section	Type	Controlling load type	DCR
8	W12X40	Column	FC axial compression	1.95
24	W12X40	Column	FC axial tension	1.38
31	W10X26	Brace	DC axial compression	1.87
56	W12X40	Column	FC axial tension	1.39
66	W12X40	Column	FC axial compression	1.94
121	W10X26	Brace	DC axial compression	1.87
1523	W12X40	Column	FC axial tension	1.29
1534	W12X40	Column	FC axial compression	2.03
1544	W12X40	Column	FC axial compression	2.04
1555	W12X40	Column	FC axial tension	1.28
569	W12X40	Column	FC axial compression	1.13
590	W12X40	Column	FC axial compression	1.02
7	W10X26	Brace	DC axial compression	1.02
9	W10X26	Brace	DC axial compression	1.02

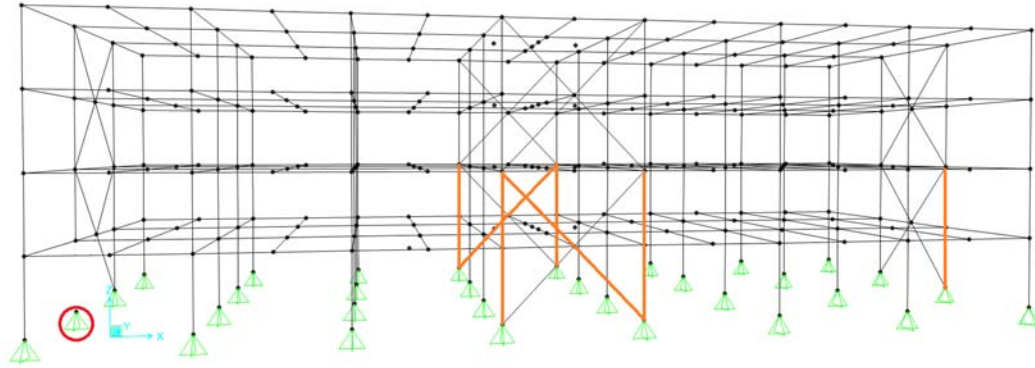


Figure 58. Configuration A1B column removal 1 failed members.

The torsion effect was only marginally improved over A1. Torsion can be seen in the deflected shape of the building in Figure 59. Note that the deflection is amplified in the figure. Both buildings suffered from large stresses on the braces, especially the EW braces. However, the local area around the column removal in A1B passed the acceptance criteria, suggesting that the X-bracing configuration has potential to limit disproportionate collapse, provided that torsion can be limited.

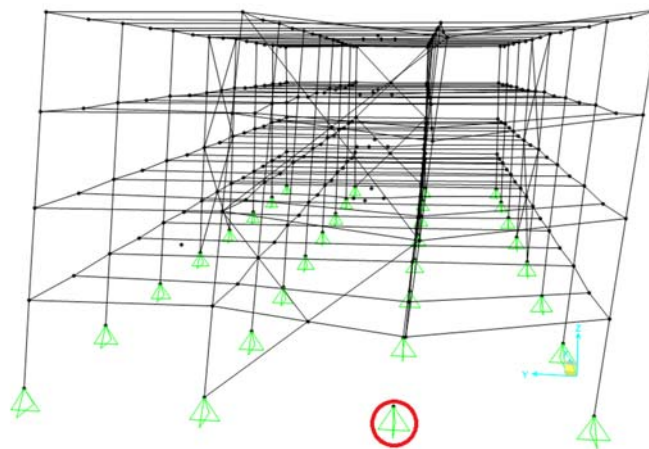


Figure 59. A1B column removal 1 deflected shape.

#### 4.4.5 Configuration A2

This section details the column removal procedure and results as applicable to Configuration A2.

##### 4.4.5.1 Column Removal Locations

Five columns were removed from A2 (Figure 60). Column removal 1 included members 1544 and 121 (brace); removal 2 included member 251; removal 3 included member 1532; removal 4 included member 1551; and removal 5 included members 243 and 166 (brace). Initially, since the NS sides of the building featured the same bracing configuration as A1, columns were not planned

to be removed on these sides of the building. However, due to the torsion observed in A1 and the added stiff-story of A2, column removal 5 was added.

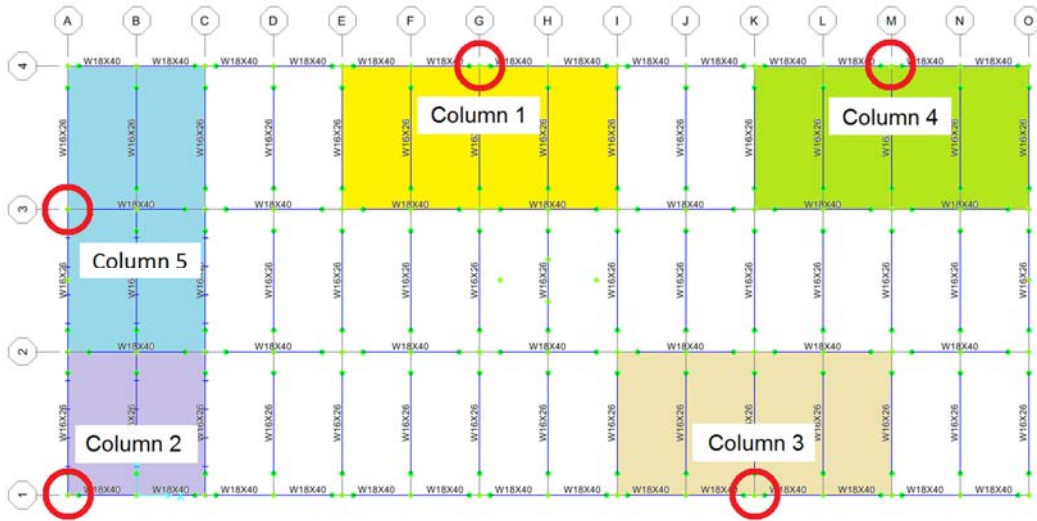


Figure 60. Configuration A2 column removals.

#### 4.4.5.2 M-factors

The m-factors for all beams, girders, and beam-to-column connections used to determine the increased loads for A2 are shown in Table 65. Most connections in the structure are simple shear tabs with  $d_{bg} = 6"$ . The connections to the braces include a gusset plate, with double angles connecting to the beams. For double angle connections,  $d_{bg} = 3"$ . Table 65 shows that the smallest m-factor for each column removal case is 1.50, based on primary double angle connections. The additional m-factors used to determine acceptance criteria were the same as those found for A1 in Section 4.4.4.2.

Table 65. Configuration A2 m-factors for determining increased loads.

Removed Column	Level	Beam / Girder	Primary or Secondary	Beam / Girder m-factor	Connection m-factor
1 (G-4)	2, 3, 4	W18X40	Primary	6.00	1.50*
	Roof	W18X40	Primary	6.00	5.16†
	2, 3	W18X40	Secondary	10.00	7.73†
	2, 3, 4, roof	W16X26	Secondary	6.17	7.73†
2 (A-1) 3 (K-1) 4 (M-4)	4	W18X40	Primary	6.00	1.50*
	roof	W18X40	Primary	6.00	5.16†
	2, 3, 4, roof	W16X26	Secondary	6.17	7.73†
	2, 3	W18X40	Secondary	10.00	7.73†
5 (A-3)	2, 3, 4	W16X26	Primary	3.81	1.50*
	roof	W16X26	Primary	3.81	5.16†
	2, 3, 4, roof	W16X26	Secondary	6.17	7.73†
	2, 3, 4, roof	W18X40	Secondary	10.00	7.73†

\*Double angle connection

†Shear tab connection

#### 4.4.5.3 Column Removal Loads

Since double angle m-factors controlled for all column removal cases, the column removal loads are all the same. The applied loads were the same as those applied to A1; for details see Section 4.4.4.3.

#### 4.4.5.4 Results

The procedures outlined in Sections 2.5.5, 2.5.6, and 2.5.7 were used for the rest of the evaluation of A2. See Appendix C for the spreadsheet with results and acceptance criteria. The members not passing the acceptance criteria are shown in Table 66 and are highlighted in Figure 61, Figure 62, and Figure 63. Column removals 1 and 2 each had 1 column failure, while removal 5 had 6 column failures and 1 beam failure. Removals 3 and 4 had no failing members. As in A1, torsional effects were observed, although the stiff-story of A2 helped reduce the number of member failures.

Table 66. A2 column removal results.

Column Removal 1 (G-4)				
Frame #	Section	Type	Controlling load type	DCR
1555	W12X40	Column	FC axial compression	1.04
Column Removal 2 (A-1)				
Frame #	Section	Type	Controlling load type	DCR
1519	W12X40	Column	FC axial compression	1.05
Column Removal 3 (K-1)				
<i>No failures</i>				
Column Removal 4 (M-4)				
<i>No failures</i>				
Column Removal 5 (A-3)				
Frame #	Section	Type	Controlling load type	DCR
1523	W12X40	Column	FC axial compression	1.03
1555	W12X40	Column	FC axial compression	1.02
69	W12X40	Column	FC axial compression	1.61
90	W12X40	Column	FC axial compression	1.29
91	W16X26	Beam	DC bending	1.01
587	W12X40	Column	FC axial compression	1.39
591	W12X40	Column	FC axial compression	1.07

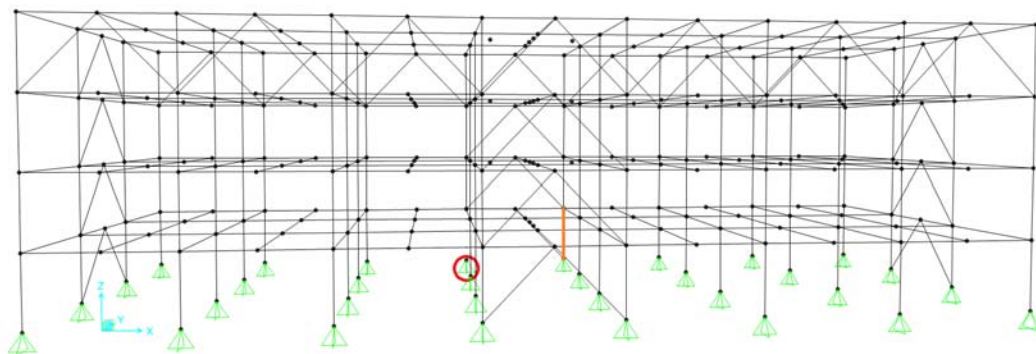


Figure 61. Configuration A2 column removal 1 failed members.

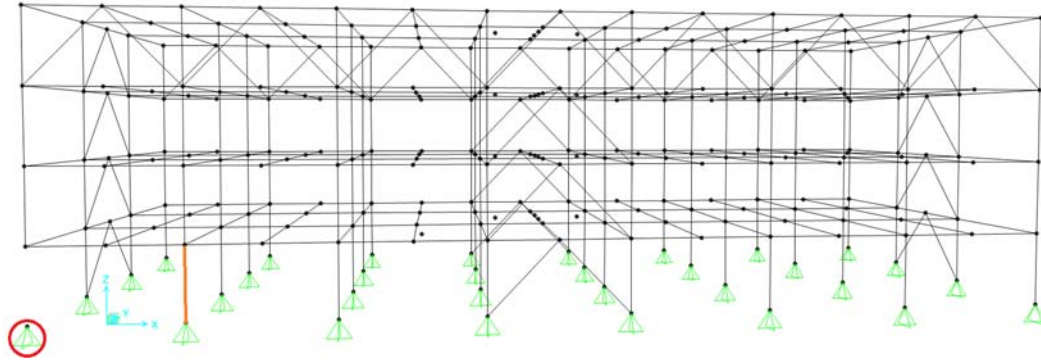


Figure 62. Configuration A2 column removal 2 failed members.

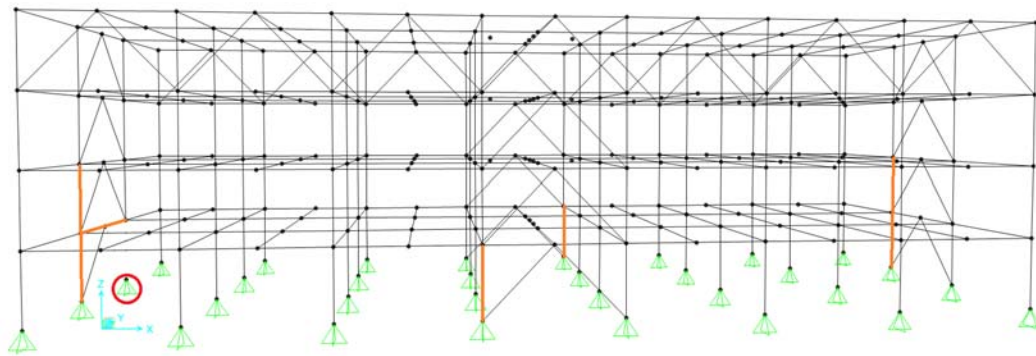


Figure 63. Configuration A2 column removal 5 failed members.

The torsion effect was most clearly seen in column removal 5, which was similar to column removal 2 in A1. The deflected shape of the building is shown in Figure 64. Note that the deflection is amplified in the figure. Although 7 members failed throughout the structure, this number is less than the 15 that failed in A1 removal 2. Because of this reduction, the stiff-story in A2 appeared to have helped resist the damaging effect of torsion by increasing overall structural rigidity.

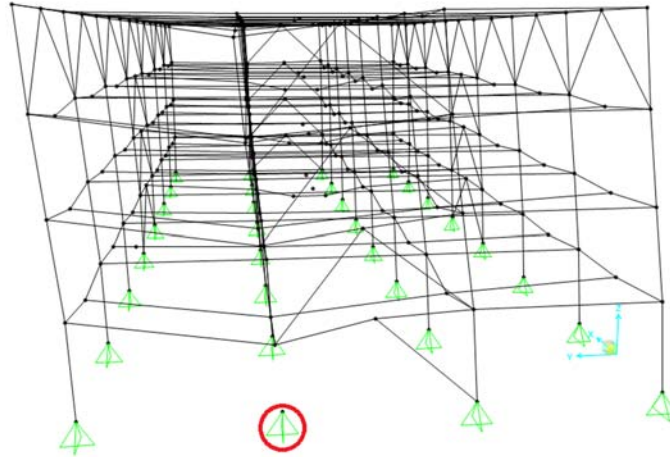


Figure 64. A2 column removal 5 deflected shape.

The lack of failed members in both column removals 3 and 4 suggests that the stiff-story helped to redistribute the loads from the affected area.

#### 4.4.6 Configuration A3

This section details the column removal procedure and results as applicable to Configuration A3. A3 was identical to A2 except that stiff-story chevron braces were added on the NS sides of the building using W10X30 members. This addition created a wraparound stiff-story along the whole fourth floor.

##### 4.4.6.1 Column Removal Locations

Five columns were removed from A3 (Figure 65). These locations were identical to the removal locations for A2.

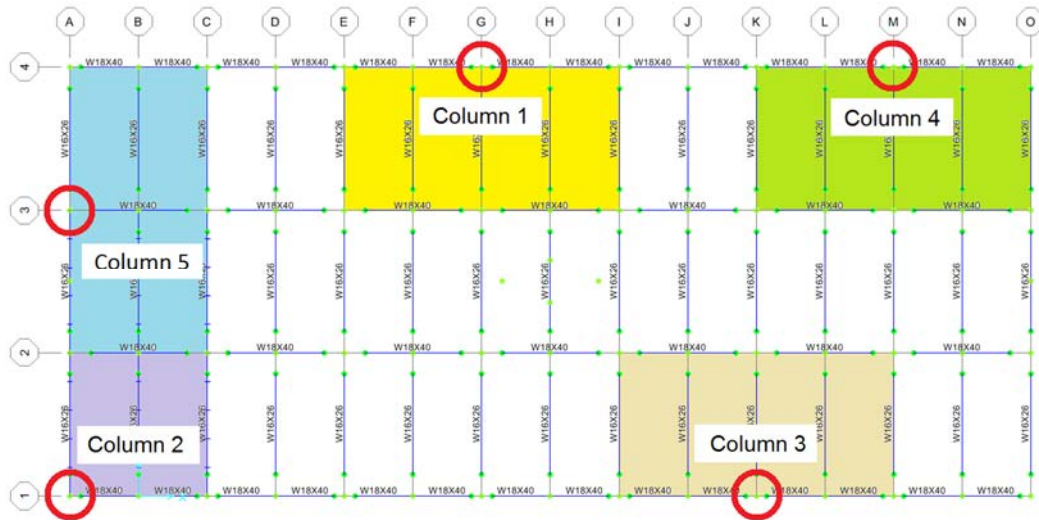


Figure 65. Configuration A3 column removals.

#### 4.4.6.2 M-factors

The m-factors for all beams, girders, and beam-to-column connections used to determine the increased loads for A3 are shown in Table 67. Most connections in the structure are simple shear tabs with  $d_{bg} = 6"$ . The connections to the braces include a gusset plate, with double angles connecting to the beams. For double angle connections,  $d_{bg} = 3"$ . Table 67 shows that the smallest m-factor for each column removal case is 1.50, based on primary double angle connections. The additional m-factors used to determine acceptance criteria were the same as those found for A1.

Table 67. Configuration A3 m-factors for determining increased loads.

Removed Column	Level	Beam / Girder	Primary or Secondary	Beam / Girder m-factor	Connection m-factor
1 (G-4)	2, 3, 4	W18X40	Primary	6.00	1.50*
	roof	W18X40	Primary	6.00	5.16 <sup>†</sup>
	2, 3	W18X40	Secondary	10.00	7.73 <sup>†</sup>
	2, 3, 4, roof	W16X26	Secondary	6.17	7.73 <sup>†</sup>
2 (A-1)	4	W18X40	Primary	6.00	1.50*
	roof	W18X40	Primary	6.00	5.16 <sup>†</sup>
	4, roof	W16X26	Primary	3.81	5.16 <sup>†</sup>
	2, 3	W16X26	Secondary	6.17	7.73 <sup>†</sup>
	2, 3	W18X40	Secondary	10.00	7.73 <sup>†</sup>
3 (K-1) 4 (M-4)	4	W18X40	Primary	6.00	1.50*
	roof	W18X40	Primary	6.00	5.16 <sup>†</sup>
	2, 3, 4, roof	W16X26	Secondary	6.17	7.73 <sup>†</sup>
	2, 3	W18X40	Secondary	10.00	7.73 <sup>†</sup>
5 (A-3)	2, 3, 4	W16X26	Primary	3.81	1.50*
	roof	W16X26	Primary	3.81	5.16 <sup>†</sup>
	2, 3	W16X26	Secondary	6.17	7.73 <sup>†</sup>
	2, 3, 4, roof	W18X40	Secondary	10.00	7.73 <sup>†</sup>

\*Double angle connection

<sup>†</sup>Shear tab connection

#### 4.4.6.3 Column Removal Loads

Since double angle m-factors controlled for all column removal cases, the column removal loads are all the same. The applied loads were the same as those applied to A1; for details see Section 4.4.4.3.

#### 4.4.6.4 Acceptance Results

The procedures outlined in Sections 2.5.5, 2.5.6, and 2.5.7 were used for the rest of the evaluation of A3. See Appendix C for the spreadsheet with results and acceptance criteria. The members not passing the acceptance criteria are shown in Table 68 and are highlighted in Figure 66. Column removal 1 was the only removal with a member failure; this member was an adjacent column. Even then, the column was only 4% overstressed. No other members failed in removal

1. Removals 2-5 had no failing members. Unlike the configurations without a NS stiff-story, torsion from NS side column removals was not an issue.

Table 68. A3 column removal results.

Column Removal 1 (G-4)				
Frame #	Section	Type	Controlling load type	DCR
1555	W12X40	Column	FC axial compression	1.04
Column Removal 2 (A-1)				
<i>No failures</i>				
Column Removal 3 (K-1)				
<i>No failures</i>				
Column Removal 4 (M-4)				
<i>No failures</i>				
Column Removal 5 (A-3)				
<i>No failures</i>				

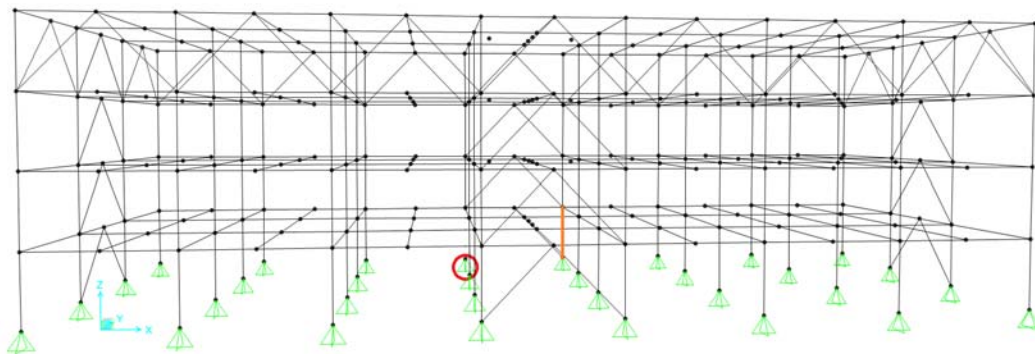


Figure 66. Configuration A3 column removal 1 failed members.

A3 performed very well, with only one member failure out of five column removals. Compared to A2, which had identical column removals and structure except for the lack of the NS stiff-story, A3 performed much better. A3 had only 11% of the failures that A2 had (1 compared to 9). Additionally, the W12X40 column that failed had a DCR of only 1.04. Using the AISC Steel Construction Manual Table 4-1, changing the column size to a W8X40 would provide an extra 4.6% compression capacity, which could reduce the DCR to 1.00. Changing to a W12X45 would provide an extra 12.5% compression capacity. The deflected shape of A3 is shown in Figure 67. Note that the deflection is amplified in the figure. Comparing the deflected shape of A3 with that

of A2 in Figure 64; the drift of the building is clearly less. Less torsional drift resulted in no member failures for A3 removal 5.

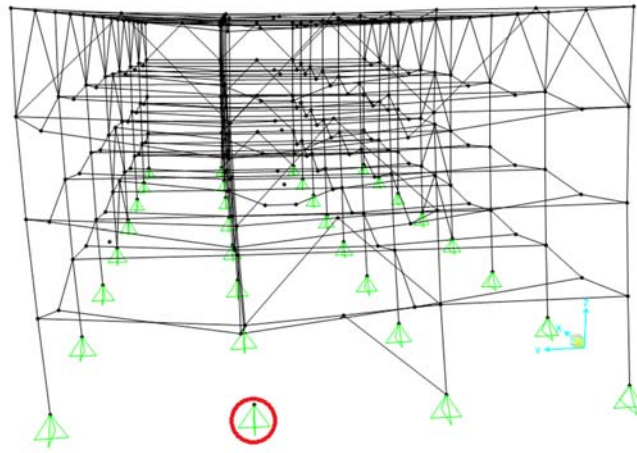


Figure 67. A3 column removal 5 deflected shape.

#### 4.4.7 Configuration B1

This section details the column removal procedure and results as applicable to Configuration B1.

##### 4.4.7.1 Column Removal Locations

Three columns were removed from B1 (Figure 68). Column removal 1 included members 251 and 57 (brace); removal 2 included member 1540 and 159 (brace); and removal 3 included member 569 and 577 (brace). Initially, since the NS sides of the building featured the same bracing configuration as A1, columns were not planned to be removed on these sides of the building. However, due to the torsion seen in A1, column removal 3 was included.

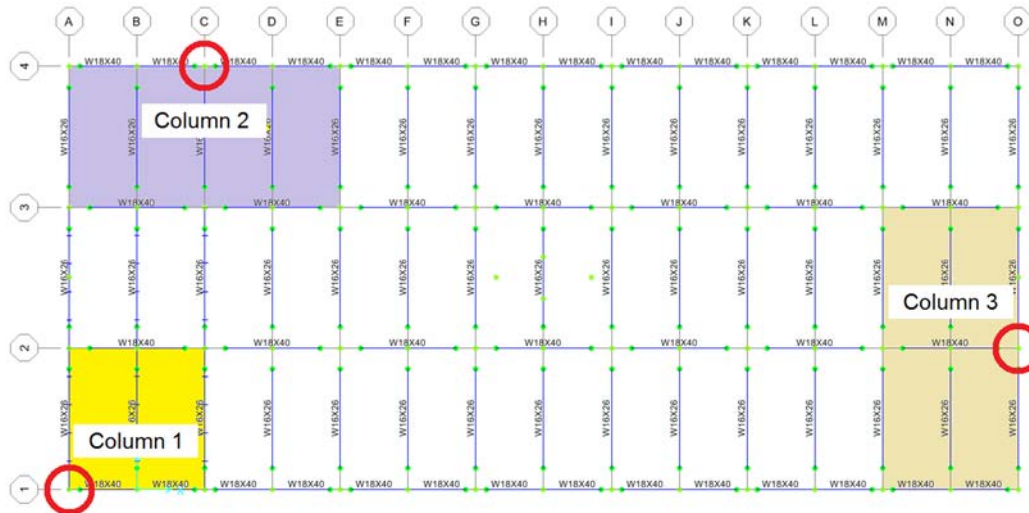


Figure 68. Configuration B1 column removals.

#### 4.4.7.2 M-factors

The m-factors for all beams, girders, and beam-to-column connections used to determine the increased loads for B1 are shown in Table 69. Most connections in the structure are simple shear tabs with  $d_{bg} = 6"$ . The connections to the braces include a gusset plate, with double angles connecting to the beams. For double angle connections,  $d_{bg} = 3"$ . Table 69 shows that the smallest m-factor for each column removal case is 1.50, based on primary double angle connections. The additional m-factors used to determine acceptance criteria were the same as those found for A1.

Table 69. Configuration B1 m-factors for determining increased loads.

Removed Column	Level	Beam / Girder	Primary or Secondary	Beam / Girder m-factor	Connection m-factor
1 (A-1)	2, 3, 4	W18X40	Primary	6.00	1.50*
	roof	W18X40	Primary	6.00	5.16†
	2, 3, 4, roof	W16X26	Secondary	6.17	7.73†
2 (C-4)	2, 3, 4	W18X40	Primary	6.00	1.50*
	roof	W18X40	Primary	6.00	5.16†
	2, 3, 4, roof	W16X26	Secondary	6.17	7.73†
	2, 3	W18X40	Secondary	10.00	7.73†
3 (O-2)	2, 3, 4	W16X26	Primary	3.81	1.50*
	roof	W16X26	Primary	3.81	5.16†
	2, 3, 4, roof	W16X26	Secondary	6.17	7.73†
	2, 3, 4, roof	W18X40	Secondary	10.00	7.73†

\*Double angle connection

†Shear tab connection

#### 4.4.7.3 Column Removal Loads

Since double angle m-factors controlled for all column removal cases, the column removal loads are all the same. The applied loads were the same as those applied to A1; for details see Section 4.4.4.3.

#### 4.4.7.4 Acceptance Results

The procedures outlined in Sections 2.5.5, 2.5.6, and 2.5.7 were used for the rest of the evaluation of B1. See Appendix C for the spreadsheet with results and acceptance criteria. The members not passing the acceptance criteria are shown in Table 66 and are highlighted in Figure 69 and Figure 70. Column removal 1 had no failures, removal 2 had one failure, and removal 3 had eleven failures. As in the other configurations without wraparound stiff stories, torsional effects were observed, although the extra braced frames in the EW direction helped reduce torsional effects slightly compared to A1, although the more member failures occurred than in A2 column removal 5.

Table 70. B1 column removal results.

Column Removal 1 (A-1)				
<i>No failures</i>				
Column Removal 2 (C-4)				
Frame #	Section	Type	Controlling load type	DCR
369	W12X40	Column	FC axial compression	1.17
Column Removal 3 (O-2)				
Frame #	Section	Type	Controlling load type	DCR
59	W12X40	Column	FC axial compression	1.08
1530	W12X40	Column	FC axial compression	2.07
1540	W12X40	Column	FC axial compression	1.55
1551	W12X40	Column	FC axial tension	1.01
69	W12X40	Column	FC axial compression	1.43
251	W12X40	Column	FC axial compression	1.38
572	W16X26	Beam	DC bending	2.02
587	W12X40	Column	FC axial compression	1.80
591	W12X40	Column	FC axial compression	1.31
593	W12X40	Column	FC axial compression	1.64
89	W6X15	Brace	DC axial compression	1.01

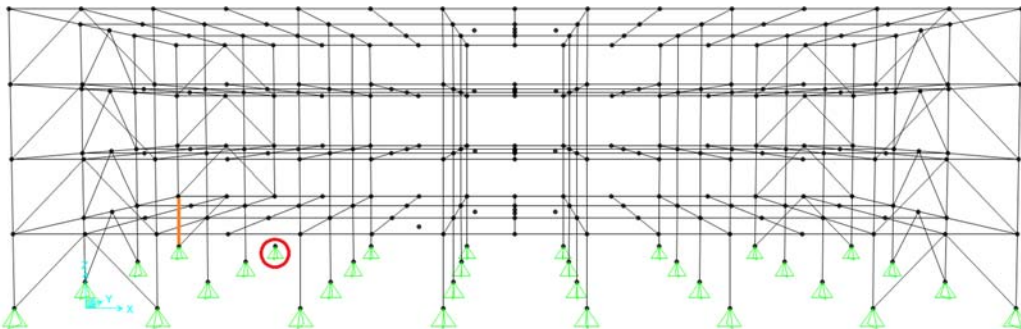


Figure 69. Configuration B1 column removal 2 failed members.

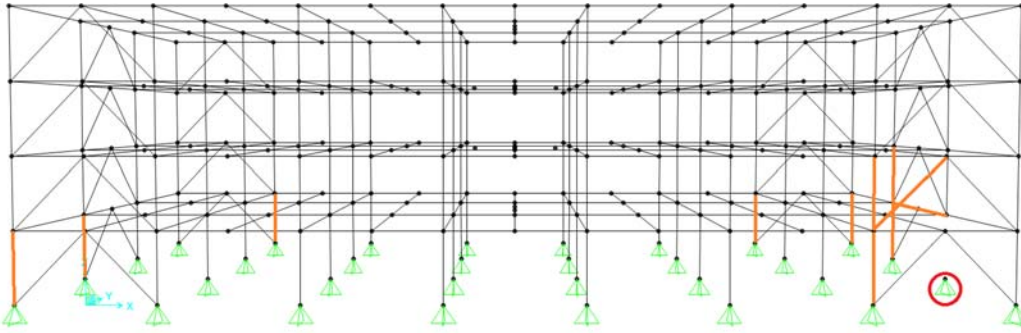


Figure 70. Configuration B1 column removal 3 failed members.

The torsion effect was most clearly seen in column removal 3, which was similar to column removal 2 in A1. The deflected shape of the building is shown in Figure 71. Note that the deflection is amplified in the figure. Although 11 members failed throughout the structure, this number is less than the 15 that failed in A1 removal 2. Because of this reduction, the modified bracing configuration in B1 appears to moderately help resist the damaging effect of torsion by increasing overall structural rigidity. Note that the brace sizes in B1 are smaller than in A1, A1B, and A2.

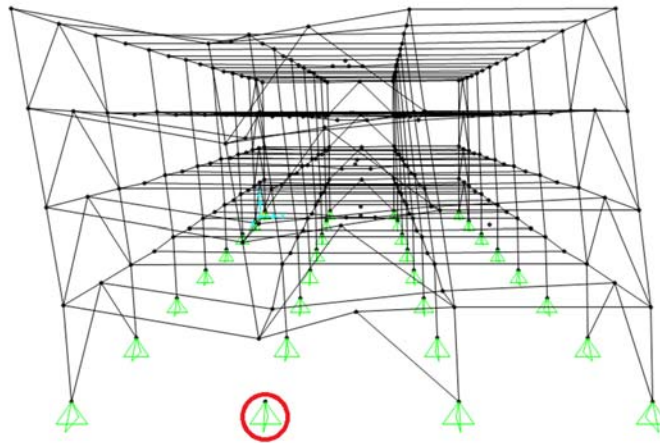


Figure 71. B1 column removal 3 deflected shape.

#### 4.4.8 Configuration B2

This section details the column removal procedure and results as applicable to Configuration B2.

##### 4.4.8.1 Column Removal Locations

Five columns were removed from B2 (Figure 72). Column removals 1-3 were identical to B1; removal 4 included member 1553 and removal 5 removed member 1534. Column removals 1-3

were supported by the LFRS bracing, while removal 4 and 5 were supported solely by B2's stiff-story.

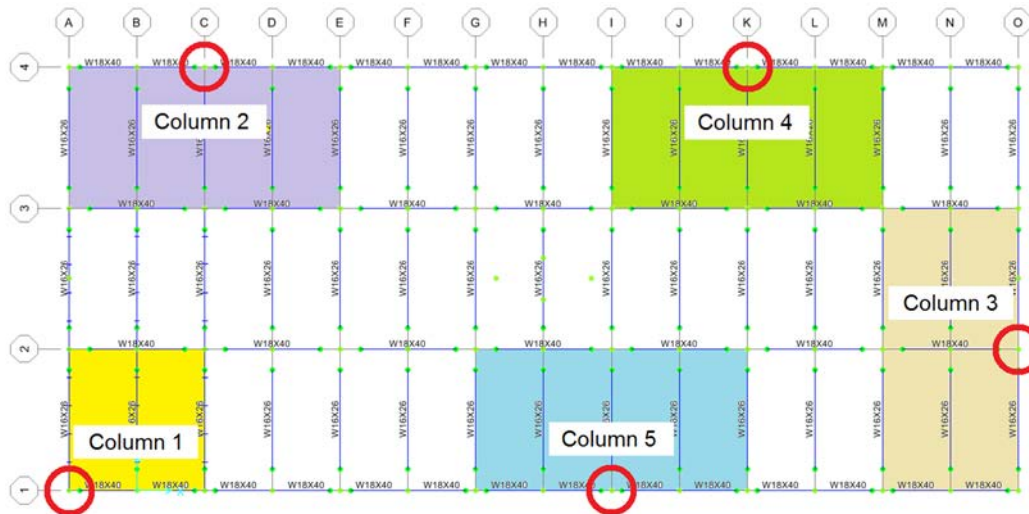


Figure 72. Configuration B2 column removals.

#### 4.4.8.2 M-factors

The m-factors for all beams, girders, and beam-to-column connections used to determine the increased loads for B2 are shown in Table 71. Most connections in the structure are simple shear tabs with  $d_{bg} = 6"$ . The connections to the braces include a gusset plate, with double angles connecting to the beams. For double angle connections,  $d_{bg} = 3"$ . Table 71 shows that the smallest m-factor for each column removal case is 1.50, based on primary double angle connections. The additional m-factors used to determine acceptance criteria were the same as those found for A1.

Table 71. Configuration B2 m-factors for determining increased loads.

Removed Column	Level	Beam / Girder	Primary or Secondary	Beam / Girder m-factor	Connection m-factor
1 (A-1)	2, 3, 4	W18X40	Primary	6.00	1.50*
	roof	W18X40	Primary	6.00	5.16†
	2, 3, 4, roof	W16X26	Secondary	6.17	7.73†
2 (C-4)	2, 3, 4	W18X40	Primary	6.00	1.50*
	roof	W18X40	Primary	6.00	5.16†
	2, 3, 4, roof	W16X26	Secondary	6.17	7.73†
	2, 3	W18X40	Secondary	10.00	7.73†
3 (O-2)	2, 3, 4	W16X26	Primary	3.81	1.50*
	roof	W16X26	Primary	3.81	5.16†
	2, 3, 4, roof	W16X26	Secondary	6.17	7.73†
	2, 3, 4, roof	W18X40	Secondary	10.00	7.73†
4 (K-4) 5 (I-1)	4	W18X40	Primary	6.00	1.50*
	roof	W18X40	Primary	6.00	5.16†
	2, 3, 4, roof	W16X26	Secondary	6.17	7.73†
	2, 3	W18X40	Secondary	10.00	7.73†

\*Double angle connection

†Shear tab connection

#### 4.4.8.3 Column Removal Loads

Since double angle m-factors controlled for all column removal cases, the column removal loads are all the same. The applied loads were the same as those applied to A1; for details see Section 4.4.4.3.

#### 4.4.8.4 Acceptance Results

The procedures outlined in Sections 2.5.5, 2.5.6, and 2.5.7 were used for the rest of the evaluation of B2. See Appendix C for the spreadsheet with results and acceptance criteria. The members not passing the acceptance criteria are shown in Table 72 and are highlighted in Figure 73. Column removals 1, 2, 4, and 5 had no failures, while removal 3 had seven member failures. Torsional effects caused failures in removal 3, which is similar to the NS column removal removals in the other configurations. Like A2, however, the stiff-story of B2 helped reduce the number of member failures.

Table 72. B2 column removal results.

Column Removal 1 (A-1)				
<i>No failures</i>				
Column Removal 2 (C-4)				
<i>No failures</i>				
Column Removal 3 (O-2)				
Frame #	Section	Type	Controlling load type	DCR
59	W12X40	Column	DC minor axis bending *	1.12
1530	W12X40	Column	FC axial compression *	1.13
69	W12X40	Column	FC axial compression	1.40
90	W12X40	Column	FC axial compression	1.03
572	W16X26	Beam	DC bending	1.06
587	W12X40	Column	FC axial compression	1.65
591	W12X40	Column	FC axial compression	1.29
Column Removal 4 (K-4)				
<i>No failures</i>				
Column Removal 5 (I-1)				
<i>No failures</i>				

\*The minor moment demand in the DC model was very large relative to capacity

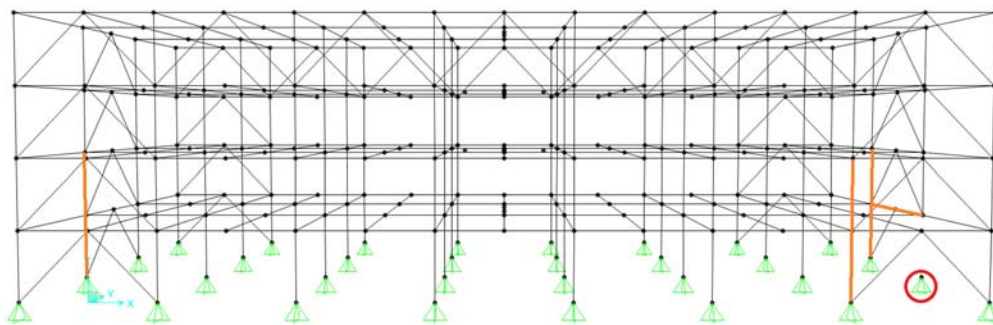


Figure 73. Configuration B2 column removal 3 failed members.

The torsion effect was most clearly observed in column removal 3. The deflected shape of the building is shown in Figure 74. Note that the deflection is amplified in the figure. Note that the brace sizes in B2 are smaller than in configurations A1-A3.

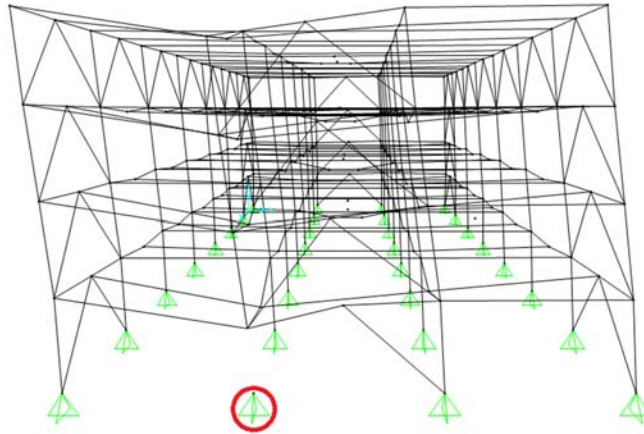


Figure 74. B2 column removal 3 deflected shape.

#### 4.4.9 Configuration B3

This section details the column removal procedure and results as applicable to Configuration B3. B3 was identical to B2 except that stiff-story chevron braces were added on the NS sides of the building using W10X30 members. This addition created a wraparound stiff-story along the whole fourth floor.

##### 4.4.9.1 Column Removal Locations

Five columns were removed from B3 (Figure 75). These locations were identical to the removal locations for B2.

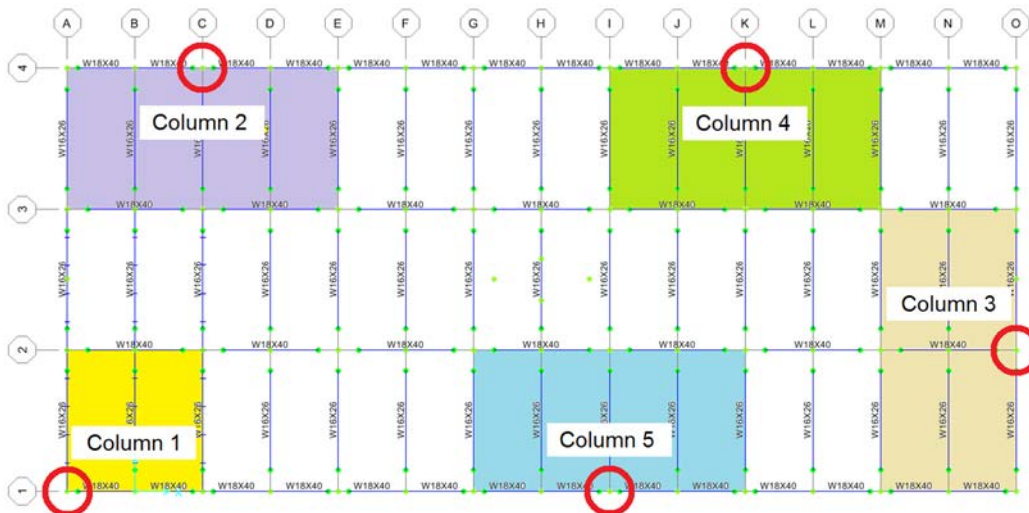


Figure 75. Configuration B3 column removals.

#### 4.4.9.2 M-factors

The m-factors for all beams, girders, and beam-to-column connections used to determine the increased loads for B3 are shown in Table 73. Most connections in the structure are simple shear tabs with  $d_{bg} = 6"$ . The connections to the braces include a gusset plate, with double angles connecting to the beams. For double angle connections,  $d_{bg} = 3"$ . Table 73 shows that the smallest m-factor for each column removal case is 1.50, based on primary double angle connections. The additional m-factors used to determine acceptance criteria were the same as those found for A1.

Table 73. Configuration B3 m-factors for determining increased loads.

Removed Column	Level	Beam / Girder	Primary or Secondary	Beam / Girder m-factor	Connection m-factor
1 (A-1)	2, 3, 4	W18X40	Primary	6.00	1.50*
	roof	W18X40	Primary	6.00	5.16†
	4, roof	W16X26	Primary	3.81	5.16†
	2, 3	W16X26	Secondary	6.17	7.73†
2 (C-4)	2, 3, 4	W18X40	Primary	6.00	1.50*
	roof	W18X40	Primary	6.00	5.16†
	2, 3, 4, roof	W16X26	Secondary	6.17	7.73†
	2, 3	W18X40	Secondary	10.00	7.73†
3 (O-2)	2, 3, 4	W16X26	Primary	3.81	1.50*
	roof	W16X26	Primary	3.81	5.16†
	2, 3	W16X26	Secondary	6.17	7.73†
	2, 3, 4, roof	W18X40	Secondary	10.00	7.73†
4 (K-4) 5 (I-1)	4	W18X40	Primary	6.00	1.50*
	roof	W18X40	Primary	6.00	5.16†
	2, 3, 4, roof	W16X26	Secondary	6.17	7.73†
	2, 3	W18X40	Secondary	10.00	7.73†

\*Double angle connection

†Shear tab connection

#### 4.4.9.3 Column Removal Loads

Since double angle m-factors controlled for all column removal cases, the column removal loads are all the same. The applied loads were the same as those applied to A1; for details see Section 4.4.4.3.

#### 4.4.9.4 Acceptance Results

The procedures outlined in Sections 2.5.5, 2.5.6, and 2.5.7 were used for the rest of the evaluation of B3. See Appendix C for the spreadsheet with results and acceptance criteria. The members not passing the acceptance criteria are shown in Table 74 and are highlighted in Figure 76 and Figure 77. Column removals 1, 2, and 3 had no failures, while removals 4 and 5 together had three column failures. Torsional effects were mitigated by the NS stiff-story and did not contribute to any member failures. The only column failures that occurred were due to removals of columns solely supported by the EW stiff-story. This suggests that the W6X15 stiff-story braces were inadequate to redistribute the loads from the removed columns. Worth noting, however, is that the member failures in removals 4 and 5 were due to DCRs that were only 1-2% higher than those of B2 removals 4 and 5, which did not have any failures. Changing the section size to a W8X40 or W12X45 could reduce the DCR to less than 1.00.

Table 74. B3 column removal results.

Column Removal 1 (A-1)				
<i>No failures</i>				
Column Removal 2 (C-4)				
<i>No failures</i>				
Column Removal 3 (O-2)				
<i>No failures</i>				
Column Removal 4 (K-4)				
Frame #	Section	Type	Controlling load type	DCR
1555	W12X40	Column	FC axial compression	1.01
Column Removal 5 (I-1)				
Frame #	Section	Type	Controlling load type	DCR
1523	W12X40	Column	FC axial compression	1.01
1532	W12X40	Column	FC axial compression	1.00

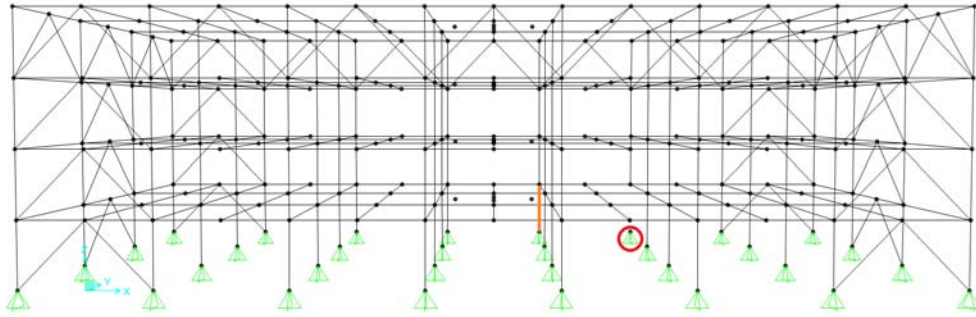


Figure 76. Configuration B3 column removal 4 failed members.

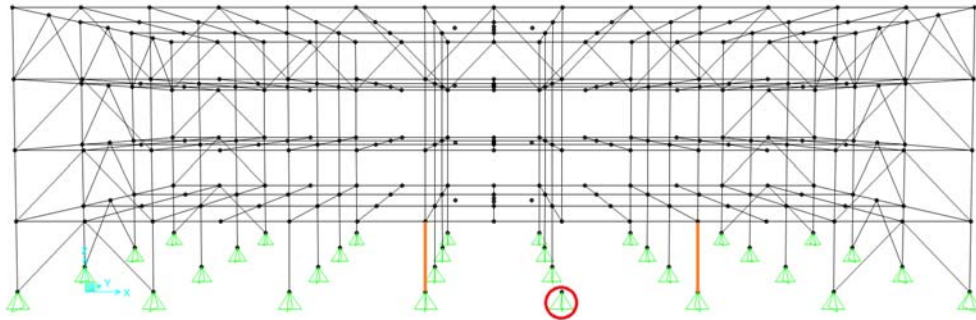


Figure 77. Configuration B3 column removal 5 failed members.

Compared to B2, which had identical column removals and structure except for the lack of the NS stiff-story, B3 performed better. B3 had four fewer member failures than B2 (3 compared to 7). The deflected shape of B3 is shown in Figure 78. Note that the deflection is amplified in the figure. Compare the deflected shape of B3 with that of B2 in Figure 74; the drift of the building is clearly less. Less torsion-caused drift resulted in no member failures for B3 removal 3.

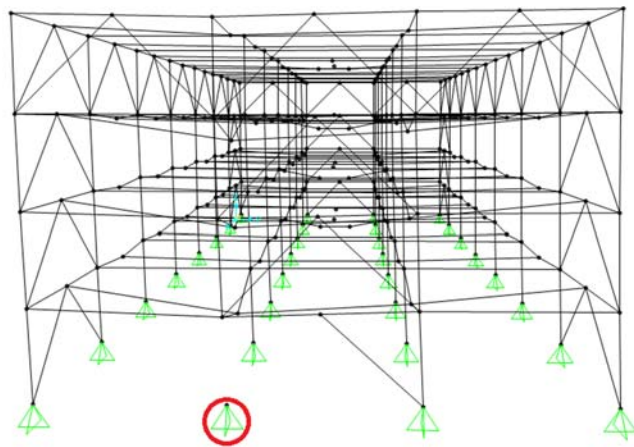
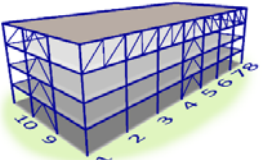
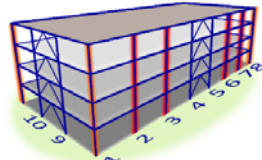
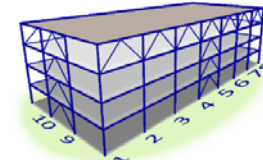
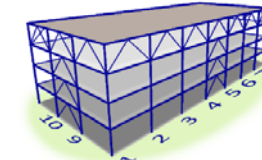
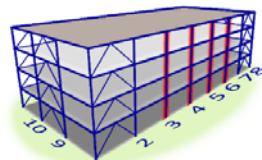
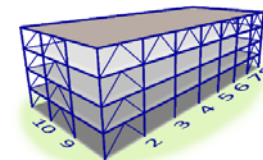
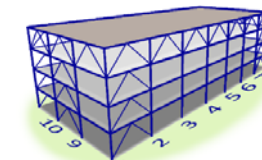


Figure 78. B3 column removal 3 deflected shape.

#### 4.4.10 Summary and Concluding Remarks

Table 45 summarizes the results from all seven buildings analyzed. CM refers to the number of columns whose removal would result in a collapse mechanism. Only A1 and B1 have possible collapse mechanisms. All other configurations prevent collapse mechanisms by using stiff-stories.

Table 75. Lamar Construction results summary.

 A0 CM = 0 RE = 24	 A1 CM = 12 RE = 34	 A2 CM = 0 RE = 18	 A3 CM = 0 RE = 2
	 B1 CM = 8 RE = 24	 B2 CM = 0 RE = 14	 B3 CM = 0 RE = 4
CM = collapse mechanism RE = elements requiring redesign			

A summary of both series (A and B) is presented next:

A series:

- The A series involved buildings with one braced frame at each NS exterior frame and one braced frame for each external frame in the EW direction, between columns 4-5. A1 did not have a stiff-story element; A2 had a stiff-story at the upper level in the EW direction; A3 was similar to A2, but had a stiff-story in the NS direction also. A0 is similar to A2, but its stiff-story geometry is similar to the one in the original building.
- Configuration A1 is very vulnerable. Because it does not employ a stiff-story, it has 12 columns which, if removed, would result in a collapse mechanism.
- While A2 employed a stiff-story, it had 18 members requiring redesign. Removing column marked 9 or 10 caused a plan rotation. This rotation is responsible for most of the elements requiring redesign.
- The plan rotation was seen for all configurations. Additional stiffness in the NS direction would help reduce this issue. For example, configuration A3 had significant reduction in the number of members requiring redesign since the stiff-story employed in the NS

direction provided continuity with the stiff-story in the EW direction and additional resistance against the plan torsion.

- The only column failed in column A3 was one FC column under case 4. The DCR was only 1.04. Thus, basically no failure is found in A3. Thus, it can be concluded that A3 is a successful configuration as originally designed. Future work should include designing columns part of the stiff-story for column loss to prevent any members from exceeding DCR limits.

#### B series:

- Buildings in the B series were identical in overall geometry to the A series. The only difference being that two braced frames for each external frame in the EW direction were employed. In the NS direction, only one braced frame at each NS exterior frame was employed. B1 did not have a stiff-story element; B2 had a stiff-story at the upper level in the EW direction; B3 was similar to B2, but had a stiff-story in the NS direction also.
- B1 has 8 columns vulnerable, resulting in CM under static analysis. B2 and B3 have stiff stories which prevent any failure mechanism.
- For B1, column removal 2 resulted in failure of column 1. This was caused by all the extra load going to column 1. B2 did not have failure when removing column marked 2 because the load in that removed column is transferred through the stiff-story to two adjacent columns, not only 1.
- For B1, removing column marked 1 did not cause any failure because the area of increased loads for column marked 1 (corner column) is smaller compared to column marked 2, thus less demand on the adjacent column.
- B2 only had failures when removing columns marked 9 or 10 because of the torsion issue. However, where the stiff-story was placed (from columns 1 to 8) no failure was observed.
- For B2, when a column 2 to 7 is lost the load is redistributed to 2 adjacent columns. B1 has 4 of those 6 columns vulnerable, depending on the connections and the slab (not modeled in these analyses).
- For B1 and B2, cases 1 and 8, the load is redistributed only to 1 adjacent column (2 or 7 respectively). However, because these are corner columns the tributary area is half of the tributary area in cases 2 to 7, resulting in a similar demand at the adjacent members.
- B2 and B3 behaved almost identically. B3 had 1 FC member failure when removing column marked 3 and 1 FC member fail under when removing column marked 4,

however, the DCRs were 1.01. Those same members did not fail for B2, however, the DCRs were just under 1.0.

- The stiff-story in the short direction included for configuration B3 eliminated any torsion and resulted in no members requiring redesign when removing columns marked 9 and 10.

Observations made from a comparison between series A and series B are presented next:

A1 vs. B1:

- B1 has 8 vulnerable columns while A1 has 12. Removing any of those columns would result in a CM in the static analysis. Contribution from the connection and the slab could help; however, based on previous studies, that alone would not be sufficient.
- Both buildings have torsion issues (removing columns marked 9 or 10).

A2 vs. B2:

- Both buildings behaved very similarly.
- Both buildings had torsion issues when columns marked 9 or 10 were removed, resulting in seven members failed for each building.
- A2 had one member fail (DCR = 1.05) when removing column marked 1 and one member fail when removing column marked 4 (DCR = 1.04). B2 did not have failure for either of those two column removal cases. However, the DCR ratios are just under 1.0, thus, having very similar results.

A3 vs. B3:

- Both buildings had similar behavior.
- Both buildings had 1 failure when removing column marked 4 (DCR = 1.04 and 1.01)
- B3 had 1 member fail when removing column marked 3 (DCR = 1.01)
- Torsion was reduced for both buildings. The stiff-story in the short direction worked together with the stiff-story in the long direction to reduce the lateral deformation of the braced frames in the short direction.

The analysis results from the configurations that featured stiff stories showed that the stiff-story concept can, when adequately designed, redistribute loads throughout the structure. Many column removals from the configurations supported by stiff stories had no member failures. Some had one or two column failures, which could easily be remedied with a slightly larger section size. The torsional effect was the primary problem encountered; once it was mitigated, failures were limited to the local column removal area.

## 5 Alternative Framing Strategies

### 5.1 Introduction

This chapter summarizes observations and evaluations of alternative framing strategies. Specifically, the American Zinc and Lamar configurations studied in Chapters 3 and 4 were assessed for relative robustness. Best practices for integration of stiff stories with the lateral force resisting systems (LFRSs) were also noted.

### 5.2 Initial development of indices

Some initial development of factors and indices to quantify vulnerability, robustness and efficiency, was conducted prior to completion of the column removal analyses for American Zinc and Lamar building configurations. The objective was to provide guidance for comparing configurations and determining the optimal balance of structural robustness and efficiency. Most of these factors and indices were later revised based on analysis results. However, the initial, basic approach still formed the foundation for evaluation of alternative framing strategies. The basic approach is described in this section.

The configuration alternatives were compared using factors based on the number of vulnerable columns, and amount of bracing or moment connections. Vulnerable columns were defined as columns lacking adjacent lateral bracing or moment connections that could provide an alternate load path in the event of column loss. The total number of vulnerable exterior columns was used in determining a “vulnerability factor” to compare the configurations. Corner columns were given more weight in the vulnerability factor, because tests on gravity framing systems had shown less resistance to collapse at these locations (Johnson et al., 2014).

To evaluate the amount of support given to columns adjacent to lateral bracing or moment connections, a “support factor” was also created. The support factor accounts for the support due to lateral bracing or moment connections on the exterior columns. In its initial development, the support factor considered the total number of braces or moment connections attached to a column at levels above the first story. For corner columns, the number of lateral braces or moment connections attached to the column was multiplied by a weighting factor to represent the more critical position of the corner columns. Ground floor lateral braces or moment connections were not included in the support factor, because ground floor braces would be required to be removed in a column removal analysis.

The total number of braced or moment-connected bays was modified into a “bracing factor” which represents the decimal percentage of exterior bays within the story that are laterally braced or moment-connected. A braced bay was defined as a 1-story, 1-bay section with diagonal braces or moment connections. The bracing factor,  $B_F$ , shown in Equation 16, was established as a simple way of representing the relative efficiency of the combined stiff-story and lateral bracing system.

$$B_F = \gamma_B \cdot \frac{n_{BBEW} + n_{BBNS}}{n_B} \quad \text{Equation 16}$$

Where:

- $n_{BBEW}$  is the number of braced bays in the EW direction;
- $n_{BBNS}$  is the number of braced bays in the NS direction;
- $n_B$  is the total number of exterior bays on structure (80 for the Lamar configurations); and
- $\gamma_B$  is the bracing factor weighting multiplier of 5, to convert the factor to a scale of 0 to 5.

The vulnerability factor and the support factor were then combined into a “robustness index.” The intent of the robustness index was to identify configurations that maximize structural robustness and minimize the number of vulnerable columns. The “efficiency index,” was a combination of the support factor and the bracing factor.

The support factor, robustness index, and efficiency index were scaled such that higher numbers are more desirable. For the vulnerability factor and bracing factor, lower numbers are more desirable. These factors and indices were assessed and revised with respect the column removal analysis results.

### 5.3 Evaluation of Alternative Framing Strategies

After completion of the column removal analyses of the various configurations for the American Zinc and Lamar building, these factors were revisited. Based on the analysis results, the collection of factors and indices was simplified to two representative factors, a revised support factor,  $S_F$ , and the bracing factor,  $B_F$ . With this reduction to two factors, some redundancy among factors and indices was eliminated. Furthermore, the two factors better reflected the scope of the parametric study, which was based on relatively simple building configurations and one design approach, and did not include economic considerations. The revised support factor provides some

indication of the relative robustness of the system, while the bracing factor provides an indication of the relative effectiveness of a particular framing configuration in resisting collapse.

For convenience, the tables summarizing the number of collapse mechanisms (CM) and the number of elements requiring redesign (RE) are repeated in Table 76 and Table 77. Note that the different framing configurations were designed for gravity and lateral loads only; column loss and alternate paths were not considered.

Table 76. American Zinc results summary.

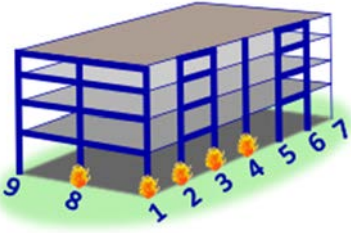
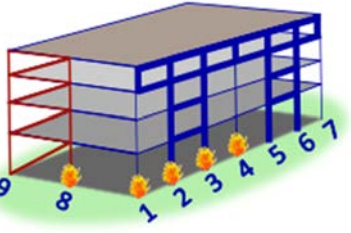
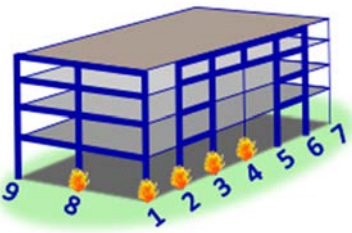
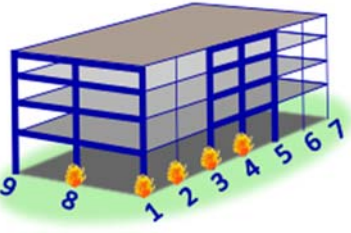
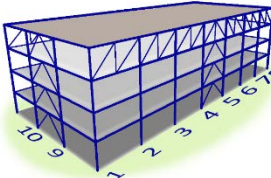
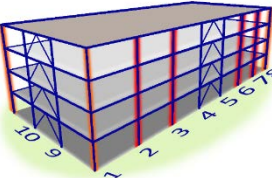
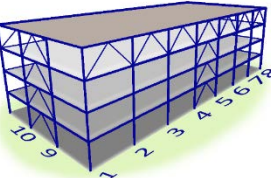
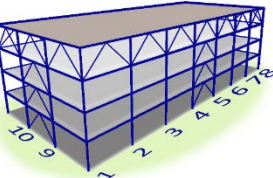
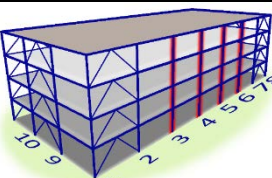
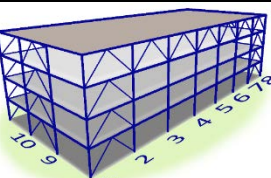
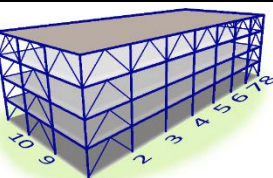
 <p>C1 CM = 0 RE = 0</p>	 <p>C2b CM = 0 RE = 1</p>	 <p>C3b CM = 0 RE = 0</p>
 <p>D1 CM = 4 RE = 0</p>		
<p>CM = collapse mechanism RE = elements requiring redesign</p>		

Table 77. Lamar Construction results summary.

 <p>A0 CM = 0 RE = 24</p>	 <p>A1 CM = 12 RE = 34</p>	 <p>A2 CM = 0 RE = 18</p>	 <p>A3 CM = 0 RE = 2</p>
	 <p>B1 CM = 8 RE = 24</p>	 <p>B2 CM = 0 RE = 14</p>	 <p>B3 CM = 0 RE = 4</p>
<p>CM = collapse mechanism RE = elements requiring redesign</p>			

From the column removal analysis results, it was determined that the support factor should be revised to be based simply on the percentage of exterior columns that are supported by a braced frame, moment frame, or stiff-story. For these case study buildings, each column from ground to roof would count as one column. For a taller building, which might have stiff stories at intervals over its height, this accounting of columns may need to be revised. The stiff stories are effective at preventing CMs for any sections of columns below.

For Lamar configuration A1, the support factor,  $S_F$ , would then be based on 8 columns supported (or 40% of 20 exterior columns), and for B1, the factor would be based on 12 columns supported (or 60%). The weighting factor for the corner columns was eliminated, since the location of the column did not appear to have any bearing on collapse. The percentage of columns was multiplied by 10 to place the support factor on a scale of 0 to 10.  $S_F$  is 10 for any configuration with a stiff-story and LFRS supporting all exterior columns. As shown in Figure 79, there is now a direct correlation of support factor,  $S_F$ , to number of collapse mechanisms (CM). CM could also be converted to a scale of 0 to 10. Or, both CM and  $S_F$  could be represented as percentages to more clearly show that CM and  $S_F$  are essentially complements of one another (e.g., 60% of columns supported translates into 40% of columns collapsing, while 100% of columns supported ( $S_F = 10$ ) results in no collapse mechanisms).

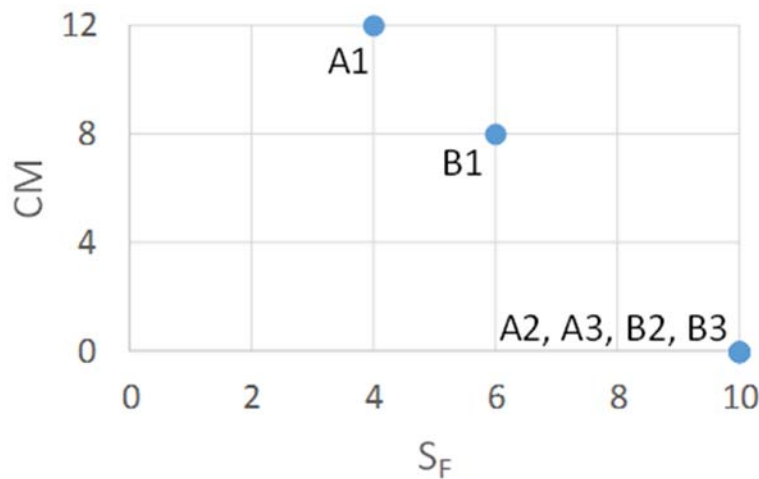


Figure 79. Support factor,  $S_F$ , versus collapse mechanisms, CM, for the Lamar configurations

The bracing factor equation remained the same. Relative efficiency, or effectiveness, of different framing solutions would vary by designer. However, if following the same design approach used in this study, and if defining higher effectiveness by lower numbers of members requiring

redesign, then the bracing factor ( $B_F$ ) provides some indication of relative effectiveness of a given configuration. Again, note that column loss was not considered in the design of the different configurations studied. Furthermore, relative economy was not within the scope of the study. Relative economy of framing solutions would depend on designer, fabricator, regional factors, and so on.

The relationship between bracing factor and relative effectiveness can be seen in a plot of  $B_F$  versus RE (Figure 80). A higher  $B_F$  generally means a lower number of members requiring redesign. For most of the configurations studied, a higher bracing factor,  $B_F$ , is preferred. The exceptions are configurations A3 and B3, discussed in more detail later. Note that the bracing factor comparison should be made for framing systems with the same type of LFRS (i.e., all braced frame configurations). The bracing factor only applies in the case of braced frames, essentially all Lamar configurations in this study. However, some general observations (in the following paragraph) also apply to the one American Zinc configuration that included braced frames in the short direction (C2b).

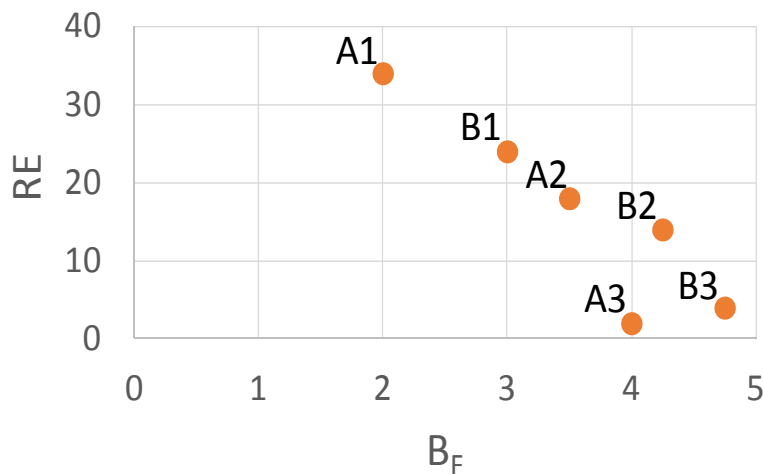


Figure 80. Bracing factor,  $B_F$ , versus elements requiring redesign, RE, for the Lamar configurations.

For buildings with braced frames, some effectiveness can be gained by running the stiff-story around the entire perimeter of the building, as in Configurations A3 and B3 for the Lamar building. This helps to reduce effects of plan torsion when a column in a braced frame is removed. This benefit can be seen in Figure 80; the two configurations with the lowest RE values are Configurations A3 and B3. The converse can be seen in the American Zinc configuration with the

braced frame but stiff-stories only in the long direction of the building (Configuration C2b). Meanwhile, for the two Lamar configurations with stiff-stories continuous around the perimeter, a lower bracing factor,  $B_F$ , reflects the more efficient A3 configuration.

#### *5.4 Integration with Lateral Force Resisting Systems*

The evaluation of the alternative configurations for American Zinc and Lamar also demonstrated that essentially any stiff-story solution that ties in with the LFRS and supports all columns will be robust. This can be seen in a comparison of the revised support factor,  $S_F$ , and the number of collapse mechanisms (CMs). For both buildings, this comparison shows that buildings without stiff stories will have CMs at all columns that are unsupported.

#### *5.5 Conclusions*

Early on in this study, thought was given to robustness of alternative framing strategies and the parameters necessary to quantify relative robustness. Based on the literature, a collection of factors and indices were developed to characterize relative vulnerability, robustness and efficiency. These factors and indices were revised and simplified to two factors based on the results of the column removal analyses for the American Zinc and Lamar configurations. The revised support factor provides some indication of the relative robustness of the system, while the bracing factor provides an indication of the relative effectiveness of a particular framing configuration in resisting collapse. Meanwhile, any stiff-story framing strategy that is integrated with the LFRS and supports all columns will be robust.

## 6 Nonlinear Analysis

### 6.1 Introduction

This chapter documents the nonlinear column removal analyses of the American Zinc and Lamar sister buildings, performed using SAP2000.

The basis of the nonlinear analysis was formed by the work described in Main and Sadek (2012) and Francisco (2014). Specifically, the reduced fiber method was used to represent the shear connections, and the strong/weak strip method with support fastener adjustments was used to represent the composite floor slab. Both of these methods were translated from Abaqus to SAP2000 with a few adjustments. Results from basic SAP2000 models were verified with Abaqus.

### 6.2 Modeling

The nonlinear analyses were performed by modifying the .sdb files created from the linear analysis, which already included the building frame geometry. Simplified gravity connections and slab representations were incorporated into these models.

SAP2000 was used to conduct the analyses in place of Abaqus because it is more commonly used in the design industry. Also, one of the primary advantages of using SAP2000 over Abaqus is the ease of model creation. SAP2000 allows for copying and replicating of frame and link elements, whereas Abaqus requires each part to be imported, as well as the unique creation of every wire-based connector element. SAP2000's focus on frame elements also allows for easier visualization of internal frame forces (bending moments). On the other hand, SAP2000's graphics engine is outdated, resulting in significant rendering delays. Ultimately, the decision to use SAP2000 was dictated by the goal of this analysis, which is to provide input and recommendations to designers through use of commercially common software.

#### 6.2.1 Shear Tab Connection Fiber Representation

Fiber connection models are used to represent the combined axial and bending behavior of shear tab connections in a realistic way. Shear tab connections are typically idealized as pinned connections, but, in a nonlinear column removal analysis, it is important to realistically represent the actual moment and tension resisting behavior in order to accurately assess the capacity of the structure. This is achieved by representing each bolt as a nonlinear fiber that has both axial and shear properties. Load-deformation curves are specified for the nonlinear bolt springs, based on work from Main and Sadek, 2012. These bolt fibers are connected by a series of rigid links that represent the actual dimensions of the shear connection. A shear tab fiber is used to account

for out-of-plane movement in the plate, while a gap element is used to represent gap closure (Main and Sadek, 2012). When the beam rotates due to a column loss scenario, there is the potential for the beam flange to conflict with the column; this gap spring is used in locations where closure of the beam setback gap is possible. Figure 81b shows an example of the shear tab connection fiber configuration and its components. The strong/weak strips shown in Figure 81a are representative of the composite slab and will be described further in Section 6.2.2.

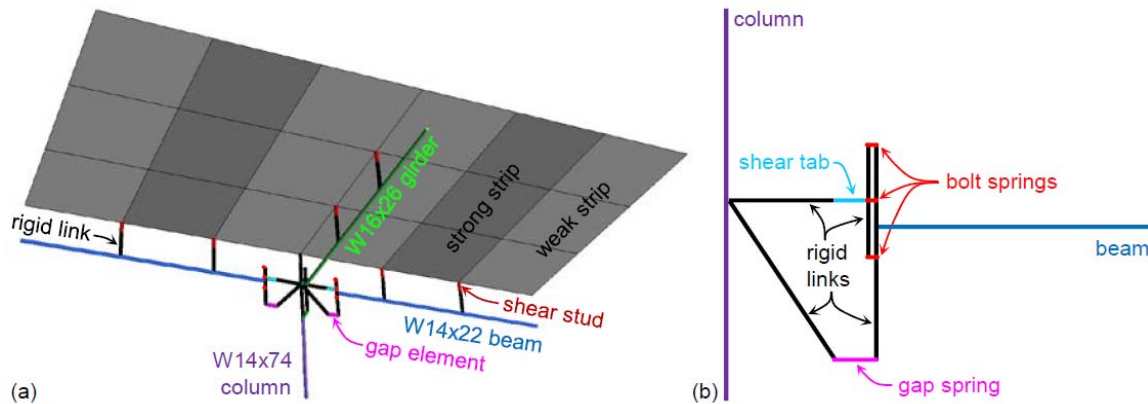


Figure 81. Reduced Model Construction in Main and Sadek (2012): (a) composite floor system; (b) beam-to-column connection.

Each different beam to girder or girder to column connection requires a unique fiber representation because differences in the depths or orientation of the connected W-shapes can influence connection behavior. Therefore, the first step in creating the fiber connections is identifying each unique shear connection in the building based on member sizes, beam copes, connection geometry, etc.

Figure 82 illustrates examples of two basic fiber representations for the American Zinc building. These are W16 beams with 3-bolt connections. The main goal of the fibers is to link the centerlines of the connector elements. The connecting point is always at the center of the bolt group. Using traditional connection detailing and accounting for differences, such as lowering bolt locations to accommodate beam copes, each connection was modeled with property geometric offsets.

Zero length springs, which are outlined in the Main and Sadek (2012) approach, are not possible in SAP2000 because two points cannot exist in the same location. This led to the creation of an offset at the bolt fibers. The bolt fibers are given a nominal 0.5" length, which is offset from the bolt centerline 0.25" in either direction, as shown. Comparisons conducted with an equivalent Abaqus model showed that this change did not affect connection behavior.

The shear tab element is used to represent the out-of-plane rigidity and torsional rigidity of the shear tab. Its parameters are based on properties of detailed finite element models of the 3-bolt shear tab (Main and Sadek 2012).

To maintain consistency with the linear analysis approach, a 1/4" thick plate and 3/4" A325N bolts were assumed for the gravity connections. In the Lamar building, 4-bolt connections were used with W18 girders, which resulted in different properties for the shear tab and bolt fibers. Additionally, W16 beams framed into W18 girders so the bottom flange of the beams did not need to be coped and the gap element was located at the beam bottom flange, unlike the top of the cope, as shown in Figure 82b.

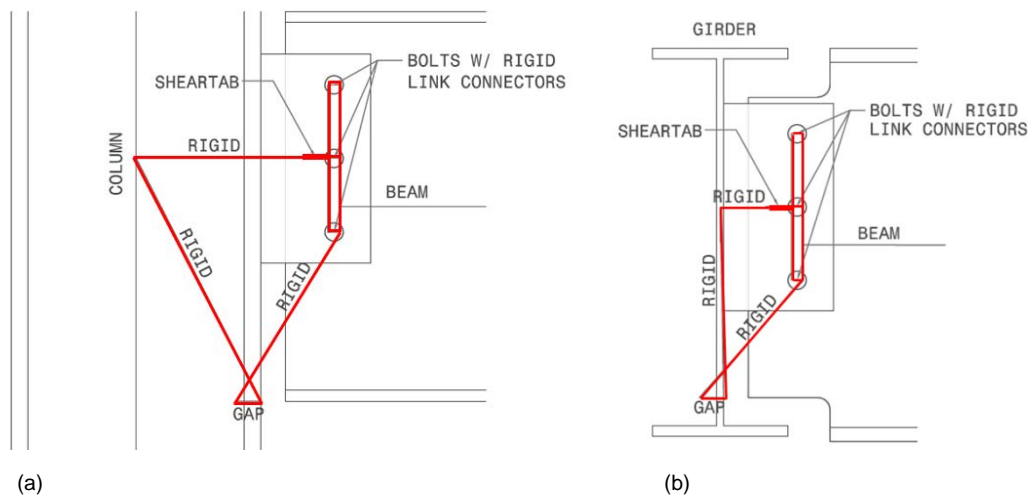


Figure 82. Fiber representation examples: (a) beam-to-column flange; (b) beam-to-girder.

The gap element required some iteration because the default 'gap element' definition in SAP2000 does not work for this configuration. Because link elements in SAP2000 use local coordinate systems for their backbone behavior, closing the gap was impossible due to the simultaneous rotation of the connection. Therefore, an arbitrary 1" element was defined that extends beyond the simulated edge of the connected element, as shown in Figure 82. This gap element is designed to open, rather than close; therefore, the rigid links at the gap element cross over each other (Figure 82). The backbone curve of the element is set to have zero stiffness up to 1" of axial extension, at which point the element becomes extremely stiff (essentially rigid). While the behavior may be slightly different than an actual gap element, it was determined to be a good approximation. The gap elements only need to be created at connections where gap closure is possible, namely at the ends of beams and girders that are away from the removed column (where

a moment creates compression at the bottom of the connection). The displacements that are reached in most of the column removal models are also not large enough to reach closure, so implementing the gap elements may not be necessary unless it is observed that closure might be possible.

#### 6.2.1.1 Limitations of the Connection Modeling

The connection models are used to represent standard shear tab connections; whenever the framing geometry prevents this connection from being used, there are model limitations. The lateral connections, connection offsets due to differing beam depths, and extended shear tabs are among these limitations.

Fiber connection modeling per Main and Sadek (2012) only encompasses shear tab gravity connections. All of the moment connections in the Vierendeel truss of the American Zinc building were modeled as fully fixed. Additionally, all gusset plate connections for the braced frames and the roof truss in the Lamar building were modeled as ideally pinned. Further studies would be needed to capture this connection behavior using a modified version of the reduced fiber connection modeling approach.

The connection point for the gravity framing members to the supporting member corresponds to the centerline of the shear tab connection. The elevations of these beams are dictated by the connection geometry in Figure 82 and by matching the top-of-steel elevations. Therefore, when beams frame into a deeper girder, as shown below in Figure 83, this creates a vertical offset and a lack of support. Particular attention should be taken to these locations and a rigid link should be added as necessary in order for the beams to be supported by the girder. It is recommended that the deflected shape of the analyzed model should be scaled significantly in order to identify potential disconnects in the modeling, which is very plausible due to all of the connector elements and different connection details.

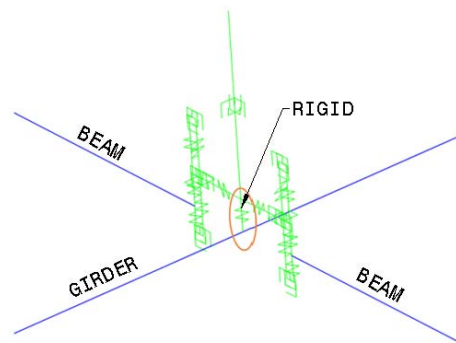


Figure 83. Beams framing into interior girder, showing need for rigid link for support.

Beams framing into the column web would likely use an extended shear tab configuration; however, instead of designing this specifically, and in order to conform to the limitations of Main and Sadek's work, a standard shear tab was used with the assumption that the tab would be braced at the top and bottom by stiffener plates. Work from Liu and Astaneh-Asl (2000) shows that extended shear tabs with stiffener plates exhibit comparable rotations and behavior compared to simple shear tabs.

### 6.2.2 Slab Representation

The representation of the composite slab in the American Zinc building is based directly on work from Main and Sadek (2012) and Francisco (2014). The strong/weak strip approach with support fastener (e.g., puddle weld or shear stud) adjustments was used, with modifications to fit the new dimensions. Additional work also included an investigation of the effects of slab continuity.

A typical 3" steel deck with a 3.25" lightweight concrete topping (for a total slab thickness of 6.25") was assumed, based on the models used in Francisco (2014). The dead load calculations used in the building design of the American Zinc building and the subsequent linear column removal models assumed a 3" steel deck with a 4.5" normal weight concrete topping (total of 7.5"). However, a slab thickness of 6.25" was used for the nonlinear models because that thickness was used for all preliminary Abaqus and SAP2000 comparisons; additionally, it is more commonly used in industry. For these reasons, the Lamar sister building was later designed with a 6.25" composite slab, in order to establish consistency between the linear and nonlinear analyses.

The strong/weak strip approach consists of layered nonlinear shell elements which are split into alternating strips, representing the ribbed nature of the composite slab (Figure 84). The strong strip, representing the thickest portion of the slab, has the following layers: steel deck, concrete, welded wire reinforcement (WWR), and another concrete layer. The weak strip, representing the thinner portion of the slab, has a dummy layer, a WWR layer and a concrete layer. The dummy layer is a null layer made of a material with negligible stiffness and strength, and allows for consistency between the shell reference surface in the strong and weak strips. To be conservative, there is not a steel layer in the weak strip due to both the weakness of the slab in the transverse direction and the reduced engagement of the steel in the longitudinal direction. This configuration also assumes the WWR is placed directly on the deck (not represented in Figure 84).

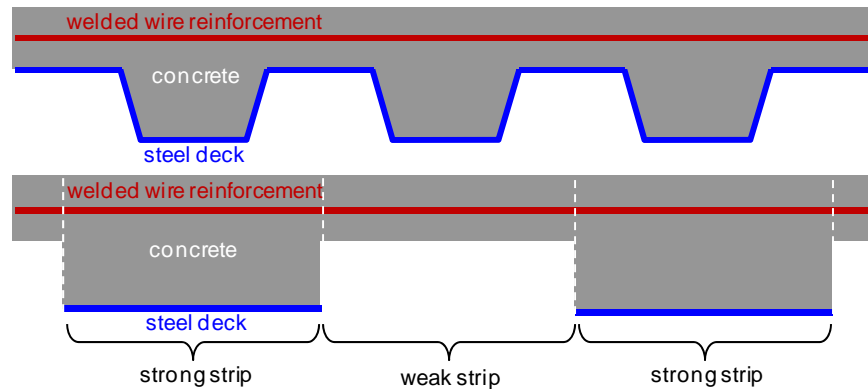


Figure 84. Example of strong/weak strip formulation [Main and Sadek (2012)].

In addition to the strong and weak strips, a third shell element definition was created called “StrongStripPW.” This element definition has the same layers as the strong strip, except the steel layer has a reduced thickness and altered material properties which are intended to mimic the behavior of the support fastener connection. More detail about this modification due to support fasteners can be found in Francisco (2014).

A typical layout of these shell elements is shown in Figure 85. The strong and weak strips alternate, while the adjusted strong strips are placed at locations where the metal deck would be expected to terminate (i.e., girder lines). The size of these shell elements is not based on the width of the ribs in the metal deck profile; instead, the elements are roughly 24” x 24” (dependent on the bay geometry), which was a recommendation of Main and Sadek (2012) that was determined to be a good compromise between computational efficiency and resolution for visualization of stresses. It was also shown that by locating the weak strips along girder lines, the widths of the strips could be increased without a change in overall system behavior. Thus, shell elements in the sister buildings were modeled with dimensions as close to 24”x24” as the bay geometry would permit. This allowed the use of the same material properties as in the 24” x 24” elements studied previously by others, specifically with regard to the support fastener adjustments. Larger changes in element size would require re-evaluation of those adjustment properties.

It is also important to note that the shell elements nearest the major columns (i.e., the columns that extend all the way from the ground to roof level) were removed, accounting for the possible lack of continuity in those locations. However, the shell elements near the minor columns in the American Zinc building (e.g., B-3) were retained.



Figure 85. Typical shell element layout of one bay in American Zinc building.

The orientation of the local axes of the slab elements is crucial for designating the strong and weak direction of the deck. When copying shell (area) elements, it is best to avoid using the ‘mirror’ function, especially when dealing with composite layout shell elements because it inverts the local axes of the affected elements, flipping the order of the layers.

The connections between the shell elements and the beams and girders are accomplished using link elements representing shear studs. The shear studs have nonlinear spring properties in both shear directions, based on those outlined in Main and Sadek (2012). Because the spacing of the connectors is approximately 24”, twice that of the expected 12” (one every rib), the force component of the shear stud backbone curve is doubled. This is not necessarily critical because,

as long as the shear studs do not reach failure, their behavior has been shown to have little effect on the overall response.

#### 6.2.2.1 Roof Representation

Representation of the roof proved to be difficult. Roof deck is typically shallower than floor deck (1.5" compared to 3"), and does not include concrete topping.

Several techniques were attempted in SAP2000 to model the roof deck. First, the strong/weak strip approach was modified such that only the strong strips would be in place, and they would only include the steel layer (i.e., no concrete layers) with equivalent thicknesses for membrane and bending behavior. The SAP2000 solver was unable to deal with this. Another attempt reduced the shell elements into truss elements representing the area of the deck (a grillage model). This provided very inconsistent results, with minimal change in the overall system response.

Due to this inconsistency, and in some cases nonsensical results, the implementation of the roof deck was discontinued and a composite slab was used instead. The roof slab was designed for the lighter loads so a thinner cross-section was used: 2" deck and 3 ¼" lightweight concrete topping. While this approach is not reminiscent of traditional buildings, it can still help to compare the relative stiffness of the column removal scenarios and the effect of the stiff-story. As an alternative, bare steel framing (without any type of deck) could have been conservatively used; however, because of the confidence and knowledge base for modeling the composite floor, it was decided to use a composite roof system. Both bare steel and composite framing were modeled for the various column removal scenarios with differing degrees of impact on the overall system behavior, as shown in the Results section. It is left to the designer's discretion to determine how to appropriately model the roof system.

#### 6.2.2.2 Limitations of Slab Representation

The exterior moment frames in the American Zinc sister building introduced challenges in dimensional matching. Figure 86 below shows column A-3, where, in the linear analysis models, moment frame beams of different sizes frame into the same point at their centerlines, resulting in inconsistent top-of-steel levels. Similar issues with the top of steel occurred in the Lamar sister building, where the beams in the stiff-story truss and braced frames were modeled as idealized pin connections and the beam centerline was set at the story level.

Usually, the shear studs are extended to the idealized center of the composite slab (i.e.:  $d/2 + 6.25"/2$ ); however, this is not possible for the moment framing elements due to the inconsistent

top-of-steel location. Therefore, the shear stud links connecting those elements to the slab are simply set to whatever length reaches to the slab; the slab location is set by the primary gravity beams. Therefore, it is possible that the slab may conflict with the exterior moment and gusset connected members. This is also the case in the shell elements outside the affected bays, as described in Section 6.2.3.

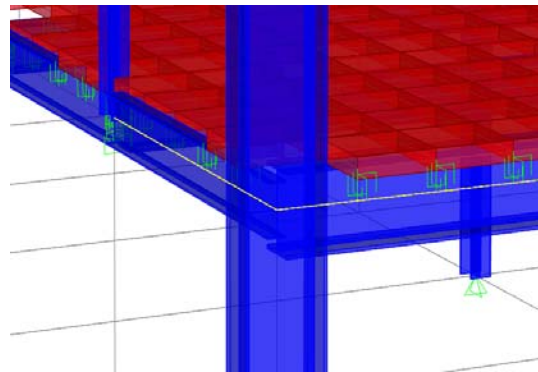
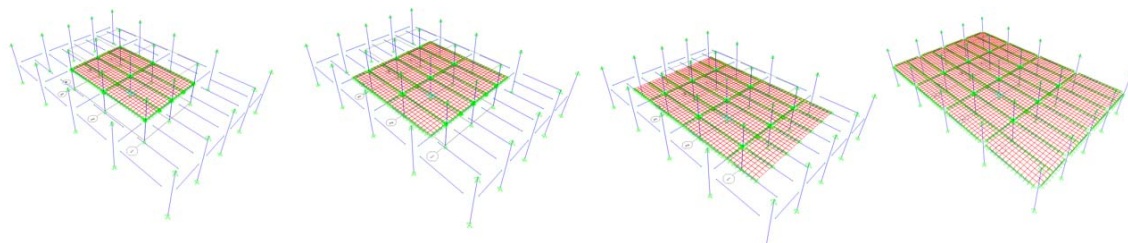


Figure 86. Moment frame beams at column A-3.

### 6.2.3 Extent of Modeling

Only the affected bays and a portion of the bays nearby were modeled with a floor slab and fiber shear tab connections, in order to maximize computational efficiency and efficacy. The amount of continuity required was investigated in models of the 20' x 30' system that was used in Main and Sadek (2012) and Francisco (2014). First, a 2 bay x 2 bay system was created with the full floor slab and fiber shear tab connections. This was modeled in both SAP2000 and Abaqus, in order to check the adequacy of the SAP2000 model. While the Abaqus model was able to reach much larger deformations, the vertical stiffness of the models were comparable (Figure 88). As previously noted, this led to the decision to continue modeling with SAP2000. Extending the 2 bay x 2 bay model to a 4 bay x 4 bay system without modification led to problems with SAP2000's solver, so a method of simplification was sought. First, two 4 bay x 4 bay models were developed. In these models, the slab was present only in the interior 2 bay x 2 bay area, with the steel framework extending beyond. One model included the fiber shear tab connections in the outer framework, while the other simplified the steel framework to assume pinned connections at shear tab locations. Results of a central column removal analysis showed little difference between these two models, except a higher displacement was reached before the analysis stopped running in the pinned connection case. This led to the implementation of only using the fiber connections in the immediately affected bay.

Further study was conducted regarding the contribution of continuity of the composite slab into bays beyond the affected bays. Using the 4 bay x 4 bay model with the pinned connection framework in the outer bays, a series of models were created with differing amounts of continuity. This progression is shown in Figure 87, starting with shell elements modeled in only the bays adjacent to the affected column (Reduced Frame). One introduced shell elements in the longitudinal direction that extended halfway in the next bay (Reduced Parallel 1/2). Another extended halfway in the longitudinal direction and halfway in the transverse direction (Reduced Both 1/2). A final model had the slab in all bays (Reduced Both). It's important to note that the shear stud connection between the beams and girders was maintained, although the beams and girders were not at their true heights in the outermost bays. This did not appear to have a significant effect on the behavior. Viewing results of a central column removal analysis for each of these models showed that continuity added stiffness to the system, in both the longitudinal and transverse directions. They also affected the SAP2000 solver, being unable to find convergence at an earlier displacement. The difference between extending the slab for half the bay versus the full bay was small (Figure 88), so further models were decided to include only that one half bay extension in both directions.



(a) Reduced Frame (b) Reduced Parallel  $\frac{1}{2}$  (c) Reduced Both  $\frac{1}{2}$  (d) Reduced Both

Figure 87. Progression of slab continuity models.

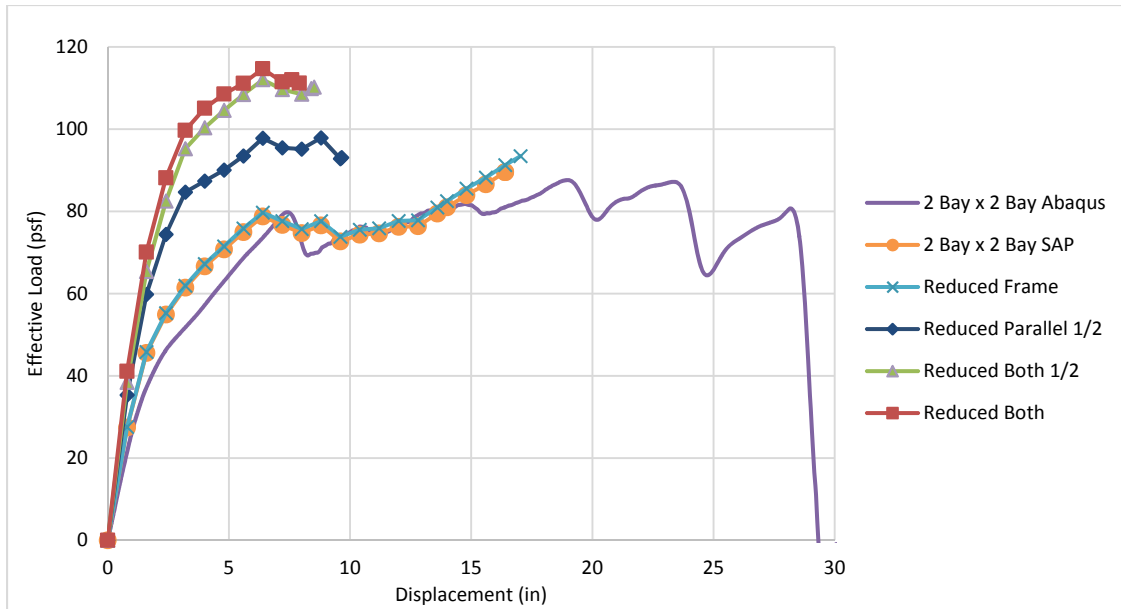


Figure 88. Results of progression of slab continuity models.

The extent of modeling can be seen below for the Alternate Column (E-2) removal scenario of the Lamar building. The blue shaded region shows the extents of the shell modeling for the slab. The pink shaded region shows where fiber shear connections are modeled (except for the moment connections).

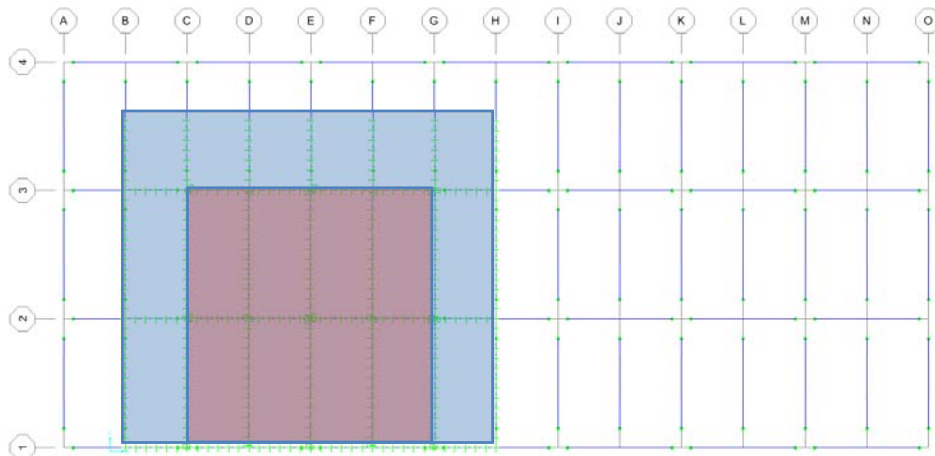


Figure 89. Extent of modeling for alternate column (E-2) scenario.

In the areas where the slab is not modeled, diaphragm constraints are used at each of the column nodes so that the structure moves rigidly together, as it would with a floor diaphragm, while also allowing out-of-plane deformations. Different diaphragm constraints should be created and applied at each level. Models were studied with and without constraints, and it was found that

using constraints in areas outside of the modeled slab portion is the best representation of actual results, which can be seen in the comparison below. When not using joint constraints, joint deformations occurred at nodes that were multiple bays away from the removed column, which is unrealistic behavior.

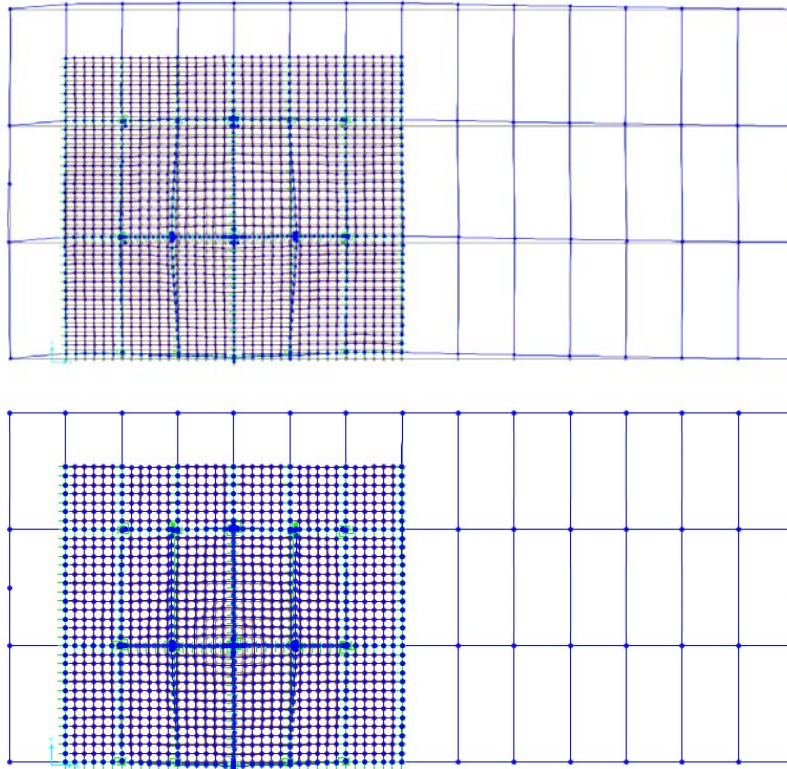


Figure 90. Deflected shape without constraints (above) and with constraints (below).

As can be seen in the lower graphic of Figure 90, the slab bows out at the perimeter of the affected bay. It is hypothesized that this is due to the compression ring that forms in the slab in a column removal scenario. While it was expected that the deflected shape should bow inwards toward the removed column, results were compared to results for comparable Abaqus models and found to correlate with the vertical deflections and behavior of the column removal case, confirming confidence in this approach.

### 6.3 Column Removal Analyses

Using the modeling methods described, various column removal scenarios were studied in SAP2000. Interior gravity columns C-2 (Central) and E-2 (Alt) were removed first because they consisted only of interior gravity connections that were most similar to the models described in

Main and Sadek (2012) and Francisco (2014). Upon satisfactory results of these scenarios, additional scenario models were constructed, matching the linear column removal scenarios.

For the American Zinc building, each of the column removal scenarios along the perimeter included at least two moment connections to the column. Again, the strong/weak strip approach and fiber connection modeling has not been previously tested for use with moment connected bays, so the results of these analyses must be carefully considered. Similar caution should be used when considering the stiff-story truss level of the Lamar building, which consists of brace connections.

For the application of the column removal itself, a load pattern was defined called 'DISP' (short for displacement) that was a dead load and had 0 for a self-weight multiplier. The load associated with this pattern was an applied 40" downward displacement at the base of the removed column. In other words, the column at the ground floor is not actually removed; it is merely pulled downward to simulate removal.

This load pattern is then used in a load case called 'DISP1'. This is a nonlinear static load case that considers P-Delta plus large displacements. The load application is set to displacement control, using a monitored displacement. The joint at the base of the 'removed' column is set as the monitored degree of freedom, and loading is monitored to a displacement magnitude of 40". This seemed to give the best results, although some variation of the nonlinear parameters was attempted to try to get better convergence, with very limited success. 50 steps were set to be saved, although all 50 were very rarely reached.

As noted several times, the SAP2000 solver had difficulty reaching the large displacements that were observed in the Abaqus models. However, this is not necessarily an adequate comparison, since the Abaqus models were quasi-static explicit time integration models, while the SAP2000 solver used in these column removal models was a nonlinear static case. A time history analysis is an option in SAP2000, but even more difficulties were experienced while trying to obtain results using that option. This option should be further investigated as a potential avenue for analysis.

### 6.3.1 Post-Processing

With the nonlinear static analysis, the model will run until it reaches the maximum number of steps (in this case, 100). That takes into account null steps, which are steps where the system fails to converge. This begins happening at various levels of displacement, and can be observed in the 'Analyzing' window. As the system fails to converge, it will reduce the step size. Once the step

size reaches a point where scientific notation is necessary, convergence will very rarely be reached on any subsequent step, and the analysis can safely be stopped.

Once the analysis is stopped either manually or by reaching the maximum number of steps, a load vs. displacement curve can be generated. This is done by pressing F12 (or Display -> Show Plot Functions) to bring up the 'Plot Function Trace Display Definition' box. This allows the user to define plot functions. Once the user defines a function that tracks the displacement of the node, as well as the reaction at that point, an overall load vs. displacement plot of the structure can be created. An additional option is to track the axial load in the columns at each level. The axial load in the column at the first story should be equal to the reaction at the bottom. By subtracting the load in the 2<sup>nd</sup> story column from the 1<sup>st</sup> story column, the load the 2<sup>nd</sup> story floor is taking can be determined. By dividing this load by the tributary area of that column, an effective distributed load can be determined. This procedure can be continued up to the top of the building, where the axial load in the 4<sup>th</sup> floor column is the load that the roof resists (which is expected to be much less than the other floors).

To export the data into Excel, the desired functions should be set as 'Vertical Functions', and displacement should be set as the 'Horizontal Plot Function'. After clicking 'Display' to check that things look correct, the data can be saved using the 'Save Named Set' button. Then, by either pressing CTRL+T (or Display -> Show Tables), and checking the box under 'Analysis Results, Structure Output, Named Set Data', the output data will show up in a table. The data in the table can then be exported in to Excel, where the analysis described above can be more easily performed.

## 6.4 Results

### 6.4.1 Results for American Zinc Sister Building

Load versus deformation plots were generated for each of the buildings and their respective column removal cases. As will be shown below, these results show a sensible progression of stiffness. However, the models tended to converge at varying and unpredictable times throughout the analysis, making it difficult to determine what caused these varying levels of convergence. In general, more elements seem to make it more likely that SAP will have issues with the solver, but this pattern was violated many times.

The hope was to be able to compare the gravity connection rotations achieved in the analysis with the experimental connections; however, the analysis failed to converge prior to achieving expected rotations. For instance, the Alternate Column in the American Zinc building deformed

6.4" (0.026 radians), which is well below the experimental rotations (0.1+ radians) and those determined in Liu and Astanteh-Asl (2000). Therefore, this procedure should not be used to determine the strength or rotation capacity of the system. Instead, it should only be used as a qualitative or comparative tool to explore different stiff-story configurations and orientations.

Figure 91 shows the load vs. displacement diagram for each of the column removal scenarios in the American Zinc building.

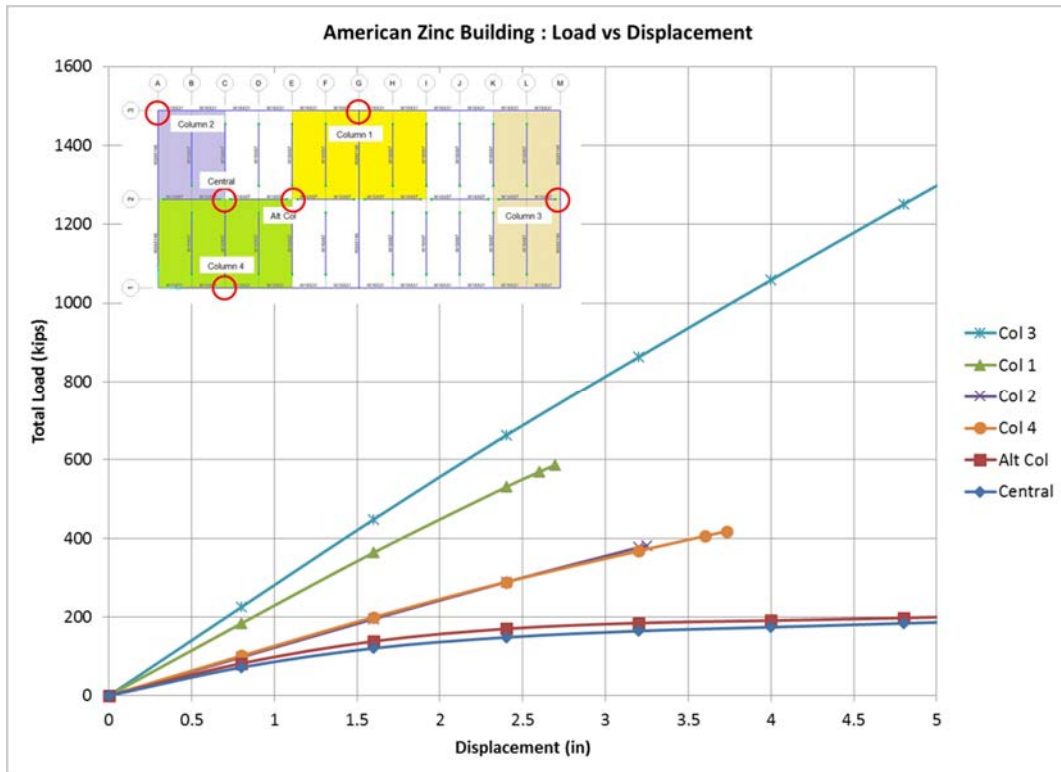


Figure 91. Column removal load vs. displacement for American Zinc sister building.

The results match with expected trends. The stiffest case, Column 3, is the column along the short edge of the building with very large beams framing into the moment connections (part of the NS lateral force resisting system). The second stiffest case, Column 1, has 3 moment connections framing into the column, with one of these connections a part of the NS lateral force resisting system. The middle range of stiffness, Columns 2 and 4, are the corner column removal case and a second edge column removal case, respectively. The corner column removal case has two moment connections, one of which is a part of the NS lateral force resisting system. The Column 4 edge removal case also only had two moment connections, but both were part of the Vierendeel truss system.

The two cases with the lowest stiffness are the two interior column removal cases, for which all beam-column connections are shear connections. The Alt Column case shows slightly more stiffness and capacity, which can be attributed to the additional continuity of slab that exists at that location.

As would be expected, the internal column removal cases experience nonlinear stiffness behavior. All of the perimeter column removal cases resulted in linear stiffness until failure to converge occurred. Again, it is still unknown what caused the analyses to terminate at deformations that were lower than expected and it is unclear what the stiffness would look like if the solver were able to process larger deformations. This is certainly a limitation of the approach that would benefit from additional study.

The maximum force achieved in the 'removed' column at the final step where analysis failed to converge was converted to an equivalent area load based on the tributary area of the column. This was calculated for each of the column removal cases and then compared to the loads calculated via the linear static procedure (deformation-controlled), as shown in Table 78. Each of the exterior columns in the nonlinear models exceeds the design loads calculated in the linear approach, which is expected and encouraging.

Table 78. Comparison of equivalent area load determined by nonlinear approach vs area load calculated with linear static procedure.

	Floor Load	Roof Load
Column 1	560 psf	484 psf
Column 2	735 psf	606 psf
Column 3	1450 psf	1167 psf
Column 4	415 psf	290 psf
Linear Static	333 psf	209 psf

As mentioned previously, a reliable method for modeling roof deck was never determined in SAP2000; instead, a composite slab was modeled at the roof because there was confidence and confirmation (through Abaqus comparisons) that the composite slab was being adequately modeled. A typical roof deck construction would have resulted in a system that is more stiff than a bare steel roof and less stiff than a composite roof system. For this reason, both bare steel and composite roof scenarios for each of the column cases were evaluated. In general, it was determined that the roof system did not contribute greatly to the overall stiffness of the 4-story building being studied (Figure 92). Similar results were found with the Lamar building.

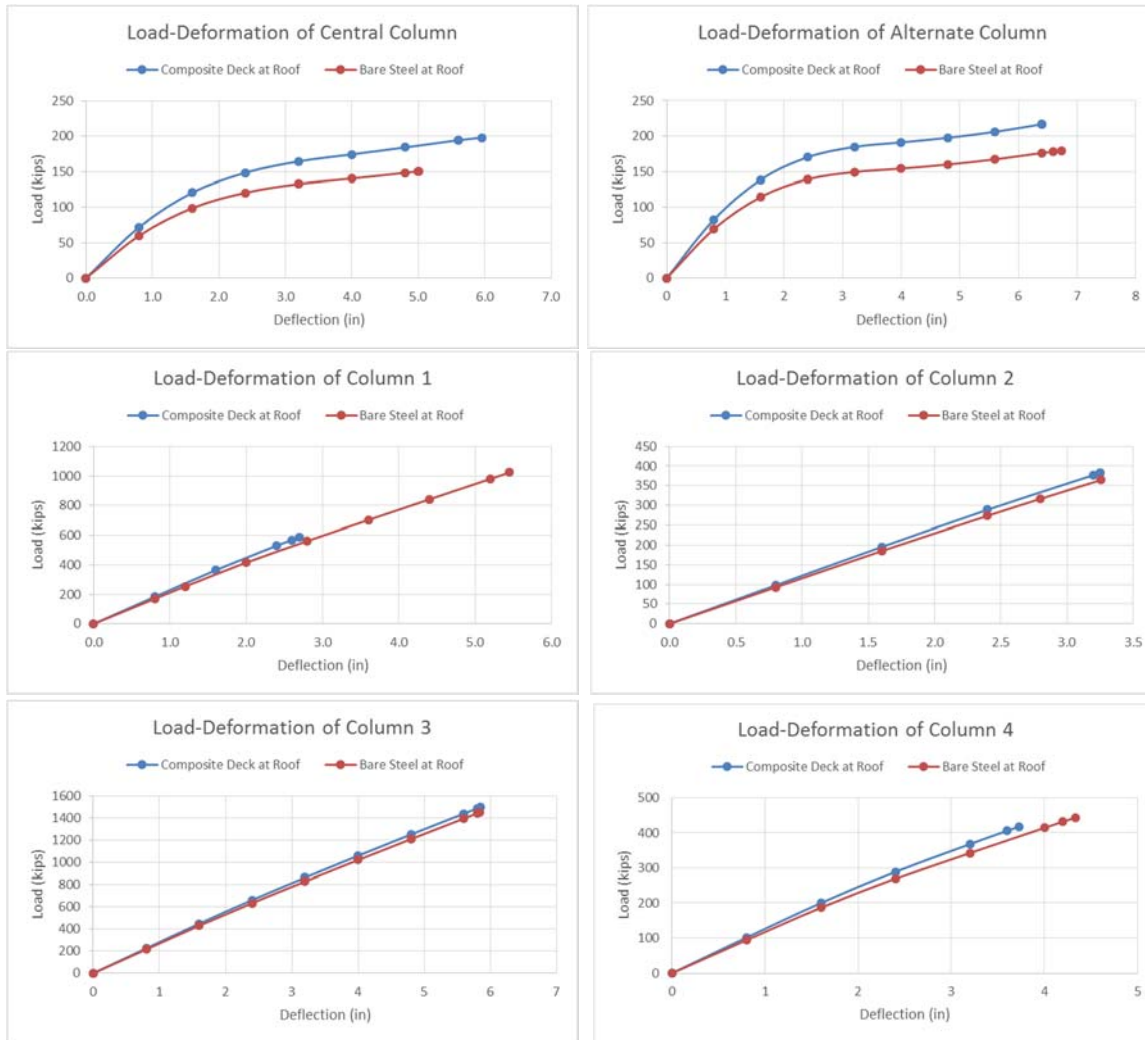


Figure 92. Influence of composite slab at roof: load vs. displacement for American Zinc building.

Despite the uncertainty in the level of convergence and roof deck modeling, the impact of the “stiff-story” concept can still be shown by comparing the sister building to a building with the same framing, but gravity connections along the perimeter. As can be seen in the column removal scenarios in Figure 93, the system is significantly stiffer with the Vierendeel truss. The effect of this change is not as significant with Columns 1 and 2, because they are stiffened by the moment frame connections that remain in the North-South direction. There is no effect to the Column 3 scenario because this is at the short end of the building, where there was not a truss. The same is true for the interior column removal cases. However, for the Column 4 scenario, the effect of the truss is very apparent, as the stiffness of the system without the truss appears to take on the same decaying stiffness behavior as the interior column removal cases.

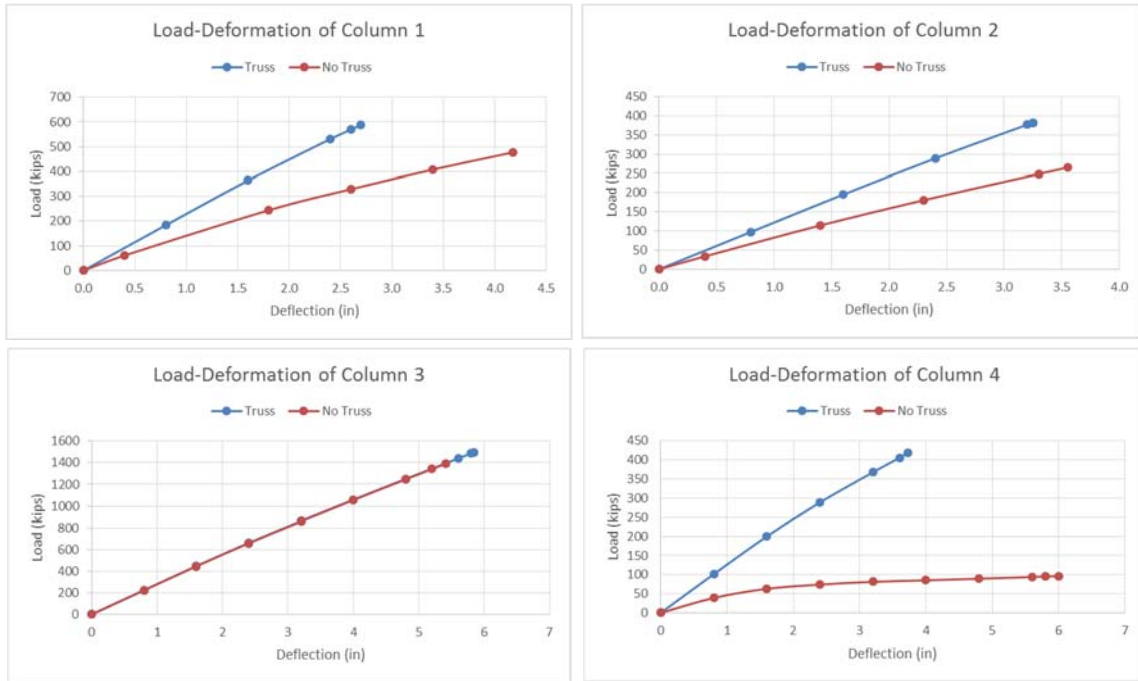


Figure 93. Column removal load vs. displacement comparison with and without Vierendeel truss.

#### 6.4.2 Results for Lamar Sister Building

Figure 94 shows the load vs. displacement diagram for each of the column removal scenarios in the Lamar building.

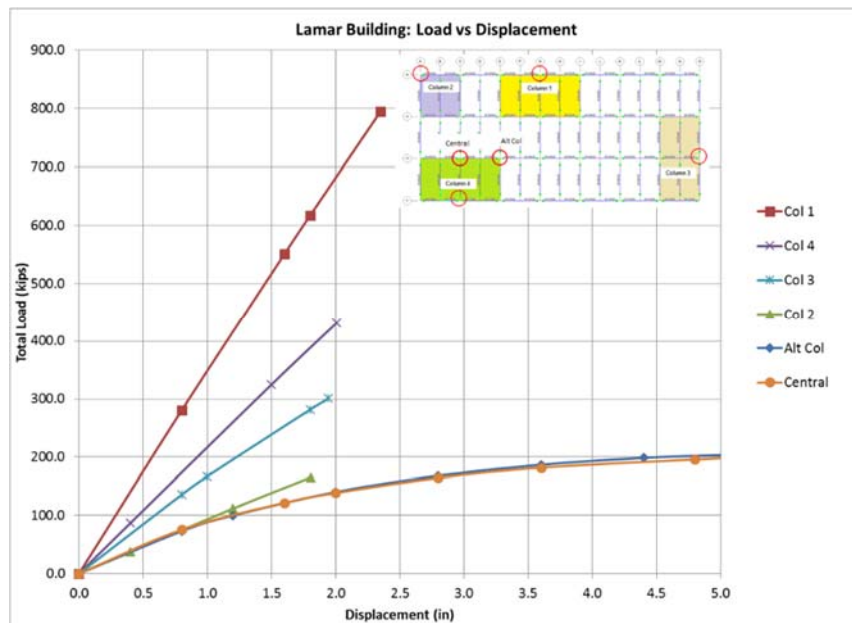


Figure 94. Column removal load vs. displacement for Lamar sister building.

Again, the results match with expected trends. The stiffest case, Column 1, occurs at a braced frame location, as shown in Figure 95. Whenever the column removal occurs at a braced frame location, as with Columns 1 and 3, the adjacent brace is removed per the UFC procedure. The braces above and adjacent to the removed column still provide substantial stiffness.

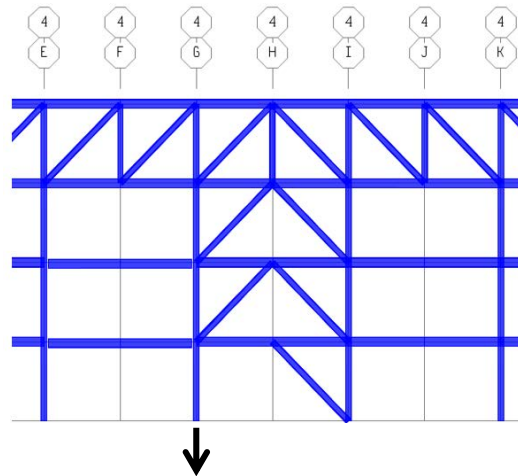


Figure 95. Column 1 removal scenario.

Column 4 is the second stiffest. It occurs at a location along the continuous roof truss. Because it is noticeably more stiff than Column 3, which occurs at a braced frame (but not along the roof truss), this shows the positive influence of the continuous roof truss on the system stiffness.

Column 2, the corner column, has the lowest stiffness of the exterior column scenarios because it occurs at the end of the truss (Figure 96). Had the truss continued in the NS direction, the Column 2 removal scenario would have likely been stiffer. Columns closer to the braced frames at column lines G and I are notably stiffer.

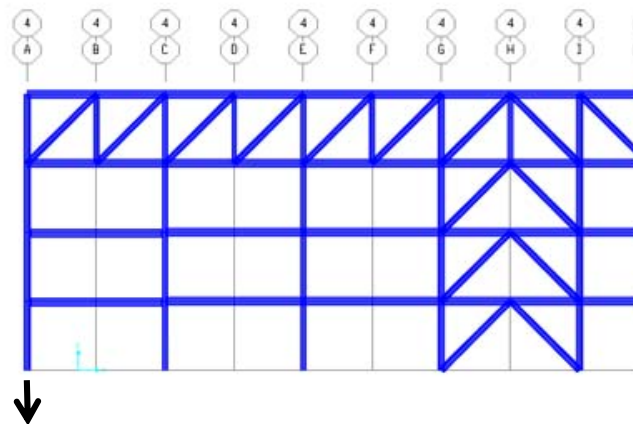


Figure 96. Column 2 removal scenario.

As with the American Zinc building, the two cases with the lowest stiffness are the two interior column removal cases, which are made up entirely of gravity shear connections. Again, the interior columns experience the most noticeable nonlinear stiffness behavior and also reached higher deformations before convergence and solver issues arose.

To demonstrate the advantage of the roof truss, the same analyses were conducted, except without the truss. These results are shown in Figure 97 for each of the exterior column removal cases. Columns 1 and 3 are at braced frame locations so the benefit of the roof truss is less apparent.

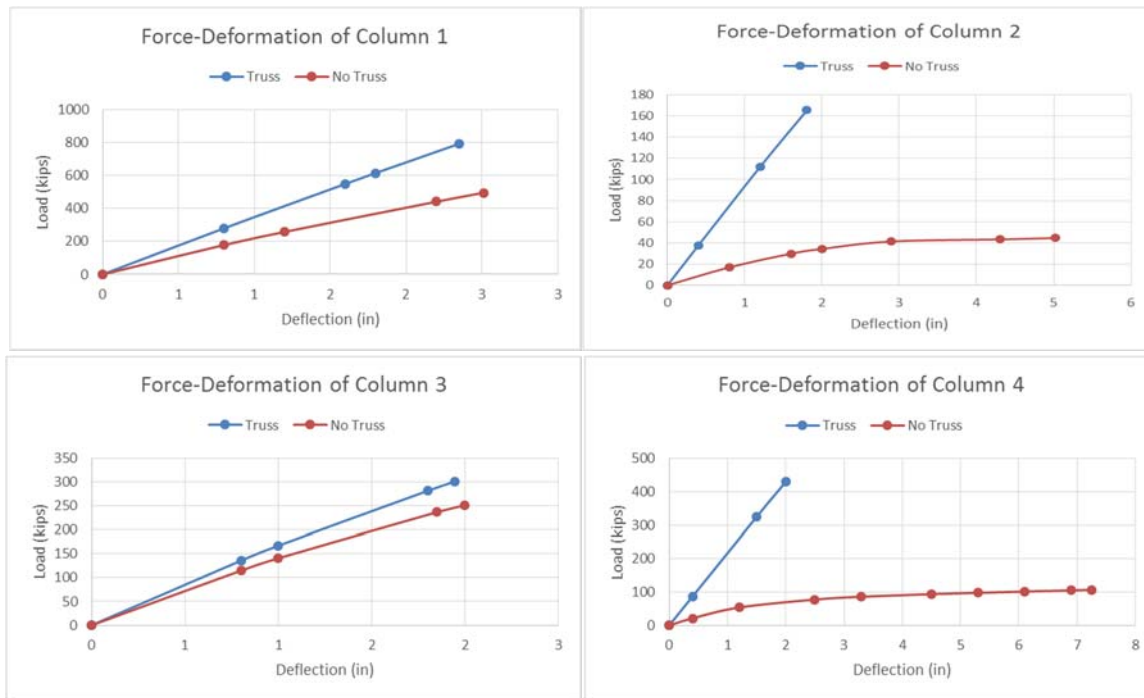


Figure 97. Column removal load vs. displacement comparison with and without roof truss.

Because of the unknowns with the level of convergence and, in an effort to further validate the procedure, the results were compared to a force-controlled analysis in which the level one column was removed and the maximum load at the column for each of the deformation-controlled cases was applied in the force-controlled models. The result of this comparison can be seen in Figure 98 for the Column 4 removal scenario and helps to confirm the linear stiffness behavior at the exterior column cases. Additionally, basic 2-D bare steel frame analyses were conducted to ensure that the force and deformation results were of the same order of magnitude and comparable stiffness.

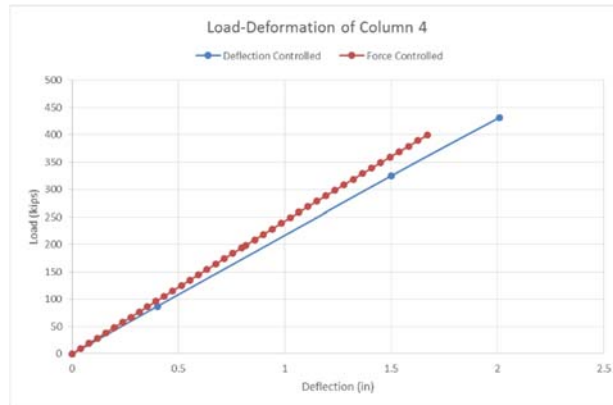


Figure 98. Column removal load vs. displacement with force-controlled and deformation-controlled loading for Lamar building.

### 6.5 Conclusions

Implementation of the nonlinear column removal models in SAP2000 for the American Zinc Sister Building and the Lamar Sister building was a limited success. The reduced modeling approaches for the shear connections and for the composite slab translated from Abaqus to SAP2000 reasonably well, and were easier to implement on a full building scale due to the available copy features in SAP2000. However, difficulty was encountered attempting to implement a time history response analysis in SAP, necessitating the use of a nonlinear static analysis instead. This had its advantages, namely quicker analysis, but it was inconsistent in how many steps would be recorded before failure to converge was reached. Further investigation may be required.

Reasonable results were obtained for the six column removal scenarios that were investigated for each building. System-level stiffness matched expected trends, although a comparison of strength was not obtained due to the inconsistency in convergence. However, equivalent area loads were determined from the nonlinear approach and compared to design loads in the linear static procedure. Care must also be taken when analyzing the results, as use of the strong/weak strip approach with support fastener adjustments in conjunction with moment connections or gusset plate connections was not within the scope of Francisco (2014).

The procedure outlined above provides another method for evaluating a building's robustness, using conventionally available software and with recommendations and guidance for modeling. By referring to Main and Sadek (2012) and comparing with simplified 2x2 bay Abaqus models, it ensured confidence in the stiffness results; it is recommended that the user take advantage of similar indicators to ensure the efficacy of their own models. Despite limitations, this method validates the alternative framing strategy approach and highlights the benefits of the stiff-story concept.

*Note: It is not recommended that the designer switch between versions of SAP2000 during analysis. Most of the models were unaffected by a version upgrade; however, one resulted in a fatal analysis error and others failed to converge at even earlier steps.*

## 7 Experimental Investigation

### 7.1 Introduction

One of the main aspects of the project was to perform an experimental study of the rotational capacity of simple beam-column connections subject to extreme deformations caused by column removal. Although it is intended that the stiff stories would limit the deformation of the connections above the failed column, a balance between safety and cost would inevitably result in some deformations which need to be predicted and accommodated. While there have been a number of tests targeted at studying the behavior of beam-column connections under extreme deformations, only a very limited number of tests deal with simple gravity connections. This chapter presents results obtained from the half-scale tests performed at LeTourneau University.

### 7.2 Test Frame

Specimens were tested in a self-reacting frame, shown in Figure 99. The self-reacting frame is composed of a 40ft long W24X162 beam, attached to two W12X79 columns. Column base plates were bolted to anchor rods casted inside 2.5ft x 5ft x 1.5ft concrete foundation blocks. Diagonal braces (2 L5" x 3 1/2" x 1/2") were added to the frame to reduce deflections in the columns due to the expected large catenary action developed at the beam specimens. 1/2" plate stiffeners were added to the test frame at all locations where concentrated forces were expected.

Specimens were restrained against out-of-plane deformations by four lateral braces. These braces, shown in Figure 100, were made from 4"x4" Southern Pine lumber. To reduce the possibility of friction from the contact of the specimen and the wood braces, a 1/16" smooth panel was installed at the surface of the 4"x4" brace. In addition, lubricant was added to the brace surface.



Figure 99. Test frame.



Figure 100. Photo of test frame and specimen showing lateral braces.

### 7.3 Test Specimens

Nine half-scale specimens consisting of two-span gravity frames with a missing center column were tested. These specimens were composed of W8x10 beams attached to W8X24 column stubs by means of shear tabs or double angle connections. Connections were sized for the gravity frame scenario of an external girder shown in Figure 101 (marked EG). The connection demand was calculated based on a 96 psf dead load and a 50 psf live load. An additional cladding load of 12 psf was used for the external girder. The connection demand resulted in a force of 31.4 kips which was reduced, to 15.7 kips, for the half-scale designs. Half-scale elements were chosen so that the dimensions were as close as possible to the half-scale ratio. These dimensions included the thickness of the web, the depth of the beam, the thickness and length of the flange, and the thickness of the column web. Plates in shear tab connections were reduced to half the thickness and half the spacing between bolts.

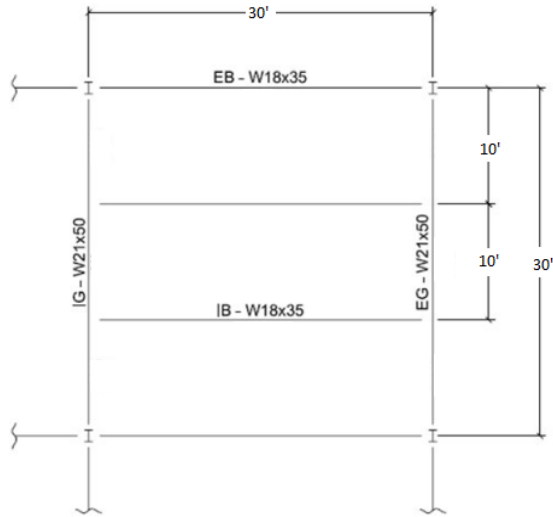


Figure 101. Plan view of the steel gravity framing system used for calculating demands. (based on Weigand, 2014)

Table 79 shows a test matrix describing the 5 different connection types tested. Connection types 1 and 2 used double angle connections. Both tests are similar, the only difference being the attachment to the columns flanges; Connection 1 is all bolted while for Connection 2 the double angles were welded to the webs of the beams. Connection types 3, 4 and 5 had shear tab connections with four bolts. Connection types 3 and 4 differed only in the bolt diameter used. Connection 3 used (4) 3/8" J429 Gr. 5 bolts in a single vertical row while Connection 4 used (4) 1/2" A325 bolts, also in a single vertical row. For Connection 3, the bolt diameter was scaled by a factor of two from 3/4" to 3/8". For Connection 4, the area of the bolts was scaled, 1/2" bolts (0.2 in<sup>2</sup>) were used to represent the 3/4" bolts (0.44 in<sup>2</sup>) used in the full scale connection. Connection types 4 and 5 differed only in the arrangement of the bolts and the geometry of the shear plate; Connection 4 had the (4) 1/2" bolts in a single vertical row, but for Connection 5, two vertical rows of (2) 1/2" bolts were used. Connection 5 was created with the intention of reducing the distance from the center of gravity of the bolt group to the center of the individual bolts, and therefore increase the capacity of the connection.

Table 79. Test matrix.

Connection Type No.	Connection Type	Bolts	No. Specimens	Span ft (m)
1	Bolted-bolted double angles	(3) 3/8" (J429 Gr. 5)	2	15ft (4.57m)
2	Welded-bolted double angles	(3) 3/8" (J429 Gr. 5)	2	15 ft (4.57m)
3	Shear tab (conventional)	(4) 3/8" (J429 Gr. 5) (single row)	2	15 ft (4.57m)
4	Shear tab (conventional)	(4) 1/2" (A325) (single row)	2	15 ft (4.57m)
5	Shear tab (extended)	(4) 1/2" (A325) (two rows)	1	15 ft (4.57m)

Connections 1, 2 and 3 used 3/8" hexagonal cap screw J429 grade 5 bolts. The strength of these bolts is similar to that of A325 bolts. 1/2" A325 bolts were used for connections 4 and 5. All bolts were installed "snug-tight". A 20ft-lbs torque was applied to all 3/8" diameter bolts and 50ft-lbs to all 1/2" bolts to maintain a uniform torque throughout and to prevent tension rupture during installation of the smaller 3/8" bolts. Figure 102 shows a drawing of Connection 1, including the location of the double angle connection. A similar detail applies to Connection 2, with the difference that the angle is welded to the beam's web by means of 3/16" welds. Figure 103 shows the center beam-column connection (left) and the right beam-column connection (right). Note that the beam specimens were connected to a column specimen at the center column, but also at both left and right ends. The left and right column specimens were bolted to the test frame.



#### 7.4 Instrumentation and Loading Protocol

The instrumentation used for the experiments is illustrated in Figure 105. A pressure transducer was used to determine the load being applied to the specimen by means of an Enerpac RC2514 ram which has a 14.25" stroke and a 50 kip capacity (marked 1 in Figure 105). Displacement was measured at the location of the missing column by means of a Unimeasure PA-15-L7M linear position transducer (marked 2). Six linear strain gages were placed at the flanges and at the web of both specimen beams, at a distance of two times the depth of the beam specimen away from the column stubs (marked 3 to 8). These strain gages were used to estimate the tensile forces in the specimens. These gages also provided insights regarding the initial flexural response of the beam-column connections. Finally, an inclinometer was used to measure the true rotation at the beam, near the removed column (marked 9).

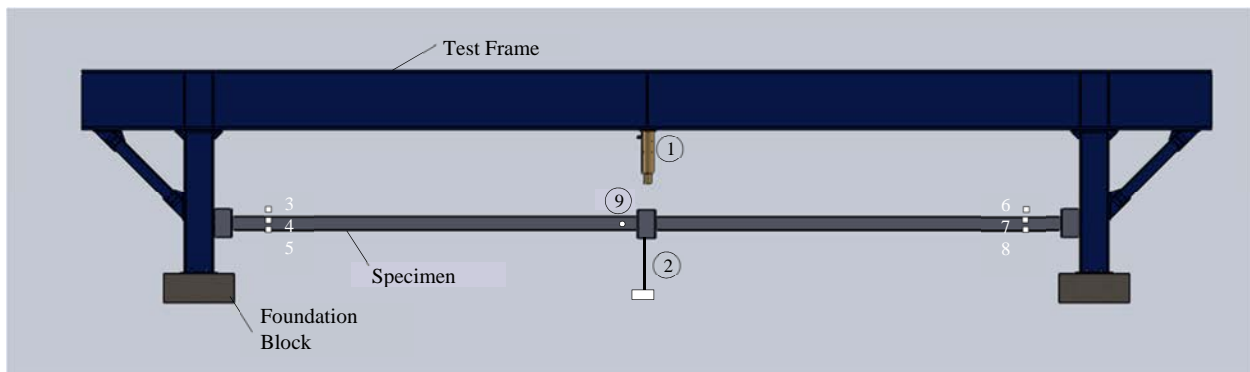


Figure 105. Instrumentation.

The deformation of the specimen and the instantaneous rotations were also tracked by using a high-definition camera. Data was logged by means of a Micro Measurements System 8000 and a National Instruments USB 6210 data acquisition system. Data was recorded every 0.01 seconds.

Specimens were initially supported under the two beams, leveled and tightened. Once the data collection started, the supports were removed and the specimens deflected under their own self-weight. The center column was then loaded by means of an Enerpac 2514 ram connected to an Enerpac air pump or hand pump. The load rate was measured at approximately 60 lbs. per second. Pressure was applied until the ram reached its maximum stroke of 14.25 inches. At that point the pressure was released, and additional plates were added between the column and the ram. The test was then continued until failure was achieved.

## 7.5 Calculations

Most measurements of interest for this experimental program were collected directly from the instruments (i.e., deflection, rotation, applied vertical load). However, the axial (catenary) force that develops in the beams was calculated from the six strain gages. To determine the axial force, the average strain was first determined as shown by Equation 17. This strain is then used in Equation 18 to determine the axial force.

$$\varepsilon = \frac{\varepsilon_{top\ flange}}{4} + \frac{\varepsilon_{web}}{2} + \frac{\varepsilon_{bottom\ flange}}{4} \quad \text{Equation 17}$$

$$\text{Axial force} = \varepsilon * E * A_{beam} \quad \text{Equation 18}$$

Where  $E$  is Young's modulus for steel, 29,000 ksi, and  $A_{beam}$  is the cross-sectional area of the beam which was 2.96 in<sup>2</sup> for the W8x10 beams used.

Another parameter measured during the experiments was the rotation of the beam at the beam to center column connection. This rotation was measured directly using an inclinometer, but also calculated using the basic geometric relationship shown in Equation 19.

$$\theta = \tan^{-1} \left( \frac{\Delta}{L} \right) \quad \text{Equation 19}$$

Where:

$\theta$  = rotation (radians);

$\Delta$  = deformation of central column measured by the displacement transducer; and

$L$  = single span length.

## 7.6 Material Testing

Tensile testing was performed to determine the yield and ultimate strength of the steel members used. Coupons were extracted from the W8x10 beams, the L2 X 2 X ¼ angles used for the double angle connections, and from the ¼" plate used for the shear tabs. For the angles and the beam sections (flange and web), coupons were removed relative to the longitudinal axis of the section as shown in Figure 106. Testing was performed in accordance with the ASTM E8 standard (ASTM, 2008) for tensile tests of plate-type materials. Figure 107 shows the dimensions of the tensile coupons. The dimensions of these specimens, fabricated by water jet cutting, were verified with calipers and recorded in **Error! Reference source not found.**, which shows the three measurements taken for width and thickness, and the average values.



Figure 106. Base material for tensile coupons.

Table 80. Dimensions of coupon specimens.

Coupon ID	Stock Material	Grade	Top width (in)	Mid width (in)	Bottom width (in)	Avg. width (in)	Top thickness (in)	Mid thickness (in)	Bottom thickness (in)	Avg. thickness (in)
Flange 1	W8 x 10	A992	0.499	0.500	0.499	0.499	0.196	0.196	0.196	0.196
Flange 2	W8 x 10	A992	0.485	0.484	0.486	0.485	0.215	0.215	0.214	0.214
Flange 3	W8 x 10	A992	0.491	0.490	0.490	0.490	0.202	0.213	0.213	0.212
Flange 4	W8 x 10	A992	0.490	0.491	0.490	0.490	0.220	0.221	0.220	0.220
Web 1	W8 x 10	A992	0.484	0.483	0.485	0.484	0.166	0.167	0.165	0.166
Web 2	W8 x 10	A992	0.489	0.490	0.493	0.490	0.165	0.165	0.165	0.165
Angle 1	L2 x 2 x ¼	A36	0.500	0.499	0.500	0.499	0.241	0.241	0.241	0.241
Angle 2	L2 x 2 x ¼	A36	0.497	0.496	0.500	0.497	0.245	0.245	0.246	0.245
Plate 1	6 x 20 x ¼	A36	0.506	0.500	0.502	0.502	0.252	0.250	0.251	0.251
Plate 2	6 x 20 x ¼	A36	0.503	0.503	0.501	0.502	0.256	0.254	0.252	0.254
Plate 3	6 x 20 x ¼	A36	0.499	0.497	0.499	0.498	0.251	0.251	0.250	0.250

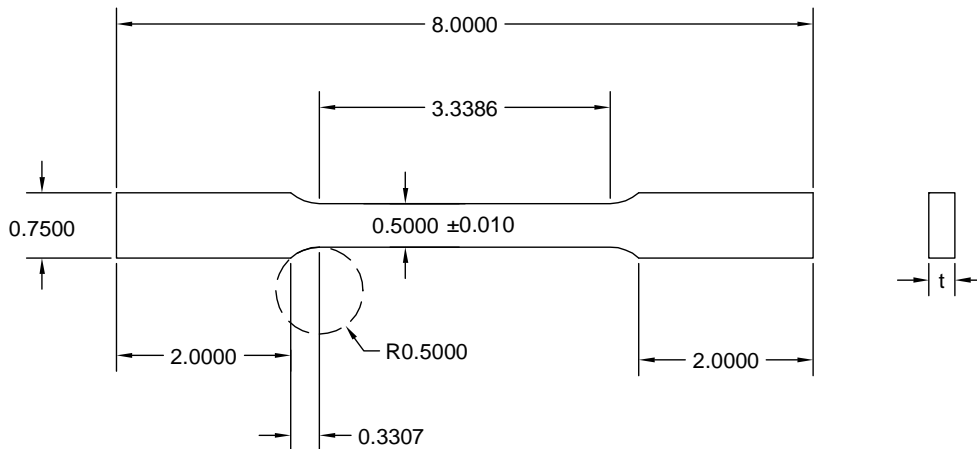


Figure 107. Tensile coupon dimensions (inches).

An Instron 5582 universal testing machine was utilized to load the specimens to failure (Figure 108). A video extensometer was mounted on the testing machine to measure gage elongation. Results were collected by the supporting computer software.



Figure 108. Material coupon loaded in Instron 5582 testing machine.

For every coupon tested, raw data values for loading and extension were recorded in an excel spreadsheet and later used to compile engineering stress-strain response curves. Engineering stress,  $\sigma_{eng}$ , and engineering strain,  $\epsilon_{eng}$ , were calculated by means of Equation 20 and Equation 21.  $P$  is the load applied and  $A$  is the cross-sectional area of the coupon. The  $\delta_{gauge}$  is the elongation within the initial coupon gauge length,  $L_{gauge}$ .

$$\sigma_{eng} = \frac{P}{A} \quad \text{Equation 20}$$

$$\epsilon_{eng} = \frac{\delta_{gauge}}{L_{gauge}} \quad \text{Equation 21}$$

The yield strength, ultimate tensile strength and the percentage elongation were calculated and are shown in Table 81. Yield stresses fell within the range of 51-54 ksi for the A992 beams, 46-49 ksi for the A36 angles, and 41-43 for the A36 plates.

Table 81. Tensile test results.

Coupon ID	$\sigma_y$ , upper (ksi)	$\sigma_u$ , (ksi)	Percent Elongation (%)
Flange 1	53	66.4	26
Flange 2	51	67.3	23
Flange 3	51	68	21
Flange 4	51	65	26
Web 1	54	67	23
Web 2	53	67	20
Angle 1	46	74	-
Angle 2	49	72	-
Plate 1	42	74	20
Plate 2	41	74	21
Plate 3	43	74	20

## 7.7 Test Results

This section discusses the results obtained from the nine half-scale tests previously described.

### 7.7.1 Connection Type 1: Specimens 1 and 2

Figure 109 shows a plot of the applied vertical force versus the vertical deflection measured by the displacement transducer. Note that both test specimens underwent approximately 5" of deflection upon removal of the missing column supports (point 1 in Figure 109). This deflection was caused by the self-weight of the specimen plus the filler plates (approximately 410 lbs.) used under the ram. Load was applied until the maximum stroke of 14.25 inches was reached (point 2), at that point the load was removed and additional filler plates were added to increase the stroke. The specimen was subsequently loaded until failure of the first bolt (i.e., one of the top bolts in the double angle to column flange connection) was reached (point 3). At that point, significant prying deformation of the angles was observed. This behavior was observed for both specimens and is further discussed below. The maximum vertical load applied by the ram was approximately 8,000 lbs., corresponding to a deflection of about 20 inches, for both specimens. After fracture of the top bolt in the double angle to column flange connection, the load carried by the specimen exhibited a sharp drop. Additional bolts in the same double angle to column flange connection continued rupturing and causing subsequent drops in the load carried (points 4 to 6). For test 2, the displacement transducer was removed before full failure of the specimen, to avoid damage to the transducer. Further discussion of the failure progression is given below.

Figure 110 shows a photo of test 2 before failure of the connection. Both test specimens failed at exterior beam to column connections and not at the connection where the column was missing (and load was applied). Specifically, the six bolts connecting the angles to the column flanges ruptured in combined tension and shear. Test 1 failed at the left exterior connection (see Figure 111), while Test 2 failed at the right exterior connection (see Figure 112). While rupture of the bolts was the controlling failure mode, large inelastic bearing deformations were observed in the web (see Figure 113). All web holes in a given bolt row experienced some bearing deformation, the top holes at the exterior connections and the bottom holes of the interior connection had the most significant bearing, followed by the middle bolts. The maximum bearing deformation observed was about  $\frac{1}{4}$ ".

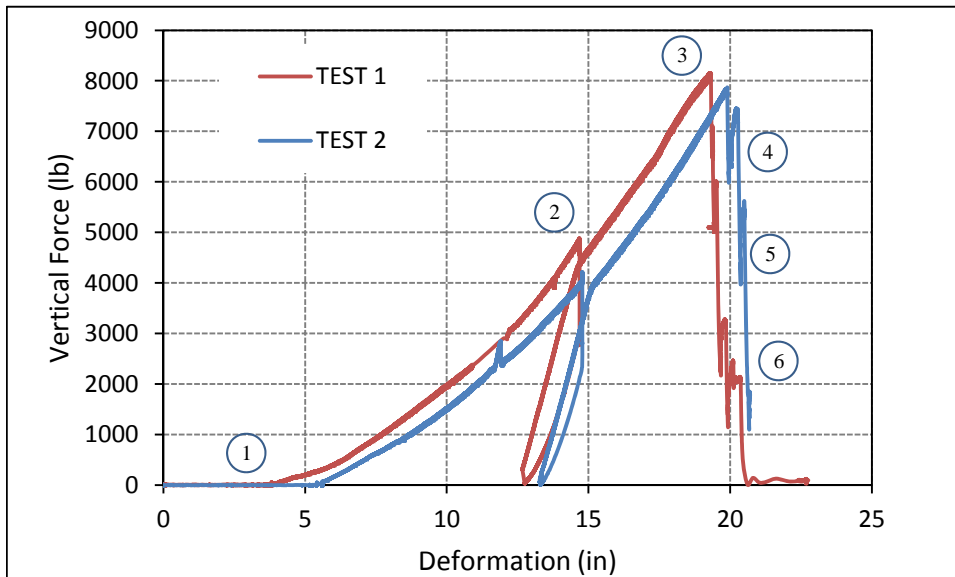


Figure 109. Applied vertical force vs. deflection at missing column.



Figure 110. Test 2 undergoing large deformations.



Figure 111. Failure of top two bolts on right angle, Test 1.



Figure 112. Failure of bolts during Test 2.



Figure 113. Bearing deformations of the bolt holes in the beam's web.

The axial (catenary) force developed in the beams due to the large deformations was derived from the measured strains. It is plotted in Figure 114 against the vertical deflection of the missing column. Both tests reached catenary forces of approximately 28 kips.

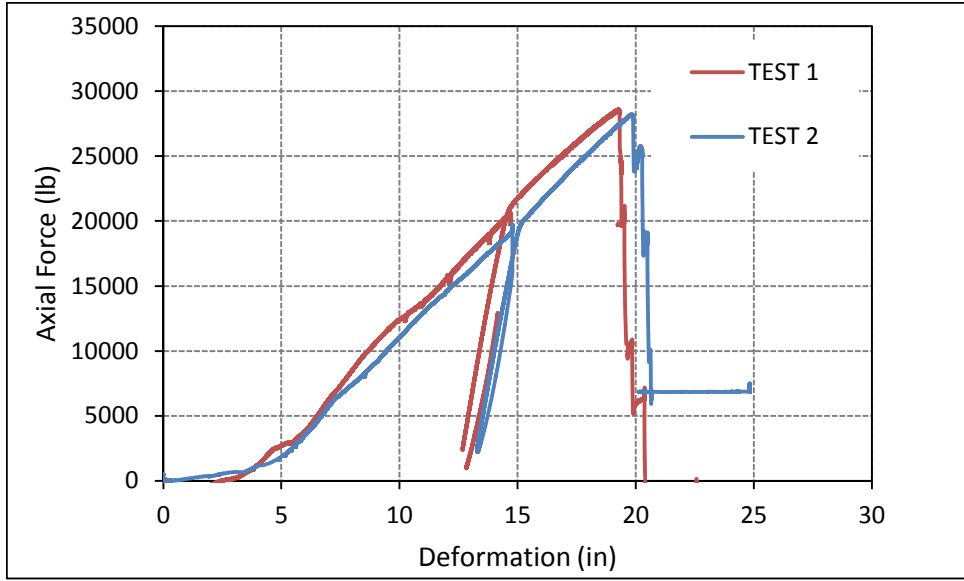


Figure 114. Catenary force vs. vertical deflection of missing column.

Plots of applied vertical force versus the measured and calculated rotations, for Test 1 (left) and Test 2 (right), are shown in Figure 115. It can be observed that the rotation derived from the vertical deflection yields similar results. The beam specimens remained elastic and rotated mostly as a rigid body. Thus, most of the rotation was concentrated in double angle deformations and bolt hole elongation.

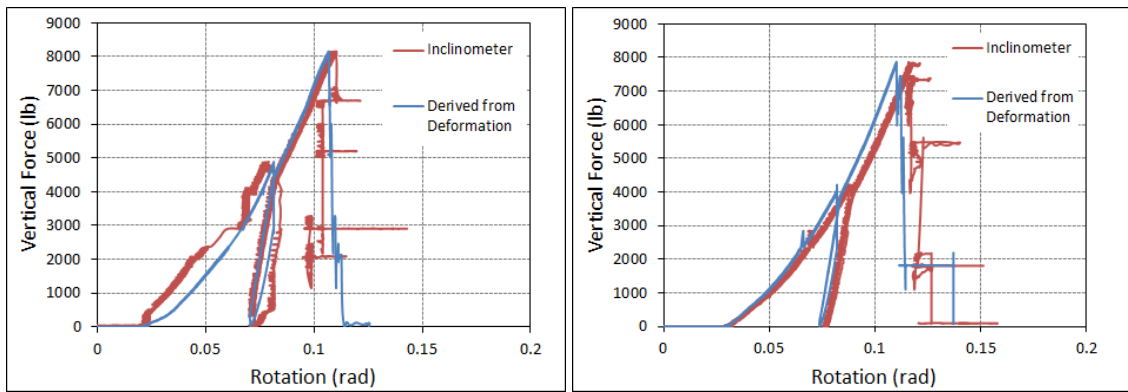


Figure 115. Force vs. rotation measured and derived for Test 1 (left) and Test 2 (right).

A summary of the main results is presented in Table 82.

Table 82. Summary of connection 1 main results.

	Test 1	Test 2	Average
Maximum Vertical Load	8,093 lb (36.0 kN)	7,822 lb (34.8 kN)	7,958 lb (35.4 kN)
Maximum Axial Force	28,512 lb (126.8 kN)	28,151 lb (125.2 kN)	28,332 lb (126.0 kN)
Maximum Deformation of Central Column at First Failure	19.3 in (490.2 mm)	19.9 in (505.5 mm)	19.6 in (497.8 mm)
Rotation at Failure	0.106 rad (6.1 deg)	0.11 rad (6.3 deg)	0.108 rad (6.2 deg)
Failure Mode	Rupture of bolts at exterior column connection.	Rupture of bolts at exterior column connection.	N/A

While bolt failure was the controlling limit state, other test specimen components also experienced damage. The outer column stubs experienced almost no visible damage. The inner column stub also experienced little visible damage. The exterior angle connections were subjected to a significant prying action at the column face which deformed the angles 3/16" out of plane. There is also a small amount of bearing elongation at the angles attached to the beam's web; however, most of the bearing occurred in the web and not the angles. The angles at the center column also exhibited significant prying deformations, but to a lesser degree, only deforming 1/16" out of plane.

#### 7.7.2 Connection Type 2: Specimens 3 and 4

Connection Type 2 was almost identical to Connection 1, the only difference being that the double angle connections were welded to the beam and not bolted. As for Connection 1 (specimens 1 and 2), specimen 3 failed when a top bolt connecting the angle to the column flange fractured. This failure occurred at an applied vertical load of 3,580 lbs. and approximately 12.2 in. of deflection. The axial force at that point was 22,984 lbs. on average; the maximum axial force was 26,500 lbs. Figure 116 shows the load versus displacement plot for this test. Because data from the string pot and inclinometer was not properly recorded, the deflection was approximated using video analysis from the high definition video created. Thus, unloading and reloading portions are not properly identified in Figure 116. Figure 117 shows the strain history for all six strain gages. The progression of events recorded during test 3 is summarized in Table 83.

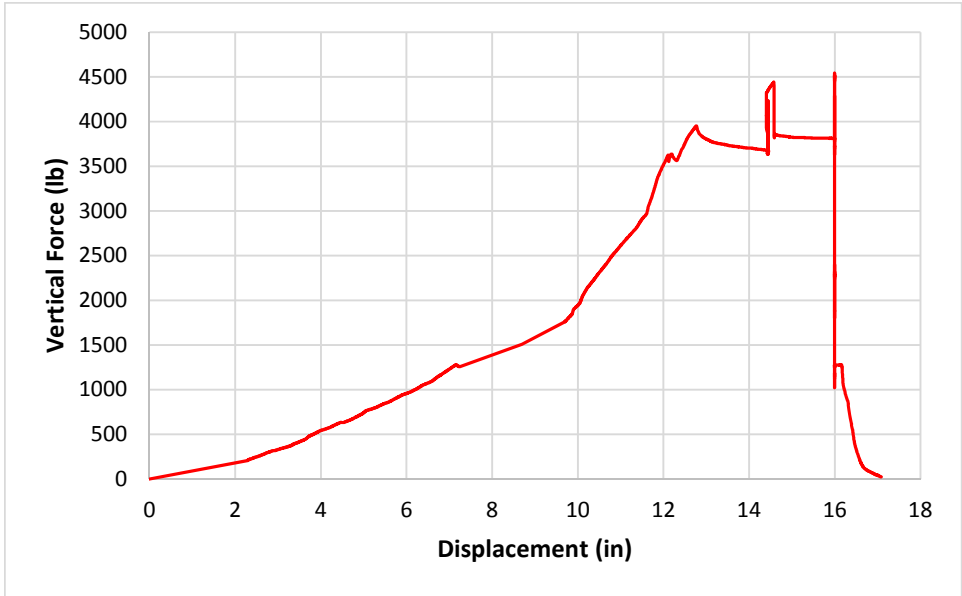


Figure 116. Test 3 vertical load versus displacement plot.

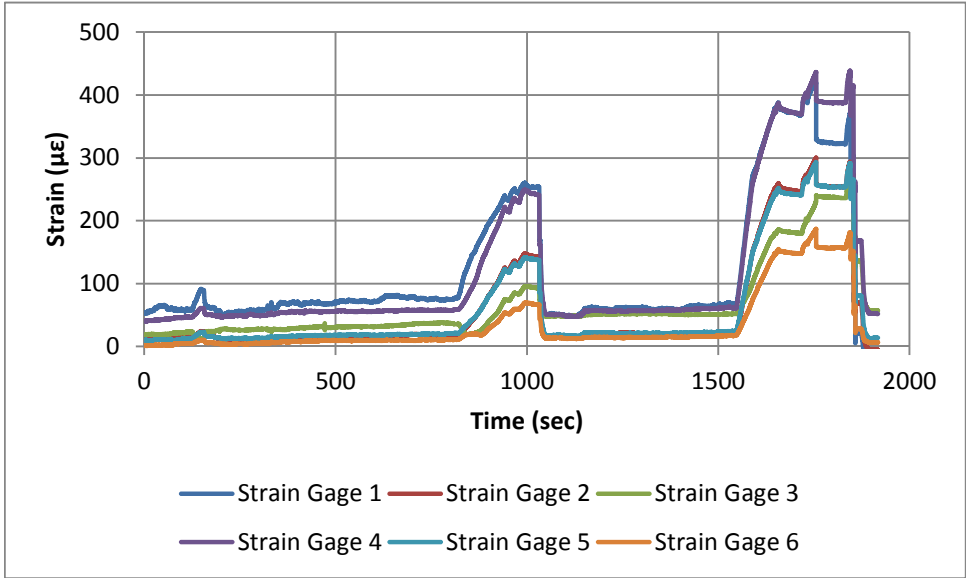


Figure 117. Test 3 strain history.

Table 83. Test 3 progression of events.

No.	Description of event
1	Start of test
2	Unloaded system, problem with ram. Added 2 filler blocks
3	First bolt failure: left column, back side, top bolt
4	Second bolt failure: left column, back side, middle bolt
5	Third bolt failure: left column, back side, bottom bolt
6	Fourth bolt failure: center column, right side, back side, bottom bolt
7	Fifth bolt failure: right column, back side, top bolt
8	Sixth bolt failure: left column, front side, top bolt
9	Seventh bolt failure: left column, front side, middle bolt. END OF TEST

Unlike tests 1 and 2, which used bolts at the angle web interface, no bearing deformations were present, making this connection detail stiffer. Prying deformations were significant, measuring approximately  $\frac{1}{2}$ " (Figure 118).



Figure 118. Test 3 prying deformations.

Specimen 4 was the second sample of Connection Type 2 tested. This specimen behaved in a very similar fashion to specimen 3, as expected. Failure occurred at the bolts connecting the double angles to the columns flanges, on the right column, starting from the top bolt (Figure 119). Significant prying deformations were observed, reaching  $\frac{1}{2}$ " at failure (Figure 119). A vertical load versus deflection plot is shown in Figure 120. Test 4 had its first bolt failure at a vertical load of 5,400 lbs. (marked 2), an axial force of 22,219 lbs. and 14.38 in. of deflection. After it experienced its initial failure, the proceeding 4 failures occurred in quick succession (marked 4 to 7). It withstood a maximum vertical load of 5,406 lbs., and at this point the axial force was 22,326 lbs.

with 14.2 in. of deflection. The maximum axial force of approximately 24,000 lbs. occurred at 15.3 in. of deflection, and the vertical load at this point was 5,178 lbs. Features of the vertical load vs. displacement plot (Figure 120) are explained in Table 84. The axial force, plotted against vertical displacement, is shown in Figure 121. The resultant axial force at the location of the strain gages was under compression for the first six inches.



Figure 119. Test 4 bolt fracture.

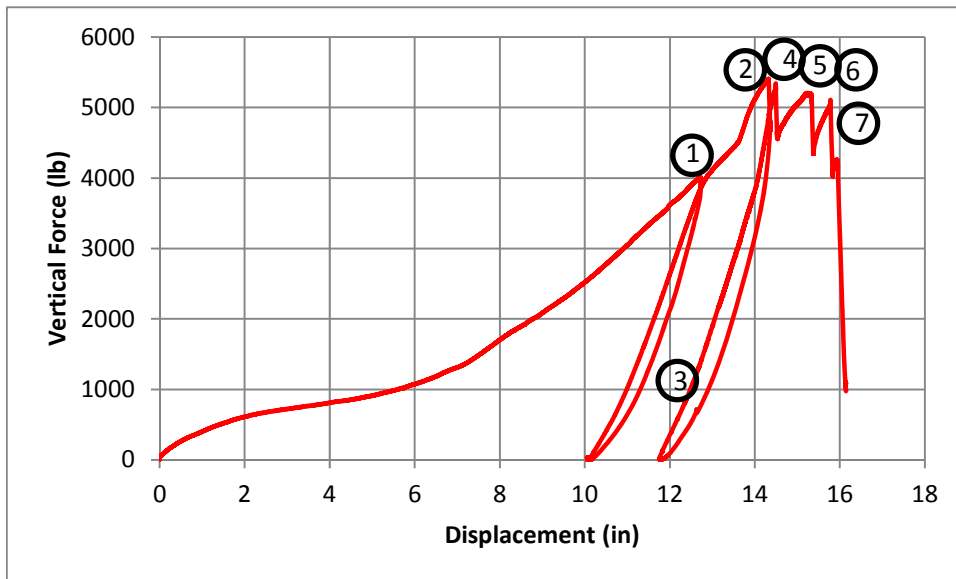


Figure 120. Test 4 vertical load versus displacement.

Table 84. Test 4 progression of failure.

No.	Description of event
1	Unloaded system because ram was out of stroke
2	First bolt failure: right column, front side, top bolt
3	Unloaded system to switch to hand pump; leak in air pump
4	Second bolt failure: center column, left side, back side, bottom bolt
5	Third bolt failure: right column, front side, middle bolt
6	Fourth bolt failure: right column, front side, bottom bolt
7	Fifth bolt failure: right column, back side, top bolt. END OF TEST
Note:	At one of the peaks, two bolts failed. Sixth bolt failure: right column, back side, middle bolt

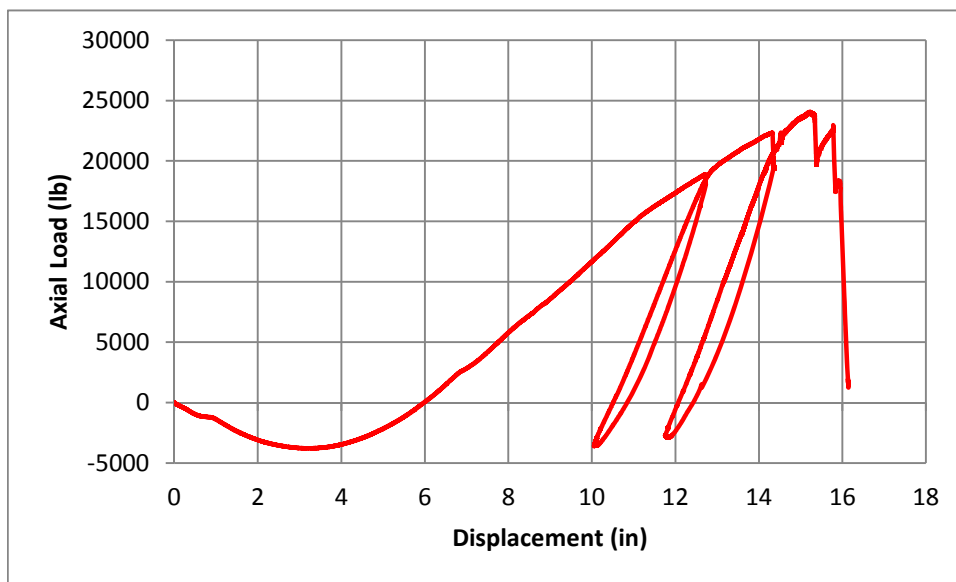


Figure 121. Test 4 axial force versus displacement.

A summary of the main results for Connection Type 2 (tests 3 and 4) is provided in Table 85. On average, this specimen held 4.97 kips of vertical load, equivalent to 2.49 kips of shear at the connections, and an axial force of 25.3 kips. At first failure the specimen had a rotation of 0.074 radians on average.

Table 85. Specimen 2 results.

	Test 3	Test 4	Average
Maximum Vertical Load	4,541 lb (20.2 kN)	5,406 lb (24.1 kN)	4,974 lb (22.1 kN)
Maximum Axial Force	26,500 lb (117.9 kN)	24,061 lb (107.0 kN)	25,280 lb (112.4 kN)
Maximum Deformation of Central Column at First Failure	12.2 in (310.0 mm)	14.3 in (364.0 mm)	13.3 in (337.8 mm)
Rotation at First Failure	0.068 rad (3.9 deg)	0.08 rad (4.6 deg)	0.074 rad (4.2 deg)
Failure Mode	Rupture of bolts	Rupture of bolts	-

### 7.7.3 Connection Type 3: Specimens 5 and 6

Specimens 5 and 6 used shear tab connections with 3/8" bolts. For specimen 5, failure occurred when a bolt fractured at an applied vertical load of 1,072 lbs. The axial force at the beams had reached 9,233 lbs. and the displacement at the center (missing) column was 6.3 in. The specimen reached a maximum vertical load of 1,162 lbs. at 8.5 in. of deflection just before the third bolt failure. The maximum axial force reached was 10,383 lbs. at a deflection of 7.6 in., just before the second bolt failed. Figure 122 shows a graph of the vertical load versus deflection, and Table 86 describes key parts identified in that figure. A graph of the axial force (average of the two beams) is shown in Figure 125. The test was stopped when five bolts failed in shear. Figure 123 shows the shear tab on the right side of central (missing) column when three of the four bolts had failed, on the left, and the beam after it had been removed, on the right. Bearing deformations were almost unnoticeable.

This test sustained greater loads after an initial failure occurred. This is believed to be caused by bolt demands being more evenly distributed since the distance from edge bolts to the center of gravity of the bolt group decreased.

Figure 124 shows strain, in micro strain, versus displacement for test 5. The strain values are as expected with strains larger in the top flange and lower in the bottom. As is seen in the graph, the strain in strain gage 1 reduced significantly after the second bolt failure (top bolt in left column). Strain gage 3 is not included in Figure 124 because it malfunctioned.

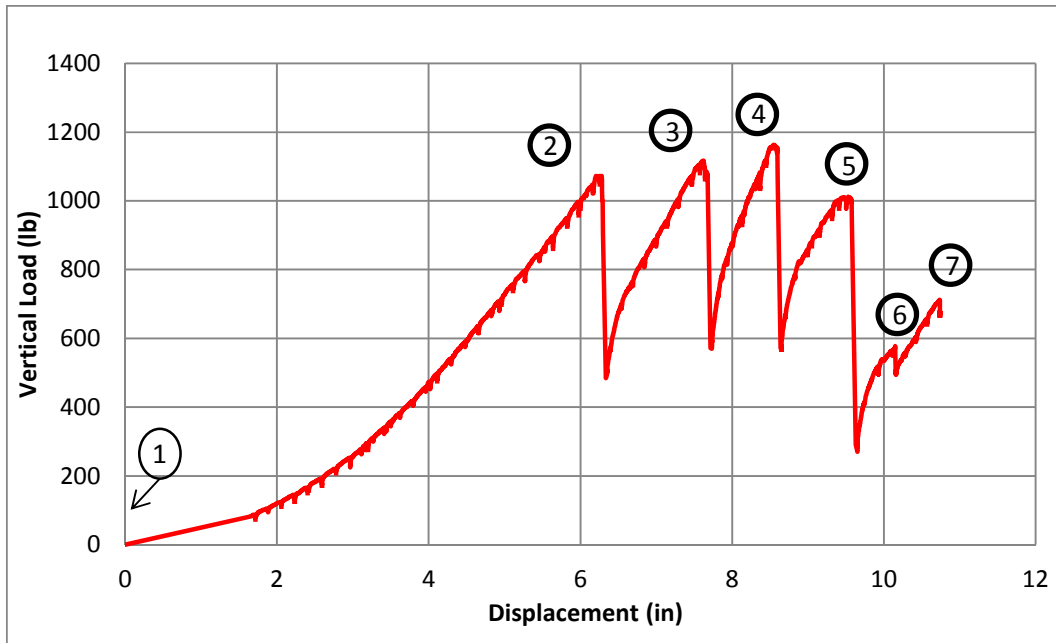


Figure 122. Test 5 vertical load vs. displacement.

Table 86. Test 5 progression of events.

No.	Description of event
1	Beginning of test, load cell did not work. Test restarted
2	First bolt failure: center column, right side, bottom bolt
3	Second bolt failure: left column, top bolt
4	Third bolt failure: center column, right side, second from bottom
5	Fourth bolt failure: center column, right side, third from bottom
6	Heard loud noise (bolt failure)
7	Fifth failed bolt fell out of hole. END OF TEST



Figure 123. Test 5 shear tab with failed bolts (left), bearing deformations (right).

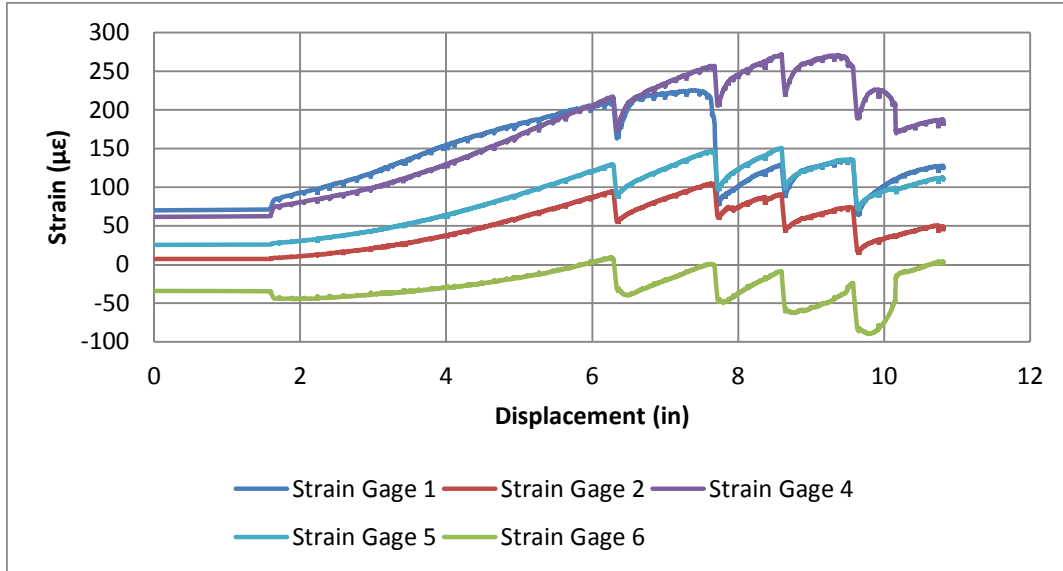


Figure 124. Test 5 strain vs. displacement.

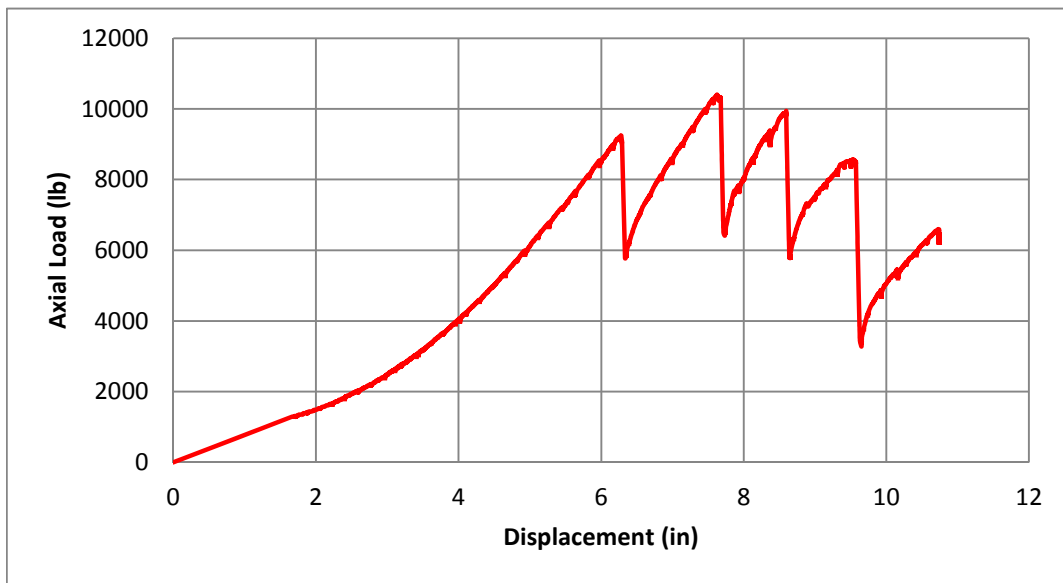


Figure 125. Test 5 axial force versus displacement.

Figure 126 shows the vertical load compared to measured and derived (calculated) rotations. While the measured rotation had significant noise, the values closely align which confirms the accuracy of the measured rotation. The rotation at first failure was 0.035 radians.

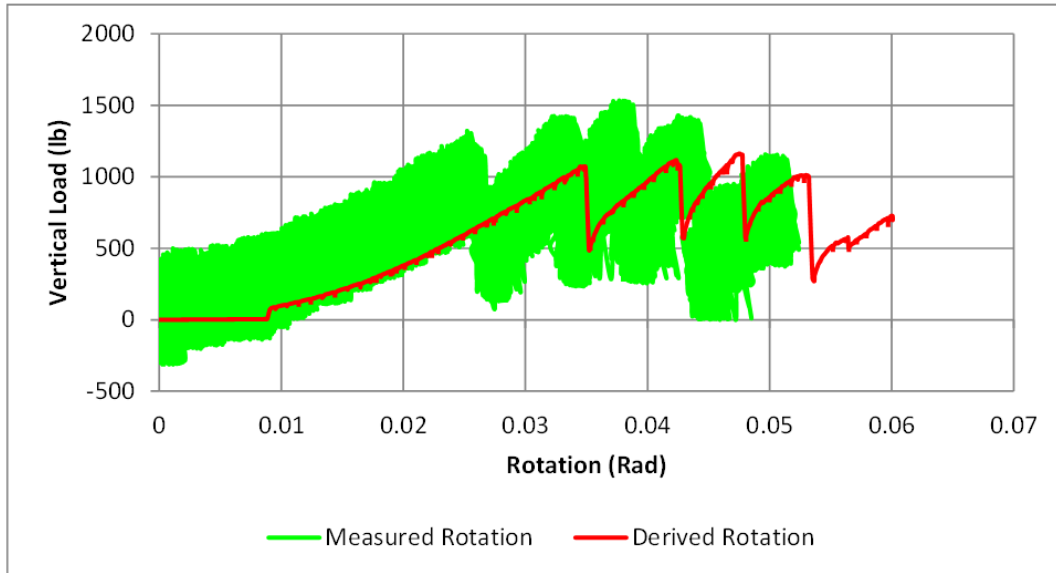


Figure 126. Test 5 vertical load versus rotation.

Figure 127 and Figure 128 show the vertical load versus displacement and the axial force versus displacement plots for test 6. Several points of interest during the test, including the progression of failure of the bolts, are numbered in Figure 127 and explained in Table 87. The maximum vertical load was 1,457 lb. (point 3), while the maximum axial force was 16,027 lb. at 8.5 in. of vertical displacement in the center column. This maximum load coincided with the first bolt failure. After the first bolt failed, the applied load dropped to approximately 800 lbs. The test was then resumed and further load was applied until the subsequent bolts failed. The controlling failure mechanism was shear of the bolts, which was the same mechanism as test 5. Bearing deformations were measured at the beams webs and shear tabs; however, these were almost unnoticeable (Figure 129).

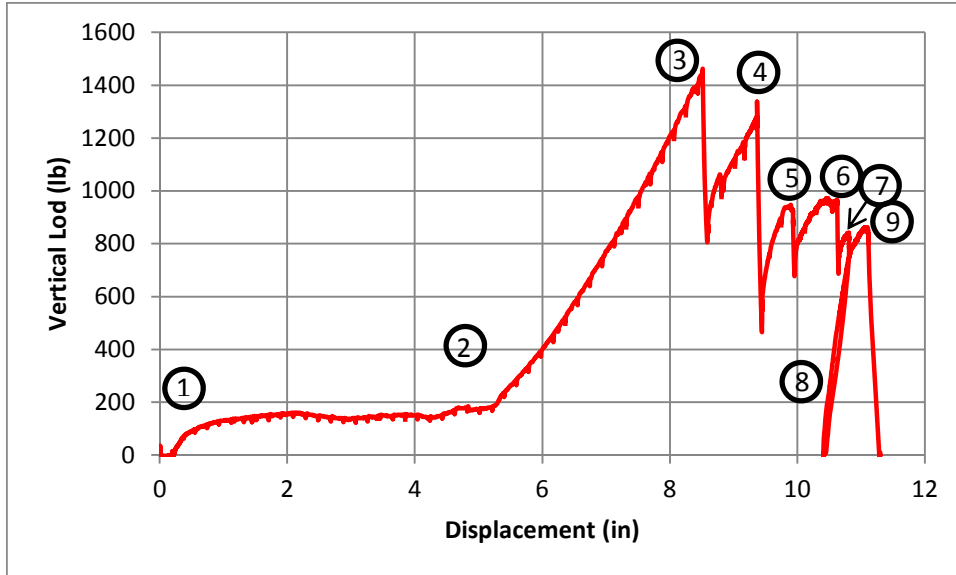


Figure 127. Test 6 vertical load versus displacement.

Table 87. Test 6 progression of events.

No.	Description of event
1	Removal of supports and initial displacement
2	No significant tension in the beams until this point
3	First bolt failure: center column, right side, bottom bolt
4	Second bolt failure: location not clear. Inferred the bolt was the left column, top bolt
5	Left column, top bolt fell out
6	Third bolt failure: location not clear. Inferred center column, right side, 2nd bolt from bottom
7	Fifth bolt Failure: location not clear. Inferred center column, right side, 3rd bolt from bottom
8	Fully unloaded to add filler blocks because ram reached end of stroke
9	Center column, right side, 3rd bolt from bottom bolt fell out. END OF TEST



Figure 128. Test 6 axial force vs. displacement.



Figure 129. Test 6 bearing deformations.

Figure 130 shows strain versus deflection plots for all six strain gages in test 6. As was expected, strain gages 3 and 6, placed at the bottom flanges, go into compression initially. After large deformations, the entire cross section is in tension.

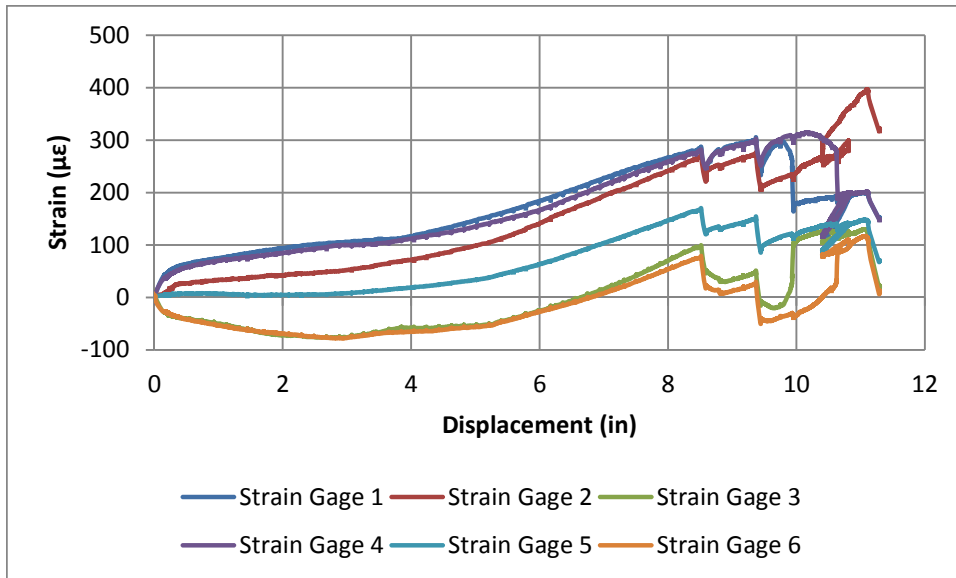


Figure 130. Test 6 strain vs. displacement.

Figure 131 shows vertical load versus rotation plots for both derived and measured rotation. These two agree very well until failure of the first bolt was reached. The maximum rotation at first failure was 0.047 radians.

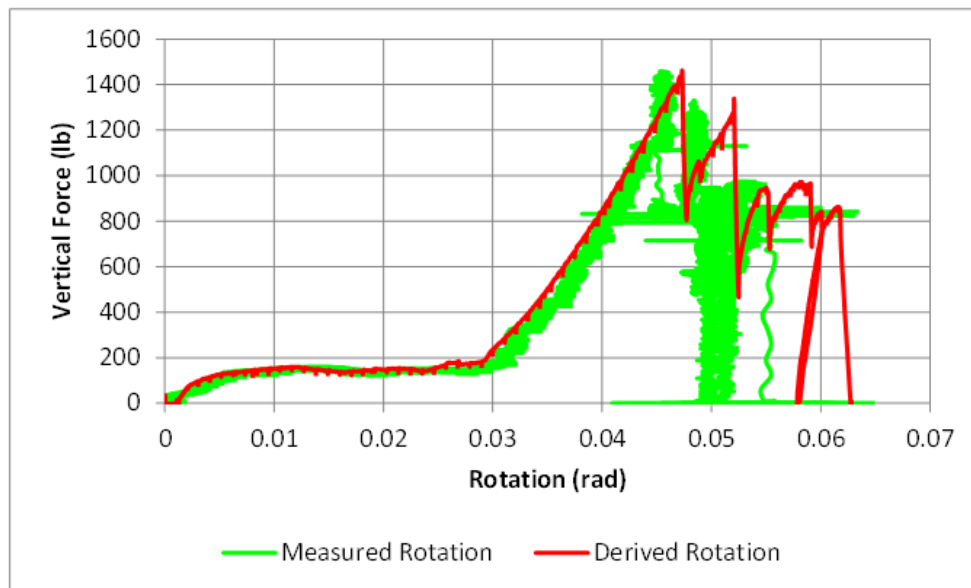


Figure 131. Test 6 vertical load versus rotation.

Results for connection detail 3 are summarized in Table 88. On average, this specimen held 1.3 kips of vertical load, equivalent to 0.65 kips of shear at connections, and 13.2 kips of axial force. The average rotation when first failure occurred was 0.041 radians.

Table 88. Summary of connection Type 3 results (Test 5 and 6).

	Test 5	Test 6	Average
Maximum Vertical Load	1,162 lb (5.2 kN)	1,457 lb (6.5 kN)	1,310 lb (5.8 kN)
Maximum Axial force	10,383 lb (46.2 kN)	16,027 lb (71.3 kN)	13,205 lb (58.7 kN)
Maximum Deformation of Central Column at First Failure	6.3 in (159.5 mm)	8.5 in (215.9 mm)	7.4 in (187.7 mm)
Rotation at First Failure	0.035 rad (2.0 deg)	0.047 rad (2.7 deg)	0.041 rad (2.4 deg)
Failure Mode	Rupture of bolts	Rupture of bolts	-

#### 7.7.4 Connection Type 4: Specimens 7 and 8

Shear tab connections with four ½" A325 bolts in a single vertical row were used in specimens 7 and 8. Figure 132 and Figure 133 show plots of the vertical and axial force, plotted against displacement, for test 7. As was the case with Connection Type 3, bolt shear was the controlling limit state. The first bolt failure occurred at 3,909 lb. of vertical load and 22,319 lb. of axial force, corresponding to a 10.6 in. deflection. After two bolts had failed, the connection reached the maximum vertical load of 4,551 lb. and 25,230 lb. of axial force at 13.2 in. of displacement. All of the bolts failed in shear due to the combined shear and axial forces; however, bearing deformations of up to nearly 1/8" were observed (Figure 134).

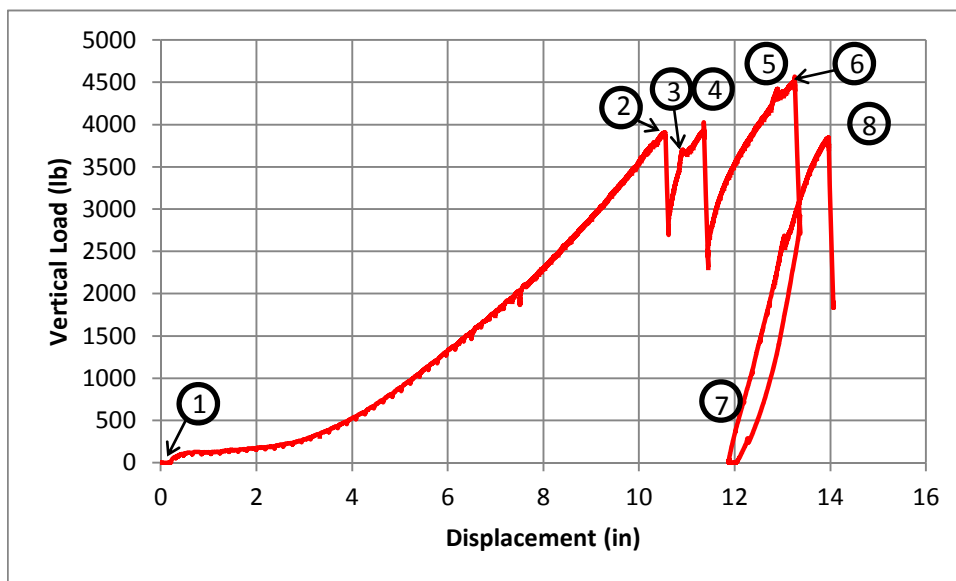


Figure 132. Test 7 vertical load versus displacement.

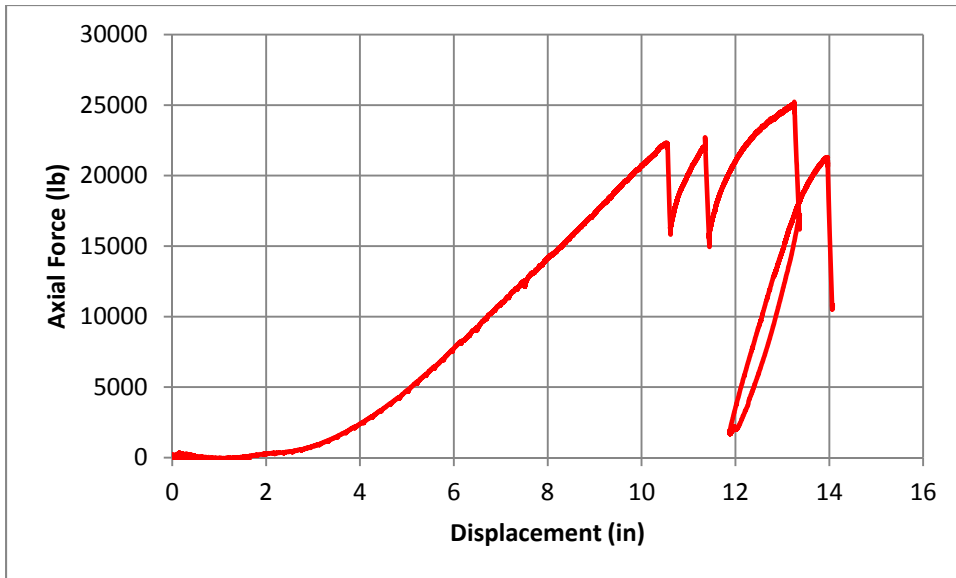


Figure 133. Test 7 axial force vs. displacement.



Figure 134. Bearing deformations in test 7 (center column, right side).

Table 89 shows a summary of the main observations identified in Figure 132. Note that the specimen was unloaded and reloaded because the ram ran out of stroke (marked 7). Filler plates were added to increase the stroke length and the test was continued until a fourth bolt failed (marked 8).

Table 89. Test 7 progression of events.

No.	Description of event
1	Removal of supports and initial displacement
2	First bolt failure: center column, right side, bottom bolt
3	Center column, right side, bottom bolt head fell out of hole
4	Second bolt failure: center column, right side, second from bottom bolt
5	Center column, right side, second from bottom bolt head fell out
6	Third bolt failure: left column, top bolt
7	Unloaded to add 2 blocks because ram reached end of stroke
8	Fourth bolt failure: center column, right side, third from bottom bolt. END OF TEST

Figure 135 displays the strain from test 7. Strain gages 4 and 6 (top and bottom gages on the right side beam) did not function for this test. For that reason, the axial force was calculated from the left beam alone, and not the average of both beams. As for previous tests, the rotation was also derived from the displacement and measured using an inclinometer. Figure 136 shows the derived rotation, exhibiting a rotation of 0.06 radians when the first bolt failed. Measured rotation was excluded from the graph because it had significant noise.

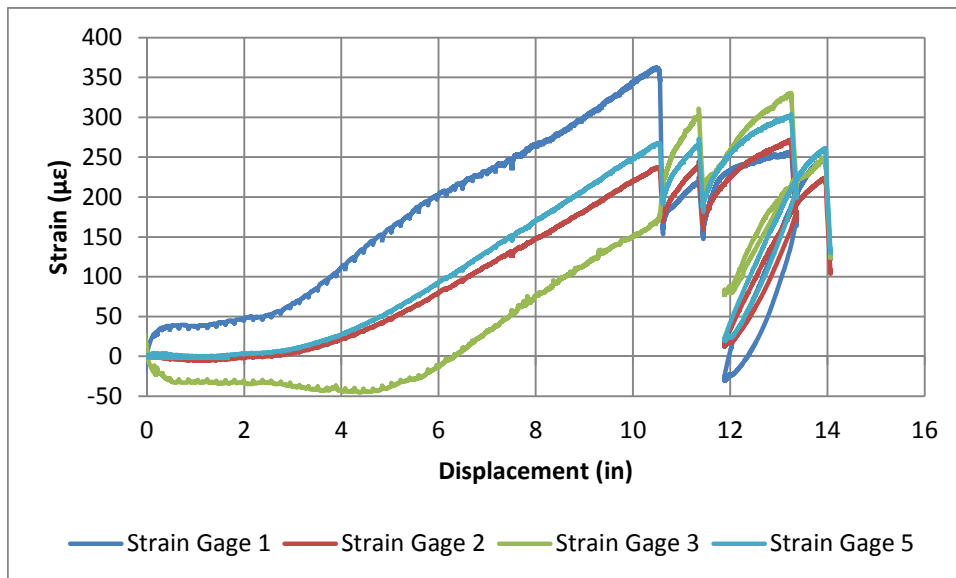


Figure 135. Test 7 strain vs. displacement.

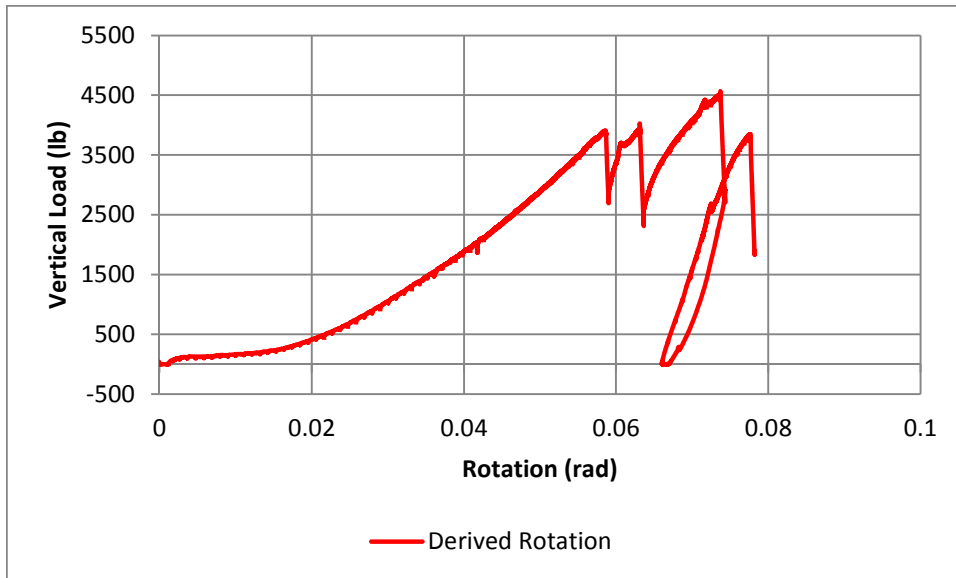


Figure 136. Test 7 derived rotation.

Figure 137 shows a plot of the vertical load applied to the center column versus the column displacement, for test 8. Significant events are identified in that figure and explained in Table 90. This specimen deflected almost 6 inches before it started to increase in load significantly. The maximum vertical load was 4,441 lb. and maximum axial force was 26,445 lb. (Figure 138), at 12.8 in. of displacement. This load was achieved right before the first bolt had shear failure. Although shear of the bolts controlled, bearing deformations were observed, especially at the beam’s web, with a maximum measured deformation of over 1/16” (see Figure 139).

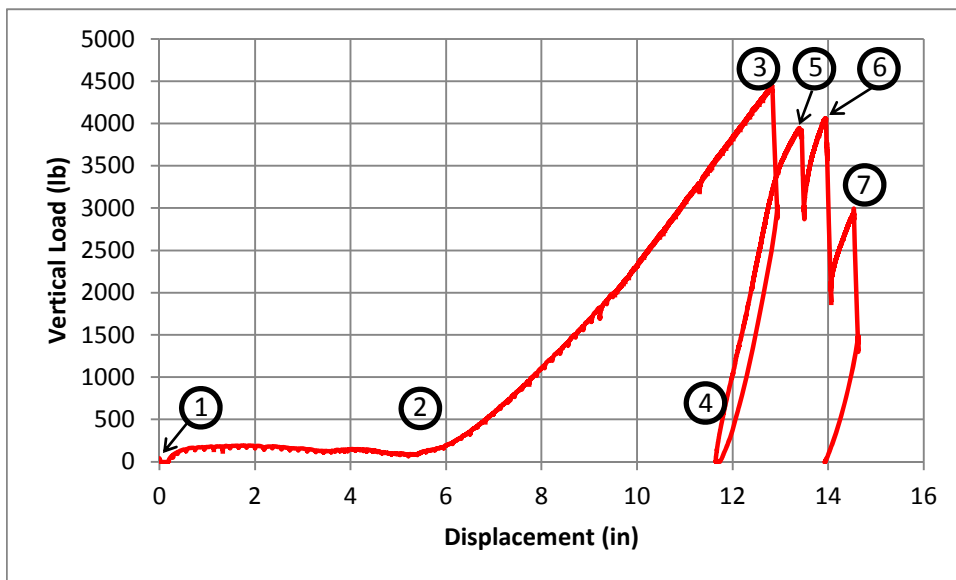


Figure 137. Test 8 vertical load vs. displacement.

Table 90. Test 8 progression of events.

No.	Description of event
1	Removal of supports and initial displacement
2	Axial tension in the beams begins
3	First bolt failure*
4	Unloaded to add 3 blocks because ram reached end of stroke
5	Second bolt failure*
6	Third bolt failure: center column, right side, 2nd from bottom bolt
7	Fourth bolt failure: center column, right side, third from bottom bolt. END OF TEST
*	The first two bolts to fail were the center column, right side, bottom bolt and the left column, top bolt, but order they failed is unknown.

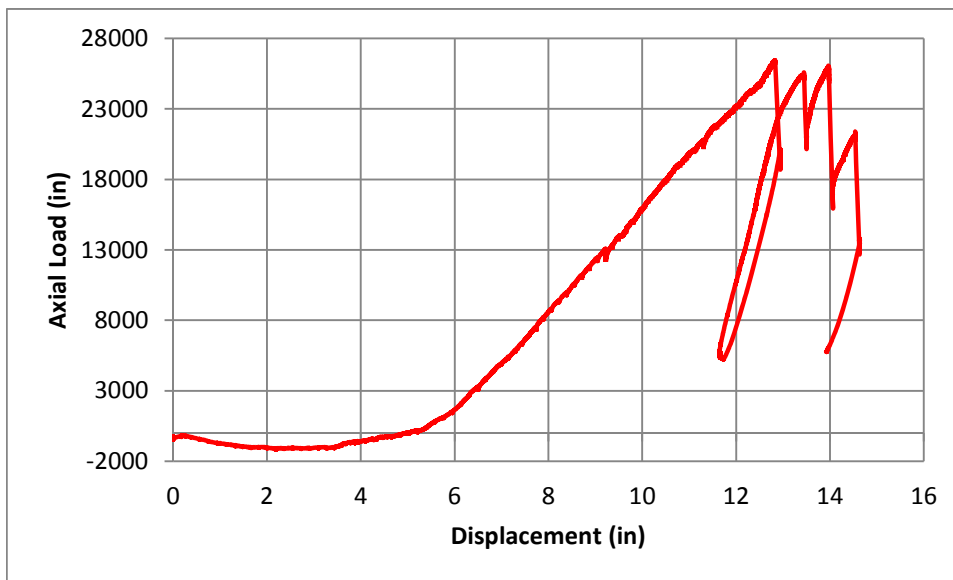


Figure 138. Test 8 axial force vs. displacement.



Figure 139. Test 8 bearing deformations.

Figure 140 shows strain vs. displacement plots for the strain gages in test 8. The strain was as expected with greater tension on the top flanges. Strains measured at the webs (2 and 5) are practically identical for the entire duration of the test. The bottom flange experienced compression for approximately the first half to the test. Strain gage 6 is excluded from the graph since it malfunctioned.

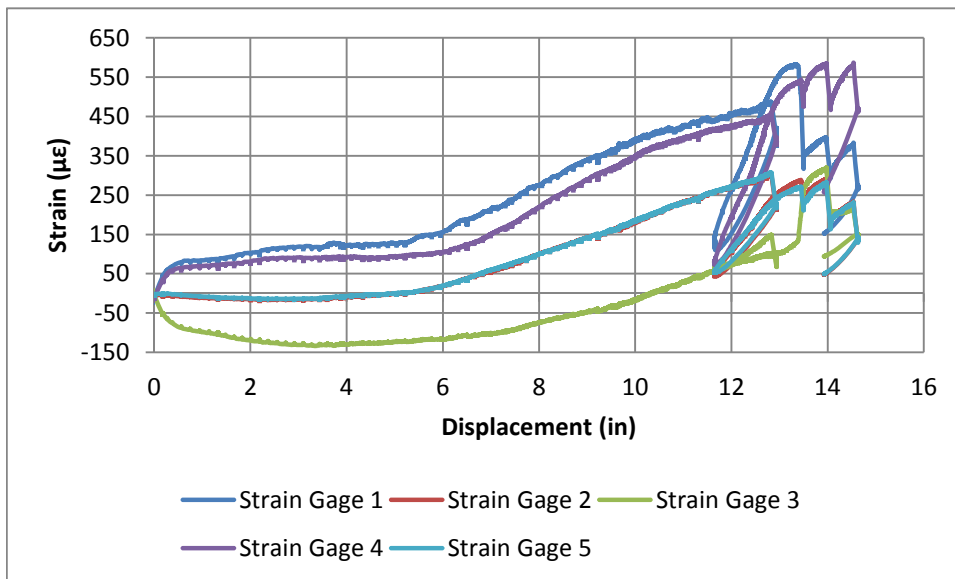


Figure 140. Test 8 strain vs. displacement.

Figure 141 shows the specimen rotation, measured and derived, plotted against the vertical load. The measured rotation had significant noise and stopped working at approximately 0.05 radians of rotation. From the derived rotation it can be seen that the first bolt failure occurred at a rotation of approximately 0.07 radians.

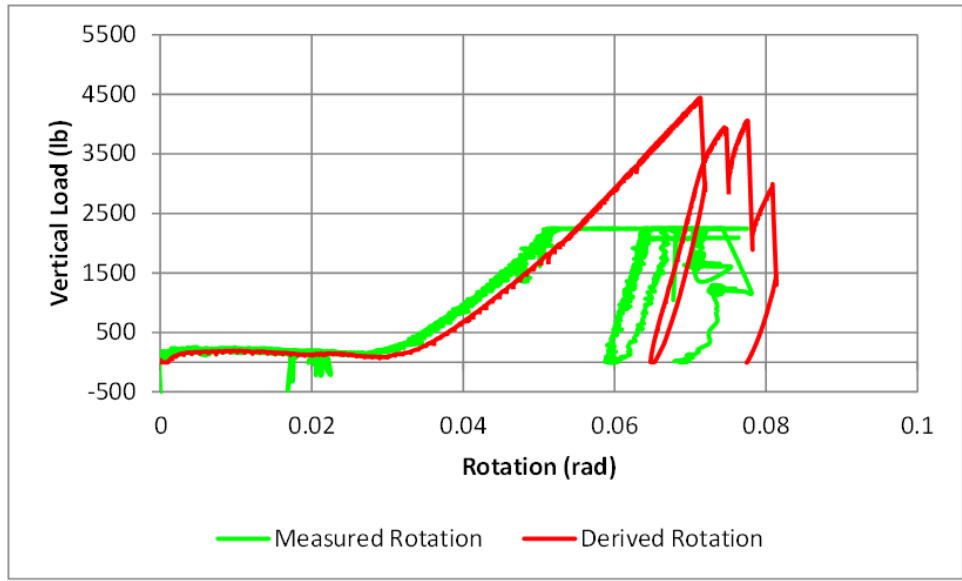


Figure 141. Test 8 vertical load vs. rotation.

Results for Connection 4 are summarized in Table 91. On average, the maximum vertical load resisted was 4.5 kips, equivalent to 2.25 kips of shear at connections, and a maximum axial force of 25.8 kips. The maximum rotation at first failure was 0.065 radians.

Table 91. Summary of Connection Type 4 results (Test 7 and 8).

	Test 7	Test 8	Average
Maximum Vertical Load	4,551 lb (20.2 kN)	4,441 lb (19.8 kN)	4,496 lb (20.0 kN)
Maximum Axial Force	25,230 lb (112.2 kN)	26,445 lb (117.6 kN)	25,838 lb (114.9 kN)
Maximum Deformation of Central Column at First Failure	10.6 in (268.2 mm)	12.8 in (325.1 mm)	11.7 in (296.7 mm)
Rotation at First Failure	0.06 rad (3.4 deg)	0.07 rad (4.0 deg)	0.065 rad (3.7 deg)
Failure Mode	Rupture of bolts	Rupture of bolts	-

7.7.5 Connection Type 5: Specimen 9

Specimen 9, shown in Figure 142 under large deflections, had shear tab connections with (4) 1/2” A325 bolts arranged in two vertical rows. This configuration would not classify as conventional,

per AISC (AISC, 2010). Figure 143 shows the vertical load versus displacement plot, with the main events numbered and described in

Table 92. The maximum vertical load sustained by this specimen was 5,680 lbs. at a displacement of 12.4 in. At that load a bolt failed in shear. The axial force, seen in Figure 144, had reached 36,037 lbs. at that displacement. Note that axial force is only plotted until first failure occurred because strain gages had significant noise afterwards. The test was stopped when four bolts had failed in shear. The two top bolts on the right column shear tab and the two bottom bolts on the left side of the center column failed (Figure 145). Bearing deformations were observed, but these were small, near 1/16" at most.



Figure 142. Test 9 central (missing column) under large deformations.

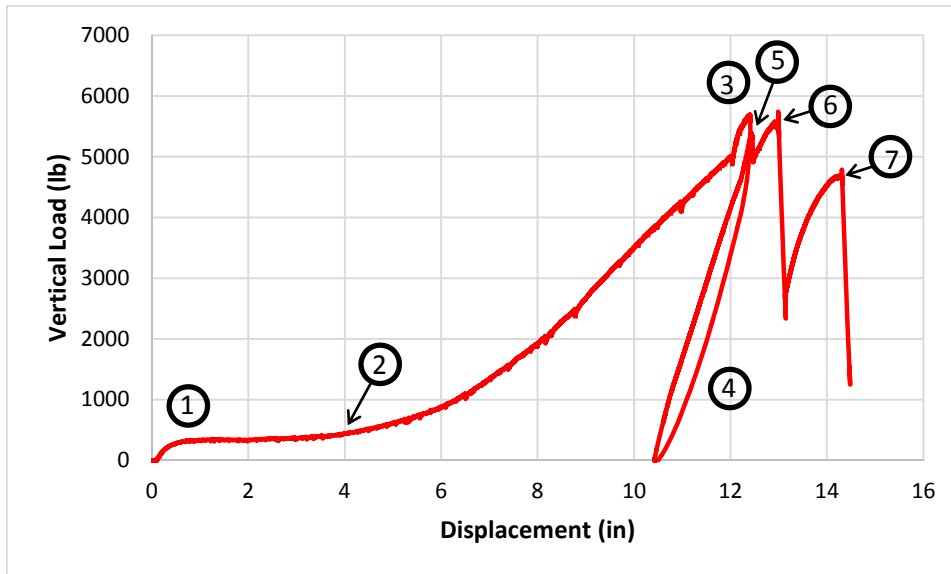


Figure 143. Vertical load vs. displacement for test 9.

Table 92. Test 9 progression of events.

No.	Description of event
1	Removal of supports and initial displacement
2	Axial tension in the beams begins
3	First bolt failure*
4	Unloaded to add spacer blocks since ram reached end of stroke
5	Second Bolt Failure*
6	Third bolt failure*
7	Fourth bolt failure: center column, left side, bottom bolt. END OF TEST
*	Exact order is unknown

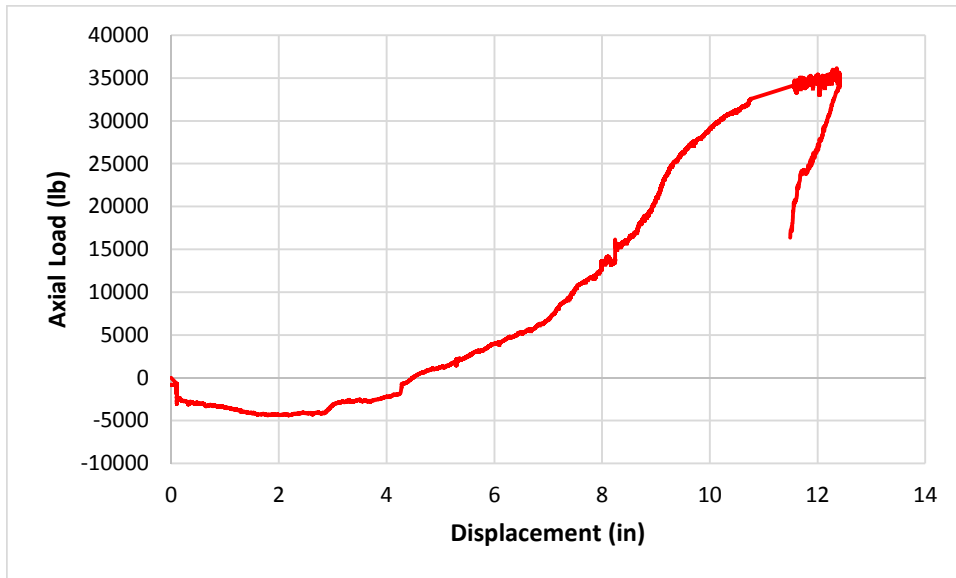


Figure 144. Axial force vs. displacement for test 9.

Figure 146 shows a plot of axial force versus derived rotation. At first failure, the maximum rotation was 0.068 radians.

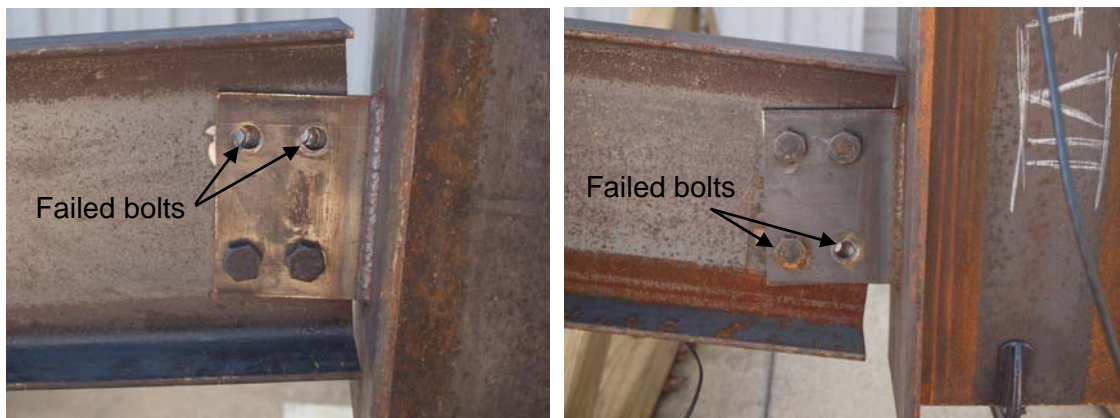


Figure 145. Failed bolts, center column (left) and right column.

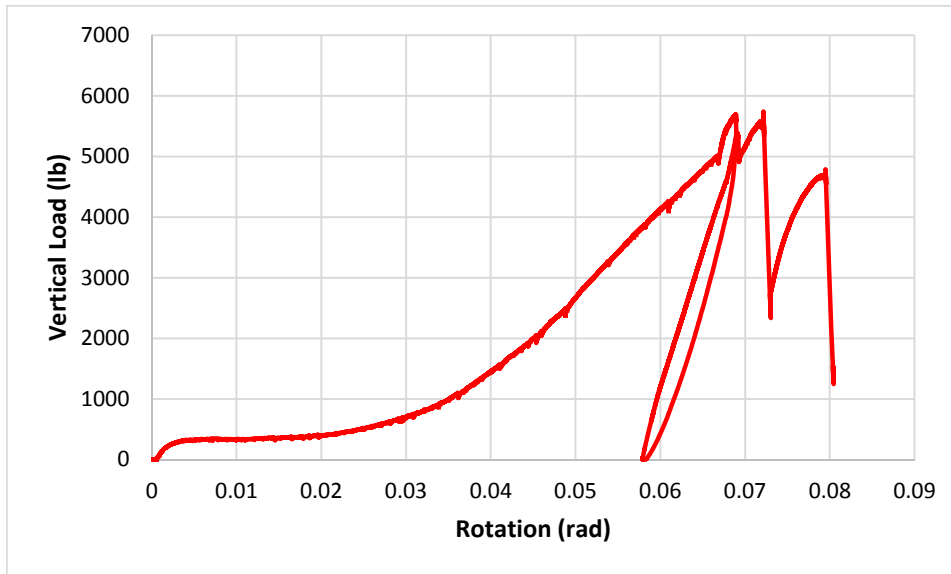


Figure 146. Axial force vs. rotation for test 9.

A summary of the main results for Connection 5 are presented in Table 93.

Table 93. Summary of Connection 5 results (Test 9).

	Test 9
Maximum Vertical Load	5,680 lb (25.3 kN)
Maximum Axial Force	36,037 lb (160.3 kN)
Maximum Deformation of Central Column at First Failure	12.4 in (315.0 mm)
Rotation at First Failure	0.068 rad (3.9 deg)
Failure Mode	Rupture of bolts

### 7.8 Summary and Conclusions

Five different connection types were tested: two specimens for types 1 through 4 and one for type 5, resulting in a total of 9 tests. The average value for vertical load, axial force, deformation, and rotation at first failure are provided in Table 94. All bolted double angle connections (Connection 1) supported the highest vertical load and had the highest rotation at failure (first bolt failure). This connection had three 3/8" bolts in double shear, connecting the angles to the beam's web, and

six bolts (three per angle) in tension connecting the angles to the column flanges. The bolts in tension failed and significant prying deformations of the angles were observed. Large bearing deformations were observed at the webs of the beams. Connection 2 was similar to Connection 1; however, it was welded to the beam's web instead of bolted. Connection 2 had similar axial force capacity as Connection 1. The maximum vertical load, however, was significantly lower. Of all specimens, double angle connections had the higher rotational capacity.

Connection types 3, 4 and 5 had shear tab connections with four bolts. Connection 3 used a conventional shear tab connection, with a ¼" plate welded to the column flange by means of 3/16" welds and beam attached to the web by means of (4) 3/8" J429 Gr. 5 bolts. Connection 4 had a similar detail, but the bolts used were ½" A325. These connection details were chosen to only differ in the bolt diameter size. The 3/8" bolt diameter represents half the diameter of the typical ¾" bolt, while the ½" bolt diameter represents approximately half the area of the ¾" bolt. Connection 4 was able to withstand more than three times the vertical load carried by Connection 3 and approximately twice the axial force. Connection 4 also had a higher rotational capacity at first failure. Connection 5 used an extended shear tab connection with (4) 1/2" bolts arranged in two vertical rows. This specimen had a similar rotational capacity to Connection 4, but it had an increased vertical and axial force capacity. The vertical load carried was 26% higher than in Connection 4 and the axial force carried was 29% higher. For illustration purposes, the vertical load vs. displacement relationship for test 6 (Connection 3), test 8 (Connection 4) and test 9 (Connection 5) are shown in Figure 147.

Table 94. Summary of results.

Connection Type No.	Connection Type	Max. Vertical Load, kip (kN)	Max. Axial Force, kip (kN)	Max. Deformation at first failure, in. (mm)	Rotation at Failure, rad
1	Bolted-bolted double angles	7.9 (35.4)	28.3 (126.0)	19.6 (497.8)	0.108
2	Welded-bolted double angles	5.0 (22.1)	25.3 (112.5)	13.25 (336.6)	0.074
3	Shear tab – 3/8" (10 mm) single row	1.3 (5.8)	13.2 (58.7)	7.4 (188.0)	0.041
4	Shear tab – ½" (13 mm) single row	4.5 (20.0)	25.8 (114.8)	11.7 (297.2)	0.065
5	Shear tab – ½" (13 mm) two rows	5.7 (25.3)	36.0 (160.3)	12.4 (315.0)	0.068

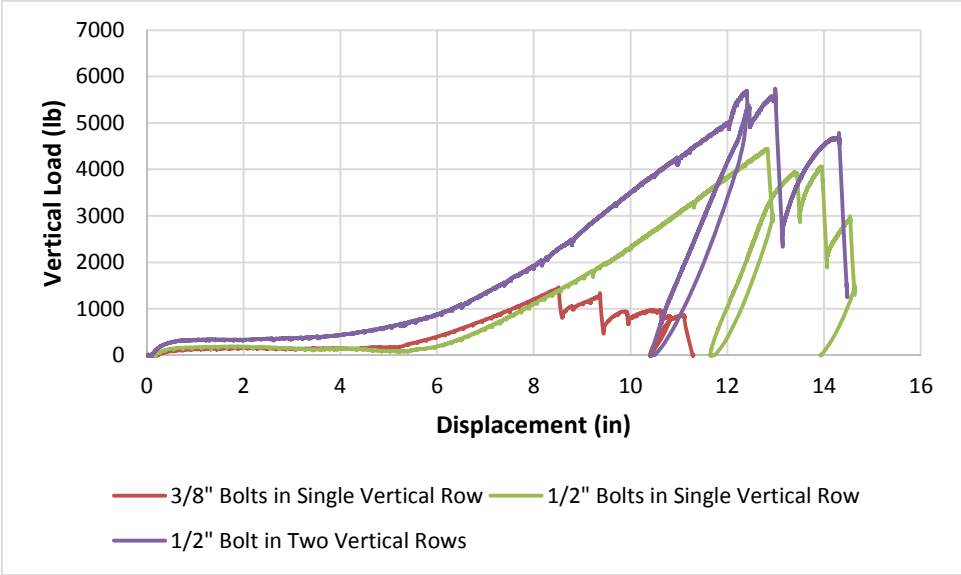


Figure 147. Vertical load vs. displacement for specimens 3, 4 and 5.

## 8 Conclusions

The primary objectives of the study were to: 1) evaluate the concept of using stiff stories to limit deformations in the case of column loss, and 2) add to the body of knowledge on behavior of beam-column gravity connections under column loss cases.

The research tasks included surveying existing buildings with large cantilevers or spans at the ground level. Two of these buildings were selected as inspiration for the two case study buildings with stiff stories. The results of linear column removal analyses (alternate path linear static analysis) were used to assess alternative framing strategies for these case study buildings and to evaluate the effectiveness of the different configurations studied. Observations and recommendations were made with respect to stiff-story configurations and their integration with the lateral force resisting system. Nonlinear column removal analyses were also conducted, and guidance with respect to incorporating nonlinear connection and slab effects was provided. Half-scale push-down tests of frames with simple connections were conducted, providing information on double angle and conventional single-plate connections, as well as single-plate connections with two vertical rows of bolts.

Initial research on robustness of alternative framing strategies established various parameters, factors, and indices that could be used to quantify relative robustness. This collection of factors and indices was developed to characterize relative vulnerability, robustness and efficiency. These factors and indices were later revised and simplified to two factors based on the results of the alternate path linear static analyses for the American Zinc and Lamar configurations. The revised support factor provides some indication of the relative robustness of the system. For steel frame buildings designed following an approach similar to that used in this study, the bracing factor provides an indication of the relative effectiveness of a particular framing configuration in resisting collapse. The most effective configurations have stiff stories that are continuous around the perimeter of the building, reducing potential problems with torsion in the event of column loss. Meanwhile, any stiff-story framing strategy that is integrated with the LFRS and supports all columns will be robust.

Implementation of the nonlinear column removal models in SAP2000 for the American Zinc Sister Building and the Lamar Sister building was a limited success. These models included nonlinear connection behavior as well as contribution from the slab using a strong/weak strip approach. Nonlinear static analysis in SAP2000 was inconsistent in how many steps would be recorded

before failure to converge was reached. However, reasonable results were obtained for the six column removal scenarios that were investigated for each building. System-level stiffness matched expected trends, and equivalent area loads determined from the nonlinear approach compared well to design loads from the linear static procedure. Note that the strong/weak strip approach with support fastener adjustments in conjunction with moment connections or gusset plate connections was not within the scope of Francisco (2014). Further investigation may be required on this aspect of the modeling, as well as on issues with convergence. Despite some current limitations, this method validated the alternative framing strategy approach and highlighted the benefits of the stiff-story concept.

Five different connection types were tested. All bolted double angle connections supported the highest vertical load and had the highest rotation at failure (first bolt failure). The bolts in tension failed, and significant prying deformations of the angles were observed. Large bearing deformations were observed at the webs of the beams. Double angle connections welded to the beam's web instead of bolted were also tested. These had similar axial force capacity as the all-bolted connections. The maximum vertical load, however, was significantly lower. Of all specimens, double angle connections had the higher rotational capacity.

Three different shear tab (single-plate) connections with four bolts were tested. One connection was a conventional shear tab connection, with a  $\frac{1}{4}$ " plate welded to the column flange by means of  $\frac{3}{16}$ " welds and beam attached to the web by means of (4)  $\frac{3}{8}$ " J429 Gr. 5 bolts. The next connection had a similar detail, but the bolts used were  $\frac{1}{2}$ " A325. The  $\frac{3}{8}$ " bolt diameter represents half the diameter of the typical  $\frac{3}{4}$ " bolt, while the  $\frac{1}{2}$ " bolt diameter represents approximately half the area of the  $\frac{3}{4}$ " bolt. The  $\frac{1}{2}$ " bolt connection was able to withstand more than three times the vertical load carried by the  $\frac{3}{8}$ " bolt connection and approximately twice the axial force. The  $\frac{1}{2}$ " bolt connection also had a higher rotational capacity at first failure. The last used an extended shear tab connection with (4)  $\frac{1}{2}$ " bolts arranged in two vertical rows. This specimen had a similar rotational capacity to Connection 4, but it had an increased vertical and axial force capacity. The vertical load carried was 26% higher than the conventional  $\frac{1}{2}$ " bolt shear tab, and the axial force carried was 29% higher.

## 9 References

ASTM (2015), E8/E8M Standard Test Methods for Tension Testing of Metallic Materials, ASTM International, West Conshohocken, PA. [www.astm.org](http://www.astm.org)

AISC (2010), *Specification for Structural Steel Buildings*, ANSI/AISC 360-05, American Institute of Steel Construction, Chicago, IL.

AISC (2011), *Steel Construction Manual*, 14<sup>th</sup> ed., American Institute of Steel Construction, Chicago, IL.

ASCE (2010), *Minimum Design Loads for Buildings and other Structures – ASCE/SEI 7-10*, American Society of Civil Engineers, Reston, Virginia.

ASCE (2007), *Seismic Rehabilitation of Existing Buildings*, ASCE/SEI 41-06, American Society of Civil Engineers, Reston, Virginia.

Department of Defense (DoD) (2009). *Design of building to resist progressive collapse*, UFC 4-023-03, Washington, D.C.

Department of Defense (DoD) (2013). *DoD Minimum Antiterrorism Standards for Buildings*, UFC 4-010-01, Washington, D.C.

Department of Defense (DoD) (2014). *Structural Engineering*, UFC 3-301-01, Washington, D.C.

Francisco, T. (2014). "Structural Integrity of the Composite Slab in Steel Composite Framing Systems." (Doctoral dissertation). Purdue University.

International Code Council (2009). *International Building Code*. Falls Church, VA.

Johnson, E.S., Weigand, J.M., Francisco, T., Fahnestock, L.A., Liu, J. and Berman, J.W. (2014) "Large-Scale Testing of a Steel-Concrete Composite Floor System Under Column Loss Scenarios," 2014 ASCE Structures Congress, Boston, MA, April 3-5, 2014, 10 pages.

Lamar Corporation (n.d.). Portfolio. Retrieved December 15, 2013, from <http://www.lamarconstruction.com/portfolio/details/169/>.

Liu, J.; Astaneh-Asl (2000). "Cyclic Testing of Simple Connections Including Effects of Slabs." *Journal of Structural Engineering*, 126(1), 32-39.

Main, J.A.; Sadek, F. (2012). "Robustness of Steel Gravity-Frame Systems with Single-Plate Shear Connections, NIST Technical Note 1749." National Institute of Standards and Technology, Gaithersburg, MD.

National Register of Historic Places (1998). American Zinc, Lead and Smelting Company Building.

Sintelar, D. South and east elevation's looking northwest. Photograph. 1997.

Stoakes, C. D., Fahnestock, L. A. (2011). "*Cyclic Flexural Testing of Concentrically Braced Frame Beam-Column Connections*," *Journal of Structural Engineering*, No. 137, p. 739-747.

Wong, E. (2013) personal communication by telephone and e-mail, LamarStructure.zip, July 26, 2013.

## Appendix A

### A. Gravity Loads for American Zinc building and for the Chauderon Administration building - Based on ASCE 7-10

Occupancy Category III (Table 1-1)

Surface Roughness Categories (6.5.6.2)

#### 1. Live loads (Table 4-1: office building)

1<sup>st</sup> story: 80 psf (office) + 20psf (partition)= 100psf

2<sup>nd</sup> story: 80 psf (office) + 20psf (partition)= 100psf

Roof: 20 psf

#### 2. Snow loads (Chapter 7)

7.3 Flat Roof Snow Loads,  $p_f$

$$P_f = 0.7 C_e C_t I P_g > I P_g$$

$$C_e = 1.0 \text{ (Table 7-2)}$$

$$C_t = 1.0 \text{ (Table 7-3)}$$

$$I = 1.0 \text{ (Table 7-4)}$$

$$P_g = 20 \text{ psf (Figure 7-1)}$$

$$P_f = 0.7 * 1.0 * 1.0 * 1.0 * 20 = 14$$

$$\text{Also, } P_f = I P_g = 1.0 * 20 = 20 \text{ psf}$$

$$\text{Therefore, } P_f = 20 \text{ psf}$$

#### 3. Dead Loads

Composite concrete steel deck: 40 psf

Mechanical: 5psf

Tile: 16 psf

DL=61 psf

4. Combination of Loads (ASCE 7-10 Ch. 2)

Story 1: LL (100psf), DL(61 psf)

Story 2: LL (100psf), DL(61 psf)

Roof: Lr(20psf), S (20psf), DL(61 psf)

DL= 61 psf

Lr = 20 psf

S = 20 psf

LL = 100 psf

Story 1:

1)  $1.4*(D) = 85.4$  psf

2)  $1.2*D+1.6*L = 233.2$  psf

3)  $1.2*D+1.6*S+L = 173.2$  psf

Story 2:

4)  $1.4*(D) = 85.4$  psf

5)  $1.2*D+1.6*L = 233.2$  psf

6)  $1.2*D+1.6*S+L = 173.2$  psf

Story 3:

7)  $1.4*(D) = 85.4$  psf

8)  $1.2*D+1.6*L = 233.2$  psf

9)  $1.2*D+1.6*S+L = 173.2$  psf

Story 4/Roof:

10)  $1.4*(D) = 85.4$ ?

11)  $1.2*D+1.6*L+0.5*S = 106.2$  psf

12)  $1.2*D+1.6*S+L = 125.2$  psf

## B. Wind Loads for the American Zinc and Lamar Buildings

AZ Wind Loads			
<b>Exterior Wall Area</b>			
E-W wall area (sq ft):	5856	Floor 1 (sq ft):	1586
		Floors 2-3 (sq ft):	1342
		Floor 4 (sq ft):	671
N-S wall area (sq ft):	2568	Floor 1 (sq ft):	695.5
		Floors 2-3 (sq ft):	588.5
		Floor 4 (sq ft):	294.25
<b>Wind Pressures (psf):</b>			
Windward (floor 1):	13.8	E-W leeward:	14.0
Windward (floor 2):	16.1	E-W side:	17.8
Windward (floor 3):	17.9	N-S leeward:	14.0
Windward (floor 4):	19.3	N-S side:	17.8
<b>E-W Case:</b>		<b>N-S Case:</b>	
<i>All forces in kips</i>		<i>All forces in kips</i>	
<b>Story</b>	<b>Windward</b>	<b>Leeward</b>	<b>Total E-W</b>
1	21.8868	22.204	44.0908
2	21.6062	18.788	40.3942
3	24.0218	18.788	42.8098
4	12.9503	12.9503	25.9006
<b>Total</b>	<b>80.4651</b>	<b>72.7303</b>	<b>153.1954</b>
<b>Story</b>	<b>Windward</b>	<b>Leeward</b>	<b>Total E-W</b>
1	9.5979	9.737	19.3349
2	9.47485	8.239	17.71385
3	10.53415	8.239	18.77315
4	5.679025	4.1195	9.798525
<b>Total</b>	<b>80.4651</b>	<b>30.3345</b>	<b>65.620425</b>
<b>Lateral Load Controlling Case:</b>		<b>Lateral Load Controlling Case:</b>	
<i>All forces in kips</i>		<i>All forces in kips</i>	
	<b>E-W</b>	<b>N-S</b>	
Earthquake	159.92	159.92	
Wind	153.20	65.62	
Controlling	159.92	159.92	
	<b>E-W</b>	<b>N-S</b>	
Earthquake	159.92	159.92	
Wind	153.20	65.62	
Controlling	159.92	159.92	

### Lamar Wind Loads

<b>Exterior wall areas:</b>			
E-W wall area:	4056 ft <sup>2</sup>	per floor:	1014 ft <sup>2</sup>
N-S wall area:	9100 ft <sup>2</sup>	per floor:	2275 ft <sup>2</sup>
<b>Wind pressures:</b>			
Windward (floor 1):	22.3 psf	E-W leeward:	13.8 psf
Windward (floor 2):	24.2 psf	E-W side:	24.5 psf
Windward (floor 3):	25.9 psf	N-S leeward:	19.1 psf
Windward (floor 4):	27.2 psf	N-S side:	24.5 psf

<b>E-W Case:</b>			
<i>All forces in kips</i>			
Story	Windward force	Leeward force	Total E-W
1	22.61	13.99	36.61
2	24.54	13.99	38.53
3	26.26	13.99	40.26
4	13.79	7.00	20.79
<b>Total</b>	<b>87.20</b>	<b>48.98</b>	<b>136.18</b>

<b>N-S Case:</b>			
<i>All forces in kips</i>			
Story	Windward force	Leeward force	Total N-S
1	50.73	43.45	94.19
2	55.06	43.45	98.51
3	58.92	43.45	102.38
4	30.94	21.73	52.67
<b>Total</b>	<b>195.65</b>	<b>152.08</b>	<b>347.73</b>

<b>Lateral Load Controlling Case:</b>		
<i>All forces in kips</i>		
	E-W	N-S
Earthquake	112.33	112.33
Wind	136.18	347.73
<b>Controlling</b>	<b>136.18</b>	<b>347.73</b>

Appendix B. m-factor according to ASCE 41 (ASCE, 2007)

American Zinc

		$P/P_{CL} < 0.2$				$0.2 \leq P/P_{CL} \leq 0.5$				Fixed Connection
		Primary		Secondary		Primary m-pl = 6		Secondary m-sl = 10		
Section		m-1	m-2	m-3	m-4	m-1	m-2	m-3	m-4	
1	W10x60	3.95	NA	6.54	NA	3.95	NA	6.54	NA	NA
2	W14x176	6.00	NA	10.00	NA	6.00	NA	10.00	NA	NA
3	W16x45	NA	5.86	NA	9.76	NA	5.86	NA	9.76	1.96
4	W16x57	6.00	NA	10.00	NA	6.00	NA	10.00	NA	1.96
5	W16x67	4.13	NA	6.86	NA	4.13	NA	6.86	NA	1.96
6	W18x86	5.49	NA	9.14	NA	5.49	NA	9.14	NA	1.91
7	W18x119	6.00	NA	10.00	NA	6.00	NA	10.00	NA	1.56
8	W24x146	6.00	NA	10.00	NA	6.00	NA	10.00	NA	1.78
9	W24x162	6.00	NA	10.00	NA	6.00	NA	10.00	NA	1.78
10	W24x279	6.00	NA	10.00	NA	6.00	NA	10.00	NA	NA

Lamar

<b>F</b> Beam Columns-Flexure m-factors						Lamar A1, A2 3/24/2015		
$F_y$	$F_{ye}$	$52/\sqrt{F_{ye}}$	$65/\sqrt{F_{ye}}$	$300/\sqrt{F_{ye}}$	$260/\sqrt{F_{ye}}$	$460/\sqrt{F_{ye}}$	$400/\sqrt{F_{ye}}$	
50	55	7.01	8.76	40.45	35.06	62.03	53.94	$P/P_{CL} = 0.252$

$P/P_{CL} < 0.2$						Primary		Secondary	
	Section	$b_f / 2t_f$	$\leq 52 / \sqrt{F_{ye}}$	$h/t_w$	$\leq 300 / \sqrt{F_{ye}}$	m-1	m-2	m-3	m-4
1	W10X26	6.56	OK	34.0	OK	6.00	NA	10.00	NA
2	W10X30	5.70	OK	29.5	OK	6.00	NA	10.00	NA
3	W10X33	9.15	KO	27.1	OK	1.25	NA	2.00	NA
4	W12X40	7.77	KO	33.6	OK	3.95	NA	6.54	NA
5	W12X58	7.82	KO	27.0	OK	3.81	NA	6.31	NA

$0.2 \leq P/P_{CL} \leq 0.5$						Primary		Secondary	
	Section	$b_f / 2t_f$	$\leq 52 / \sqrt{F_{ye}}$	$h/t_w$	$\leq 260 / \sqrt{F_{ye}}$	m-pl = 5.22		m-sl = 8.7	
						m-1	m-2	m-3	m-4
1	W10X26	6.56	OK	34.0	OK	5.22	5.22	8.70	NA
2	W10X30	5.70	OK	29.5	OK	5.22	5.22	8.70	NA
3	W10X33	9.15	KO	27.1	OK	1.25	NA	2.00	NA
4	W12X40	7.77	KO	33.6	OK	3.50	NA	5.80	NA
5	W12X58	7.82	KO	27.0	OK	3.39	NA	5.61	NA

			$52/\sqrt{F_{ye}}$	$65/\sqrt{F_{ye}}$	$418/\sqrt{F_{ye}}$	$640/\sqrt{F_{ye}}$	<b>P</b> rimary beams	Lamar	A1
Fy	Fye							m-factors	2/10/2015
50	55	7.01	8.76	56.36	86.30				

	Section	bf (in)	tf (in)	h (in)	tw (in)	bf / 2tf	$< 52/\sqrt{F_{ye}}$	h/tw	$< 418/\sqrt{F_{ye}}$	m-1	m-2
1	W18X40	6.015	0.525	17.9	0.315	5.73	OK	50.9	OK	8.93	6.73
2	W16X26	5.5	0.345	15.69	0.25	7.97	KO	56.8	KO	3.81	5.94
If limit checks are both "OK," then use m-factor of 6. Otherwise, use lowest of m-1 or m-2 not less than 2.00											

Based on ASCE 41-06 Table 5-5 (p. 111) LS values

			$52/\sqrt{F_{ye}}$	$65/\sqrt{F_{ye}}$	$418/\sqrt{F_{ye}}$	$640/\sqrt{F_{ye}}$	<b>S</b> econdary beams	Lamar	A1
Fy	Fye							m-factors	2/10/2015
50	55	7.01	8.76	56.36	86.30				

	Section	bf (in)	tf (in)	h (in)	tw (in)	bf / 2tf	$< 52/\sqrt{F_{ye}}$	h/tw	$< 418/\sqrt{F_{ye}}$	m-1	m-2
1	W18X40	6.015	0.525	17.9	0.315	5.73	OK	50.9	OK	15.12	11.28
2	W16X26	5.5	0.345	15.69	0.25	7.97	KO	56.8	KO	6.17	9.90
If limit checks are both "OK," then use m-factor of 10. Otherwise, use lowest of m-1 or m-2 not less than 3.00											

Based on ASCE 41-06 Table 5-5 (p. 111) LS values

<b>C</b>	onnections	Lamar	A1
	m-factors		2/10/2015
		Primary	Secondary
<b>Double Angles</b>	$d_{bg}$ (in)=	3	
<i>Smallest value from:</i>			
Shear in bolt	5.48	8.22	
Tension in bolt	1.50	4.00	
Flexure in angles	8.32	12.13	
<b>Simple Shear Tab</b>	$d_{bg}$ (in)=	6	
	5.16	7.73	
<i>Based on UFC 4-023-03 Table 5-1 (p. 67)</i>			

### Appendix C. Column Removal Results

American Zinc		Column Removal		Column Removal Results Spreadsheet																				3/24/15							
<b>C1</b>		<b>1</b>		Force Control																Deformation Control						Check Total					
Fr. ID	Section	Type	Primary?	Axial			Moment				$P_{UF}/P_{CL} > 0.5$		Shear			Axial			Moment			$P_{UF}/P_{CL} < 0.2$		$0.2 \leq P_{UF}/P_{CL} \leq 0.5$		Tension		Check Total			
				$P_{UF}$ Kip	$P_{CL}$ Kip	$P_{FI}$ Kip	$M_{UFx}$ Kip-ft	$M_{CLx}$ Kip-ft	$M_{UFy}$ Kip-ft	$M_{CLy}$ Kip-ft	$P_{UF}/P_{CL}$	FC?	DCR	$V_{UF}$ Kip	$V_{RF}$ Kip	DCR	$P_{UD}$ Kip	$P_{CE}$ Kip	$P_{TE}$ Kip	$M_{UDx}$ Kip-ft	$M_{CEx}$ Kip-ft	$M_{UDy}$ Kip-ft	$M_{CEy}$ Kip-ft	m-fact.	DCR	m-fact.	DCR		m-fact.	DCR	
A	B	C		FCV	FCVH	FCV	FCV	FCV	FCV	FCV	FCV	FCS	FCS	FCS	DCV	DCV	DCV	DCV	DCV	DCV	DCV	DCV	DCV	DCV	DCV	DCV	DCV	DCV			
1	W18X86	Beam	Secondary	-0.001	972.76	342.45	1148.4	8370	0.032	2178	0.000	n	NA	9.939	265	0.038	0	972.76	1138.5	4750	8370	1E-13	2178	9.14	0.06	NA	NA	NA	NA	0.06	y
10	W18X119	Beam	Primary	-0.001	1358.2	531.00	-1199	11790	-0.03	3109.5	0.000	n	NA	15.97	373.4	0.043	0	1358.2	1579.5	-8466	11790	-6E-14	3109.5	6	0.12	NA	NA	NA	NA	0.12	y
100	W24X279	Column	Primary	-60.94	3250.1	531.00	108.06	37575	-54.49	8685	0.019	n	NA	0.492	930.2	0.001	-283.6	1682	1935	-2375	18810	79.914	4194	6	0.03	NA	NA	NA	NA	0.03	y
101	W24X279	Column	Primary	-34.97	3250.1	531.00	131.39	37575	-8.714	8685	0.011	n	NA	1.456	930.2	0.002	-179.9	1682	1935	-1832	18810	-16.34	4194	6	0.02	NA	NA	NA	NA	0.02	y
102	W24X279	Column	Primary	-16.39	3250.1	342.45	-55.4	37575	-9.139	8685	0.005	n	NA	0.69	930.2	0.001	-67.69	1682	1935	2779.1	18810	0.52	4194	6	0.03	NA	NA	NA	NA	0.03	y
103	W14X176	Column	Primary	-191.7	2013.5	342.45	209.2	14400	-69.46	7335	0.095	n	NA	1.205	379	0.003	-463.1	2013.5	2331	60.694	14400	-191.3	7335	6	0.05	NA	NA	NA	NA	0.05	y
104	W18X86	Beam	Secondary	-0.001	972.76	531.00	746.71	8370	-0.032	2178	0.000	n	NA	6.646	265	0.025	0	972.76	1138.5	3145.6	8370	-1E-13	2178	9.14	0.04	NA	NA	NA	NA	0.04	y
108	W14X176	Column	Primary	-139.6	2154.5	765.00	72.578	14400	-69.42	7335	0.065	n	NA	1.425	379	0.004	-318.7	2154.5	2331	14261	14400	-190.6	7335	6	0.20	NA	NA	NA	NA	0.20	y
109	W14X176	Column	Primary	-86.65	2154.5	765.00	28.72	14400	24.001	7335	0.040	n	NA	0.576	379	0.002	-193.9	2154.5	2331	7868.6	14400	41.733	7335	6	0.11	NA	NA	NA	NA	0.11	y
11	W18X119	Beam	Primary	-0.001	1358.2	765.00	659.93	11790	-0.03	3109.5	0.000	n	NA	7.807	373.4	0.021	0	1358.2	1579.5	4224.1	11790	2E-14	3109.5	6	0.06	NA	NA	NA	NA	0.06	y
110	W14X176	Column	Primary	-31.85	2154.5	531.00	-150.4	14400	0.0079	7335	0.015	n	NA	1.6	379	0.004	-60.35	2154.5	2331	-13783	14400	-0.559	7335	6	0.17	NA	NA	NA	NA	0.17	y
114	W14X176	Column	Primary	-123	2154.5	531.00	762.54	14400	-54.72	7335	0.057	n	NA	11.06	379	0.029	-955.7	2154.5	2331	13924	14400	-109.4	7335	6	0.19	NA	NA	NA	NA	0.19	y
115	W14X176	Column	Primary	-74.56	2154.5	531.00	-569.1	14400	-6.689	7335	0.035	n	NA	8.319	379	0.022	-602.6	2154.5	2331	11357	14400	23.671	7335	6	0.15	NA	NA	NA	NA	0.15	y
116	W14X176	Column	Primary	-28.75	2154.5	531.00	-792.5	14400	-0.036	7335	0.013	n	NA	10.78	379	0.028	-239.7	2154.5	2331	-17232	14400	0.169	7335	6	0.21	NA	NA	NA	NA	0.21	y
12	W18X86	Beam	Secondary	-0.001	972.76	531.00	1148.5	8370	0.032	2178	0.000	n	NA	9.939	265	0.038	0	972.76	1138.5	4750.1	8370	2E-14	2178	9.14	0.06	NA	NA	NA	NA	0.06	y
120	W24X146	Column	Primary	-138	1682	342.45	-1664	18810	-25.28	4194	0.082	n	NA	23.65	482.4	0.049	-525.2	1682	1935	-5144	18810	80.009	4194	6	0.09	NA	NA	NA	NA	0.09	y
121	W24X146	Column	Primary	-84.8	1682	531.00	1250.8	18810	-4.075	4194	0.050	n	NA	18.61	482.4	0.039	-331.2	1682	1935	-3893	18810	-16.28	4194	6	0.06	NA	NA	NA	NA	0.06	y
122	W24X146	Column	Primary	-33.48	1682	531.00	1881.6	18810	0.313	4194	0.020	n	NA	25.23	482.4	0.052	-128.3	1682	1935	5777.2	18810	0.377	4194	6	0.06	NA	NA	NA	NA	0.06	y
126	W14X176	Column	Primary	-94.61	2154.5	531.00	-107.2	14400	9.373	7335	0.044	n	NA	1.132	379	0.003	-584.5	2154.5	2331	-5365	14400	-67	7335	6	0.09	NA	NA	NA	NA	0.09	y
127	W14X176	Column	Primary	-58.01	2154.5	531.00	55.609	14400	-3.107	7335	0.027	n	NA	0.605	379	0.002	-367.9	2154.5	2331	-3861	14400	18.447	7335	6	0.06	NA	NA	NA	NA	0.06	y
128	W14X176	Column	Primary	-21.76	2154.5	531.00	-104.2	14400	0.268	7335	0.010	n	NA	0.997	379	0.003	-141.6	2154.5	2331	5834.5	14400	0.537	7335	6	0.07	NA	NA	NA	NA	0.07	y
13	W18X86	Beam	Secondary	-0.001	972.76	531.00	1148.5	8370	-0.032	2178	0.000	n	NA	9.939	265	0.038	0	972.76	1138.5	4750.1	8370	2E-13	2178	9.14	0.06	NA	NA	NA	NA	0.06	y
132	W14X176	Column	Primary	-121.8	2154.5	342.45	741.98	14400	12.192	7335	0.057	n	NA	10.73	379	0.028	-310.4	2154.5	2331	-2519	14400	-45.35	7335	6	0.06	NA	NA	NA	NA	0.06	y
133	W14X176	Column	Primary	-73.69	2154.5	531.00	-543.8	14400	3.113	7335	0.034	n	NA	7.941	379	0.021	-193.5	2154.5	2331	-1767	14400	16.13	7335	6	0.04	NA	NA	NA	NA	0.04	y
134	W14X176	Column	Primary	-28.37	2154.5	531.00	-746.3	14400	-0.151	7335	0.013	n	NA	10.18	379	0.027	-67.97	2154.5	2331	3142	14400	-0.012	7335	6	0.04	NA	NA	NA	NA	0.04	y
138	W14X176	Column	Primary	-165.3	2013.5	531.00	-441.7	14400	12.049	7335	0.082	n	NA	2.3	379	0.006	-425.3	2013.5	2331	542.09	14400	-45.39	7335	6	0.05	NA	NA	NA	NA	0.05	y
139	W14X176	Column	Primary	-166.8	2013.5	531.00	-450	14400	54.777	7335	0.083	n	NA	2.345	379	0.006	-1271	2013.5	2331	-7248	14400	109.24	7335	6	0.13	NA	NA	NA	NA	0.13	y
14	W18X119	Beam	Primary	-0.001	1358.2	531.00	-1221	11790	-0.03	3109.5	0.000	n	NA	15.9	373.4	0.043	0	1358.2	1579.5	-9737	11790	-2E-13	3109.5	6	0.14	NA	NA	NA	NA	0.14	y
140	W24X146	Column	Primary	-185.7	1491.2	531.00	-783	18810	-24.98	4194	0.125	n	NA	4.128	482.4	0.009	-704.8	1491.2	1935	-1985	18810	80.362	4194	6	0.08	NA	NA	NA	NA	0.08	y
141	W24X146	Column	Primary	18.585	1682	342.45	-2619	18810	26.698	4194	0.011	n	NA	36.18	482.4	0.075	-107.2	1682	1935	-4060	18810	106.76	4194	6	NA	NA	NA	3.00	0.06	0.07	y
142	W24X146	Column	Primary	12.523	1682	531.00	-1597	18810	-5.486	4194	0.007	n	NA	23.85	482.4	0.049	-66	1682	1935	-2249	18810	-19.03	4194	6	NA	NA	NA	3.00	0.03	0.05	y
143	W24X146	Column	Primary	9.829	1682	531.00	2927.8	18810	-0.432	4194	0.006	n	NA	37.37	482.4	0.077	-13.66	1682	1935	4282.5	18810	-0.52	4194	6	NA	NA	NA	3.00	0.04	0.08	y
144	W24X146	Column	Primary	-72.26	1682	531.00	712.97	18810	26.142	4194	0.043	n	NA	10.21	482.4	0.021	-235.2	1682	1935	433.25	18810	106.76	4194	6	0.03	NA	NA	NA	NA	0.03	y

Lamar		Column Removal		Column Removal Results Spreadsheet																				3/24/2015								
<b>A1</b>		<b>1 (G-1)</b>		Force Control																Deformation Control						Check Total						
Fr. ID	Section	Type	Primary?	Axial			Moment				$P_{UF}/P_{CL} > 0.5$		Shear			Axial			Moment			$P_{UF}/P_{CL} < 0.2$		$0.2 \leq P_{UF}/P_{CL} \leq 0.5$		Tension		Braces		Check Total		
				$P_{UF}$ Kip	$P_{CL}$ Kip	$M_{UFx}$ Kip-ft	$M_{CLx}$ Kip-ft	$M_{UFy}$ Kip-ft	$M_{CLy}$ Kip-ft	$P_{UF}/P_{CL}$	FC?	DCR	$V_{UF}$ Kip	$V_{RF}$ Kip	DCR	$P_{UD}$ Kip	$P_{CE}$ Kip	$P_{TE}$ Kip	$M_{UDx}$ Kip-ft	$M_{CEx}$ Kip-ft	$M_{UDy}$ Kip-ft	$M_{CEy}$ Kip-ft	m-fact.	DCR	m-fact.	DCR	m-fact.	DCR	m-fact.		DCR	
A	B	C		FCV	FCVH	FCV	FCV	FCV	FCV	FCV	FCS	FCS	FCS	DCV	DCV	DCV	DCV	DCV	DCV	DCV	DCV	DCV	DCV	DCV	DCV	DCV	DCV	DCV	DCV	DCV		
1534	W12X40	Column	Primary	-446.71	329.85	-13.79	215.63	0.03	63.00	1.354	y	1.42	1.56	105.7	0.015	-527.2	346.0	575.3	-4.80	225.93	0.01	69.30	NA	NA	NA	NA	NA	NA	NA	NA	1.42	n
1544	W12X40	Column	Primary	-401.93	329.85	-10.17	215.63	-0.03	63.00	1.219	y	1.27	1.14	105.7	0.011	-459.2	346.0	575.3	-3.26	221.53	-0.04	69.30	NA	NA	NA	NA	NA	NA	NA	NA	1.27	n

Lamar		Column Removal	Column Removal Results Spreadsheet																				3/24/2015									
A1		2	(A-2)		Force Control										Deformation Control										Check							
Fr. ID	Section	Type	Primary?	Axial		Moment				$P_{UF}/P_{CL} > 0.5$			Shear			Axial				Moment				$P_{UF}/P_{CL} < 0.2$		$0.2 \leq P_{UF}/P_{CL} \leq 0.5$		Tension	Braces	Check		
				$P_{UF}$	$P_{CL}$	$M_{UFx}$	$M_{CLx}$	$M_{UFy}$	$M_{CLy}$	$P_{UF}/P_{CL}$	FC?	DCR	$V_{UF}$	$V_{RF}$	DCR	$P_{UD}$	$P_{CE}$	$P_{TE}$	$M_{UDx}$	$M_{CEx}$	$M_{UDy}$	$M_{CEy}$	m-fact.	DCR	m-fact.	DCR	m-fact.	DCR	m-fact.	DCR	DCR	OK?
A	B	C		FC Y	FC V	FC Y	FC Z	FC A	FC A				FCS	FCS		DC Y	DC V	DC Y	DC A	DC A												
8	W12X40	Column	Primary	-484.86	329.85	-10.89	215.63	-27.18	63.00	1.470	y	1.95	1.29	105.7	0.012	-582.4	346.0	575.3	-1.33	237.19	-6.10	69.30	NA	NA	NA	NA	NA	NA	NA	1.95	n	
16	W12X58	Column	Secondary	-429.95	576.61	13.66	324.00	-31.51	121.88	0.746	y	1.05	1.46	131.8	0.011	-492.5	616.6	828.8	17.15	356.40	-37.42	134.06	NA	NA	NA	NA	NA	NA	NA	1.05	n	
24	W12X40	Column	Primary	297.03	329.85	-30.89	215.63	-14.77	63.00	0.900	y	1.28	5.16	105.7	0.049	394.6	346.0	575.3	-40.52	237.19	-20.84	69.30	1.25	NA	NA	NA	3.00	0.61	NA	NA	1.28	n
44	W10X26	Brace	Primary	-448.64	68.01	0.88	74.32	0.00	28.13	6.597	n	NA	2.51	80.3	0.031	-557.2	68.0	371.0	0.88	74.32	0.00	30.94	NA	NA	NA	NA	NA	6.00	1.37	1.37	n	
56	W12X40	Column	Primary	297.25	329.85	30.96	215.63	18.93	63.00	0.901	y	1.35	5.18	105.7	0.049	395.1	346.0	575.3	40.67	237.19	26.67	69.30	1.25	NA	NA	NA	3.00	0.67	NA	NA	1.35	n
66	W12X40	Column	Primary	-485.07	329.85	10.90	215.63	21.13	63.00	1.471	y	1.86	1.29	105.7	0.012	-582.8	346.0	575.3	1.30	237.19	4.75	69.30	NA	NA	NA	NA	NA	NA	NA	1.86	n	
122	W10X26	Brace	Primary	-447.74	68.01	0.88	74.32	0.00	28.13	6.583	n	NA	2.50	80.3	0.031	-555.5	68.0	371.0	0.88	74.32	0.00	30.94	NA	NA	NA	NA	NA	6.00	1.36	1.36	n	
1523	W12X40	Column	Primary	565.92	329.85	30.96	215.63	18.87	63.00	1.716	y	2.16	0.99	105.7	0.009	742.8	346.0	575.3	40.66	237.19	26.65	69.30	1.25	NA	NA	NA	3.00	0.88	NA	NA	2.16	n
1534	W12X40	Column	Primary	-843.47	329.85	17.87	215.63	-19.42	63.00	2.557	y	2.95	4.28	105.7	0.040	-1020.4	346.0	575.3	18.61	237.19	1.66	69.30	NA	NA	NA	NA	NA	NA	NA	2.95	n	
1544	W12X40	Column	Primary	-842.60	329.85	-17.82	215.63	-25.33	63.00	2.554	y	3.04	4.27	105.7	0.040	-1018.7	346.0	575.3	-18.48	237.19	2.08	69.30	NA	NA	NA	NA	NA	NA	NA	3.04	n	
1555	W12X40	Column	Primary	565.03	329.85	-30.89	215.63	14.82	63.00	1.713	y	2.09	0.99	105.7	0.009	741.2	346.0	575.3	-40.52	237.19	20.92	69.30	1.25	NA	NA	NA	3.00	0.81	NA	NA	2.09	n
91	W16X26	Beam	Primary	-0.01	89.25	-315.02	38.00	0.04	33.64	0.000	n	NA	35.00	106.0	0.330	0.0	89.2	594.4	-398.46	37.92	0.04	33.64	3.81	2.76	NA	NA	NA	NA	NA	2.76	n	
176	W12X40	Column	Primary	-274.75	329.85	-128.83	215.63	0.35	63.00	0.833	y	1.44	2.65	105.7	0.025	-325.8	346.0	575.3	-81.67	237.19	2.60	69.30	NA	NA	NA	NA	NA	NA	NA	1.44	n	
243	W12X40	Column	Primary	-438.71	329.85	-128.82	215.63	0.35	63.00	1.330	y	1.93	15.97	105.7	0.151	-514.9	346.0	575.3	-81.64	237.19	2.61	69.30	NA	NA	NA	NA	NA	NA	NA	1.93	n	
569	W12X40	Column	Primary	-469.89	329.85	-6.17	215.63	-2.21	63.00	1.425	y	1.49	1.31	105.7	0.012	-551.4	346.0	575.3	-4.20	226.57	-1.18	69.30	NA	NA	NA	NA	NA	NA	NA	1.49	n	

Lamar		Column Removal	Column Removal Results Spreadsheet																				4/1/2015									
A1B		1	(A-2)		Force Control										Deformation Control										Check							
Fr. ID	Section	Type	Primary?	Axial		Moment				$P_{UF}/P_{CL} > 0.5$			Shear			Axial				Moment				$P_{UF}/P_{CL} < 0.2$		$0.2 \leq P_{UF}/P_{CL} \leq 0.5$		Tension	Braces	Check		
				$P_{UF}$	$P_{CL}$	$M_{UFx}$	$M_{CLx}$	$M_{UFy}$	$M_{CLy}$	$P_{UF}/P_{CL}$	FC?	DCR	$V_{UF}$	$V_{RF}$	DCR	$P_{UD}$	$P_{CE}$	$P_{TE}$	$M_{UDx}$	$M_{CEx}$	$M_{UDy}$	$M_{CEy}$	m-fact.	DCR	m-fact.	DCR	m-fact.	DCR	m-fact.	DCR	DCR	OK?
A	B	C		FC Y	FC V	FC Y	FC Z	FC A	FC A				FCS	FCS		DC Y	DC V	DC Y	DC A	DC A												
8	W12X40	Column	Primary	-613.54	329.85	0.42	215.63	-5.82	63.00	1.860	y	1.95	4.33	105.7	0.041	-750.7	346.0	575.3	-0.46	237.19	-0.09	69.30	NA	NA	NA	NA	NA	NA	NA	1.95	n	
24	W12X40	Column	Primary	442.77	329.85	-2.90	215.63	-1.78	63.00	1.342	y	1.38	3.46	105.7	0.033	583.9	346.0	575.3	-3.01	237.19	-2.08	69.30	1.25	NA	NA	NA	3.00	0.37	NA	NA	1.38	n
31	W10X26	Brace	Primary	-637.35	68.01	0.88	74.32	0.00	28.13	9.371	n	NA	2.29	80.3	0.028	-763.8	68.0	371.0	0.88	74.32	0.00	30.94	NA	NA	NA	NA	NA	6.00	1.87	1.87	n	
56	W12X40	Column	Primary	443.41	329.85	2.91	215.63	2.22	63.00	1.344	y	1.39	3.47	105.7	0.033	585.0	346.0	575.3	2.96	237.19	2.56	69.30	1.25	NA	NA	NA	3.00	0.38	NA	NA	1.39	n
66	W12X40	Column	Primary	-614.20	329.85	-0.43	215.63	5.02	63.00	1.862	y	1.94	4.34	105.7	0.041	-751.9	346.0	575.3	0.46	237.19	0.17	69.30	NA	NA	NA	NA	NA	NA	NA	1.94	n	
121	W10X26	Brace	Primary	-636.18	68.01	0.88	74.32	0.00	28.13	9.354	n	NA	2.27	80.3	0.028	-761.8	68.0	371.0	0.88	74.32	0.00	30.94	NA	NA	NA	NA	NA	6.00	1.87	1.87	n	
1523	W12X40	Column	Primary	410.24	329.85	2.90	215.63	2.18	63.00	1.244	y	1.29	2.55	105.7	0.024	551.8	346.0	575.3	2.96	237.19	2.52	69.30	1.25	NA	NA	NA	3.00	0.36	NA	NA	1.29	n
1534	W12X40	Column	Primary	-648.00	329.85	0.54	215.63	4.20	63.00	1.965	y	2.03	4.42	105.7	0.042	-785.4	346.0	575.3	1.00	237.19	-0.05	69.30	NA	NA	NA	NA	NA	NA	NA	2.03	n	
1544	W12X40	Column	Primary	-647.34	329.85	-0.54	215.63	4.96	63.00	1.963	y	2.04	4.40	105.7	0.042	-784.3	346.0	575.3	-1.01	237.19	-0.07	69.30	NA	NA	NA	NA	NA	NA	NA	2.04	n	
1555	W12X40	Column	Primary	409.60	329.85	-2.90	215.63	1.86	63.00	1.242	y	1.28	2.54	105.7	0.024	550.6	346.0	575.3	-3.01	237.19	2.14	69.30	1.25	NA	NA	NA	3.00	0.35	NA	NA	1.28	n
569	W12X40	Column	Primary	-370.02	329.85	-2.64	215.63	-0.05	63.00	1.122	y	1.13	1.16	105.7	0.011	-432.6	346.0	575.3	-1.38	237.19	4.41	69.30	NA	NA	NA	NA	NA	NA	NA	1.13	n	
590	W12X40	Column	Primary	-332.80	329.85	-2.63	215.63	-0.05	63.00	1.009	y	1.02	0.79	105.7	0.007	-395.0	346.0	575.3	-1.87	237.19	-3.12	69.30	NA	NA	NA	NA	NA	NA	NA	1.02	n	
7	W10X26	Brace	Primary	-303.85	68.01	0.88	74.32	0.00	28.13	4.468	n	NA	1.87	80.3	0.023	-414.5	68.0	371.0	0.88	74.32	0.00	30.94	NA	NA	NA	NA	NA	6.00	1.02	1.02	n	
9	W10X26	Brace	Primary	-304.49	68.01	0.88	74.32	0.00	28.13	4.477	n	NA	1.87	80.3	0.023	-415.5	68.0	371.0	0.88	74.32	0.00	30.94	NA	NA	NA	NA	NA	6.00	1.02	1.02	n	

Lamar		Column Removal	Column Removal Results Spreadsheet																				3/27/2015									
A2		1	(G-4)		Force Control										Deformation Control										Check							
Fr. ID	Section	Type	Primary?	Axial		Moment				$P_{UF}/P_{CL} > 0.5$		Shear		Axial			Moment				$P_{UF}/P_{CL} < 0.2$		$0.2 \leq P_{UF}/P_{CL} \leq 0.5$		Tension		Braces		Total			
				$P_{UF}$ Kip	$P_{CL}$ Kip	$M_{UFx}$ Kip-ft	$M_{CLx}$ Kip-ft	$M_{UFy}$ Kip-ft	$M_{CLy}$ Kip-ft	$P_{UF}/P_{CL}$	FC?	DCR	$V_{UF}$ Kip	$V_{RF}$ Kip	DCR	$P_{UD}$ Kip	$P_{CE}$ Kip	$P_{TE}$ Kip	$M_{UDx}$ Kip-ft	$M_{CEx}$ Kip-ft	$M_{UDy}$ Kip-ft	$M_{CEy}$ Kip-ft	m-fact.	DCR	m-fact.	DCR	m-fact.	DCR	m-fact.	DCR	DCR	OK?
1555	W12X40	Column	Primary	-336.08	329.85	-4.27	215.63	0.00	63.00	1.019	y	1.04	0.55	105.7	0.005	-373.6	346.0	575.3	-4.66	237.19	-0.01	69.30	NA	NA	NA	NA	NA	NA	NA	NA	1.04	n

Lamar		Column Removal	Column Removal Results Spreadsheet																				3/27/2015									
A2		2	(A-1)		Force Control										Deformation Control										Check							
Fr. ID	Section	Type	Primary?	Axial		Moment				$P_{UF}/P_{CL} > 0.5$		Shear		Axial			Moment				$P_{UF}/P_{CL} < 0.2$		$0.2 \leq P_{UF}/P_{CL} \leq 0.5$		Tension		Braces		Total			
				$P_{UF}$ Kip	$P_{CL}$ Kip	$M_{UFx}$ Kip-ft	$M_{CLx}$ Kip-ft	$M_{UFy}$ Kip-ft	$M_{CLy}$ Kip-ft	$P_{UF}/P_{CL}$	FC?	DCR	$V_{UF}$ Kip	$V_{RF}$ Kip	DCR	$P_{UD}$ Kip	$P_{CE}$ Kip	$P_{TE}$ Kip	$M_{UDx}$ Kip-ft	$M_{CEx}$ Kip-ft	$M_{UDy}$ Kip-ft	$M_{CEy}$ Kip-ft	m-fact.	DCR	m-fact.	DCR	m-fact.	DCR	m-fact.	DCR	DCR	OK?
1519	W12X40	Column	Primary	-346.12	329.85	-0.10	215.63	0.05	63.00	1.049	y	1.05	0.03	105.7	0.000	-396.6	346.0	575.3	0.00	237.19	-0.01	69.30	NA	NA	NA	NA	NA	NA	NA	NA	1.05	n

Lamar		Column Removal	Column Removal Results Spreadsheet																				3/30/2015									
A2		5	(A-3)		Force Control										Deformation Control										Check							
Fr. ID	Section	Type	Primary?	Axial		Moment				$P_{UF}/P_{CL} > 0.5$		Shear		Axial			Moment				$P_{UF}/P_{CL} < 0.2$		$0.2 \leq P_{UF}/P_{CL} \leq 0.5$		Tension		Braces		Total			
				$P_{UF}$ Kip	$P_{CL}$ Kip	$M_{UFx}$ Kip-ft	$M_{CLx}$ Kip-ft	$M_{UFy}$ Kip-ft	$M_{CLy}$ Kip-ft	$P_{UF}/P_{CL}$	FC?	DCR	$V_{UF}$ Kip	$V_{RF}$ Kip	DCR	$P_{UD}$ Kip	$P_{CE}$ Kip	$P_{TE}$ Kip	$M_{UDx}$ Kip-ft	$M_{CEx}$ Kip-ft	$M_{UDy}$ Kip-ft	$M_{CEy}$ Kip-ft	m-fact.	DCR	m-fact.	DCR	m-fact.	DCR	m-fact.	DCR	DCR	OK?
1523	W12X40	Column	Primary	-311.40	329.85	-4.48	215.63	-4.05	63.00	0.944	y	1.03	0.99	105.7	0.009	-348.3	346.0	575.3	-5.40	237.19	-5.36	69.30	NA	NA	NA	NA	NA	NA	NA	NA	1.03	n
1555	W12X40	Column	Primary	-311.98	329.85	4.48	215.63	-3.26	63.00	0.946	y	1.02	0.99	105.7	0.009	-349.2	346.0	575.3	5.40	237.19	-4.33	69.30	NA	NA	NA	NA	NA	NA	NA	NA	1.02	n
69	W12X40	Column	Primary	-467.90	329.85	40.74	215.63	0.06	63.00	1.419	y	1.61	6.10	105.7	0.058	-551.8	346.0	575.3	47.82	237.19	-0.08	69.30	NA	NA	NA	NA	NA	NA	NA	NA	1.61	n
90	W12X40	Column	Primary	-363.90	329.85	40.74	215.63	0.07	63.00	1.103	y	1.29	1.44	105.7	0.014	-431.1	346.0	575.3	47.83	237.19	-0.04	69.30	NA	NA	NA	NA	NA	NA	NA	NA	1.29	n
91	W16X26	Beam	Primary	-0.01	89.25	-135.95	42.15	0.04	33.64	0.000	n	NA	21.28	106.0	0.201	0.0	89.2	594.4	-162.73	42.27	-0.04	33.64	3.81	1.01	NA	NA	NA	NA	NA	NA	1.01	n
587	W12X40	Column	Primary	-446.15	329.85	7.08	215.63	-0.10	63.00	1.353	y	1.39	0.79	105.7	0.008	-511.8	346.0	575.3	8.49	237.19	-0.03	69.30	NA	NA	NA	NA	NA	NA	NA	NA	1.39	n
591	W12X40	Column	Primary	-340.55	329.85	7.08	215.63	-0.11	63.00	1.032	y	1.07	0.07	105.7	0.001	-393.5	346.0	575.3	8.48	237.19	-0.04	69.30	NA	NA	NA	NA	NA	NA	NA	NA	1.07	n

Lamar		Column Removal	Column Removal Results Spreadsheet																				4/15/2015									
A3		1	(G-4)		Force Control										Deformation Control										Check							
Fr. ID	Section	Type	Primary?	Axial		Moment				$P_{UF}/P_{CL} > 0.5$		Shear		Axial			Moment				$P_{UF}/P_{CL} < 0.2$		$0.2 \leq P_{UF}/P_{CL} \leq 0.5$		Tension		Braces		Total			
				$P_{UF}$ Kip	$P_{CL}$ Kip	$M_{UFx}$ Kip-ft	$M_{CLx}$ Kip-ft	$M_{UFy}$ Kip-ft	$M_{CLy}$ Kip-ft	$P_{UF}/P_{CL}$	FC?	DCR	$V_{UF}$ Kip	$V_{RF}$ Kip	DCR	$P_{UD}$ Kip	$P_{CE}$ Kip	$P_{TE}$ Kip	$M_{UDx}$ Kip-ft	$M_{CEx}$ Kip-ft	$M_{UDy}$ Kip-ft	$M_{CEy}$ Kip-ft	m-fact.	DCR	m-fact.	DCR	m-fact.	DCR	m-fact.	DCR	DCR	OK?
1555	W12X40	Column	Primary	-336.48	329.85	-4.22	215.63	0.00	63.00	1.020	y	1.04	0.54	105.7	0.005	-389.9	346.0	575.3	-4.95	237.19	0.00	69.30	NA	NA	NA	NA	NA	NA	NA	NA	1.04	n

Lamar		Column Removal	Column Removal Results Spreadsheet																				4/7/2015									
B1		2	(C-4)		Force Control										Deformation Control										Check							
Fr. ID	Section	Type	Primary?	Axial		Moment				$P_{UF}/P_{CL} > 0.5$		Shear		Axial			Moment				$P_{UF}/P_{CL} < 0.2$		$0.2 \leq P_{UF}/P_{CL} \leq 0.5$		Tension		Braces		Total			
				$P_{UF}$ Kip	$P_{CL}$ Kip	$M_{UFx}$ Kip-ft	$M_{CLx}$ Kip-ft	$M_{UFy}$ Kip-ft	$M_{CLy}$ Kip-ft	$P_{UF}/P_{CL}$	FC?	DCR	$V_{UF}$ Kip	$V_{RF}$ Kip	DCR	$P_{UD}$ Kip	$P_{CE}$ Kip	$P_{TE}$ Kip	$M_{UDx}$ Kip-ft	$M_{CEx}$ Kip-ft	$M_{UDy}$ Kip-ft	$M_{CEy}$ Kip-ft	m-fact.	DCR	m-fact.	DCR	m-fact.	DCR	m-fact.	DCR	DCR	OK?
369	W12X40	Column	Primary	-377.81	329.85	5.43	215.63	0.09	63.00	1.145	y	1.17	0.58	105.7	0.006	-458.9	346.0	575.3	7.42	237.19	0.12	69.30	NA	NA	NA	NA	NA	NA	NA	NA	1.17	n

Lamar		Column Removal		Column Removal Results Spreadsheet																				4/7/2015									
<b>B1</b>		<b>3 (O-2)</b>		Force Control										Deformation Control										Check									
Fr. ID	Section	Type	Primary?	Axial		Moment				$P_{UF}/P_{CL} > 0.5$			Shear			Axial		Moment				$P_{UF}/P_{CL} < 0.2$		$0.2 \leq P_{UF}/P_{CL} \leq 0.5$		Tension		Braces		Check Total			
				$P_{UF}$ Kip	$P_{CL}$ Kip	$M_{UFx}$ Kip-ft	$M_{CLx}$ Kip-ft	$M_{UFy}$ Kip-ft	$M_{CLy}$ Kip-ft	$P_{UF}/P_{CL}$	FC?	DCR	$V_{UF}$ Kip	$V_{RF}$ Kip	DCR	$P_{UD}$ Kip	$P_{CE}$ Kip	$P_{TE}$ Kip	$M_{UDx}$ Kip-ft	$M_{CEx}$ Kip-ft	$M_{UDy}$ Kip-ft	$M_{CEy}$ Kip-ft	m-fact.	DCR	m-fact.	DCR	m-fact.	DCR	m-fact.		DCR	DCR	OK?
59	W12X40	Column	Primary	-322.55	329.85	-18.20	215.63	1.42	63.00	0.978	y	1.08	0.25	105.7	0.002	-386.7	346.0	575.3	-22.05	237.19	30.53	69.30	NA	NA	NA	NA	NA	NA	NA	NA	1.08	n	
1530	W12X40	Column	Primary	-526.43	329.85	-11.42	215.63	-26.42	63.00	1.596	y	2.07	2.36	105.7	0.022	-633.1	346.0	575.3	-14.54	237.19	-98.22	69.30	NA	NA	NA	NA	NA	NA	NA	NA	2.07	n	
1540	W12X40	Column	Primary	-467.05	329.85	11.23	215.63	-5.32	63.00	1.416	y	1.55	2.26	105.7	0.021	-546.9	346.0	575.3	14.18	237.19	-10.06	69.30	NA	NA	NA	NA	NA	NA	NA	NA	1.55	n	
1551	W12X40	Column	Primary	218.80	329.85	20.55	215.63	-15.65	63.00	0.663	y	1.01	1.24	105.7	0.012	298.7	346.0	575.3	25.69	237.19	-20.63	69.30	1.25	NA	NA	NA	NA	3.00	0.50	NA	NA	1.01	n
69	W12X40	Column	Primary	-456.44	329.85	-6.10	215.63	1.44	63.00	1.384	y	1.43	1.17	105.7	0.011	-529.2	346.0	575.3	-7.77	237.19	2.57	69.30	NA	NA	NA	NA	NA	NA	NA	NA	1.43	n	
251	W12X40	Column	Primary	-423.06	329.85	-18.56	215.63	-0.51	63.00	1.283	y	1.38	2.19	105.7	0.021	-503.5	346.0	575.3	-14.04	237.19	-3.51	69.30	NA	NA	NA	NA	NA	NA	NA	NA	1.38	n	
572	W16X26	Beam	Primary	-0.01	89.25	-243.52	38.86	0.04	33.64	0.000	n	NA	29.50	106.0	0.278	0.0	89.2	594.4	-299.11	38.84	0.04	33.64	3.81	2.02	NA	NA	NA	NA	NA	NA	2.02	n	
587	W12X40	Column	Primary	-449.64	329.85	-92.60	215.63	-0.21	63.00	1.363	y	1.80	11.17	105.7	0.106	-529.9	346.0	575.3	-112.80	237.19	0.17	69.30	NA	NA	NA	NA	NA	NA	NA	NA	1.80	n	
591	W12X40	Column	Primary	-289.69	329.85	-92.60	215.63	-0.22	63.00	0.878	y	1.31	1.89	105.7	0.018	-342.5	346.0	575.3	-112.80	237.19	0.17	69.30	NA	NA	NA	NA	NA	NA	NA	NA	1.31	n	
593	W12X40	Column	Primary	-423.36	329.85	11.10	215.63	-19.13	63.00	1.283	y	1.64	2.19	105.7	0.021	-503.3	346.0	575.3	14.01	237.19	-33.34	69.30	NA	NA	NA	NA	NA	NA	NA	NA	1.64	n	
89	W6X15	Brace	Primary	-220.97	44.96	0.51	29.64	0.00	16.28	4.915	n	NA	0.79	41.33	0.019	-273.0	45.0	216.0	0.51	29.64	0.00	17.51	NA	NA	NA	NA	NA	NA	6.00	1.01	1.01	n	

Lamar		Column Removal		Column Removal Results Spreadsheet																				4/8/2015								
<b>B2</b>		<b>3 (O-2)</b>		Force Control										Deformation Control										Check								
Fr. ID	Section	Type	Primary?	Axial		Moment				$P_{UF}/P_{CL} > 0.5$			Shear			Axial		Moment				$P_{UF}/P_{CL} < 0.2$		$0.2 \leq P_{UF}/P_{CL} \leq 0.5$		Tension		Braces		Check Total		
				$P_{UF}$ Kip	$P_{CL}$ Kip	$M_{UFx}$ Kip-ft	$M_{CLx}$ Kip-ft	$M_{UFy}$ Kip-ft	$M_{CLy}$ Kip-ft	$P_{UF}/P_{CL}$	FC?	DCR	$V_{UF}$ Kip	$V_{RF}$ Kip	DCR	$P_{UD}$ Kip	$P_{CE}$ Kip	$P_{TE}$ Kip	$M_{UDx}$ Kip-ft	$M_{CEx}$ Kip-ft	$M_{UDy}$ Kip-ft	$M_{CEy}$ Kip-ft	m-fact.	DCR	m-fact.	DCR	m-fact.	DCR	m-fact.		DCR	DCR
59	W12X40	Column	Primary	-137.09	329.85	-3.56	215.63	14.09	63.00	0.416	n	NA	0.02	105.7	0.000	-155.8	346.0	575.3	-3.76	237.19	-115.15	69.30	NA	NA	2.11	1.12	NA	NA	NA	NA	1.12	n
1530	W12X40	Column	Primary	-278.97	329.85	-2.66	215.63	-17.41	63.00	0.846	y	1.13	0.60	105.7	0.006	-323.5	346.0	575.3	-3.75	237.19	-115.47	69.30	NA	NA	NA	NA	NA	NA	NA	NA	1.13	n
69	W12X40	Column	Primary	-445.20	329.85	-3.78	215.63	2.23	63.00	1.350	y	1.40	0.68	105.7	0.006	-508.8	346.0	575.3	-4.52	237.19	-6.19	69.30	NA	NA	NA	NA	NA	NA	NA	NA	1.40	n
90	W12X40	Column	Primary	-325.80	329.85	-5.48	215.63	-1.20	63.00	0.988	y	1.03	0.23	105.7	0.002	-374.7	346.0	575.3	-6.19	237.19	4.20	69.30	NA	NA	NA	NA	NA	NA	NA	NA	1.03	n
572	W16X26	Beam	Primary	-0.01	89.25	-147.12	41.51	0.04	33.64	0.000	n	NA	22.08	106.0	0.208	0.0	89.2	594.4	-168.94	41.97	0.04	33.64	3.81	1.06	NA	NA	NA	NA	NA	NA	1.06	n
587	W12X40	Column	Primary	-465.30	329.85	-22.59	215.63	-8.59	63.00	1.411	y	1.65	5.12	105.7	0.048	-550.1	346.0	575.3	-33.88	237.19	-0.87	69.30	NA	NA	NA	NA	NA	NA	NA	NA	1.65	n
591	W12X40	Column	Primary	-348.73	329.85	-31.79	215.63	5.26	63.00	1.057	y	1.29	1.96	105.7	0.019	-411.0	346.0	575.3	-33.89	237.19	-0.87	69.30	NA	NA	NA	NA	NA	NA	NA	NA	1.29	n

Lamar		Column Removal		Column Removal Results Spreadsheet																				4/18/2015									
<b>B3</b>		<b>4 (K-4)</b>		Force Control										Deformation Control										Check									
Fr. ID	Section	Type	Primary?	Axial		Moment				$P_{UF}/P_{CL} > 0.5$			Shear			Axial		Moment				$P_{UF}/P_{CL} < 0.2$		$0.2 \leq P_{UF}/P_{CL} \leq 0.5$		Tension		Braces		Check Total			
				$P_{UF}$ Kip	$P_{CL}$ Kip	$M_{UFx}$ Kip-ft	$M_{CLx}$ Kip-ft	$M_{UFy}$ Kip-ft	$M_{CLy}$ Kip-ft	$P_{UF}/P_{CL}$	FC?	DCR	$V_{UF}$ Kip	$V_{RF}$ Kip	DCR	$P_{UD}$ Kip	$P_{CE}$ Kip	$P_{TE}$ Kip	$M_{UDx}$ Kip-ft	$M_{CEx}$ Kip-ft	$M_{UDy}$ Kip-ft	$M_{CEy}$ Kip-ft	m-fact.	DCR	m-fact.	DCR	m-fact.	DCR	m-fact.		DCR	DCR	OK?
1555	W12X40	Column	Primary	-331.88	329.85	-0.22	215.63	0.08	63.00	1.006	y	1.01	0.04	105.7	0.000	-386.1	346.0	575.3	-0.28	237.19	0.11	69.30	NA	NA	NA	NA	NA	NA	NA	NA	NA	1.01	n

Fr. ID Section		Type Primary?		Force Control										Deformation Control								Check											
				Axial		Moment				P <sub>UF</sub> /P <sub>CL</sub> > 0.5				Shear		Axial			Moment				P <sub>UF</sub> /P <sub>CL</sub> < 0.2		0.2 ≤ P <sub>UF</sub> /P <sub>CL</sub> ≤ 0.5		Tension		Braces		Total	OK?	
A	B	C		P <sub>UF</sub> Kip	P <sub>CL</sub> Kip	M <sub>UFx</sub> Kip-ft	M <sub>CLx</sub> Kip-ft	M <sub>UFy</sub> Kip-ft	M <sub>CLy</sub> Kip-ft	P <sub>UF</sub> /P <sub>CL</sub>	FC?	DCR	V <sub>UF</sub> Kip	V <sub>RF</sub> Kip	DCR	P <sub>UD</sub> Kip	P <sub>CE</sub> Kip	P <sub>TE</sub> Kip	M <sub>UDx</sub> Kip-ft	M <sub>CEx</sub> Kip-ft	M <sub>UDy</sub> Kip-ft	M <sub>CEy</sub> Kip-ft	m-fact.	DCR	m-fact.	DCR	m-fact.	DCR	m-fact.	DCR	DCR	OK?	
1523	W12X40	Column	Primary	-333.58	329.85	0.00	215.63	0.01	63.00	1.011	y	1.01	0.02	105.7	0.000	-387.7	346.0	575.3	-0.05	237.19	-0.07	69.30	NA	NA	NA	NA	NA	NA	NA	NA	NA	1.01	n
1532	W12X40	Column	Primary	-331.43	329.85	0.00	215.63	-0.01	63.00	1.005	y	1.00	0.02	105.7	0.000	-385.5	346.0	575.3	-0.05	237.19	0.08	69.30	NA	NA	NA	NA	NA	NA	NA	NA	NA	1.00	n

Appendix D. Loads Applied to Elements in American Zinc Configuration 0 (Force and Deformation Controlled Models)

Column Removal Case 1:

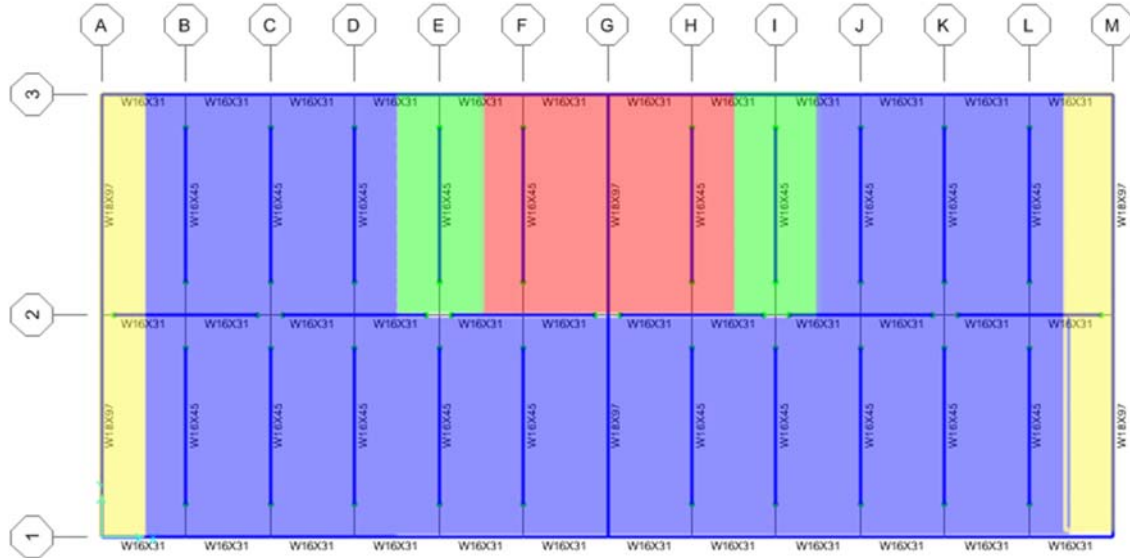


Figure 148. Load Patterns for Column 1 Removal

Table 95. Column 1 Loads (tributary width = 10' - 2")

Floor	$G_{LD}$ lb/ft	$G_{LF}$ lb/ft	G lb/ft	$\frac{1}{2}G$ lb/ft	$\frac{1}{2}G + \frac{1}{2}G_{LD}$ lb/ft	$\frac{1}{2}G + \frac{1}{2}G_{LF}$ lb/ft
2 - 4	3379.0	2503.4	1251.7	625.9	2315.3	1877.6
roof	2119.2	1568.7	784.3	392.2	1451.8	1177.6
Location	2-3: F-H		1-2: B-L 2-3: B-D, J-L	1-3: A, M	2-3: E, I	

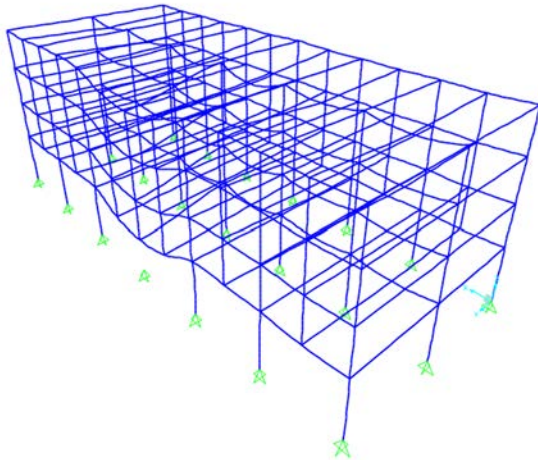


Figure 149. Deformations under column 1 removal analysis

Column Removal Case 2:

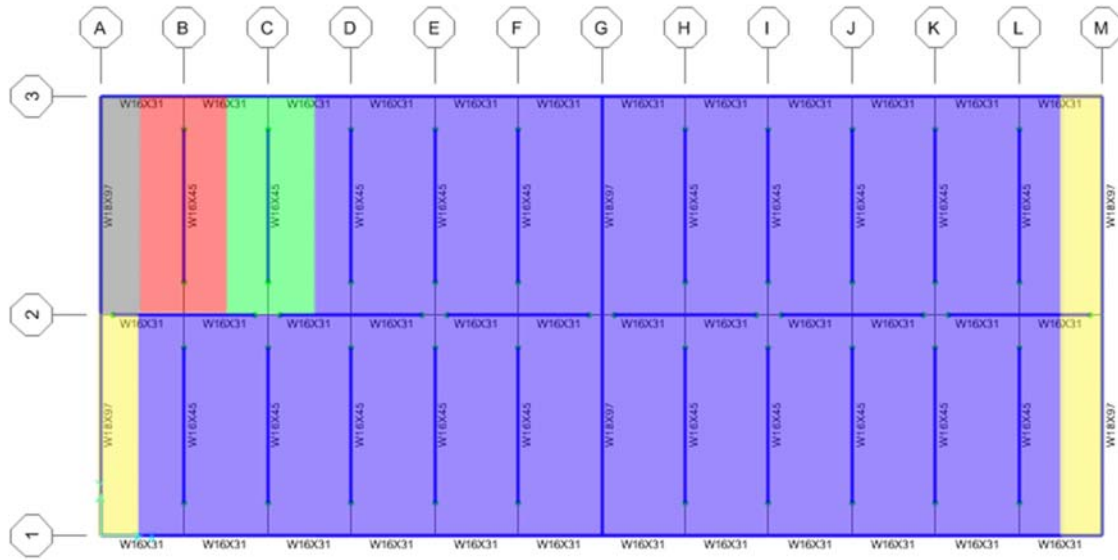


Figure 150. Load Patterns for Column 2 Removal

Table 7. Column 2 Loads (tributary width = 10' - 2")

Floor	G <sub>LD</sub>	G <sub>LF</sub>	G	½G	½G + ½G <sub>LD</sub>	½G + ½G <sub>LF</sub>
	lb/ft	lb/ft	lb/ft	lb/ft	lb/ft	lb/ft
2 – 4	3379.0	2503.4	1251.7	625.9	2315.3	1877.6
roof	2119.2	1568.7	784.3	392.2	1451.8	1177.6
Location	2-3:B		1-2: B-L 2-3:D-L	1-2: A,M 2-3: M	2-3: C	

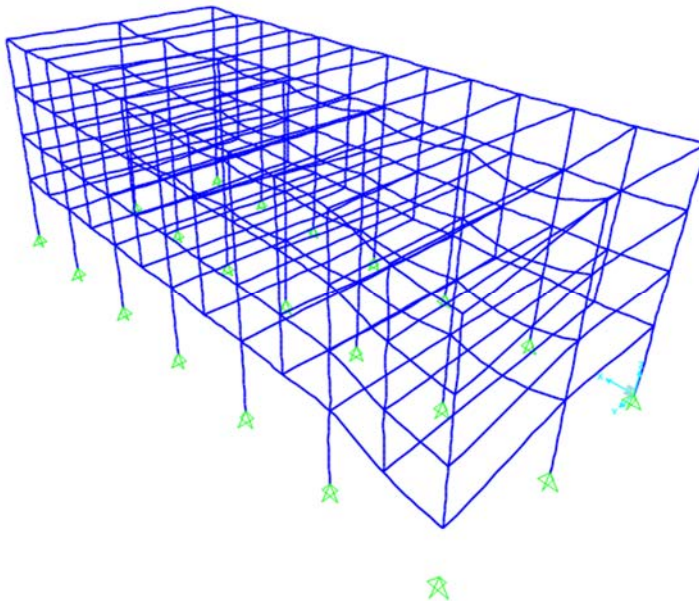


Figure 151. Column 2 Removal

Column Removal Case 3:

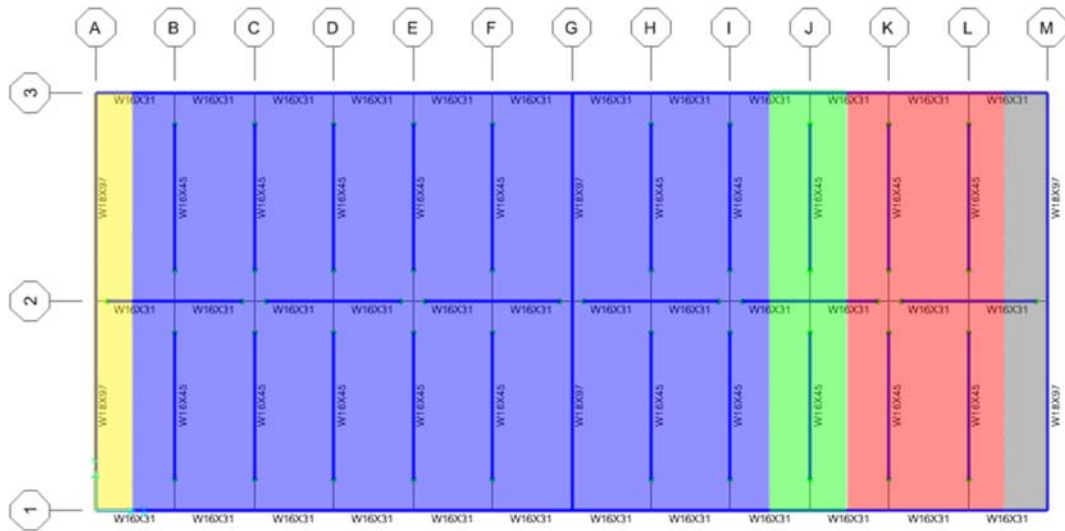


Figure 152. Load Patterns for Column 3 Removal

Table 8. Column 3 Loads (tributary width = 10' - 2")

Floor	G <sub>LD</sub>	G <sub>LF</sub>	G	½G	½G + ½G <sub>LD</sub>	½G + ½G <sub>LF</sub>
	lb/ft	lb/ft	lb/ft	lb/ft	lb/ft	lb/ft
2 – 4	3379.0	2503.4	1251.7	625.9	2315.3	1877.6
roof	2119.2	1568.7	784.3	392.2	1451.8	1177.6
Location	1-2: K, L 2-3: K, L		1-2: B-I 2-3: B-I	1-2: A 2-3: A	1-2: J 2-3: J	

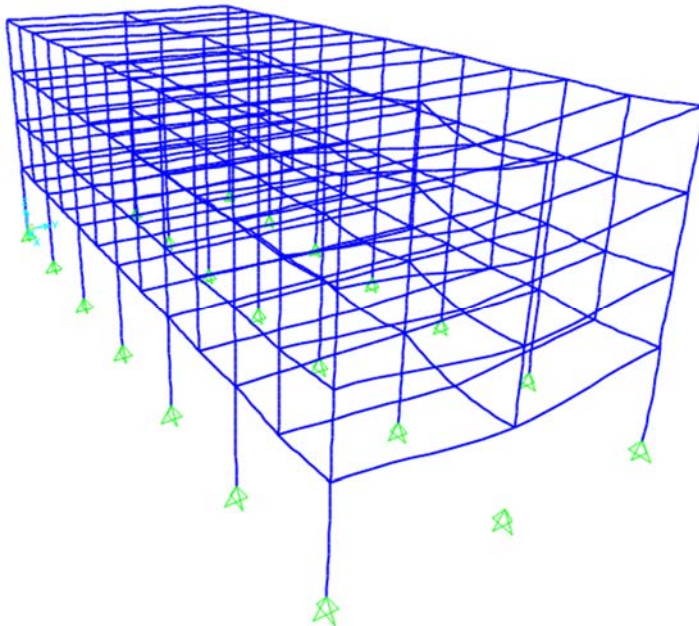


Figure 153. Column 3 Removal

Column Removal Case 4:

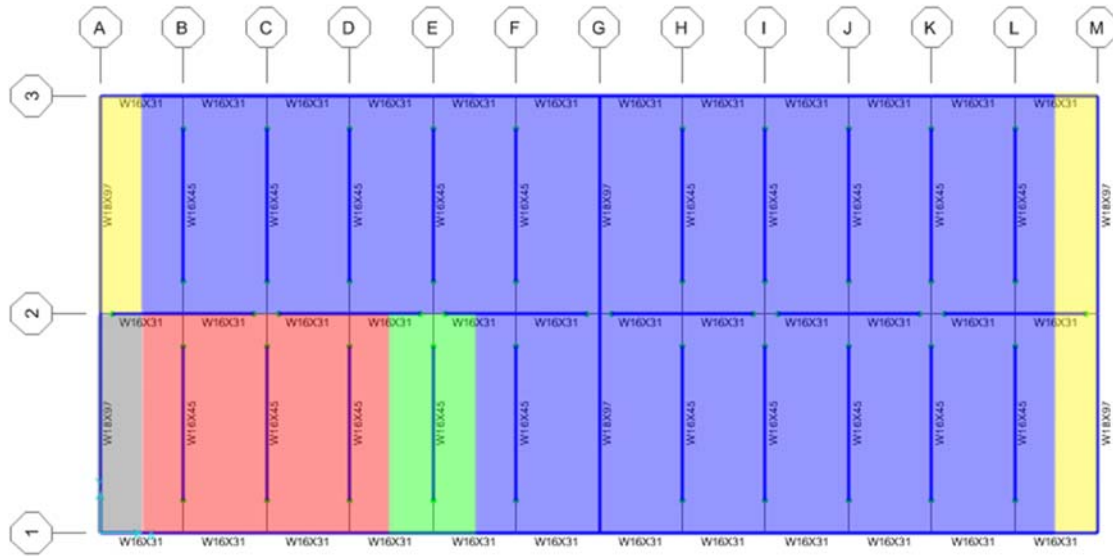


Figure 154. Load Patterns for Column 4 Removal

Table 9. Column 4 Loads (tributary width = 10' - 2")

Floor	G <sub>LD</sub>	G <sub>LF</sub>	G	½G	½G + ½G <sub>LD</sub>	½G + ½G <sub>LF</sub>
	lb/ft	lb/ft	lb/ft	lb/ft	lb/ft	lb/ft
2 - 4	3379.0	2503.4	1251.7	625.9	2315.3	1877.6
roof	2119.2	1568.7	784.3	392.2	1451.8	1177.6
Location	1-2: B-D		1-2: F-L 2-3: B-L	1-2: M 2-3: A,M	1-2: E	

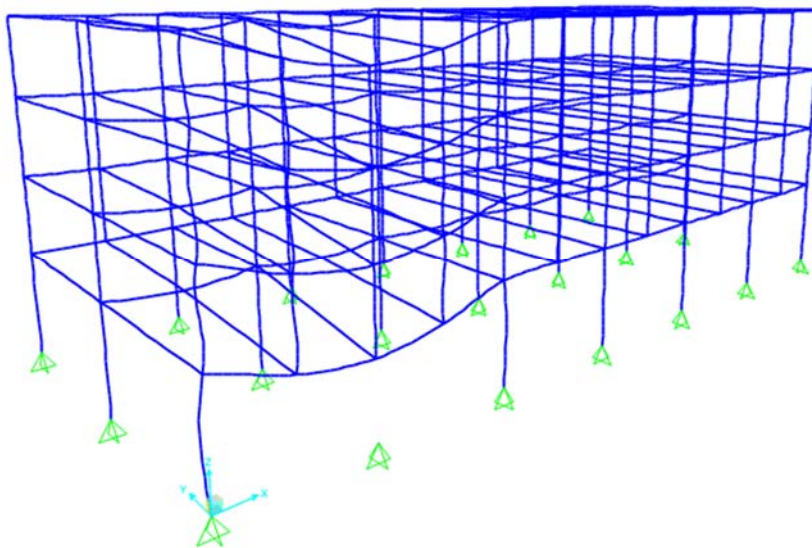


Figure 155. Column 4 Removal